The Use of CpG Oligodeoxynucleotides As Antiviral Treatments Against Orthopoxvirus Infection

Thesis

The use of CpG oligodeoxynucleotides as antiviral treatments against Orthopoxvirus infection.

Matthew Christopher Jackson

This thesis is submitted for examination for the degree of

Doctor of Philosophy to the Open University

Biomedical Sciences Department, Dstl Porton Down

March 2008

DATE OF SUBMISSION: 8 FEBRUARY 2008
DATE OF AWARD: 31 MARCH 2008

ProQuest LLC.
789 East Eisenhower Parkway
P.O. Box 1346
Ann Arbor, MI 48106 – 1346

Abstract

Complications with the current smallpox vaccine and the threat of a new smallpox epidemic have dramatically increased efforts to identify new antiviral compounds against orthopoxviruses. CpG oligodeoxynucleotides were investigated here for their ability to confer protection against vaccinia virus (VACV) in a model of orthopoxvirus infection in pre- and post-exposure settings.

Intranasal delivery of the B-class CpG 7909, prior to intranasal challenge with VACV, previously resulted in complete protection in a Balb/C mouse model of infection. Immunological analysis found that pre-stimulation with CpG resulted in the local release of pro-inflammatory cytokines such as IFN-α, IFN-γ, TNF-α and IL-6 along with chemotactic messengers such as CCL2. In addition, activated innate effector cells such as macrophages, neutrophils, and dendritic cells were identified in high numbers in the lungs of CpG treated mice prior to infection. This heightened immune response persisted throughout early VACV infection in CpG-treated animals compared to that observed in un-stimulated control mice. Mice treated with CpG-B 7909 also initiated a second wave of immune activation late in infection indicative of a more rapidly formed adaptive response. Treatment and infection of B-cell Knock-out (KO) mice and neutrophil ablated mice suggested neither B-cells nor neutrophils alone were crucial in conferring CpG-mediated protection against VACV.

The success of CpG-B 7909 as a prophylactic against VACV led to its investigation as a post-exposure therapeutic. Intranasal treatment with CpG-B

7909, 24 hours after VACV challenge, boosted the pro-inflammatory response initiated after VACV infection in the lung. This response involved increased macrophage, neutrophil, dendritic cell and NK cell responses and increased levels of pro-inflammatory cytokines, interferons and chemokines. This enabled protection of 60% of VACV infected mice. Multiple dosing of CpG post-VACV exposure did not increase levels of protection.

The effectiveness of delivering CpG-B 7909 intranasally and identification of macrophages as a highly activated cell-type during CpG-mediated protection, led to the investigation of alveolar macrophages following CpG stimulation. Using *in vitro* macrophage cell-lines, A-class (CpG-A) and semi-soft C-class (CpG-sC) CpGs induced secretion of nitric oxide and expression of cytokines/chemokines more effectively than other classes of CpG in both alveolar (MH-S) and blood monocyte/macrophage (J774) cell-lines. In addition, MH-S macrophages were shown to secrete more nitric oxide but less IL-6 and TNF-α than J774 macrophages after CpG stimulation. In an *in vitro* model of infection with VACV, pre-treatment of macrophages with CpG-B and CpG-sC significantly restricted viral replication independently of nitric oxide production. These antiviral properties led to the investigation of CpG-sC 10109 as a prophylactic against VACV *in vivo* where it conferred complete protection.

Collectively, these results suggest CpGs are highly immunostimulatory and can confer full protection against VACV when given pre-exposure. This protection correlates with the induction of a strong, local immune response prior to VACV challenge, without which, the host fails to control infection effectively.

Declaration

Unless otherwise stated, the results and data presented within this thesis were solely the work of Matt Jackson.

All animal handling and infection studies were performed by Dr Mandy Gates, Dr Roman Lukaszewski, Mrs Amanda Phelps, Mrs Lin Eastaugh and Mrs Jan Platt, Dstl. All subsequent processing of tissues for analysis were performed by M.Jackson with assistance when necessary from the above mentioned colleagues.

All statistical analysis was performed following consultation with Dr. Tom Laws, Dstl.

CpG sequences were provided by Dr Art Krieg of Coley Pharmaceuticals, Ottawa, Canada.

Acknowledgements

First and foremost I would like to thank my chief supervisor Dr Roman Lukaszewski for allowing me the opportunity to do this project and for his invaluable assistance throughout both the practical aspects and writing up of this thesis. The amount of times I heard the words "Don't Panic" can not be quantified, so once again, I thank you for keeping me on the straight and narrow. I would also like to thank my two additional supervisors, Dr Mandy Gates and Dr Di Williamson for their contributions and excellent suggestions throughout the entirety of this project.

I am also extremely grateful to all those who assisted at various stages throughout the practical work in this project. For this special thanks must go to Dr Mandy Gates, Dr Roman Lukaszewski, Amanda Phelps, Lin Eastaugh, Sarah Newstead and Jan Platt. In addition, I would like to thank Rachel Dean and Dr Tim Milne for their willingness to buddy me outside of work hours. In addition, the phenomenon that is Dr Rage Laws is acknowledged for his supreme statistical guidance and proof-reading skills. A big 'thank you' also needs to be extended to Dr Art Krieg and colleagues over at Coley Pharmaceuticals for allowing me access to their bank of CpG oligonucleotides.

In addition, I would like to thank the following people for making the writing of this thesis and the last four years as a whole, less traumatic than they could have been: Rob Deakin for managing "Da Plan"; Jack Johnson, Brian Wilson, Chris Martin, Jean-Benoit Dunckel and Nicolas Godin for musical bliss and Tim Milne,

Tom laws, Kim Pearcey and Dave Scarratt for musical venting. Extra thanks should also go the newly graduated Dr Tim Milne for endless rants and for being the proverbial rabbit for me to chase. Post-thesis but pre-viva, I thank Steve Moore, Tom Laws, Chris Lebutt and Tim Milne for Vegas baby, I don't think I've ever laughed as much.

Finally and most importantly, I thank Gems, for absolutely everything.

This thesis is dedicated to my parents Barry and Irene Jackson for always providing me with everything a son could ever want.

Table of contents

	Page
Abstract	i
Declaration	iii
Acknowledgements	iv
Dedication	vi
Table of contents	vii
List of tables and figures	xv
List of abbreviations	xxiv
1. Chapter 1. General Introduction	1
1.1. The innate immune response	1
1.1.1. Pattern recognition	2
1.1.2. Toll and the Toll-Like receptors	2
1.1.3. Non-TLR PRRs	7
1.1.4. Viral defence and PRRs	8
1.1.5. TLR recognition of viral PAMPs	11
1.1.5.1.TLR2	11
1.1.5.2.TLR3	11
1.1.5.3.TLR4	12
1.1.5.4.TLRs 7 and 8	12
1.1.5.5.TLR9	13
1.2. Immunostimulatory properties of CpG motifs	14
1.2.1. The identification of CpG motifs	14
1.2.2. Differences between bacterial and vertebrate DNA	16
1.2.3. Species differentiation and other organisms	17

1.2.4. The significance of backbone chemistry 20

1.2.5. Different classes of CpGs 21

1.2.5.1.CpG-A / D-type 22

1.2.5.2.CpG-B / K-type 23

1.2.5.3.CpG-C / C-type 24

1.2.5.4.CpG-sC / Semi-soft C-type 24

1.2.6. Immune consequences of CpG-TLR9 recognition 25

1.2.7. Therapeutic applications of CpGs 26

1.2.7.1.Use of CpGs in allergy, cancer and as vaccine adjuvants 26

1.2.7.2.The use of CpGs against infectious disease 28

1.3. Smallpox and pathogenesis 29

1.3.1. Animal models 30

1.3.2. Vaccinia virus 31

1.3.2.1.Vaccinia virus life cycle 32

1.3.3. Poxvirus immunomodulation 37

1.3.3.1.Virokines 37

1.3.3.2.Viroreceptors 40

1.3.3.3.Viral inhibition of signal transduction 44

1.3.4. Vaccination complications 48

1.3.4.1.Targeting viral enzymes and proteins 49

1.3.4.2.Targeting host enzymes 53

1.3.4.3.Targeting host systems 55

1.4. Aims of this research 57

2. Chapter 2. Materials and Methods 58

2.1. Cell culture 58

2.1.1. CpG stimulation 58

2.1.2. Nitric oxide measurements 60

2.1.3. Nitric oxide inhibition 60

2.2. Viral titrations 62

2.2.1. Cell culture infected macrophages 62

2.2.2. Viral titre calculation 62

2.3. Reverse transcription polymerase chain reaction (RT-PCR) 63

2.3.1. RNA isolation from macrophage cell-lines and primary macrophages 63

2.3.2. DNA-free treatment 64

2.3.3. RNA purification 64

2.3.4. Reverse transcription 66

2.3.5. Relative quantitation of gene expression 66

2.4. Cytokine analysis *via* protein detection 70

2.4.1. BD™ cytometric bead array (CBA) 70

2.4.2. IFN-α sandwich enzyme linked immunosorbent assay (ELISA) 70

2.5. Flow cytometry 72

2.5.1. Antibody staining 73

2.5.2. Apoptosis measurement 74

2.6. Animals and infection 74

2.6.1. Sources of animals 74

2.6.2. Infection with VACV strain IHD 75

2.6.3. CpG and PBS dosing 75

2.6.4. Bronchoalveolar lavage collection and staining 75

2.6.5. Alveolar macrophage purification 76

2.6.6. Neutrophil ablation 76

2.6.7. Technical assistance 76

2.7. Statistical methods 78

3. Chapter 3. The prophylactic use of CpG-B 7909 against VACV 79

3.1. Introduction 79

3.1.1. CpG prophylaxis and bacterial infection 79

3.1.2. CpG prophylaxis and parasitic infection 81

3.1.3. CpG prophylaxis and viral infection 81

3.2. Aims of this chapter 83

3.3. Results 84

3.3.1. Experimental outline 84

3.3.2. Cytokine responses in the lung 84

3.3.3. Cellular responses in the lung 86

3.3.3.1.Lung macrophage responses 86

3.3.3.2.Lung neutrophil responses 88

3.3.3.3.Lung dendritic cell responses 91

3.3.3.4.Lung natural killer cell responses 94

3.3.3.5.Lung B-cell responses 97

3.3.3.6.Lung T-cell responses 101

3.3.4. Cytokine responses in the spleen 101

3.3.5. Cellular responses in the spleen 104

3.3.5.1.Spleen macrophage responses 104

3.3.5.2.Spleen neutrophil responses 104

3.3.5.3.Spleen dendritic cell responses 108

3.3.5.4.Spleen natural killer cell responses 111

3.3.5.5.Spleen B-cell responses 115

3.3.5.6.Spleen T-cell responses 118

3.3.6. Cytokine responses in the sera 118

3.3.7. The role of B-cells in CpG mediated VACV protection 121

3.3.8. The role of neutrophils in CpG mediated VACV protection 123

3.4. Discussion 126

4. Chapter 4. The use of CpG-B 7909 as a post-exposure therapeutic against VACV 142

4.1. Introduction 142

4.2. Aims of this chapter 144

4.3. Results 145

4.3.1. Selection of day and dose for post-exposure CpG delivery 145

4.3.2. Effect of multiple doses of CpG-B 7909 via the intranasal route 145

4.3.3. Immunological impact of post-exposure CpG-B 7909 delivery 147

4.3.3.1.Experimental Outline 147

4.3.3.2.Cytokine responses in the lung 149

4.3.3.3.Cellular responses in the lung 149

4.3.3.3.1. Lung macrophage responses 149

4.3.3.3.2. Lung neutrophil responses 152

4.3.3.3.3. Lung dendritic cell responses 154

4.3.3.3.4. Lung natural killer cell responses 158

4.3.3.3.5. Lung B-cell responses 161

4.3.3.3.6. Lung T-cell responses 164

4.3.3.4.Cytokine responses in the spleen 164

4.3.3.5.Cellular responses in the spleen 168

4.3.3.5.1. Spleen macrophage responses 168

4.3.3.5.2. Spleen neutrophil responses 168

4.3.3.5.3. Spleen dendritic cell responses 173

4.3.3.5.4. Spleen natural killer cell responses 173

4.3.3.5.5. Spleen B-cell responses 178

4.3.3.5.6. Spleen T-cell responses 178

4.3.3.6.Cytokine responses in the sera 182

4.4. Discussion. 184

5. Chapter 5. Macrophage responses to different classes of CpG 195

5.1. Introduction 195

5.1.1. Defences at the lung surface 195

5.1.2. The role of alveolar macrophages 196

5.1.3. Variety of lung macrophages and heterogeneity 197

5.1.4. Macrophage responses to CpG 198

5.1.5. Viral infections in the lung 200

5.1.6. CpG-B 7909 and CpG-B 10103 201

5.2. Aims of this Chapter 201

5.3. Results 202

5.3.1. TLR9 is present on primary macrophages 202

5.3.2. TLR9 expression in MH-S and J774 macrophage cell-lines upon stimulation with CpG 206

5.3.3. The *in vitro* stimulatory properties of CpG-B 7909 are comparable to CpG-B 10103 208

5.3.4. Release of NO by MH-S and J774 macrophages following stimulation with CpG 210

5.3.4.1.A-class and semi-soft C-class CpGs stimulate greater NO responses than B-class and C-class CpGs in MH-S but not J774 macrophages 210

5.3.4.2.Lower concentrations of CpG do not induce higher concentrations of NO 214

5.3.5. Chemokine and cytokine production by MH-S and J774 macrophage cell-lines after stimulation with different classes of CpGs 216

5.3.5.1.CCL2 216

5.3.5.2.TNF-α 218

5.3.5.3.IL-6 222

5.3.6. Replication of VACV in unstimulated MH-S and J774 macrophages 222

5.3.7. Replication of VACV in pre-stimulated MH-S and J774 macrophages 225

5.3.8. The effect of NO inhibition on VACV replication in MH-S and J774 macrophages 229

5.3.8.1. The inhibition of NO from MH-S macrophages 230

5.3.8.2. Inhibition of NO does not alter the growth of VACV in CpG stimulated macrophages 230

5.3.9. CpGs prevent apoptosis in both MH-S and J774 macrophage cells lines 232

5.3.10. CpG-sC 10109 is protective against VACV 232

5.4. Discussion 237

6. Chapter 6. Summary Discussion 246

6.1. The immune response to VACV in naïve mice 247

6.2. The effect of CpG-B 7909 on the immune response to VACV 251

6.3. Post-exposure treatment of VACV with CpG-B 7909 258

6.4. CpGs activate macrophages and restrict VACV titres *in vitro* 262

6.5. Concluding remarks 267

7. Chapter 7. References 270

List of Tables and Figures

Page

Chapter 1. General Introduction

Table 1.1	The mammalian TLR family: Ligand recognition and cellular distribution of TLRs 1-10 in humans and TLR11 in mice.	4
Figure 1.1	TLR pathway and activation.	6
Figure 1.2	Human CpG activation and immunity.	19
Figure 1.3	Vaccinia virus life-cycle.	33
Figure 1.4	Examples of three types of poxvirus immunomodulatory strategy.	38
Table 1.2	Virus specific enzyme or protein targets.	50
Table 1.3	Host cellular enzyme targets.	54
Table 1.4	Host signalling targets.	56

Chapter 2. Materials and Methods

Table 2.1	CpG sequences used throughout.	59
Figure 2.1	The Griess Reaction.	61
Figure 2.2	Typical bioanalyser analysis of RNA samples.	65
Figure 2.3	Universal thermocycler PCR reaction programme:(Applied Biosystems 9600 Emulation).	67
Figure 2.4	Real-time PCR and fluorescence resonance energy transfer (FRET) technology.	68
Figure 2.5	Detection of reporter signal by ABI Prism 7000 SDS software.	69

Figure 2.6 Cytokine quantification through CBA protein detection. 71

Table 2.2 The Hema Gurr rapid staining procedure 77

Chapter 3. The use of CpG-B 7909 as a pre-exposure therapeutic against VACV

Figure 3.1 Measurement of lung cytokine levels in Balb/C mice pre-treated with either CpG-B 7909 or PBS throughout infection with VACV. 85

Figure 3.2 Lung macrophage numbers during VACV infection in CpG-B 7909 and PBS pre-treated groups. 87

Figure 3.3 Activation of lung macrophages during VACV infection in CpG-B 7909 and PBS pre-treated groups. 89

Figure 3.4 Lung neutrophil numbers during VACV infection in CpG-B 7909 and PBS pre-treated groups. 90

Figure 3.5 Activation of lung neutrophils during VACV infection in CpG-B 7909 and PBS pre-treated groups. 92

Figure 3.6 Lung dendritic cell numbers during VACV infection in CpG-B 7909 and PBS pre-treated groups. 93

Figure 3.7 Activation of lung dendritic cells during VACV infection in CpG-B 7909 and PBS pre-treated groups. 95

Figure 3.8 Lung natural killer cell numbers during VACV infection in CpG-B 7909 and PBS pre-treated groups. 96

Figure 3.9 Activation of lung natural killer cells during VACV infection in CpG-B 7909 and PBS pre-treated groups 98

Figure 3.10	Lung B-cell numbers during VACV infection in CpG-B 7909 and PBS pre-treated groups.	99
Figure 3.11	Activation of lung B-cells during VACV infection in CpG-B 7909 and PBS pre-treated groups.	100
Figure 3.12	Lung T-cell numbers during VACV infection in CpG-B 7909 and PBS pre-treated groups.	102
Figure 3.13	Measurement of spleen cytokine levels in Balb/C mice pre-treated with either CpG-B 7909 or PBS throughout infection with VACV.	103
Figure 3.14	Spleen macrophage numbers during VACV infection in CpG-B 7909 and PBS pre-treated groups.	105
Figure 3.15	Activation of spleen macrophages during VACV infection in CpG-B 7909 and PBS pre-treated groups.	106
Figure 3.16	Spleen neutrophil numbers during VACV infection in CpG-B 7909 and PBS pre-treated groups.	107
Figure 3.17	Activation of spleen neutrophils during VACV infection in CpG-B 7909 and PBS pre-treated groups.	109
Figure 3.18	Spleen dendritic cell numbers during VACV infection in CpG-B 7909 and PBS pre-treated groups.	110
Figure 3.19	Activation of spleen dendritic cells during VACV infection in CpG-B 7909 and PBS pre-treated groups.	112
Figure 3.20	Spleen natural killer cell numbers during VACV infection in CpG-B 7909 and PBS pre-treated groups.	113
Figure 3.21	Activation of spleen natural killer cells during VACV infection in CpG-B 7909 and PBS pre-treated groups.	114

Figure 3.22	Spleen B-cell numbers during VACV infection in CpG-B 7909 and PBS pre-treated groups.	116
Figure 3.23	Activation of spleen B-cells during VACV infection in CpG-B 7909 and PBS pre-treated groups.	117
Figure 3.24	Spleen T-Cell numbers during VACV infection in CpG-B 7909 and PBS pre-treated groups.	119
Figure 3.25	Measurement of serum cytokine levels in Balb/C mice pre-treated with either CpG-B 7909 or PBS throughout infection with VACV.	120
Figure 3.26	Effect of B-cell KO on CpG-mediated VACV protection	122
Figure 3.27	Effect of neutrophil depletion on CpG-mediated VACV protection.	124
Table 3.1	Significant differences between CpG-B 7909 and PBS treatment groups in the lungs of mice during VACV infection.	135
Table 3.2	Significant differences between CpG-B 7909 and PBS treatment groups in the lungs of mice during VACV infection.	136

Chapter 4. The use of CpG-B 7909 as a post-exposure therapeutic against VACV

Figure 4.1	Different intranasal doses of CpG-B 7909 as a post-exposure treatment in mice infected with VACV.	146
Figure 4.2	Effect of multiple dosing with CpG-B 7909 as a post-exposure treatment in mice infected with VACV.	148

Figure 4.3	Measurement of lung cytokine levels in Balb/C mice treated with CpG-B 7909 or PBS post-infection with VACV.	150
Figure 4.4	Lung macrophage numbers during VACV infection in CpG-B 7909 and PBS treated groups.	151
Figure 4.5	Activation of lung macrophages during VACV infection in CpG-B 7909 and PBS treated groups.	153
Figure 4.6	Lung neutrophil numbers during VACV infection in CpG-B 7909 and PBS treated groups.	155
Figure 4.7	Activation of lung neutrophils during VACV infection in CpG-B 7909 and PBS treated groups.	156
Figure 4.8	Lung dendritic cell numbers during VACV infection in CpG-B 7909 and PBS treated groups.	157
Figure 4.9	Activation of lung dendritic cells during VACV infection in CpG-B 7909 and PBS treated groups.	159
Figure 4.10	Lung natural killer cell numbers during VACV infection in CpG-B 7909 and PBS treated groups.	160
Figure 4.11	Activation of lung natural killer cells during VACV infection in CpG-B 7909 and PBS treated groups.	162
Figure 4.12	Lung B-cell numbers during VACV infection in CpG-B 7909 and PBS treated groups.	163
Figure 4.13	Activation of lung B-cells during VACV infection in CpG-B 7909 and PBS treated groups.	165
Figure 4.14	Lung T-cell numbers during VACV infection in CpG-B 7909 and PBS treated groups	166

Figure 4.15	Measurement of spleen cytokine levels in Balb/C mice treated with CpG-B 7909 or PBS post-infection with VACV.	167
Figure 4.16	Spleen macrophage numbers during VACV infection in CpG-B 7909 and PBS treated groups.	169
Figure 4.17	Activation of spleen macrophages during VACV infection in CpG-B 7909 and PBS treated groups.	170
Figure 4.18	Spleen neutrophil numbers during VACV infection in CpG-B 7909 and PBS treated groups.	171
Figure 4.19	Activation of spleen neutrophils during VACV infection in CpG-B 7909 and PBS treated groups.	172
Figure 4.20	Spleen dendritic cell numbers during VACV infection in CpG-B 7909 and PBS treated groups.	174
Figure 4.21	Activation of spleen dendritic cells during VACV infection in CpG-B 7909 and PBS treated groups.	175
Figure 4.22	Spleen natural killer cell numbers during VACV infection in CpG-B 7909 and PBS treated groups.	176
Figure 4.23	Activation of spleen natural killer cells during VACV infection in CpG-B 7909 and PBS treated groups.	177
Figure 4.24	Spleen B-cell Numbers during VACV infection in CpG-B 7909 and PBS treated groups.	179
Figure 4.25	Activation of spleen B-cells during VACV infection in CpG-B 7909 and PBS treated groups.	180
Figure 4.26	Spleen T-cell numbers during VACV infection in CpG-B 7909 and PBS treated groups.	181

Figure 4.27 Measurement of serum cytokine levels in Balb/C mice treated with CpG-B 7909 or PBS post-infection with VACV. 183

Table 4.1 Significant differences between CpG-B 7909 and PBS treatment groups in the lungs of mice during VACV infection. 190

Table 4.2 Significant differences between CpG-B 7909 and PBS treatment groups in the spleens of mice during VACV infection. 191

Chapter 5. Macrophage responses to different classes of CpG

Figure 5.1 Expression of TLR9 on primary alveolar macrophages. 203

Figure 5.2 Immunohistological staining of BAL samples. 204

Figure 5.3 Primary alveolar macrophages are responsive to CpG. 205

Figure 5.4 Changes in expression of TLR9 mRNA. 207

Figure 5.5 Expression of TLR9 on MH-S and J774 macrophages. 209

Figure 5.6 B-class CpGs 10103 and 7909 induce comparable cytokine responses in macrophages. 211

Figure 5.7 B-class CpGs 10103 and 7909 induce comparable NO responses in macrophages. 212

Figure 5.8 Release of NO as determined by nitrite measurement using the Griess reaction. 213

Figure 5.9 Release of NO by MH-S and J774 macrophages following stimulation with low concentrations of CpG. 215

Figure 5.10	Changes in chemokine CCL2 mRNA expression.	217
Figure 5.11	Changes in chemokine CCL2 protein release.	219
Figure 5.12	Changes in pro-inflammatory TNF-α cytokine mRNA expression.	220
Figure 5.13	Changes in pro-inflammatory TNF-α protein release.	221
Figure 5.14	Changes in pro-inflammatory cytokine IL-6 mRNA expression.	223
Figure 5.15	Changes in pro-inflammatory IL-6 protein release.	224
Figure 5.16	Growth of VACV in MH-S and J774 macrophage cell lines.	226
Table 5.1	Both CpG-B 10103 and CpG-sC 10109 significantly restrict the growth of VACV in MH-S and J774 macrophages.	227
Figure 5.17	Growth of VACV in MH-S and J774 macrophage cell lines pre-stimulated with CpG.	228
Figure 5.18	Effect of NO inhibitor L-NMMA on release of nitric oxide in MH-S macrophages following 24 hour stimulation with CpG-sC 10109.	231
Figure 5.19	Effect of L-NMMA NO inhibition on growth of VACV in MH-S cells.	233
Figure 5.20	CpGs prevent apoptosis in both MH-S and J774 macrophages.	234
Figure 5.21	CpG-sC 10109 confers protection against VACV.	236

Chapter 6. Summary Discussion

Figure 6.1	Increased inflammatory responses in the lungs of untreated VACV infected mice.	248
Figure 6.2	Increased inflammatory responses in the spleens of untreated VACV infected mice.	249
Figure 6.3	Immunological impact of CpG-B 7909 in the lung and effect on VACV titres.	252
Figure 6.4	Immunological impact of CpG-B 7909 in the spleen and effect on VACV titres.	254
Figure 6.5	VACV titres in the brains of infected mice treated prophylactically with CpG-B 7909.	255
Figure 6.6	Increased inflammatory responses following administration of CpG-B 7909 post-infection with VACV.	259
Figure 6.7	Timing of CpG delivery influences the immune response during VACV infection.	263

List of Abbreviations

ABI	Applied Biosystems
ADCC	Antibody Dependent Cellular Cytotoxicity
Ag	Antigen
AIDS	Acquired Immunodeficiency Syndrome
AM	Alveolar Macrophage
ANOVA	Analysis of Variants
AP-1	Activator Protein 1
ATF2	Activating Transcription Factor 2
AZT	Azidothymidine
β-ME	β-Mercapto-Ethanol
BAL	Bronchoalveolar Lavage
BCG	Bacille Calmette-Guerin
BD	Becton Dickinson
bp	Binding protein
CBA	Cytometric Bead Array
CBP	CREB-Binding Protein
CCL2	Chemokine Ligand 2
CCR	CC Chemokine Receptor
CD	Cluster of Differentiation
CDC	Centre for Disease Control
cDNA	Complementary DNA
CDV	Cidofovir
CEV	Cell-associated Enveloped Virus

CLR	C-type Lectin Receptor
CMV	Cytomegalovirus
CO_2	Carbon Dioxide
CpG	Cytosine-phosphate-Guanosine
CpG-A	A-class CpG
CpG-B	B-class CpG
CpG-C	C-class CpG
CpG-N	CpG Neutralising
CpG-sC	semi-soft C-class CpG
CREB	cAMP-Response Element Binding Protein
Crm	Cytokine-Response Modifier
CTL	Cytotoxic T-lymphocyte
CTP	Cytosine Triphosphate
DC-SIGN	Dendritic Cell-Specific Intercellular adhesion molecule 3-Grabbing Non-integrin
DMEM	Dulbecco's Modified Eagle's Medium
DNA	Deoxyribose Nucleic Acid
dNTP	deoxy-Nucleotide-Triphosphate
ds	Double Stranded
dTMP	deoxy Thymidine Monophosphate
dTTP	deoxy Thymidine Triphosphate
dUMP	deoxy Uracil Monophosphate
dUrd	deoxy Uridine
EBV	Epstein-Barr virus
ECACC	European Collection of Animal and Cell Cultures

EEV	Extracellular Enveloped Virus
eIF	Eukaryotic protein synthesis Initiation Factor
ELISA	Enzyme-linked Immunosorbent Assay
Fc	Fragment Crystallisable
FCS	Foetal Calf Serum
FLV	Friend Leukaemia Virus
GDP	Guanosine Diphosphate
GM-CSF	Granulocyte-Macrophage Colony-Stimulating Factor
GMP	Guanosine 5'Monophosphate
GTP	Guanosine Triphosphate
HCMV	Human Cytomegalovirus
HDP-CDV	Hexadecyloxypropyl-Cidofovir
HEPES	N-(2-hydroxyethyl)-piperazine-N'-2-ethanesulfonic acid
HIV	Human Immunodeficiency Virus
HRP	Horseradish Peroxidise
HSV	Herpes Simplex Virus
IHD-(J)	International Health Department (strain-J)
i.m.	Intramuscular
i.n.	Intranasal
i.p.	Intraperitoneal
i.t.	Intratracheal
i.v.	Intravascular
ICAM	Intracellular Adhesion Molecule
ICE	IL-1β Converting Enzyme
IEV	Intracellular Enveloped Virus

IFN	Interferon
Ig	Immunoglobulin
IkB	Inhibitor of NF-κB
IKK	Inhibitor of NF-κB Kinase
IL	Interleukin
IL-1RA	Interleukin-1 Receptor Antagonist
IMV	Intracellular Mature Virus
IP-10	IFN-γ inducible Protein 10
IRAK	IL-1 Receptor-Associated Kinase
IRF	Interferon Regulatory Factor
ISG	IFN-Stimulated Genes
ISRE	Interferon Stimulatory Response Element
IV	Immature Virus
IκB	Inhibitor of NF-κB
JAK	Janus Kinase
kb	Kilobase
KSHV	Kaposi's Sarcoma-associated Herpesvirus
L-NMMA	N^G-Methyl'L-arginine Acetate salt
LPS	Lipopolysaccharaide
LRR	Leucine Rich Repeats
LSM	Lymphocyte Separation Medium
LVS	*Francisella tularensis* Live Vaccine Strain
µg	Microgram
µl	Microlitres
µM	Micromolar

MAP	Mitogen-Activated Protein
MCMV	Mouse Cytomegalovirus
MCP	Membrane Cofactor Protein
MCV	Molluscum Contagiosum Virus
MDA	Melanoma-Differentiation-Associated
MGB	Minor Groove Binder
MHC	Major Histocompatability Complex
MIP	Macrophage Inhibitory Protein
MKK	MAP Kinase Kinase
MLD	Mean Lethal Dose
MMTV	Mouse Mammary Tumour Virus
mRNA	messenger Ribose Nucleic Acid
MVA	Modified Vaccinia Ankara,
MyD88	Myeloid Differentiation Factor 88
NED	*N*-1-napthylethylenediamine dihydrochloride
NFQ	Non-Fluorescent Quencher
NF-κB	Nuclear Factor Kappa B
NIH	National Institute of Health
NK cell	Natural Killer Cell
NLR	Nod-Like Receptor
nm	Nanometres
nM	Nanomolar
NO_2^-	Nitrite
NOD	Nucleotide-binding Oligomerisation domain
OAS	Oligoadenylate Synthetase

ODE-CDV	Octadecycloxyethyl-Cidofovir
ODN	Oligodeoxynucleotide
OMP	Orotidine Monophosphate
PAMPs	Pathogen Associated Molecular Patterns
PBMC	Peripheral Blood Mononuclear Cell
PBS	Phosphate Buffered Saline
pDC	Plasmacytoid Dendritic Cell
PE	Phycoerythrin
PKR	Protein Kinase R
PO	Phosphodiester
Poly I:C	Polyinosinic Polycytidylic
PRR	Pattern Recognition Receptor
PS	Phosphorothioate
RANTES	Regulated upon Activation, Normal T-cell Expressed, and Secreted.
RBC	Red Blood Cell
RIG	Retinoic acid Inducible Gene
RK13	Rabbit Kidney 13
RLH	RIG-Like Helicase
RNA	Ribose Nucleic Acid
rpm	revolutions per minute
RPMI	Roswell Park Memorial Institute
RSV	Respiratory Syncytial Virus
RT	Reverse Transcription
RT-PCR	Reverse Transcription Polymerase Chain Reaction

SAH	S-Adenosylhomo-cysteine Hydrolase
SAM	S-Adenosylmethionine
SARS	Severe Acute Respiratory Syndrome
SDS	Sequence Detection System
SPGF	Smallpox Growth factor
SPI	Serine Protease Inhibitor
ss	Single Stranded
STAT	Signal Transducers and Activators of Transcription
TAB	TGFβ-Activated kinase Binding protein
TAK	TGFβ-Activated Kinase
TCAV	Tacaribe Arenavirus
TGFβ	Transforming Growth Factor Beta
Th	T-helper cell
TIR	Toll-Interleukin-1 Receptor
TLR	Toll-Like Receptor
TMB	Tetramethyl-Benzidine
TNF	Tumour-Necrosis Factor
TNFR	Tumour-Necrosis Factor Receptor
TRAF	Tumour-necrosis factor Receptor Associated Factor
TREM	Triggering Receptors Expressed on Myeloid cells
TRIF	Toll/IL-1 Receptor domain-containing adaptor inducing IFN-beta
U	Units
UMP	Uracil Monophosphate
UNG	Uracil-N-glycosylase
VACV	Vaccinia Virus

vCKBPs	Viral Chemokine-Binding Proteins
vCKRs	Viral Chemokine-Receptor homologues
VCP	VACV Complement control Protein
vEGF	Viral Epidermal Growth Factor
VESPR	Virus-Encoded Semaphoring Protein Receptor
v-GAAP	Viral Golgi Anti-Apoptotic Protein
VGF	VACV-induced Growth Factor
vSEMA	Viral Semaphorin Homologue
VSV	Vesicular Stomatitis Virus
vTNFR	Virus TNF Receptor
vVEGF	Viral Vascular Endothelial Growth Factor
WR	Western Reserve
XMP	Xanthine 5'-Monophospahte

Chapter 1: General Introduction

1.1. The innate immune response

The innate immune system of multicellular organisms has evolved into a powerful system for the detection and elimination of infectious organisms. Innate immunity serves as the rapid, front-line of host defence that can be characterised by the initiation of effector mechanisms that interact immediately and directly with invading pathogenic organisms. This response is coupled with the ability to respond unchanged and equally to subsequent infections. This primitive response is a highly conserved ancient system that occurs in a vast range of species from higher order mammals, such as humans, down the phylogenetic tree to insects, metazoans and plants.

The mammalian immune system possesses a two tiered mechanism of protecting the host from infection. The innate system is characterised by the activation and recruitment of phagocytic cells such as macrophages and neutrophils along with the release of immunostimulatory cytokines, chemokines, and polyreactive IgM antibodies which can activate the complement system. In the vast majority of cases, the innate immune response proves too powerful for any invading organism and infection resolves without the development of symptomatic illness. Pathogens that are able to overcome the innate response however are faced by an adaptive immune response that is initiated by cells of the innate response. Innate immune cells such as dendritic cells and macrophages, present antigen and release effector molecules that activate the two key components of the adaptive response, B and T-lymphocytes. This typically leads to production of high affinity IgG antibodies and the generation of cytotoxic T-Lymphocytes (CTLs) through a process of clonal expansion. Ultimately,

the adaptive immune response enables the generation of immunological memory and long lasting protection.

1.1.1. Pattern recognition

Research over recent years has afforded greater insight into the host ability to discriminate between self and non-self. Studies have shown that protection of the host by the innate immune system during the early stages of an infectious challenge in part relies upon its ability to recognise a highly conserved set of molecular motifs expressed by micro-organisms. These patterns have been defined as 'pathogen-associated molecular patterns' (PAMPs) and host organisms have developed a repertoire of germline-encoded receptors throughout evolution known as pattern recognition receptors (PRRs) that are capable of recognising these particular motifs (Medzhitov & Janeway, 1997). PRRs are expressed constitutively by the host and diversity within these PRRs has resulted from the evolution of a number of different families of pattern recognition receptors that fall broadly into one of two categories, namely, those located either on the cell surface or intracellularly (endosomal and cytosolic). The most studied family of receptors are the family of Toll-like receptors (TLRs).

1.1.2. Toll and the Toll-like receptors

TLRs have been widely shown to play a crucial role in initiating the immune response and as such are fundamental to the host's ability to cope successfully with infection. Toll was first identified and characterised through studies using *Drosophila melanogaster*. These studies initially characterised Toll as an essential feature of Drosophila's embryonic development but it was later shown to be crucial in its

antifungal response (*via* activation of the antifungal peptide drosomycin) to *Aspergillus fumigatus* (Lemaitre *et al.*, 1996). Soon after this discovery, a homologous family of receptors was identified in humans and to date 13 TLRs have been described in mammals with each receptor possessing specificity for particular PAMPs. TLRs are predominantly associated with cells that are most likely to be amongst the first to encounter invading organisms such as monocytes/macrophages, neutrophils, dendritic cells and epithelial cells (Table 1.1) (Akira, Uematsu & Takeuchi, 2006; Hornung *et al.,* 2002). Notably, TLR expression is also exhibited by a variety of other non-immune cell-types that are susceptible to infection including adipocytes, vascular endothelial cells and intestinal epithelial cells. This wide degree of cellular expression ensures the innate immune response is able to detect infection rapidly and mount an appropriate and immediate immune response. To fine-tune this innate response further, TLR family members are expressed differentially among immune cells with certain TLRs only being expressed by specific cell types and receptors being positioned either on the cell-surface (TLRs 1, 2, 4, 5, 6 and 11) or intracellularly within endosomal compartments (TLRs 3, 7, 8, and 9). Variation in the location of these receptors allows the host immune system to recognise a range of both intracellular and extracellular pathogens. For instance, TLR4 is expressed at the cell surface and recognises the lipopolysaccharide (LPS) component of extracellular Gram negative bacteria (Beutler, 2000). Conversely, the endosomally located TLR9 has been widely shown to recognise unmethylated cytosine-phosphate-guanosine (CpG) dinucleotides, which are common in the genomes of most bacteria and DNA viruses but not in vertebrate genomes (Bauer *et al.*, 2001). This allows the TLRs to recognise PAMPs from a variety of micro-organisms such as bacteria, viruses, mycobacterium, spirochetes and yeasts.

TLR	Ligands	Distribution	Cellular location
TLR1	Triacyl peptides (bacteria and mycobacteria) ♦associates with and regulates TLR2 response	B-cells*** Monocytes*** NK cells** Neutrophils***	Cell surface
TLR2	Peptidoglycan (Gram$^+$ bacteria) Lipoproteins (bacteria and mycoplasma) Atypical LPS (bacteria) Porins (*Neisseria*) Haemagluttinin protein (measles virus) ♦ associates with either TLR1 or TLR6	Monocytes***** NK cells** B-cells** Neutrophils***	Cell surface
TLR3	dsRNA (Viruses) synthetic Poly (I:C)	NK cells** T-cells** DCs***	Intracellular
TLR4	LPS (Gram$^-$ bacteria) Mannam (*C.albicans*) Viral envelope proteins (RSV, MMTV) Glycoinositolphospholipids (*Trypanosoma*) HSP 60,70, Fibrinogen (Host)	Monocytes **** B-cells* Neutrophils*	Cell surface, CD14-MD2 dependent response
TLR5	Flagellin (bacteria)	Monocytes*** NK cells* Neutrophils*	Cell surface
TLR6	Microbial lipoproteins (bacterial) ♦ associates and regulates TLR2 response	Monocytes*** NK cells* Neutrophils*	Cell surface
TLR7	Synthetic Imidazoquinoline-like molecules ssRNA (virus)	pDC** B-cells** Monocytes* Neutrophils*	Intracellular
TLR8	Synthetic Imidazoquinoline-like molecules ssRNA (virus)	Monocytes** Neutrophils*	Intracellular
TLR9	CpG DNA (bacteria, virus, protozoa)	pDC*** B-cells** Neutrophils*	Intracellular
TLR10	Unknown	B-cells* pDC* Neutrophils*	Cell surface
Mouse TLR11	Uropathogenic bacteria Profilin-like molecule (*Toxoplasma gondii*)	Kidney / Bladder epithelia*** Liver Epithelia*	Cell surface

Table 1.1. The mammalian TLR family: Ligand recognition and cellular distribution of TLRs 1-10 in humans and TLR11 in mice.

** Denotes relative expression of TLR on cellular source*

Review reference (Akira, Uematsu & Takeuchi, 2006; Hornung *et al.*, 2002)

Structurally, the Toll-like receptors possess characteristic external regions that consist of multiple leucine-rich repeats (LRR) that are responsible for ligand-binding and an intracellular, cytoplasmic portion that closely resembles the cytoplasmic portion of the IL-1 receptor family (Medzhitov *et al.*, 1997). Stimulation of TLRs results in the activation of nuclear transcription factors such as NF-κB (Figure 1.1). The nuclear factor-κB (NF-κB)/REL family of transcription factors has been shown to play a central role in coordinating the expression of a wide variety of inflammatory genes (Li & Verma, 2002). Whether located at the cell surface or intracellularly, each TLR possesses a highly conserved intracellular region known as the Toll/IL-1R (TIR) domain that is homologous to both Toll and the IL-1 receptor cytoplasmic regions. The TIR component of the receptor interacts with one of five cytoplasmic adaptor proteins that also contain TIR domains and this interaction has proven crucial for signal transduction following ligand binding (O'Neill & Bowie, 2007). The predominant adaptor protein utilised by the cell is the myeloid differentiation primary response gene 88 (MyD88) (Schnare *et al.*, 2000). With the exception of TLR3, all TLR binding can initiate a common and well characterised signaling cascade that is dependant upon the recruitment of MyD88. This molecule is recruited to the TIR domain, and upon binding, signals through its N-terminal 'death domain' resulting in the immediate recruitment of IL-1 receptor-associated kinases (IRAKs) 1, 2 and 4, depending on the TLR stimulated (Wesche *et al.*, 1997; Keating *et al.*, 2007). Following the phosphorylation of IRAK-2 by IRAK-4, another critically important molecule, the tumour-necrosis factor receptor (TNFR)-associated factor 6 (TRAF6) (Cao *et al.*, 1996), becomes activated by IRAK-2 through ubiquitination (Keating *et al.*, 2007). This crucial step then permits TRAF6 to complex with TAK-1 (TGFβ-activated kinase 1) and TAB (TAK 1 binding proteins) 1 and 2. Together they activate

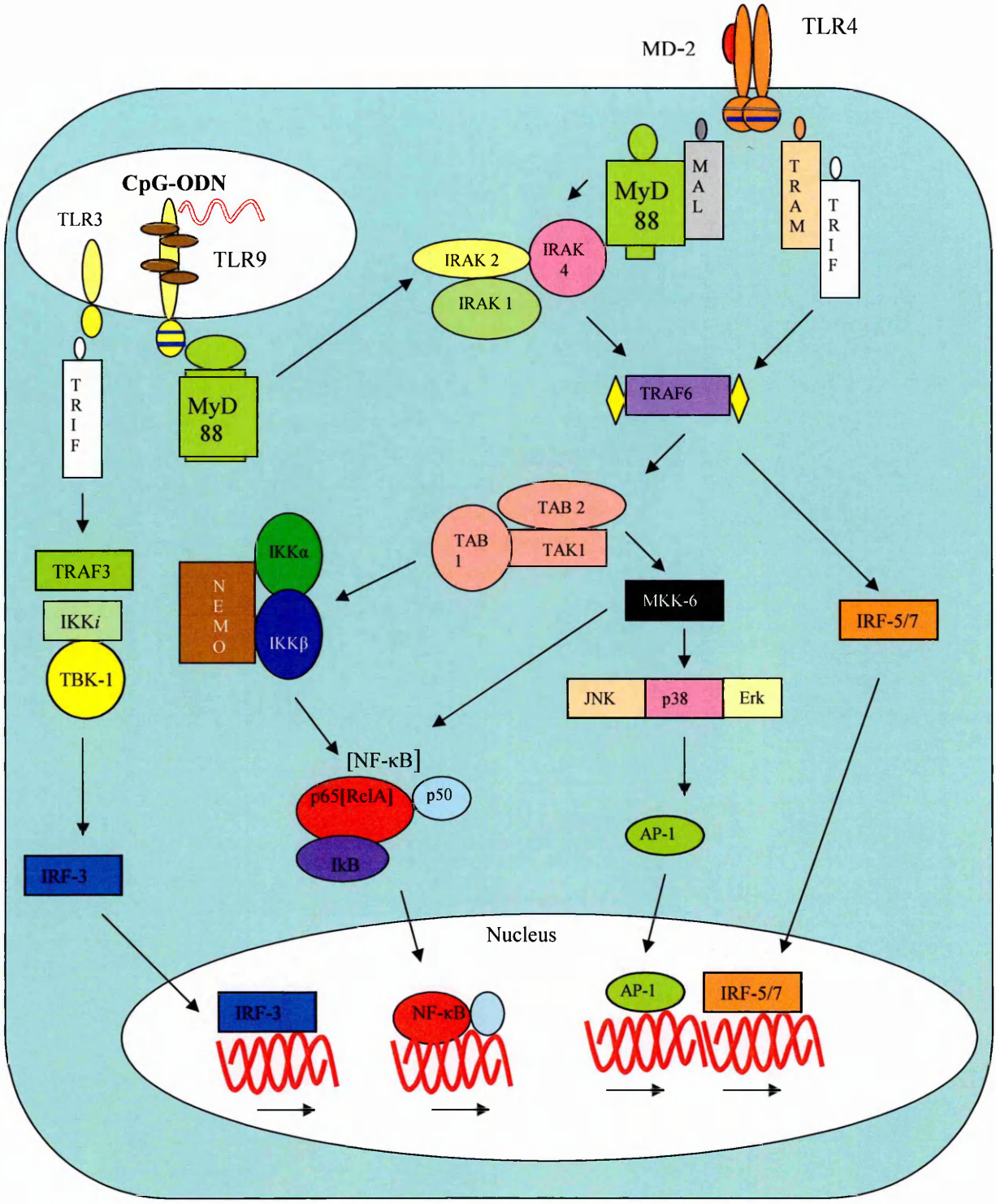

Figure 1.1. TLR pathway and activation.

Binding of ligand to TLRs results in adaptor protein recruitment (MyD88/TRIF/TRAM/MAL) that binds to the cytoplasmic TIR domain of the TLR. CpG-DNA binds to intracellular TLR9 and initiates signal transduction through a MyD88 dependent pathway. Here, signal transduction occurs through IRAK4, IRAK-1/IRAK2, TRAF-6, and the TAB1/TAB2/TAK1 complex. NF-κB activation results from activation of IKK complex (IKKα/IKKβ/NEMO) and freeing of NF-κB from its inhibitor (IκB) for nuclear translocation. The binding of ligands to TLRs can also result in activation of additional transcription factors such as AP-1 *via* JNK, p38, Erk pathways and interferon genes through IRF-5. IRF-3 activation can occur through a MyD88 independent pathway *via* TRIF through TLRs 3 or 4 and IRF-7 can initiate IFN signalling in a pathway specific to pDC and TLR7/9 signaling.

the inhibitor of NF-κB kinase complex (IKK) *via* tyrosine phosphorylation. The phosphorylation of IκB (inhibitor of NF-κB) results in the release of NF-κB allowing it to freely translocate into the nucleus of the cell. Import of NF-κB into the nucleus permits the transcription of hundreds of genes that encode mediators of inflammatory responses (reviewed in; Li & Verma, 2002). These include the synthesis of pro-inflammatory cytokines such as IL-1β, IL-6, IL-18, IL-12 and TNF-α and also the production of anti-inflammatory cytokines and mediators such as IL-10 and IL-1 receptor antagonsist (IL-1RA) to help regulate the inflammatory response. Secretion of chemokines such as IL-8, CCL2, MIP-1α/β, as well as inflammatory prostaglandins, leukotrienes and oxidants are also all under the control of NF-κB. Additional transcription factors are also activated through TLR signaling. For instance, TAK-1 is also able to simultaneously activate two members of the mitogen-activated protein (MAP) kinase kinase family MKK3 and MKK6, which are able to activate c-Jun N-terminal kinases and p38 to activate ATF2-cJun and AP-1 (Sato *et al.*, 2005;Hartmann & Krieg, 2000). IRF-5 is able to translocate into the nucleus of the cell and bind interferon stimulatory response element (ISRE) motifs present in the promoter regions of cytokine genes (Takaoka *et al.*, 2005). A comprehensive review of the signaling pathways specific for individual TLRs is beyond the scope of this thesis but can be found in the following review article (Kawai & Akira, 2007).

1.1.3. Non-TLR PRRs

In addition to the TLR pathway, a number of additional transmembrane receptor families have been shown to possess PRR properties. One such group are the C-type lectin receptors (CLRs), a family with up to 17 subgroups, several of which can bind to PAMPs and also directly to micro-organisms themselves through CLR sugar

moieties (Robinson *et al.*, 2006). CLRs are found on myeloid antigen presenting cells such as dendritic cells, macrophages and B-cells and are postulated to play a number of roles within the response to pathogenic organisms in addition to ensuring immune homeostasis. Well studied receptors within this family include DC-SIGN (dendritic cell-specific intercellular adhesion molecule 3-grabbing non-integrin) that can mediate the phagocytosis of mycobacteria (Neyrolles *et al.*, 2006). Other families include the TREM (triggering receptors expressed on myeloid cells) family of receptors (Klesney-Tait *et al.*, 2006), the siglec molecules (Crocker, 2005), collectins and also the mannose receptors that recognise mannosylated lipoarabinomannans.

Within the last few years our understanding of the molecular mechanism of pathogen recognition has been boosted even further by the discovery of two additional families of intracellular pattern recognition receptors. These comprise the NOD (nucleotide-binding oligomerisation domain)-like receptors (NLRs) and the RIG (retinoic acid inducible gene)-like helicases (RLHs). The NLRs are comprised of two predominant sub-classes, the NODs (NOD1-5) and NALPs (NALP1-14) and recognise unique bacterial components such as peptidoglycan intracellularly (Meylan, Tschopp & Karin, 2006). The RLH receptors are key to the successful initiation of the type I interferon pathways in a TLR independent fashion and are covered in the following section.

1.1.4. Viral defence and PRRs

The structural components of viruses, including viral DNA, single and double stranded RNA and surface glycoproteins, are able to activate the innate immune system. Responses against viral pathogens are dependant upon recognition of viral

PAMPs by pattern recognition receptors and subsequent induction of IFN-stimulated genes (ISGs) and production of antiviral cytokines such as the type I, II and III interferons (e.g. IFN-α/β, IFN-γ and IFN-λ respectively). Type I IFNs, (IFN-α and IFN-β in particular) are the first interferons synthesised following viral detection and can be produced by most cell types once virally infected where they act to confer an antiviral state in uninfected cells (reviewed in; Platanias, 2005). Amplification of these early type I IFNs and subsequent binding to the type I IFN receptor activates the Janus kinase and signal transducers and activators of transcription (JAK-STAT) pathway. Here, STAT1 and STAT2 combine with the IFN regulatory factor 9 to form the IFN-stimulated gene factor 3 complex, which translocates into the nucleus to bind IFN-stimulated response elements (ISRE) present in a variety of genes required for antiviral immunity (Takaoka & Yanai, 2006). This includes the induction of many pro-inflammatory cytokines including the type II interferon, IFN-γ. IFN-γ is specifically produced by activated NK cells and T-cells to perform numerous roles including macrophage activation and promoting the development of $CD4^+$ Th-1 cells and cytotoxic $CD8^+$ cells (Katze *et al.*, 2002; Haller *et al.*, 2006). The type III IFNs are less well defined and their roles in antiviral immunity are gradually being established although research has revealed a potent *in vivo* role for these interferons in a poxvirus infection model (Kotenko *et al.*, 2003; Bartlett *et al.*, 2005). Collectively, the interferon response is vital to the successful defence against viral pathogens, incorporating both arms of the host immune response. This has been shown repeatedly in virally-infected mice with a dysfunctional interferon response, rapidly leading to overwhelming infection and death (Muller *et al.*, 1994).

Control of type I IFN genes is tightly regulated by a number of transcription factors including NF-κB, ATF2-c-Jun, but predominantly by members of the interferon regulatory factor (IRF) family of transcription factors (Honda & Taniguchi, 2006). The intracellular recognition of viral PAMPs has recently been shown to occur *via* a newly identified set of cytosolic PRRs collectively known as the RLHs. These RNA helicases act as sentinels for the detection of viral RNA and consist of 2 family members, these being melanoma-differentiation-associated gene 5 (MDA5) (Andrejeva *et al.*, 2004) and Retinoic-acid-inducible gene-1 (RIG-I) (Yoneyama *et al.*, 2004). RIG-I and MDA-5 are ubiquitously expressed in most tissues and exhibit specificity for distinct sets of RNA viruses (Kato *et al.*, 2006). Both RLHs have been shown to recognise dsRNA, which is generated as an intermediate of viral transcription and recently, the exact ligand for RIG-I has been reported to be 5'-triphosphate groups on RNA (Hornung *et al.*, 2006). The sensing of viral RNA in most cell types typically leads to the serine/threonine phosphorylation of IRF-3 which enables it to homodimerise and translocate into the nucleus where it promotes the initiation of IFN-β mRNA synthesis and activation of other ISGs. Activation of IRF-7 follows shortly after to synergise with IRF-3 in the production of a variety of different IFN-α subtypes (Haller *et al.*, 2006). Additionally, dsRNA is recognised by dsRNA-dependant protein kinase (PKR), which in response to stimulation, inhibits host translation through phosphorylation of the α-subunit of eukaryotic protein synthesis initiation factor 2 (eIF-2α). This inhibition of translation thwarts the virus' ability to utilise host machinery to synthesise proteins critical to its survival (Saunders & Barber, 2003). It is perhaps very likely that additional PRRs exist that recognise dsDNA as type I IFN responses have been demonstrated to occur in response to cytosolic dsDNA that are independent of TLR or RIG-I activation (Ishii *et al.*, 2006).

A potential candidate for this has recently been identified as the DNA-dependent activator of IRFs (DAI) (Takaoka *et al.,* 2007).

1.1.5. TLR recognition of viral PAMPs

Recognition of viral PAMPs by members of the TLR family has also been widely documented with TLRs 2, 3, 4, 7, 8 and 9 being able to recognise viral ligands (Gorden *et al.*, 2006). Deficiencies in the TLR pathway have been shown to result in exacerbated viral infection, as seen in the susceptibility of MyD88 deficient mice to respiratory syncytial virus (RSV) infection (Rudd *et al.*, 2007).

1.1.5.1. TLR2

TLR2 recognises the haemagluttinin protein of wild type measles viruses, and a virion protein of human cytomegalovirus (CMV) (Bieback *et al.*, 2002; Compton *et al.*, 2003). More recently, the secretion of pro-inflammatory cytokines in response to vaccinia virus (VACV) has been suggested to rely on TLR2 activation on dendritic cells (Zhu *et al.*, 2007). In this paper, signaling was thought to initiate via TLR2 interaction with core or envelope proteins given UV-inactivated VACV generated similar levels of cytokine responses. This makes it unlikely that newly-synthesised VACV virions stimulated responses through TLR2 (Zhu *et al.,* 2007).

1.1.5.2. TLR3

TLR3 was the first TLR to be identified with antiviral properties having been widely shown to recognise dsRNA as a by-product of viral replication (Alexopoulou *et al.*, 2001). TLR3 is endosomally located and its activation recruits the adaptor protein TRIF, not MyD88 as typically utilised by all other TLRs. This subsequently results in

activation of NF-κB, the IFN response pathway *via* IRF-3 and the initiation of apoptosis (Figure 1.1) (Schroder & Bowie, 2005). The cellular distribution of TLR3 on NK cells and, in particular, myeloid DCs may also promote cross-priming and generation of virus specific $CD8^+$ T-cells (Datta *et al.*, 2003). Interestingly, TLR3 has recently been suggested to be detrimental following VACV infection (Hutchens *et al.*, 2008). Here, mice deficient in TLR3 had increased survival and reduced disease morbidity, virus dissemination and lung inflammation compared to wildtype mice (Hutchens *et al.*, 2008). This implies that TLR3 interactions with dsRNA from VACV may contribute to the pathogenesis of severe and fatal cases of poxvirus infection.

1.1.5.3. TLR4

TLR4, which is predominantly recognised as the receptor for bacterial LPS, is also able to recognise viral components and initiate a pro-inflammatory response. This has been demonstrated through TLR4 specific recognition of RSV fusion protein F as well as the envelope protein of mouse mammary tumour virus (MMTV) (Rassa *et al.*, 2002; Kurt-Jones *et al.*, 2000). Like TLR3, TLR4 activation can also be mediated *via* the adaptor protein TRIF in a MyD88 independent pathway resulting in the activation of IRF-3 (Wietek *et al.*, 2003).

1.1.5.4. TLRs 7 and 8

One cell type in particular that has proven crucial to the initiation of the interferon response is the plasmacytoid dendritic cell (pDC) (Asselin-Paturel *et al.*, 2001). Activation of pDCs *via* the intracellular TLRs 7, 8 or 9 leads to the recruitment of MyD88, TRAF-6 and IRF-5/7 which in turn leads to the synthesis of multiple type I IFN-α genes and copious release of IFN-α (Kawai *et al.*, 2004; Takaoka *et al.*, 2005).

pDCs are unique in that they constitutively express IRF-7 whereas in other cell types, IRF-7 is generally undetectable in the cells' quiescent or resting state prior to IRF-3 activation. Mouse TLR7 has been found to recognise and respond to ssRNA from numerous viruses including human immunodeficiency virus (HIV), influenza and vesicular stomatitis virus (VSV) whilst TLR8 has also been shown to recognise HIV in humans (Heil *et al.*, 2004; Diebold *et al.*, 2004).

1.1.5.5. TLR9

TLR9 on pDCs can also be activated by the presence of CpG motifs present in the genomes of DNA viruses such as herpes-simplex virus-1 and 2 (HSV-1 and HSV-2) (Krug *et al.*, 2004; Lund *et al.*, 2003) and present in synthetic CpG oligodeoxynucleotides (CpGs). Numerous studies have shown that TLR9 deficiency in mice results in extreme susceptibility to viral infection and an inability to induce necessary antiviral responses (Tabeta *et al.*, 2004). In contrast, mice lacking TLR9 have been shown to mount normal IFN-α responses in response to highly attenuated strains of VACV questioning the importance of TLR9 in iniating responses to VACV infection (Waibeler *et al.,* 2007). The finding that CpG motifs from prokaryotic DNA can stimulate the immune system and the subsequent development of CpGs has stimulated extensive research into the potential therapeutic uses of these synthetic compounds. Over the last decade they have been used as vaccine adjuvants, in cancer and allergy treatments and as protective agents in their own right.

1.2. Immunostimulatory properties of CpG motifs

1.2.1. The identification of CpG motifs

Evidence for bacterial preparations being able to confer a therapeutic effect to cancer patients was reported as far back as 1893 by Coley (Coley, 1893) following successful treatment of sarcomas. However, the effects of bacterial DNA specifically were questioned and generally considered to be immunologically inert. The concept of DNA acting purely as a genetic code was first questioned in studies dating back to 1963 where DNA from viruses was reported to induce the production of interferon (Rotem *et al.*, 1963). It was not until 1984, when bacterial DNA was first reported to confer a therapeutic effect against tumours (Tokunaga *et al.*, 1984), that the field of CpG research began to take shape.

In a series of pioneering studies where the anti-tumour effect of DNA from *Mycobacterium bovis* bacille Calmette-Guerin (BCG) was analysed, it was shown that a purified fraction of BCG DNA (designated MY-1), was able to activate natural killer cells (NK cells) and B-cells and to initiate the production of type I and type II interferons (Yamamoto *et al.*, 1992b; Messina *et al.*, 1991). Significantly, these results could not be reproduced using vertebrate DNA and were abolished by pre-treatment of the MY-1 fraction with DNase. Yamamoto *et al* showed that it was possible to recreate the stimulatory effects of bacterial DNA using synthetic oligodeoxynucleotides (ODN) containing unique self-complementary palindromic sequences (Yamamoto *et al.*, 1992a). Closer examination of these hexameric stimulatory palindromes revealed one common feature, namely the presence of a central cytosine and guanosine dinucleotide motif and two flanking base pairs. Analysis of bacterial and vertebrate DNA revealed that bacterial DNA seemed to

feature far more of these active palindromes than vertebrate DNA did, although at the time the flanking sequences of the CpG motif were not thought to be so critical. Methylation of CpGs was also not originally thought to have a deleterious effect on the stimulatory ability of DNA (Kuramoto *et al.*, 1992). This was contradicted by results published by Pisetsky and colleagues who demonstrated that methylation of poly-(dC,dG) was sufficient to abolish its stimulatory effects (Messina *et al.*, 1993).

A number of these concepts were later revised in a seminal paper by Krieg and colleagues in experiments where massive stimulation of B-cells using particular ODNs was demonstrated (Krieg *et al.*, 1995). It was shown that the stimulatory effect of CpG ODNs could be eliminated if the cytosine base of the CpG motif was substituted for a 5-methyl cytosine. Conversely, methylation of any other cytosine bases, not part of the CpG dinucleotide, was shown to have no effect on the immunostimulatory capacity. This work also highlighted that the stimulatory strength of ODNs featuring the CpG motif lay primarily in the context of bases immediately adjacent to the CpG dinucleotide and did not require the motif to be in a palindromic sequence. Altering the positions of the CpG motif could also be shown to reduce the degree of immune stimulation. This allowed the identification of a sequence motif that afforded optimal stimulation and helped define the characteristics of oligonucleotides that would prove most stimulatory. In a mouse model, it was recognised that oligonucleotides with a CpG dinucleotide flanked by two 5' purines and two 3' pyrimidines (5'-Pu-Pu-CpG-Pyr-Pyr-3') proved most stimulatory (Ballas *et al.*, 1996). Ideally, these motifs were preceded on the 5′ side by an ApA, GpA, or GpT and followed with a TpT. Soon after came the discovery that CpG dinucleotides sandwiched between cytosine and guanosine bases in the sequence CCGG were

practically inert (Krieg *et al.*, 1998). These CCGG motifs were identified as being able to specifically neutralise the immunostimulatory effects of stimulatory CpG motifs and were coined CpG-N motifs. The significance of these findings helped shape the idea that the mammalian immune system might be able to use differences between bacterial and its own DNA to initiate a response to infection.

1.2.2. Differences between bacterial and vertebrate DNA

There are a number of key differences between bacterial DNA and vertebrate DNA (Stacey *et al.*, 2003). Firstly, CpG dinucleotide motifs in bacterial DNA are present at the level expected given random base utilisation (estimated as 1 per 16 bases). In contrast, vertebrate DNA features only a quarter of this CpG content, suggesting a high degree of CpG suppression (Bird, 1987). Secondly, cytosine methylation in vertebrate CpG motifs (approximately 70%) differs substantially from bacterial DNA, where the vast majority of CpG motifs are unmethylated (Razin & Friedman, 1981). Thirdly, CpG dinucleotide motifs in vertebrate DNA are typically flanked by the immune-neutralising sequences described by Krieg (Krieg *et al.*, 1998). Genomic sequence analysis of the human genome also revealed the suppression of those CpG motifs that have proven to be most stimulatory (e.g GACGTT). Finally, mammalian DNA is capped with specialised DNA-protein structures called telomeres that are rich in hexameric TTAGGG motifs. These motifs are rare in bacteria, and have proven to be highly immunosuppressive through down-regulation of IL-12 and IFN-γ production (Gursel *et al.*, 2003; Shirota *et al.*, 2004). These TTAGGG motifs have emerged as potential therapeutic agents in their own right (Klinman *et al.*, 2005).

The combination of these factors has led to the hypothesis that the presence of bacterial DNA or mimicking synthetic ODNs can be detected by cells of the innate immune system and can initiate a rapid immune response. Recent years have seen a prolific advance in our understanding of how CpG motifs are recognised by cells of the immune system and the signaling cascade that results in immune cell activation. Advances in our understanding of ODN chemistry have facilitated the development of a variety of structurally different CpG ODNs that can differentially activate particular cells of the immune system.

1.2.3. Species differentiation and other organisms

Bacterial DNA itself has been shown to vary in its stimulatory capacity, with DNA from different species of bacteria resulting in differing levels of immune activation. DNA from *Escherischia coli* is highly effective at stimulating immune cell activity, whilst DNA from *Clostridium perfringens* induces a weak immune response (Neujahr *et al.*, 1999). This variation may be due to differences in the quantity and quality of internal stimulatory CpG motifs, along with the presence of immune neutralising motifs.

Although the vast majority of work related to CpG stimulation originates from the immunostimulatory properties of bacterial DNA, it is of note that other organisms possess DNA that also proves to be stimulatory. Much work has focused on the genomes of viruses and the notable degree of variation in their CpG content (Karlin *et al.*, 1994). It is has been demonstrated that nearly all pathogenic vertebrate viruses exhibit a high degree of CpG suppression. This is believed to be part of an evolutionary defence mechanism to limit the host's response to infection. Viruses that

exhibit the smallest degree of CpG content are most able to establish long-lasting infections such as HIV, where only one fifth of the expected numbers of CpG motifs are present (Karlin *et al.*, 1994). In addition, both adenovirus type 2 and 5 have about 5-fold higher concentration of CpG-N motifs to help further suppress the host response and limit inflammation (Krieg *et al.*, 1998).

Drosophila extracts have been shown to have stimulatory properties along with DNA from nematodes and this is a result of the high degree of unmethylated CpG motifs present in the genome (Sun *et al.*, 1996; Sun *et al.*, 1997). Studies have demonstrated that the optimal CpG motif in human responses is the hexameric GTCGTT motif (Hartmann & Krieg, 2000) and a wide variety of other vertebrate species has also been investigated for their responsiveness to CpGs. Cows, sheep, goats, pigs, as well as cats and dogs have all been shown to respond to the GTCGTT motif that optimally stimulates human immune cells, suggesting a high degree of evolutionary conservation (Rankin *et al.*, 2001). However, not all vertebrates share this preference for the GTCGTT motif as the study by Rankin *et al.*, 2001, revealed that inbred strains of mice and rabbits responded best to the motif GACGTT. Studies have revealed that the amino acid sequence for the human TLR9 receptor differs by 24% from the mouse TLR9 amino acid sequence, and this may explain the difference in CpG motif preference between the two species (Hemmi *et al.*, 2000).

It is known that the cells of the immune system that express TLR9 differ between different species as well. In humans, it has been suggested that B-cells and pDCs are the only cell types to express TLR9 (Hornung *et al.*, 2002) (Figure 1.2) although other research has recently suggested TLR9 expression may also be functional in human

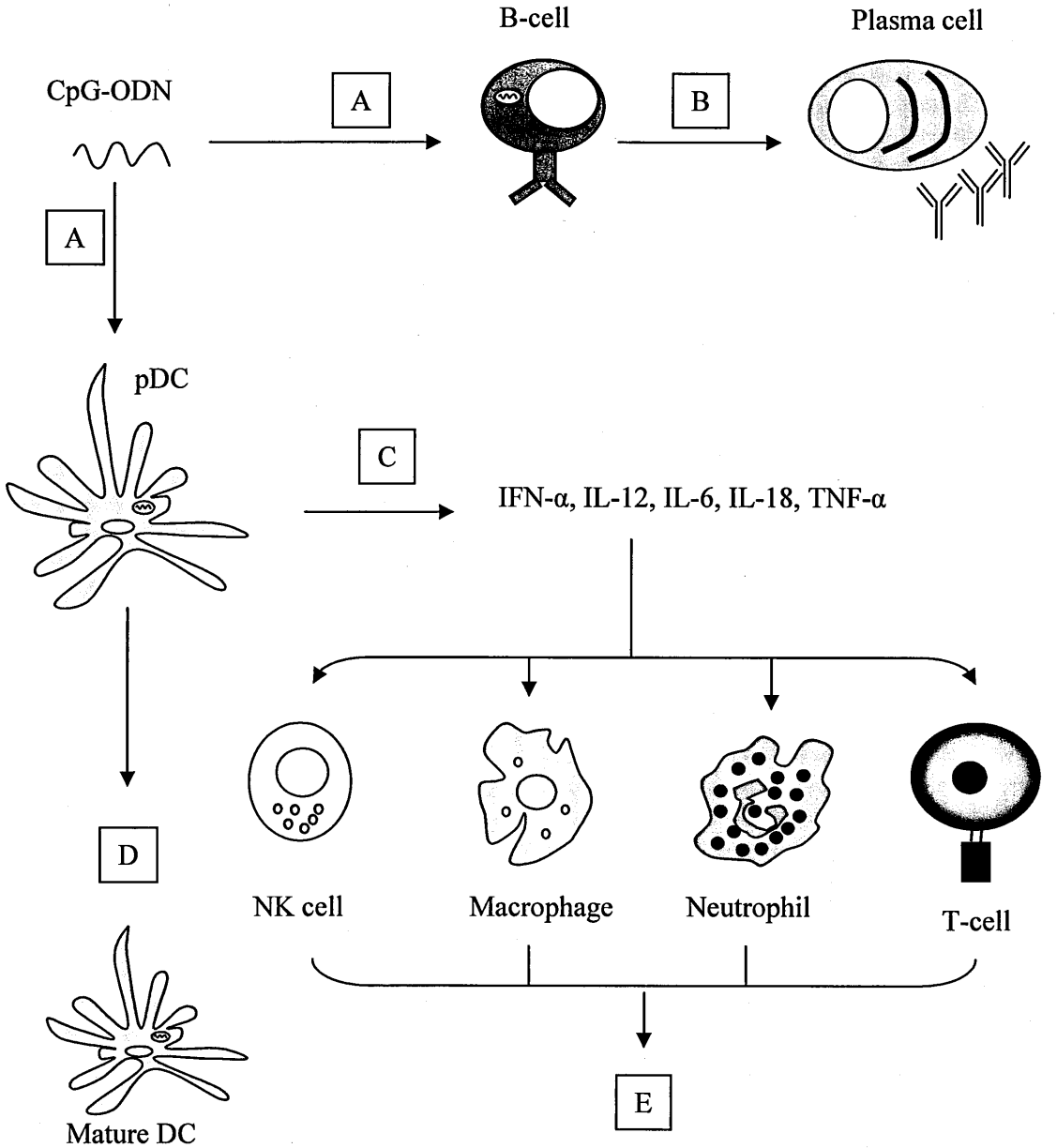

Figure 1.2. Human CpG activation and immunity.

CpG-ODN or bacterial DNA is recognised by endosomally located TLR9 on pDCs or B-cells (**A**). Activation of B-cells results in cytokine release and B-cell proliferation and differentiation into antibody secreting plasma cells (**B**). Binding of CpG to plasmacytoid dendritic cells (pDCs) results in pro-inflammatory cytokine release (**C**) prompting dendritic cell activation and maturation (**D**). This is coupled with the activation of additional immune cell types including NK cells, macrophages, neutrophils and T-cells and subsequent release of cytokines and pro-inflammatory mediators (**E**).

neutrophils (Hayashi *et al.*, 2003) and pulmonary epithelial cells (Platz *et al.*, 2004). Despite the uncertainty surrounding the exact cell types responding to CpGs directly through TLR9 activation in humans, it is clear that pDCs and B-cells are also key TLR9 expressing cells in mice. Here, immune cells of the myeloid lineage such as monocytes, macrophages and myeloid dendritic cells have also been shown to respond directly to stimulation with CpGs (Iwasaki & Medzhitov, 2004). It is also clear that in order to stimulate TLR9, DNA needs to enter the cell and associate with TLR9 in endosomal compartments. This occurs once TLR9 relocates from the endoplasmic reticulum to lysosomes containing CpG-DNA where the signaling cascade is initiated following TLR9 receptor dimerisation (Latz *et al.*, 2004; Latz *et al.*, 2007). This signaling cascade is dependent upon MyD88 and results in the activation of transcription factors such as NF-κB and AP-1 and subsequent induction of inflammatory gene mRNA synthesis (Kumagai, Takeuchi & Akira, 2008). This process can be inhibited by the addition of lysosomal inhibitors such as chloroquine and bafilomycin, which prevent endosomal maturation and subsequent CpG-TLR9 binding and signal transduction (Hacker *et al.*, 1998). More recently, a TLR9 independent cytosolic pathway of DNA recognition has also been suggested by Nagata and colleagues (Okabe *et al.*, 2005) in which binding of DNA that has escaped lysosomal degradation is reported to induce activation of the innate immune system.

1.2.4. The significance of backbone chemistry

Studies have shown that the backbone of synthetic DNA can alter its stimulatory abilities (Sester *et al.*, 2000). CpG constructs created using a modified nuclease-resistant backbone, such as a phosphorothioate (PS) backbone, confer far greater resistance against degradation and protection from cell nucleases than non-modified

phosphodiester (PO) backbones (Zhao *et al.*, 1993; Stein *et al.*, 1988). The PS backbone also enhances the ability of ODNs to bind to cell membranes and consequently results in more successful cellular uptake. The effect of these backbone modifications varies depending on the cell type taking up the oligonucleotides in question. CpGs constructed with a PS backbone are far more potent at activating B-cells than the same sequence CpG motif constructed with a PO backbone (Krieg *et al.*, 1996). In contrast, ODNs on a pure PS backbone are not as potent at activating macrophages and NK cells as ODNs with mixed PS and PO content (Boggs *et al.*, 1997). The chemical composition of CpGs has helped in the development of a variety of different classes of CpGs that preferentially activate particular cells of the immune system.

1.2.5. Different classes of CpGs

There are currently three main classes of synthetic CpG typically varying between 8-30 bases in length. Many factors have contributed to the development of these different CpG classes. These include the number and spacing of CpG motifs (2-4 motifs being optimal), the sequence specificity and the presence of either poly G regions or other stimulatory sequences at the terminal ends of the oligonucleotide. In addition, another important aspect is the oligonucleotide backbone chemistry. Native DNA possesses a phosphodiester backbone and CpGs are often totally or partially modified to a nuclease-resistant phosphorothioate backbone which serves to prolong the *in vivo* half-life and immunostimulatory power of the ODN. These classes result in different patterns of immune activation.

1.2.5.1. CpG-A / D-type

CpG-A ODNs (sometimes referred to as "D-type" CpGs), are constructed using a mixed phosphodiester and phosphorothioate backbone and are potent induces of IFN-α production from plasmacytoid dendritic cells (Krug *et al.*, 2001). This activation also directly induces pDC maturation and strongly activates NK cells indirectly (Ballas *et al.*, 1996). These A-class CpGs are able to induce a far more potent IFN-α response than that resulting from actual bacterial DNA and are comparable to bacterial DNA in their NK stimulatory capacity. However, although able to bind TLR9 on B-cells, they promote a poor response as measured by the degree of proliferation and maturation (Verthelyi *et al.*, 2001).

CpG-A typically contain either a single hexameric purine-pyrimidine-CG-purine-pyrimidine motif (Verthelyi *et al.*, 2001) or multiple CpG motifs that are flanked by self-complementary bases that are palindromic (Krug *et al.*, 2001). These self-complementary bases have the potential to form a stem-loop structure and two-dimensional computer analysis suggests that this may expose the CpG at the apex. The central CpG motifs and vast majority of the A-class ODN is built with a PO backbone; however, the ends of the ODN are modified to feature 5' and 3' PS ends. The modified PS ends are also typically complemented with poly-G motifs that are able to interact with those on adjacent ODNs to form G-tetrads (Kerkmann *et al.*, 2005). It has been suggested that these motifs act to improve cellular uptake, NK cell activation and IFN-α production by pDCs.

Example type: CpG 2336 (Coley, Ca)

G*G*G GACGACGTCGTGG*G*G*G*G*G

** denotes phosphorothioate bonds, all others bonds are phosphodiester.*

1.2.5.2. CpG-B / K-type

CpG-B ODNs differ in many ways from their CpG-A relatives. The most basic of these differences stems from the fact that CpG-B ODNs are constructed using only a PS backbone, making them incredibly resistant to degradation. CpG-B motifs encode multiple CpG motifs that are optimal when flanked by a thymidine immediately 5' and either a TpA or TpT on the 3' side. From an immunological perspective, these factors combine to promote an extremely potent stimulation of B-cells, as determined by enhanced cellular proliferation, increased expression of co-stimulation markers and IgM antibody and IL-6 cytokine production (Verthelyi *et al.*, 2001; Yi *et al.*, 1996a). However, in contrast to CpG-A, CpG-B are only able to induce a limited stimulatory effect on pDCs and NK cells, resulting in limited production of IFN-α and IFN-γ (Verthelyi *et al.*, 2001). Finally, B-class ODNs do not feature the self-complementary CpG-flanking regions that are typical of CpG-A ODNs and as such do not typically form higher-ordered structures. Reports have shown that forcing B-class motifs into a higher ordered structure on microparticles and other such delivery systems will promote a more typical A-class response as determined by enhanced IFN-α production (Kerkmann *et al.*, 2005).

Example type: CpG-B 7909 (Coley, Ca) (Commercial No: PF-3512676)

TCGTCGTTTTGTCGTTTTGTCGTT

1.2.5.3. CpG-C / C-type

The C-class of CpGs are a mixture of the A and B classes and are designed to have immunostimulatory properties of both these types of CpG (Hartmann *et al.*, 2003). They are constructed using only a phosphorothioate backbone (like CpG-B) and also commonly feature multiple CpG motifs. In addition, whilst internal CpG motifs may be similar to those often seen in CpG-B class ODNs (e.g. TCG dimer at the 5' end), they are also sometimes peripheral to a central CpG motif embedded within a palindromic sequence characteristically seen in CpG-A ODNs (e.g. GTCGTT) (Hartmann *et al.*, 2003). They are also constructed without poly-G motifs, which are typical of A-class CpG ODNs, but do possess palindromic 3'ends which promote the formation of duplexes that are essential for IFN-α production (Vollmer *et al.*, 2004). These factors combine to create a class of CpGs that are capable of strongly stimulating B-cells to secrete IL-6 and to express co-stimulatory molecules, whilst also activating pDCs and NK cells resulting in IFN-α and IFN-γ release (Marshall *et al.*, 2003).

Example type: CpG 2395 (Coley, Ca)

5'- TCGTCGTTTTCGGCGCGCGCCG – 3'

3'-GCCGCGCGCGGGTTTTGCTGCT-5'

1.2.5.4. CpG-sC / Semi-soft C-type

Recently, a modified C-type CpG has been designed. This CpG bares close resemblance to the characteristics of the C-type oligonucleotide described above (section 1.2.5.3), but differs primarily in the chemical composition of its oligonucleotide backbone. Here, the PS backbone present in the C-type CpGs has

been part replaced with phosphodiester bonds between the CG dinucleotide motifs to form a mixed PS-PO backbone. This modification increases the ODN's susceptibility to nuclease degradation and consequently, this new type of CpG is currently being referred to as a softer version of the C-class ODN or a semi-soft C-class. Recently, the use of CpG-sC 10109 as an adjuvant in anthrax studies has been investigated and reported to significantly boost the immunogenicity of the BioThrax® vaccine (Gu *et al.,* 2007). No reports of the stimulatory effects of CpG-sC on individual cell-types have currently been published.

Example type: CpG 10109 (Coley, Ca)

TCGTC*G TTTTAC*GGCGCC*GTG CCG

** denotes phosphodiester bonds, all others bonds are phosphorothioate.*

1.2.6. Immune consequences of CpG-TLR9 recognition

Stimulation of TLR9 by CpGs results in two separate types of immune response, these being a rapid activation of innate cells and a subsequent enhancement of the antigen-specific immune response (reviewed in; Krieg, 2002). Direct stimulation of cells expressing TLR9 results in rapid release of pro-inflammatory cytokines such as IFN-α, IL-12, IL-18, IL-6 and TNF-α, along with secretion of chemokines such as IL-8, IFN-γ inducible protein 10 (IP-10) and CCL2 (Krieg *et al.*, 1995; Yi *et al.*, 1996b; Krug *et al.*, 2001; Klinman *et al.*, 1996). This is accompanied by an increase in expression of both MHC and co-stimulatory molecules such as CD40, CD80 and CD86 on antigen presenting cells, as well as cellular maturation to boost the host's ability to present antigen to T-cells (Krieg *et al.*, 1995). This is aided by the up-regulation of the chemokine receptor CCR7 on these cell types, which directs cellular

traffic to the T-cell zones of the lymph nodes. The direct stimulation of TLR9 on both naïve and memory B-cells functions synergistically with the B-cell receptor to facilitate their rapid proliferation and differentiation into antibody secreting plasma cells (Jung *et al.*, 2002). Additionally, Fcγ receptors can be upregulated on B-cells and polymorphonuclear leukocytes such as neutrophils, to enhance levels of antibody dependent cellular cytotoxicity (ADCC) (Krieg, 2002). The direct, or indirect, activation of neutrophils (Weighardt *et al.*, 2000) and macrophages by CpGs also increases cellular migration along chemotactic gradients, and enhances phagocytosis and respiratory burst defences (Gao *et al.*, 2002). NK cells are also rapidly activated following CpG stimulation, demonstrating enhanced responsiveness to IL-12 (Sivori *et al.*, 2006) and pDC derived IFN-α and TNF-α resulting in IFN-γ release and increased cytotoxicity (Marshall *et al.*, 2006). Together, these cell types promote the formation of a highly skewed Th-1 cytokine milieu, which consequently affects the development of Th-0 $CD4^+$ cells and drives them to adopt a Th-1 phenotype (Klinman *et al.*, 1996). CpGs can also augment the function of antigen-specific $CD8^+$ T-cells and enhance their survival (Beloeil *et al.*, 2003).

1.2.7. Therapeutic applications of CpGs

1.2.7.1. Use of CpGs in allergy, cancer and as vaccine adjuvants

The immunostimulatory properties of CpGs have led to their use in a variety of different therapeutic applications. Over the last decade, they have been investigated as adjuvants to pre-existing or newly developing vaccines, as cancer and allergy treatments and as therapeutic agents against disease (reviewed in; Krieg, 2006). Most of these studies have occurred in mice, although currently six CpGs are in human clinical trials. These human trials are examining the therapeutic effect of CpGs as

vaccine adjuvants for influenza (Cooper *et al.*, 2004), anthrax (Klinman, 2006) and hepatitis B (Halperin *et al.*, 2003), as cancer therapies for non-Hodgkins lymphoma (Link *et al.*, 2006) and metastatic melanoma (Speiser *et al.*, 2005) and as direct treatment against hepatitis C (McHutchison *et al.*, 2006) and asthma (Racila & Kline, 2005).

The potent adjuvant effects of CpGs are presumed to be a result of the Th-1 cytokine phenotype that they promote and as such they are currently surpassing any other commonly used adjuvant system such as alhydrogel/alum salts, which typically generate a Th-2 milieu. The induction of a Th-1 cytokine environment by CpG greatly enhances the function of APCs, T-cells and B-cells, as well as inducing IgG class switching (He *et al.*, 2004; Sparwasser *et al.*, 2000; Jegerlehner *et al.*, 2007). Ultimately the CpG adjuvant effect could permit the reduction in number of vaccinations required and therefore the amount of antigen and costs required to reach vaccine efficacy. In addition, they may also improve the vaccine's long-term protective activity by encouraging sustained antibody levels (Krieg, 2006). The success of CpGs against allergic responses is likely to stem from the Th-1 type cytokine patterns produced following CpG administration. This Th-1 induction counteracts the negative effects of Th-2 dominated allergic responses (Lin *et al.*, 2004; Kline *et al.*, 1998; Kitagaki *et al.*, 2002). The mode of action for this effect may however be more complicated than a simple switch in cytokine production and has been suggested to also induce T-regulatory cells (Jain *et al.*, 2002). As a cancer therapy, CpGs have been well documented to have anti-tumour activity (Krieg, 2007). Within this field, use of CpGs as a monotherapy have yielded some success against small tumours, but CpGs have needed to be combined with other effective anti-

tumour approaches to be effective against larger tumours. Here, it is suggested that T-cells play an important role in tumour rejection, having been primed by TLR9 activated pDCs to develop into tumour-specific effector $CD8^+$ cells instead of maintaining tolerance (Krieg, 2006). The use of CpGs in this capacity is leading the way to becoming the first fully licensed therapeutic CpG.

1.2.7.2. The use of CpGs against infectious disease

Studies have shown that administration of CpGs can offer protection against a wide variety of bacterial, viral and parasitic infections (Krieg, 2006). In total, these experiments have all shown a variety of direct and indirect CpG mediated effects that have typically included the release of Th-1 associated cytokines such as IL-12, IL-6 and IFN-γ as well as the activation of numerous cell-types including macrophages, dendritic cells and NK cells, as well as B and T-lymphocytes. The exact protective effects of CpG treatment are likely to vary between different micro-organisms (with certain infections responding better to different classes of CpG), according to the nature of the infection and activation of those cell types most crucial to fighting it. With this in mind, in order for any CpG to be utilised as an effective and licensed therapeutic, it is fundamental that the relationship between the CpG and organism is well understood. This thesis will address whether CpGs could be used in a protective capacity against smallpox, the disease caused by infection with variola virus, using its close relative VACV as a model for infection. The next section will introduce the disease process of smallpox and provide an introduction to VACV as the laboratory virus model used throughout this project.

1.3. Smallpox and pathogenesis

Following a worldwide vaccination campaign, the late 1970s provided the world's first success at defeating a global disease when smallpox was eradicated. The etiological agent of smallpox, variola virus, proved the most formidable pathogen of the modern age killing more people throughout recorded history than all other infectious diseases combined (Fenner *et al.*, 1998). The vast majority of these deaths resulted from infection with a particularly pathogenic strain of variola known as variola major, which proved fatal in between 5-40% of those infected. A second, less virulent strain, known as variola minor, also presented but resulted in mortality in fewer than 1% of patients. Both strains of virus exhibited an extremely narrow host range with humans being the only known host for infection and person to person spread being a well-documented phenomenon. Clinically, infection with variola typically occurred *via* the aerosol route, allowing the virus to infect the mucosal tissue of the airways and migrate into the lymphatic system and local lymph nodes (Stanford *et al.*, 2007). After a period of multiplication in the lymph nodes, the host typically developed an asymptomatic primary vireamia by the fourth day that allowed the virus to spread to other parts of the body and induce a secondary vireamia typically around four days later. This asymptomatic phase was known to last up to 17 days prior to the onset of clinical symptoms such as fever and malaise and the explosion of the characteristic macropapular rash on the mucosa of the mouth, pharynx and face. This rash then continued to spread systemically and often managed to quilt the entire body of the infected patient 10 days after symptom onset, at which point the rash became pustular. Death of the patient was often attributed to the toxaemia associated with the infection and massive inflammatory responses but could also result from haemorrhagic and malignant forms of variola infection. (Fenner *et al.*, 1998). The

vaccination campaign centred on the use of VACV, a close relative of variola, as a live vaccine. Today, complications with the smallpox vaccine, that are unacceptable by modern standards, and fears over the deliberate release of variola on a new generation of unvaccinated individuals have led to an increased effort to design an effective new approach to combating infection. Given the exquisite host specificity of variola for humans, research into the pathogenesis of disease using variola virus has not been possible. Consequently, research has focused on animal models using highly related orthopoxviruses to expand on the limited amount currently known of the disease processes associated with smallpox.

1.3.1. Animal models

A variety of animal models have been well established to study orthopoxvirus infection. These include studies using poxviruses such as ectromelia and VACV in mice, monkeypox in primates and myxoma virus in rabbits (Smith & Kotwal, 2002). The use of these viruses in animal models is somewhat limited by the specificity of these viruses for certain hosts. For instance, ectromelia is a natural mouse pathogen that can not infect primates whereas VACV can infect a broad range of species (Stanford *et al.,* 2007). In mouse models, both ectromelia and VACV have proven excellent animal models in a vast array of studies (Smith & Kotwal, 2002). Ectromelia infection in mice typically follows inoculation of the virus into the footpad of the mouse resulting in an acute infection (mousepox) that mimics variola infection in humans (Chaudhri *et al.,* 2006). However, the specificity of ectromelia for mice makes studies investigating the efficacy of drug treatments impossible to transfer into higher order animals such as primates. This limits the use of ectromelia virus as a model for othropoxvirus infection. In contrast, intranasal infection of mice with

VACV also results in an acute infection that can be compared with existing information from human infections (Xu *et al.,* 2004). This makes the use of VACV the most useful orthopoxvirus in studies looking to assess the efficacy of particular antiviral treatments and the virus of choice to use in studies throughout this thesis.

1.3.2. Vaccinia virus

Vaccinia virus, like variola, is an orthopoxvirus and member of the family *poxviridae*, a complex family of large brick-shaped DNA viruses that replicate in the cytoplasm of host cells. VACV possesses a large linear double-stranded genome of approximately 200kb and a variety of different strains of vaccinia have been characterised to date including Copenhagen (Goebel *et al.*, 1990), modified vaccinia Ankara (MVA) (Antoine *et al.*, 1998), western reserve (WR), lister (Garcel *et al.*, 2007) and International health department (IHD). These strains all have a highly conserved central region of approximately 100kb that contains the majority of the essential genes needed for replication. Within this region, 90 genes are conserved amongst all poxviruses (Upton *et al.*, 2003), which helps explain the morphological and functional similarities amongst family members. Away from this central region non-essential genes, or those not critical for ensuring competent replication, are found. These genes encode various proteins responsible for virus virulence and host range tropism and are not as conserved as the central region. Instead, this section contains a number of deletions, mutations and transpositions and these differences contribute to the unique characteristics of each poxvirus in terms of host range, pathogenesis and immunomodulatory capacity. Unlike other poxviruses that are restricted in their host range (e.g. camelpox, variola), vaccinia is able to infect a wide

range of hosts, including humans and its large number of genes enables it to replicate in the majority of mammalian cells.

1.3.2.1. Vaccinia virus life cycle

Replication of VACV takes place in the cytoplasm of the host cell and occurs almost entirely independently of the cell nucleus (Figure 1.3). The infection process begins with the attachment of VACV virions to the surface of the targeted cell. Both the attachment and entry processes of VACV into the cell are poorly understood and both processes are complicated as a result of two infectious forms of VACV virion being produced. These virions take the form of the intracellular mature virus (IMV) and the extracellular enveloped virus (EEV) and are structurally and antigenically different from one another (Boulter & Appleyard, 1973). Currently, evidence suggests that IMV particles possess a single lipid bilayer that is embedded with non-glycosylated viral proteins, although a two-membrane model has also been proposed (Moss, 2006). Regardless of whether IMVs possess one or two membranes, EEV particles are known to possess one extra. Consequently the entry processes of IMV and EEV virions into the cell are thought to differ as well. A number of virion proteins have been suggested to help facilitate attachment of VACV to the cell, since no specific cellular receptor for vaccinia has been clearly identified to date. This research is further advanced for IMV with virion proteins H3L (Lin *et al.*, 2000), A27L (Chung *et al.*, 1998) and D8L (Hsiao *et al.*, 1999) all presumed to play a part. EEV virions possess at least five virus-encoded surface proteins in their outer membrane including A33R, A34R, A56R, B5R and F13L but evidence for a direct role of any of these proteins in cellular attachment has not being convincingly presented. The IMV receptors are all thought to interact with cell glycosaminoglycans such as heparan or

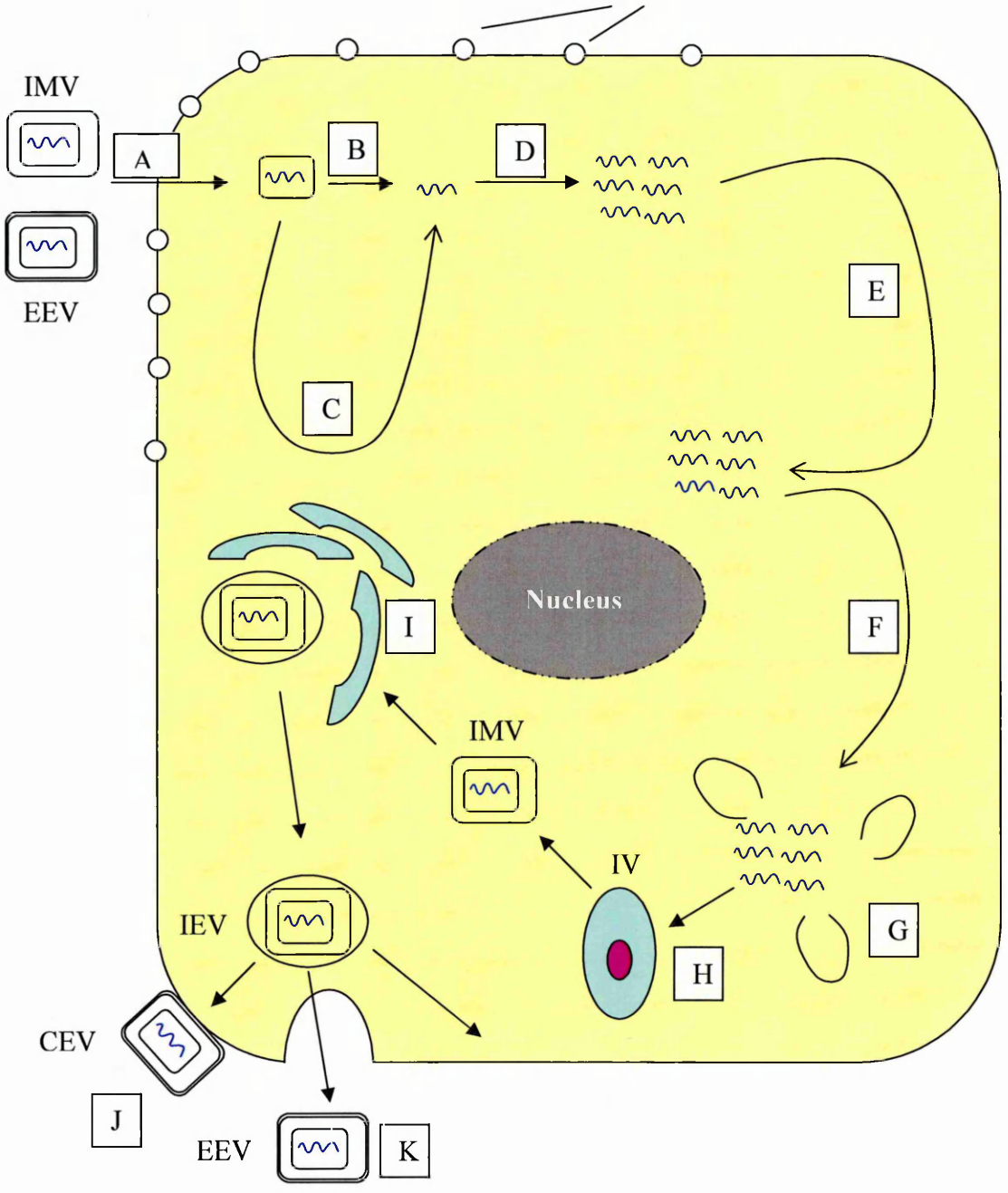

Figure 1.3. Vaccinia virus life-cycle.

Intracellular mature virus (IMV) or Extracellular enveloped virus (EEV) particles enter the cell *via* an ill-defined process (most likely fusion) that may involve glycosaminoglycans (**A**). Once inside, the virus core uncoats to release viral DNA (**B**). This is then followed by the transcription and translation of early viral genes (**C**), viral DNA replication (**D**) and finally intermediate (**E**) and late (**F**) gene processing. New particles begin to form in crescent shapes (**G**) before morphing into a non-infectious immature virus (IV) (**H**) and then intracellular mature virus particles (IMV). IMVs then acquire additional membranes *via* the golgi apparatus or early endosomes (**I**) to become intracellular enveloped virus particles (IEV). IEV fuses to the cell surface to become cell-associated virus (CEV) (**J**) or gets released from the cell as a free EEV particle (**K**).

chondroitin sulphates or components of the extracellular matrix. The ubiquitous presence of glycosaminoglycans on most cells would help to explain the ability of VACV to invade so many different cell types.

Once attached, IMV and EEV are thought to adopt similar strategies for entering the cell although different strategies have been proposed (Vanderplasschen *et al.*, 1998). IMV entry is thought to occur *via* one of three mechanisms. The most accepted mechanism is that VACV IMV fuses with the plasma membrane of the cell and gains entry (Armstrong *et al.*, 1973) whilst another suggests that the virus actually uncoats outside of the cell without fusion and then somehow crosses the external membrane (Locker *et al.*, 2000). Thirdly, bound IMV may be endocytosed and then may fuse with the vesicular membrane of the endosome to free the core virus particle into the cytoplasm (Moss, 2006). It is possible that both endosomal and plasma membrane entry paths are used depending on the strain of virus and type of cell being infected. Either way, there appears to be at least one virion protein that is conserved (VACV-A28) and is likely to be involved throughout the fusion/entry process (Senkevich *et al.*, 2004). Entry of EEV is no more clear-cut as suggestions for cell entry include fusion with the plasma membrane or entry *via* endocytosis and acidified envelope degradation (Ichihashi, 1996). Current reviews suggest that the fusion process is mediated by a group of viral proteins associated with the IMV membrane that are conserved across all poxviruses (Moss, 2006).

Having entered the cell and lost all outer membranes, the virus core moves through the cytosol towards the centre of the cell along microtubules (Carter *et al.*, 2003) (Figure 1.3). Within twenty minutes, VACV begins to synthesise viral mRNA using

its own endogenous DNA-dependent RNA polymerase and encapsulated transcription factors to transcribe and translate early genes required for replication and survival. Approximately half of the entire genome is transcribed here and a number of these early proteins prompt the dissolution of the virus core to release genomic DNA into the cytoplasm allowing it to act as a template for DNA replication. DNA synthesis begins one to two hours post-infection next to the site of the uncoated core and viral factories then begin to develop. This process also mediates the transcription of the intermediate class of genes that, unlike the early genes, are thought to require assistance from the host's own transcription factors to synthesise proteins (Rosales *et al.*, 1994). The intermediate genes encode a number of proteins, some of which are necessary for late gene transcription to occur and tend to reach their peak synthesis at approximately two hours. Throughout the translation of early and intermediate VACV genes, host cellular mRNA translation begins to be inhibited selectively by small non-translated poly-A mRNAs (Bablanian *et al.*, 1991). This contributes to a reduction in host cellular mRNAs and a rise in VACV mRNAs, resulting in a marked shift towards the preferential synthesis of VACV polypeptides. As late gene transcription occurs, the synthesis of many of the proteins required for assembling new virus particles is seen. These late genes also encode enzymes that are packaged within newly formed virions to instigate the next cycle of infection.

As late genes are continuously synthesised, the assembly of new virus particles occurs in cytoplasmic factories that have been shown to be free of any cellular organelles (Ichihashi *et al.*, 1971). The first morphologically distinct structures produced within these factories are crescent-shaped, which soon grow to form ovals and incorporate a variety of host-derived lipids and virus proteins. These initial structures are known as

immature virus particles (IV) and are non-infectious. These soon grow to form new infectious IMV particles by acquiring a number of external membranes (Figure 1.3). These IMV particles accumulate to great numbers, becoming the predominant infectious progeny virus within each infected cell. A number of IMVs leave the virus factories along microtubules, utilising the A27L membrane protein (Sanderson *et al.*, 2000) and may acquire a double outer membrane from either the trans-golgi network (Schmelz *et al.*, 1994), early endosomes (Tooze *et al.*, 1993; van Eijl *et al.*, 2002) or perhaps membranes from both sources (Husain & Moss, 2003; Moss, 2006) to form intracellular enveloped virus (IEV). The IEV continues along microtubules serving as an intermediary virus particle until it reaches, and then fuses with, the plasma membrane, losing one of its external membranes in the process. Once fused, the virion is exocytosed and becomes the cell-associated enveloped virus (CEV) if it remains attached to the cell wall or extracellular enveloped virus (EEV) if it is released from the cell completely. Whether an IEV remains cell-associated or is released is dependent on the strain of virus as well as the infected host cell itself. For instance, VACV IHD strain has been shown to release approximately 50-fold more EEV than the WR strain. This may be due to a point mutation within the A34R gene locus that encodes a lectin-like protein (McIntosh and Smith, 1996). By this stage, host protein synthesis is usually completely shut off and host DNA replication may also have been inhibited, possibly as a result of VACV encoded endonucleases (Dales, 1990; Buller & Palumbo, 1991).

To continue the spread of infection, CEVs are propelled towards neighbouring cells *via* actin polymerisation (Cudmore *et al.*, 1995; Stokes, 1976) and are predominantly thought to mediate the local cell-cell spread of infection. EEVs, in contrast, are free to

initiate long range spread of infection systemically if they can avoid neutralisation by the host immune response. The third and most dominant way for infection to progress is the non-specific release of streams of IMV particles after the death of the infected cell and subsequent cell lysis. This only occurs following the completion of the infectious virus cycle and, as such, is too slow to promote the rapid spread of virus but is key in promoting the local dissemination of infectious virus progeny.

1.3.3. Poxvirus immunomodulation

In order to survive and prosper within the host, viruses have evolved ways to avoid or manipulate the host antiviral immune response so that they are able to establish their habitat, complete their replication cycle and find additional viable cells to infect. Viruses are able to modulate host response mechanisms like apoptosis, complement, antibodies, pro-inflammatory cytokines and chemokines as well as lymphocyte function and signaling. Large DNA viruses, such as herpesviruses and poxviruses are particularly able to encode multiple classes of immunomodulatory proteins capable of fighting these host defence systems because of their large genomes and array of non-essential genes. VACV has been shown to possess an arsenal of immunomodulatory proteins that serve to promote its continued survival within the host. The defensive strategies utilised by poxviruses can be grouped into three broad main categories: virokines, viroreceptors and viral proteins that interfere with signaling and effector pathways (Figure 1.4).

1.3.3.1. Virokines

Virokines are virally encoded proteins that are synthesised during replication and secreted from the infected host cell into the extracellular environment. The vast

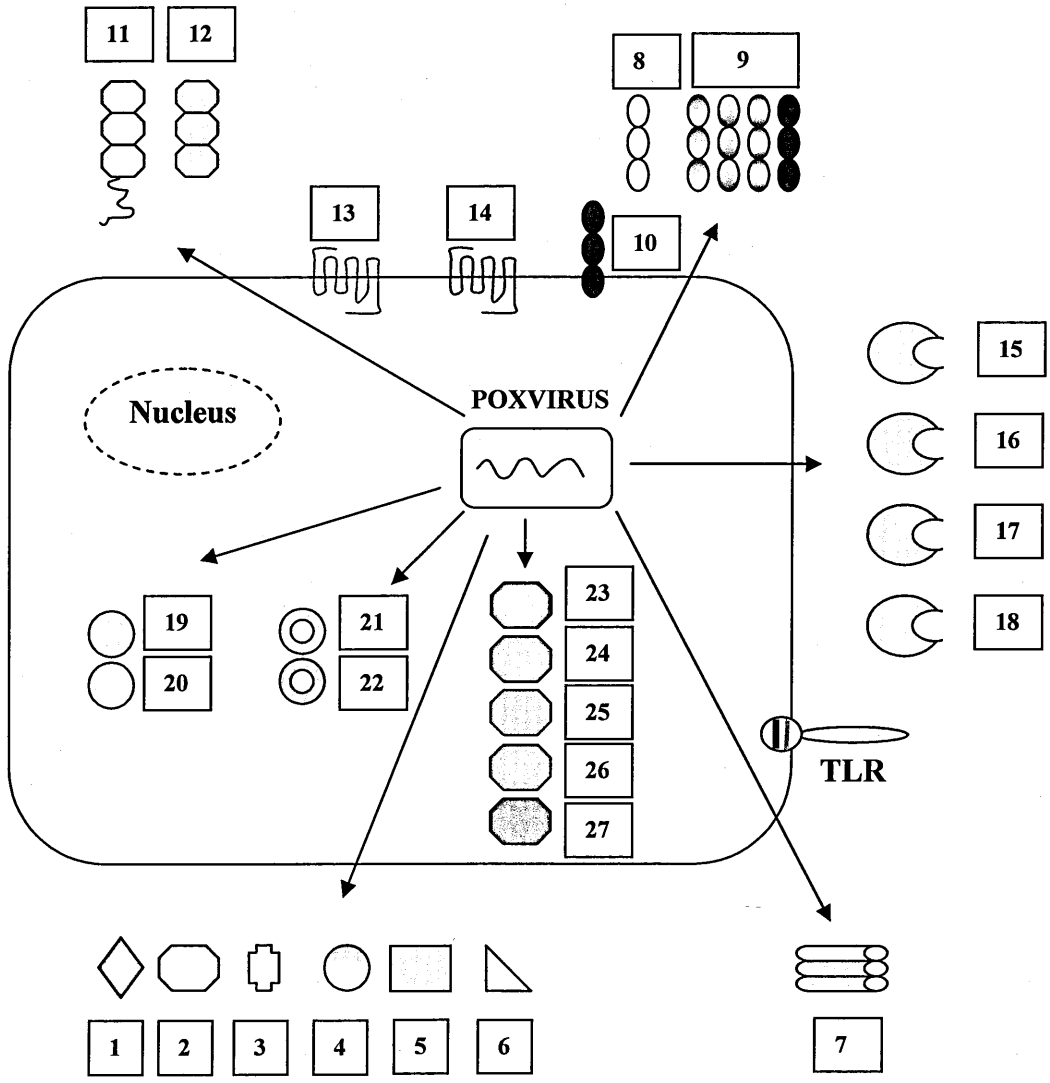

Figure 1.4. Examples of three types of poxvirus immunomodulatory strategy.

Virokines
1. vvEGF*
2. vvSEMA*
3. Orf IL-10
4. Orf vVEGF
5. Orf GIF
6. Myxoma SERP
7. VCP*

Viroreceptors
8. Cowpox crmE
9. Pox crmB/C/D/E*
10. crmE/TNF-R*
11. IL-1βR*
12. IFN-γR*
13. Swinepox CXCR1
14. Capripox CCR-1
15. IFN-α/β BP*
16. IL-18 BP*
17. vCKBP1 (M-T7)
18. vCKBP2 (35KDa) *

Signal transduction
19. SPI-1*
20. SPI-2*
21. K3L*
22. E3L*
23. A46R*
24. A52R*
25. N1L*
26. K1L*
27. M2L*

*VACV encoded

majority are mimics of host cytokines or chemokines and are thought to have been acquired by the virus throughout evolution following capture of host genes. Many of these mimicking proteins share a high percentage of the structural and functional characteristics of the host protein that they mimic. Several poxviruses have been shown to secrete virokines including the parapoxvirus orf, which produces a viral IL-10 homologue (Imlach *et al.*, 2002), an inhibitor of granulocyte-macrophage colony-stimulating factor (GM-CSF) and Interleukin-2 (IL-2) collectively known as GIF (Deane *et al.*, 2000) and vascular endothelial growth factor (VEGF) (Wise *et al.*, 1999). VACV has been shown to release a homologue of epidermal growth factor referred to as vEGF, which enhances cell proliferation (Brown *et al.*, 1985), presumably to increase the number of cells available for infection.

Another identified virokine produced by VACV is vSEMA (viral semaphorin homologue). Semaphorins serve a dual role as both chemoattractants and chemorepellants in the host system and are involved in directing axons during the development of the nervous system (Spriggs, 1999). The VACV vSEMA protein (encoded by A39R in WR) binds the semaphorin receptor VESPR (virus-encoded semaphoring protein receptor) in macrophages and, in doing so, is thought to prompt the synthesis and expression of cytokines and adhesion molecules (Gardner *et al.*, 2001). vSEMA has also been shown to bind the plexin C1 receptor in dendritic cells where it induces actin cytoskeleton rearrangement and also prevents integrin-mediated adhesion and chemokine-induced migration. (Walzer *et al.*, 2005).

Other non-poxvirus virokines identified to date include homologues for a number of other cytokines and chemokines including IL-6 and macrophage inflammatory protein

2 (vMIP2) produced by Karposi's sarcoma-associated herpesvirus (KSHV), and IL-10 homologues secreted by both Epstein-Barr virus (EBV) and human cytomegalovirus (HCMV). These cytokines serve a variety of pro- and anti-inflammatory functions in the host and viral homologues are likely to manipulate these functions to suit their own purpose. The release of key viral chemokine homologues may serve to promote virus dissemination and growth or assist in re-directing the host response to avoid detection and neutralisation. This has been seen with the release of the vCXC1 protein encoded by HCMV which induces neutrophil chemotaxis to either assist in the dissemination of virus or recruitment of fresh cells for infection (Penfold *et al.*, 1999)

1.3.3.2. Viroreceptors

Viroreceptors have been shown to play a fundamental role in the survival of viruses during infection. They act as viral mimics of chemokine and cytokine receptors and can be either released extracellularly or retained intracellularly/on the cell surface to block or bind host cytokines and chemokines. Closer examination of the virus genes that encode these receptors show that they possess sequence similarity to the extracellular binding domains of the host cytokine receptors but do not share any homology with the transmembrane or signaling domains. Consequently, viroreceptors act as decoy receptors, competing for and 'mopping up' free cytokines and chemokines in the local environment to prevent the binding of the intended host messenger molecules to true receptors. So far, a wide variety of these receptors have been identified in a range of pox and herpesviruses.

Myxoma virus has been shown to encode a soluble vTNFR (virus TNF receptor), encoded by the T2 gene, that prevents the dimerisation of the TNF receptor which is

required for signal transduction. This enables the virus to neutralise the activity of TNF and act as a potent virulence factor (Schreiber *et al.*, 1996). A variety of other poxviruses (including cowpox, vaccinia, variola and ectromelia) have also been shown to encode different TNF receptor homologues from the one encoded by myxoma. These sets of TNF-like receptors have been grouped into a family of receptors and are commonly known as cytokine-response modifiers (Crm). To date CrmB, CrmC, CrmD and CrmE have been identified, with each virus encoding either one or a subset of these receptors (Loparev *et al.*, 1998; Reading *et al.*, 2002). The majority of these TNF-receptors are secreted from the infected cell but, as Reading and colleagues have shown, there is also evidence for membrane bound TNF-binding activity *via* CrmE in cells infected with certain strains of VACV including Lister, USSR and Evans (Reading, Khanna & Smith, 2002).

Soluble cytokine receptors also exist for IL-1β (vIL-1βR) and IFN-γ (vIFN-γR), both of which are secreted and produced by VACV. IL-1β is a pyrogenic cytokine and the decoy IL-1β receptor encoded by the B15R gene of VACV (WR) is able to efficiently block the febrile response (Alcami & Smith, 1992). Likewise, the B8R gene of VACV WR encodes for a vIFN-γR and binds IFN-γ from various species (Alcami & Smith, 1995). Recently, the IFN-γ binding protein (IFN-γ bp) of ectromelia virus has been shown to play a pivotal role in reducing the strength of the host inflammatory response (Sakala *et al.*, 2007).

In addition to cytokine receptors, homologues of key cytokine binding proteins have also been discovered that are produced by ectromelia virus, cowpox, VACV, variola and molluscum contagiosum virus. These include homologues of the IFN-α/β binding

protein encoded by the B18R gene in VACV (WR) (Colamonici *et al.*, 1995). The VACV IFN-α/β receptors have been shown to bind to the host cell surface to prevent IFN binding to genuine IFN receptors (Alcami *et al.*, 2000). In addition, numerous IL-18 binding proteins (IL-18bp) have been reported in the literature. IL-18 is a key cytokine involved in driving the interferon response during the onset of infection, through the activation of NK cells (Tomura *et al.*, 1998). The viral IL-18 binding proteins have been shown to possess very little homology to the mammalian IL-18 receptors and instead mimic the shape of mammalian IL-18 binding proteins (IL-18bp) that are thought to help regulate IL-18 activity (Smith *et al.*, 2000). In VACV, deletion mutants lacking the IL-18bp (encoded by VACV (WR) gene C12L) have been shown to be markedly attenuated *in vivo* and enable a more vigorous IFN-γ and cytotoxic T-cell response to develop (Reading & Smith, 2003a).

Viral chemokine-receptor homologues (vCKRs) are best described for herpesviruses such as KSHV, HCMV and mouse cytomegalovirus (MCMV) and are not well characterised in the genomes of poxviruses. However, several genes encoding vCKRs have been identified in poxvirus genomes based purely on their sequence similarity with host receptors. These include the CXCR1 homologue of swinepox (Massung *et al.*, 1993) and the CC-chemokine receptor homologue of capripoxvirus (Cao *et al.*, 1995), but no specific function has been assigned to these proteins. Unlike the vast majority of cytokine-receptor homologues, these vCKRs are not secreted but are membrane bound and possess the characteristic seven-transmembrane structure of host chemokine receptors. Herpesvirus vCKRs have been shown to sequester chemokines from the extracellular milieu of infected cells and influence cellular proliferation and signal transduction (Arvanitakis *et al.*, 1997). It is possible that the

vCKR homologues encoded by poxviruses may also perform similar functions during infection although this has yet to be conclusively reported.

Two families of soluble chemokine-binding proteins (vCKBPs) have been described that use distinct methods of combating host chemokines. The first family (type I) is comprised of a solitary member known as chemokine binding protein 1 (vCKBP1), encoded by the M-T7 gene from myxoma virus. This protein was originally identified as a soluble IFN-γ receptor (Mossman *et al.*, 1995), and is secreted from the infected cell to bind a wide variety of CC, CXC and C-chemokines with relatively low affinity (Lalani *et al.*, 1997). The second family, comprising of vCKBP2 produced by both myxoma and VACV, has been shown to exhibit greater specificity than vCKBP1 for binding CC-chemokines such as RANTES (regulated upon activation, normal T-cell expressed and secreted) (Graham *et al.*, 1997; Burns *et al.*, 2002). The low–affinity binding of vCKBP1 is thought to interfere with the positioning and presentation of chemokines to cell surface GAG proteins whereas the stronger affiliation between vCKBP2 proteins actually inhibits the interaction of the chemokines with their intended targets.

Finally, the complement system has also been shown to be a target for virus immunomodulatory proteins. The best studied of these belongs to VACV and is the complement control protein (VCP). This protein resembles human complement 4b binding protein (C4b-BP) (Kotwal & Moss, 1988) and mimics the biological functionality of a number of complement control proteins including factor H, membrane cofactor protein (MCP) and decay-accelerating factor (DAF) (Sahu *et al.*, 1998). VCP is known to thwart both the classical and alternative complement

pathways by binding to C3 and C4 and encouraging the destruction of the C3 convertase (Kotwal *et al.*, 1990). This ensures the complement system is blocked at multiple sites to prevent the formation of the final membrane attack complex and release of additional pro-inflammatory mediators such as C3a/C4a/C5a. This results in reduced cellular influx and inflammation (Isaacs *et al.*, 1992). By hindering the complement system, VCP serves as a key virulence factor and enables VACV to escape a key arm of the innate immune response to promote its own survival within the host.

1.3.3.3. Viral inhibition of signal transduction

Poxviruses possess a variety of mechanisms to interfere with key signaling pathways in the host cell to promote their survival within the cell. One key strategy utilised by a variety of poxviruses is blocking cellular apoptosis. Apoptosis has long been established as an effective way of protecting the host from viral infection because early induction of cell death can prevent pathogen replication by rendering host macro-molecular machinery inactive (Zimmermann *et al.*, 2001). In addition, apoptotic cells can be phagocytosed rapidly by other cells of the immune system before the inflammatory intracellular contents of the cell are released. A number of proteins in the cell's apoptotic pathway are targeted by viral proteins to prolong the life of the infected cell so that the virus is able to replicate to higher titres (Benedict *et al.*, 2002). In VACV a number of proteins have been identified that may prevent apoptosis. Most recently, a protein encoded by both VACV and camelpox has been identified by Gubser and colleagues and has been termed viral golgi anti-apoptotic protein (v-GAAP) (Gubser *et al.*, 2007). This protein was found to be highly homologous to the human GAAP, a transmembrane protein of the Golgi apparatus,

which prevents apoptosis. Over-expression of v-GAAP was shown to prevent apoptosis *in vitro*, whilst deletion of v-GAAP from VACV was shown to effect virulence *in vivo* (Gubser *et al.*, 2007). Other anti-apoptotic proteins encoded by VACV include a serine protease inhibitor (serpin/SPI) known as SPI-2 (encoded by VACV WR B13R), which blocks apoptosis triggered by binding of both TNF-α to the TNF receptor 1 and Fas ligand to CD95 Fas receptor (Dobbelstein & Shenk, 1996; Kettle *et al.*, 1995). VACV SPI-2 is a potent inhibitor of cysteine aspartate protease-1 (caspase-1), an enzyme previously known as ICE (IL-1β converting enzyme). Caspase-1 is the functional form of pro-caspase, an enzyme that naturally exists in the cell in an inactive state. In its active state, caspase-1 plays an important role in apoptosis by initiating the proteloytic caspase cascade (Concha & Abdel-Meguid, 2002). VACV SPI-2 has been shown to inhibit this process by blocking the cleavage event necessary to convert the inactive pro-caspase into active caspase-1 and thus prevent the initiation of apoptosis. It has been suggested that apoptosis involves many other caspases such as caspase-8, and these may also be potential targets for other poxvirus serpins, such as cytokine response modifier A (CrmA), encoded by cowpox, that may inhibit apoptosis (Zhou *et al.*, 1997). An additional serpin encoded by VACV known as SPI-1 (encoded by VACV (WR) B22R gene) may synergise with SPI-2 to induce complete inhibition of apoptosis (Macen *et al.*, 1996).

The inhibition of caspase-1 by VACV SPI-2 also has a profound anti-inflammatory effect. Active caspase-1 is directly responsible for the cleavage of both pro-IL-1β and pro-IL-18 into their functional forms (Giamila & Charles, 1999). Pro-caspase-1 has been shown to be at the heart of the variety of multi-protein assembly units known as inflammasomes (Martinon *et al.*, 2002). Along with pro-caspase-1, inflammasomes

typically consist of a NOD-like receptor, other cellular caspases and adaptor molecules specific for each inflammasome (Mariathasan & Monack, 2007). Upon inflammasome activation, pro-caspase-1 is cleaved into its functional form. Therefore, by inhibiting caspase-1, VACV SPI-2, along with related serpins from other poxviruses, blocks the conversion of the non-functional form of cytokines to the functional form and thus prevents the synthesis of key cytokines that have a multi-faceted role in inflammation. Some groups looking at the virulence of poxviruses lacking SPI-1 and SPI-2, using deletion studies, have reported an increase in virulence (Tscharke *et al.*, 2002), although other groups have contradicted this finding (Kettle, *et al.,* 1995). Thus, it remains unclear how much VACV SPI-2 contributes to virulence in an *in vivo* system.

In addition to inhibiting the extracellular compounds of the IFN response, VACV also targets intracellular components of the IFN signaling cascade. Upon binding to cellular receptors, IFN induces the expression of a number of pathways (section 1.1.4) and enzymes. Two of these enzymes, IFN-induced dsRNA-dependent protein kinase (PKR) and 2'-5'-oligoadenylate synthetase (2'-5' OAS), are activated by the copious amounts of dsRNA produced during viral replication (Honda & Taniguchi, 2006). PKR, a ubiquitously expressed serine/threonine kinase, phosphorylates itself to become activated and then phosphorylates the eukaryotic translation factor 2α (eIF-2α) to inactivate it. This inactivation stops the translation of essential proteins and thus results in apoptosis. The VACV gene product encoded by K3L produces an eIF-2α mimic, which prevents PKR phosphorylation of eIF-2α and thus prevents the inactivation of eIF-2α. This, in turn, prevents translational arrest and allows the cell to continue synthesising its necessary proteins (Davies *et al.*, 1992). 2'5'-OAS functions

to activate a latent cellular RNase known as RNase L. RNAse L prevents protein synthesis by cleaving RNA molecules and thus preventing their translation into protein. VACV also targets this process by binding dsRNA with a protein encoded by the gene E3L, and prevents the activation of RNase L and subsequent RNA degradation (Langland *et al.*, 2006; Chang *et al.*, 1992). This, in turn, also acts as an additional method of viral inhibition of apoptosis as deletion of E3L in virus mutants accelerates the rate of cellular apoptosis (Kibler *et al.*, 1997).

Another significant method of interfering with the cellular regulation of key molecules is through targeting of the TLR pathway. The significance of TLRs as pattern recognition receptors of invading organisms was discussed in section 1.1.2. Viruses have evolved to target numerous elements in the signaling pathway to disrupt the transduction of pro-inflammatory signals. Several proteins in particular have been shown to play significant, yet different, roles in virally-induced TLR immunomodulation. VACV protein A46R has been shown to target the intracellular TIR domains of both the IL-1 and toll-like receptors (Bowie *et al.*, 2000; Stack *et al.*, 2005). Binding of A46R to the TIR domain may prevents the co-localisation of important adaptor molecules such as MyD88, TRAM, TRIF and Mal. Other VACV proteins target the signaling pathway further downstream. A52R has been shown to associate with both IRAK2 and TRAF6 and prevent their respective associations with other key cellular components, or disrupt signaling complexes, thus preventing further signal transduction (Harte *et al.*, 2003) The intracellular N1L protein of VACV has been reported to associate with several proteins of the IKK complex, one suggested target being TBK1, and its deletion has been shown to cause marked attenuation *in vivo* (DiPerna *et al.*, 2004; Bartlett *et al.*, 2002). VACV K1L has been shown to

inhibit the degradation of IκBα by interacting with the IKK complex and thus prevent the activation of NF-κB (Shisler & Jin, 2004). Additionally, the VACV M2L protein has been shown to interfere with the ERK2 pathway and prevent NF-κB activation (Gedey *et al.*, 2006). Most recently, a new protein referred to as K7 from VACV has been shown to inhibit both NF-κB activation and the initiation of antiviral immune pathways (Lucas *et al.*, 2007). This protein was initially identified as having sequence similarity to VACV A52R, although the specifics of where in the immune signaling pathway it acts have yet to be elucidated.

1.3.4. Vaccination complications

The smallpox vaccine led to the worldwide eradication of smallpox disease in the late 1970's. Whilst it was successful, the vaccination campaign was also plagued with complications due to a higher incidence of side-effects than any other current or past vaccine (Fulginiti *et al.*, 2003). The majority of these side effects resulted from uncontrolled VACV replication, either at the site of inoculation or at distant sites, following accidental infection or internal dissemination. Such complications were most common in those vaccinees suffering from an underlying condition such as eczema/atopic dermatitis or an immune system deficiency (Lane *et al.*, 1970). Despite these issues, the smallpox vaccine remains the primary countermeasure against exposure to smallpox infection as no clinically approved antiviral treatments for smallpox, or any other orthopoxvirus infection, have been licensed. The current threat of variola virus being released deliberately as a biowarfare agent has further prompted demands for other vaccination approaches, such as a third generation MVA vaccine, or new antivirals against Orthopoxvirus infection (Parrino *et al.*, 2007). Research

activity has focused on developing antiviral drugs as well as immunomodulatory compounds that can modulate the host response to infection.

1.3.4.1. Targeting viral enzymes and proteins

The targeting of essential viral enzymes has proven to be very successful in a variety of viral infections, resulting in approximately 20 licensed antiviral drugs for HIV alone (Greene, 2004). Examples of this approach are listed in Table 1.2 and include azidothymidine (AZT), which inhibits HIV reverse transcriptase (Nakashima *et al.*, 1986) and acyclovir, a compound that inhibits the DNA polymerase of HSV (Freeman & Gardiner, 1996). Both of these compounds are licensed and have proven useful in the treatment of infected individuals. Nucleoside phosphonate analogues of cellular deoxyribonucleotides are another class of drug that have proven to have broad spectrum antiviral activity against DNA viruses (De Clercq, 2007). Within this class, the drug cidofovir (((S)-1(3-hydroxy-2-phosphonylmethoxypropyl)) cytosine or HPMPC or CDV) has been shown to be a potent inhibitor of viral DNA polymerases and activity has been demonstrated against adeno-, polyoma-, herpes- and poxviruses, including lethal doses of VACV (Smee *et al.*, 2001a), variola, cowpox, monkeypox and molluscum contagiosum virus (MCV) (De Clercq, 2002). Cidofovir has been shown to work by incorporating itself into the extending viral DNA chain. This is only possible following several intracellular phosphorylation steps, converting CDV into the diphosphate form where it can then cause chain termination (Magee *et al.*, 2005). Currently, CDV is unlicensed for use against poxviruses and has only obtained approval for clinical use in the treatment of CMV retinitis (Lalezari, 1997), a complication that frequently results from HIV infection. Clinical trials have also established the *in vivo* efficacy of topical CDV in humans against MCV in AIDS

Target Enzyme	Involved in:	Example
HIV reverse transcriptase	Converts viral RNA into cDNA copy	AZT (Azidothymidine) Tenofovir
HSV DNA polymerase	Viral DNA synthesis	Acyclovir
Viral DNA polymerases of a wide variety of viruses including: adeno-, polyoma-, herpes- and poxviruses.	Viral DNA synthesis	Cidofovir (CDV) and derivatives of including HDP-CDHV and ODE-CDV
HBV DNA polymerase	Viral DNA synthesis	Adefovir
HIV protease	Protein cleavage	Saquinavir, Ritonavir, Indinavir, Nelfinavir
Picornavirus protease	Protein cleavage	AG6084
Herpesvirus assemblin	Viral capsid assembly	Flavin, CL13933
Target Protein	**Involved in:**	**Example**
37 kDa palmitylated peripheral membrane protein (e.g VACV F13L)	Othopoxvirus egress (Envelope wrapping of IMV)	ST-246
F13L	Orthopoxvirus egress	Compound 14
Virus envelope proteins / glycolipids	HIV entry	Enfuvirtide

Table 1.2. Virus specific enzyme or protein targets.

Table lists examples of antiviral compounds that target virus specific proteins or enzymes.

patients and also efficacy against orf virus. (Meadows *et al.*, 1997). Whilst promising and recommended by the Centre for Disease Control (CDC) for use against complications arising from smallpox vaccination (Wharton *et al.*, 2003), its use may be hindered by the requirement for intravenous delivery and high levels of nephrotoxicity (Cundy, 1999). Extensive studies have been conducted recently *in vitro* and in animal models and currently oral derivatives based on lipid conjugates such as hexadecyloxypropyl-cidofovir (HDP-CDV) and octadecycloxyethyl-cidofovir (ODE-CDV) are being formulated to boost uptake from the small intestine and reduce levels of nephrotoxicity (Keith *et al.*, 2004; Quenelle *et al.*, 2004). These derivatives are currently exhibiting over 100 times greater activity against VACV and cowpox replication than unmodified CDV (Kern *et al.*, 2002). This may be due to an increased uptake (Aldern *et al.*, 2003) and ability to reach target tissues (Ciesla *et al.*, 2003) Other acyclic nucleoside analogues such as adefovir and tenofovir have been licensed and have proven successful in the treatment of hepatitis B virus (HBV) (Hadziyannis *et al.*, 2005) and HIV (Robbins *et al.*, 1998) respectively.

Other key viral enzymes targeted by antiviral compounds include viral proteases and neuraminadases (Table 1.2). Inhibiting viral proteases has achieved success in the treatment of HIV (e.g. saquiniavir, ritonavir, indinavir and nelfinavir), and is an approach that is being investigated to combat picornaviruses (AG6084), the capsid assembly protein assemblin in herpeseviruses (flavin, CL13933) and the hepatitis C virus (HCV) protease (Patick & Potts, 1998). Viral neuraminadases are potential targets in the treatment of influenza virus types A and B, owing to their fundamental role in permitting virus escape from the cell following replication. This has led to the design of drugs to inhibit this process (von Itzstein *et al.*, 1993; Smee *et al.*, 2001b).

This resulted in the manufacture of oseltamivir (Nicholson *et al.*, 2000) and zanamivir (Hayden *et al.*, 1997), both of which exhibit potent anti-neuraminidase activity. Antiviral compounds that target the cysteine proteinase (encoded by I7L) in VACV have been identified and reported to block viral maturation (Byrd *et al.*, 2004). This study investigated the role of this viral proteinase and demonstrated that it was responsible for essential cleavage events during maturation that lead to the formation of infectious IMV particles. Inhibition of these cleavage events was reported to restrict viral titers in *in vitro* systems (Byrd & Hruby, 2005).

The targeting of viral proteins is an additional strategy that has yielded success therapeutically (Table 1.2). The drug ST-246 has proven to be very effective against a wide range of orthopoxviruses such as VACV, monkeypox, camelpox, ectromelia and variola viruses (Yang *et al.*, 2005a). This drug works by targeting a 37-kDa palmitylated peripheral membrane protein (F13L in VACV), preventing the enveloping of IMV particles and thus inhibiting the formation of EEV particles. Studies show that this approach protects against orthopoxvirus-induced disease and, unlike CDV, can be delivered orally with much lower toxicity. Screening assays to identify new antiviral compounds have recently reported an additional compound that targets F13L and this has also proven effective at preventing viral egress and disease in initial studies (Bailey *et al.*, 2007). Other antivirals target virus envelope proteins or glycolipids used during the entry of the virus into the host cell e.g. enfuvirtide. This is currently an approach being investigated in the fight against HIV infection (Este & Telenti, 2007).

1.3.4.2. Targeting host enzymes

An alternative antiviral approach is to interfere with host cell processes and machinery that viruses require to ensure competent replication and survival within the intracellular environment. A number of studies have shown efficacy against a range of viruses including poxviruses (Table 1.3).

The targeting of cellular enzymes, such as inosine 5'-monophosphate (IMP) dehydrogenase, has received much attention. This enzyme converts IMP to xanthine 5'-monophospahte (XMP), which is required for the *de novo* biosynthesis of the purine mononucleotides such as guanosine 5'monophosphate (GMP) / diphosphate (GDP) / triphosphate (GTP). By inhibiting this enzyme, the availability of these guanosine mononucleotides is greatly reduced and this in turn inhibits both viral RNA and DNA synthesis (Robins *et al.*, 1985). This is the basis of the antiviral drug ribavirin, which inhibits VACV replication *in vivo* through its 5'-monophosphate metabolite (Sidwell *et al.*, 1973).

S-adenosylhomo-cysteine (SAH) hydrolase is another key target enzyme of antiviral compounds. This enzyme is responsible for hydrolysing SAH, a compound that inhibits S-adenosylmethionine (SAM)-dependent methyltransferase reactions. SAM acts as a methyl donor for 5'-cap formation during RNA synthesis and the inhibition of SAH hydrolase results in the accumulation of SAH and interference of key methylation steps that effect RNA stability. Inhibition of SAH hydrolase has been shown to preferentially affect viruses, such as VACV, in their replication cycle by disrupting the stability of VACV mRNA (Borchardt *et al.*, 1984). Many adenosine analogues, such as neplanocins A and C and carbocyclic 3-deazaadenosine have been

Target Enzyme	Involved in:	Examples
IMP dehydrogenase	Converts IMP to XMP	Ribavirin
SAH hydrolase	SAH hydrolysis	Neplanocins A and C Carbocyclic 3-deazaadenosine
OMP decarboxylase	Converts OMP to UMP	Pyrazofurin
CTP synthetase	Converts UTP to CTP	Cyclopentyl cytosine
Thymidylate synthetase	Converts dUMP to dTMP	5-amino-dUrd

Table 1.3. Host cellular enzyme targets.

Table lists examples of antiviral compounds that exert their effects by targeting host cellular enzyme targets

described as inhibitors of SAH hydrolase with broad spectrum activity against poxviruses, negative strand RNA viruses and a host of others (De Clercq *et al.*, 1984; De Clercq & Montgomery, 1983).

Additional enzymes useful as antiviral targets include orotidine 5'-monophosphate (OMP) decarboxylase, cytosine 5'-triphosphate (CTP) synthetase and thymilidate synthetase. OMP decarboxylase inhibitors prevent the conversion of OMP to uracil 5'monophosphate (UMP), which blocks the accumulation of UTP and CTP pools. CTP pools are also depleted by CTP synthetase inhibitors, which block the conversion of UTP into CTP. Both of these inhibitors ultimately promote depletion of either UTP or CTP reservoirs and this results in the suppression of RNA synthesis. Key examples of these compounds in action come from the effect of the OMP decarboxylase inhibitor pyrazofurin and its derivatives on the replication of a variety of viruses (Chen *et al.*, 1993) along with CTP synthetase inhibitors such as cyclopentenyl cytosine (Ce-Cyd) (De Clercq *et al.*, 1991). Thymidylate synthetase inhibitors target the thymidylate synthetase enzyme, which prevents conversion of dUMP into dTMP (deoxy thymidine monophosphate). This inhibition leads to a lack of deoxy thymidine triphosphate (dTTP) and consequently results in defective DNA synthesis. Derivatives of diphosphohexose deoxyuridine (dUrd), such as 5-amino-dUrd, have demonstrated a potent activity against VACV (De Clercq, 1980).

1.3.4.3. Targeting host systems

More recently, a variety of studies have been published that have targeted poxvirus replication by targeting host cellular signaling pathways (Table 1.4). These include the drug CI-1033, which interferes with the cellular ErbB-1 signal transduction

Target Pathway	Involved in:	Examples
ErbB-1	Physiological growth factor signalling by EGF	CI-1033
ABl-family tyrosine kinase	Actin motility	STI-571 (Gleevac)
Interferon	Antiviral state formation, cell signalling	(Pegylated) IFN-α Poly IC

Table 1.4. Host signalling targets.

Table lists examples of antiviral compounds that exert their effects by targeting host pathways

pathway (Yang *et al.*, 2005b). This pathway is activated by orthopoxvirus growth factors such as VGF in VACV/SPGF in variola (Tzahar *et al.*, 1998), and inhibition *via* CI-1033 was shown to improve protection against a lethal VACV infection (Yang *et al.*, 2005b). Additionally, targeting of the Abl-family of tyrosine kinases has also proved to be a valid approach with studies revealing a substantial drop in VACV spread following inhibition with STI-571 (Gleevac) and increased survival of infected mice (Reeves *et al.*, 2005). Alternatively, interferon is a known antiviral and methods of inducing this pathway *via* administration of poly IC have been shown to induce a protective effect against VACV in rabbits (Levy & Lvovsky, 1978). Many other systems, some virus specific, are also viable targets for antiviral therapies that aim to interfere with virus attachment through specific cellular receptors, cell entry, virus motility and replication. Many of these are also able to demonstrate potential use as antiviral strategies such as the fusion inhibitor T-20 that is approved for the treatment of HIV (Kilby *et al.*, 1998).

1.4. Aims of this research

The aims of this research are to establish the effectiveness of using CpGs as an antiviral against orthopoxvirus infection. The prophylactic or therapeutic efficacy of CpGs will be assessed in both pre-exposure and post-exposure model systems. This work will also attempt to establish the key immune parameters behind the success or failure of CpGs in protecting against orthopoxvirus infection so that the future use of CpGs as an antiviral strategy can be determined.

Chapter 2: Materials and Methods

2.1. Cell culture

Macrophage cell lines were obtained from ECACC (HPA, UK) and were maintained *in vitro* at 37°C under atmospheric conditions of 5% carbon dioxide (CO_2) and 95% humidity in vented tissue culture flasks (Corning®). MH-S cells were grown in endotoxin-free RPMI 1640 medium (Gibco® Invitrogen) and J774 cells were maintained in endotoxin-free Dulbecco's modified Eagle's medium (DMEM) (Gibco® Invitrogen). Both media were supplemented with 10% foetal calf serum (FCS) (Gibco® Invitrogen) and 2 mM L-glutamine (Sigma, UK). Rabbit kidney epithelial cells (RK-13) were obtained from ECACC (HPA, UK) and maintained in DMEM supplemented with 10% FCS, 2% HEPES-buffer, 1% tylosin, 100 U/ml penicillin, and 100 μg/ml streptomycin plus 2 mM L-glutamine (PSG), all from Sigma, UK.

2.1.1. CpG stimulation

Cells were incubated in 6, 24 or 96-well plates at a concentration of 1 x 10^6/ml overnight at 37°C to allow cells to adhere. Cell supernatants were then removed and replaced with an equivalent volume of CpG (Table 2.1) made up to the desired concentration in appropriate media. CpGs 2336, 7909, 10103, 10101, 10109, 2137 and 2243 were all obtained from Coley Pharmaceutical group (Ottawa, Canada). Plates were then re-incubated at 37°C and supernatants removed at individual time-points for subsequent analysis. Extraction of total RNA from macrophages for cytokine analysis is detailed in section 2.3.2.

CpG	Sequence	Class	Supplier
2336	G*G*GGACGACGTCGTGG*G*G*G*G*G *Mixed PS-PO backbone*	A	Coley Pharmaceuticals, Canada
10103	TCGTCGTTTTTCGGTCGTTTT *PS backbone*	B	Coley Pharmaceuticals, Canada
7909	TCGTCGTTTTGTCGTTTTGTCGTT *PS backbone*	B	Coley Pharmaceuticals, Canada
10101	*Not available* *PS backbone*	C	Coley Pharmaceuticals, Canada
10109	TCGTC*GTTTTAC*GGCGCC*GTGCCG *Mixed PS-PO backbone*	Semi-soft C	Coley Pharmaceuticals, Canada
2243	G*G*GGGAGCATGCTGG*G*G*G*G*G *Mixed PS-PO backbone*	A (control)	Coley Pharmaceuticals, Canada
2137	TGCTGCTTTTGTGCTTTTGTGCTT *PS backbone*	B (control)	Coley Pharmaceuticals, Canada

Table 2.1. CpG sequences used throughout

* Denotes phosphorothioate (PS) bonds in an otherwise phosphodiester (PO) backbone

* Denotes phosphodiester (PO) bonds in an otherwise phosphorothioate (PS) backbone

— Denotes palindromic sequence within ODN

2.1.2. Nitric oxide measurements

Production of nitric oxide (NO) was measured using the Griess reagent system (Promega, UK) as detailed in Figure 2.1. Briefly, 50 µl sample supernatants were carefully removed from individual wells following stimulation with CpG, and incubated with 50 µl sulphanilamide solution (1% sulphanilamide in 5% phosphoric acid) and 50 µl *N*-1-napthylethylenediamine dihydrochloride (NED) solution (0.1% NED in water), as detailed in manufacturer's instructions (Promega, UK). Levels of nitrite (NO_2^-), the stable end product of NO breakdown, were measured using a Thermolab multiscan plate reader at 540 nm using Ascent software 2.4.2 (Thermolab systems, UK). Standard curves were run on each plate (100 µM-0 µM) using a 0.1 M sodium nitrite standard to allow accurate calculation of nitrite concentration and determination of nitric oxide production in each sample.

2.1.3. Nitric oxide inhibition

Inhibition of nitric oxide synthesis was achieved using the generic inhibitor of nitric oxide synthase (NOS) N^G-methyl-L-arginine acetate salt (L-NMMA) (Sigma, UK). Working solutions of L-NMMA were prepared daily in fresh medium and either added alone or in combination with CpG as replacement medium for macrophages that had been incubated overnight at a concentration of 1 x 10^6/ml. Cells were then incubated at 37°C for a period of 24 hours and supernatant removed prior to further analysis or viral infection.

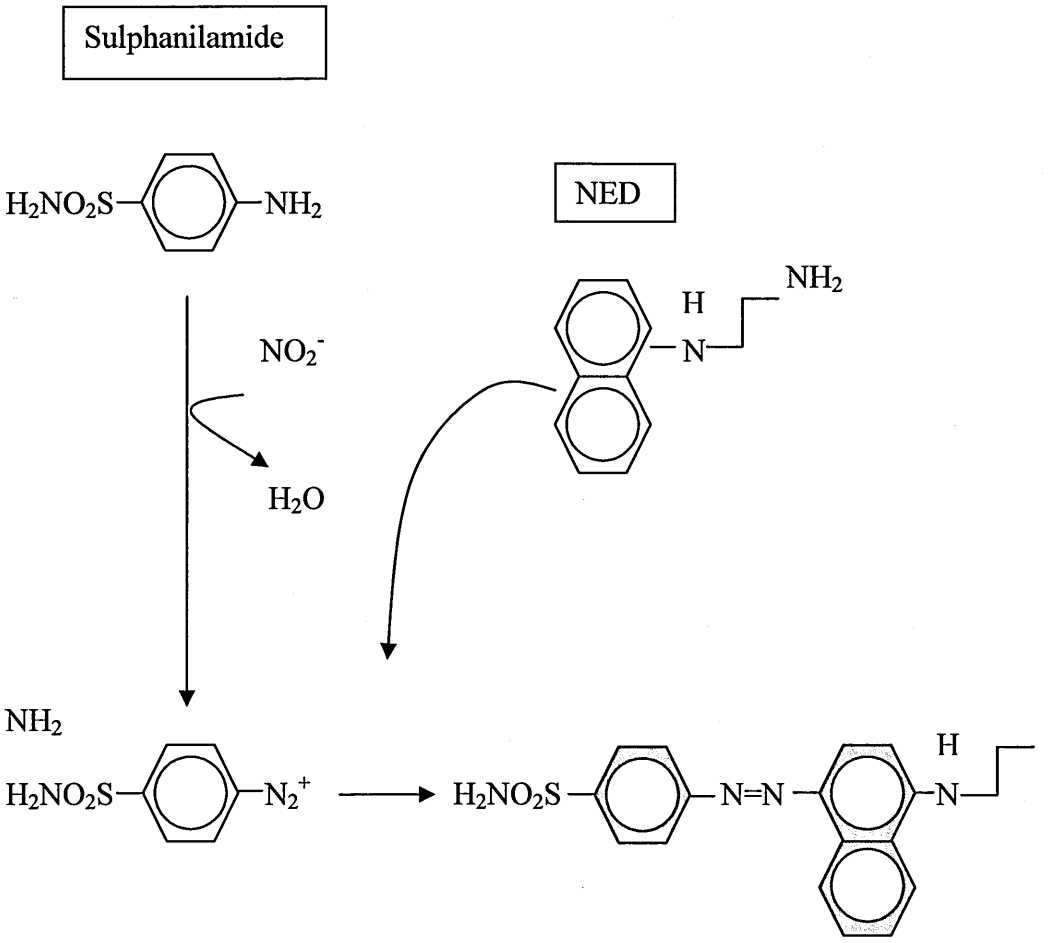

Figure 2.1. The Griess reaction.

Levels of NO are determined by measurement of nitrite (NO_2^-), a stable end product of NO breakdown. Addition of sulphanilamide and *N*-1-napthylethylenediamine dihydrochloride (NED) under acidic conditions creates a colorimetric change that is measurable at an absorbance of 540 nm.

2.2. Viral titrations

2.2.1. Cell culture infected macrophages

Macrophages at a concentration of $1x10^6$/ml were left to adhere overnight at 37°C in 24-well plates in 1 ml volumes. The following day, suspensions of VACV (strain IHD) were prepared in cell-line specific medium at a concentration of 5×10^6 plaque-forming units per ml (pfu/ml) and used to infect macrophages in triplicate. Briefly, 400 µl of medium were removed from each well and 100 µl viral suspension added and incubated for 1 hour at 37°C. After 1 hour, 500 µl of cell supernatant were removed from each well and cells washed twice with 500 µl PBS. Following the second wash, 1 ml of fresh medium was added to each well and plates re-incubated at 37°C with this point serving as time 0 hours in the infection timeline. At specific time points, plates were removed from the incubator and placed immediately into a -20°C freezer to stop the infection process.

2.2.2. Viral titre calculation

Plates were removed from the freezer, thawed and then cells scraped from the bottom of wells using a pipette tip. Triplicate wells were then merged into a 3 ml Dounce homogeniser. Wells were then washed with 100 µl PBS to ensure maximum recovery of virus and cellular debris. Cells were then homogenised with between 20-30 strokes to release the viral progeny. Homogenates were then poured into 15 ml falcon tubes and centrifuged for 10 minutes at 2000 revolutions per minute (rpm) to pellet the cell debris. Once pelleted, 2 µl aliquots of viral supernatants were added to one column of a 96-well plate containing 200µl of DMEM with 2% FCS. Remaining viral supernatant was stored at -20°C in fresh tubes for further analysis. A 1:10 dilution series of the clarified suspension was prepared across a 96-well plate using DMEM

with 2% FCS as the diluent; each dilution occupied a column of 8 wells. Once complete, 100 µl were transferred from each well and used to infect 5 x 10^4 RK13 cells/well in DMEM 2% FCS in 96-well plates. Assay plates were incubated at 37°C for 48 hours before being fixed with formal saline for a minimum of 4 hours. Finally, formal saline was then removed and cells stained with 1.5% filtered crystal violet to determine viral titres using the Reed-Müench method (Reed & Muench, 1938).

2.3. Reverse transcription polymerase chain reaction (RT-PCR)

2.3.1. RNA isolation from macrophage cell-lines and primary macrophages

Total RNA from macrophage cell-lines and primary alveolar macrophages was isolated using Ambions RNAqueous® phenol-free isolation kits. MH-S and J774 cell macrophages were grown in 96-well plates and assayed in triplicate. Preparation of cell lysates was achieved through removal of culture supernatants and addition of 250 µl of RNAqueous® lysis solution containing guanidinium isothiocyanate (Chomczynski & Sacchi, 1987) to each well. Adherent cells were scraped from the bottom of wells using a pipette tip. Triplicate wells were then merged to provide a 700 µl sample of cell lysate and mixed with 64% ethanol as described in manufacturer's instructions. Samples were then centrifuged for 15 seconds through a filter cartridge into a collection tube at 12000 rpm to bind RNA to the glass fibres in the filter as described by Boom and colleagues and Marko (Boom *et al.*, 1990; Marko *et al.*, 1982). Sample flow through was discarded and any remaining sample passed through the same filter cartridge to bind residual RNA. Bound RNA was then washed three times with 2 wash solutions, the first containing guanidinium isothiocyanate to denature residual RNAses and the second an 80% ethanol based solution to further

remove contaminants. After washing, RNA was finally eluted in 2 x 50 µl low ionic strength elution buffer pre-heated to 75°C.

2.3.2. DNA-free treatment

Extracted RNA samples were all treated using Ambion's TURBO DNA-free™ kit to remove traces of contaminating DNA. This involved addition of a one tenth sample volume of 10X TURBO DNase buffer to the RNA along with 2 µl (4 units) TURBO DNase, followed by a 30 minute incubation step at 37°C. Inactivation of TURBO DNase and removal of divalent cations was achieved through mixture of sample with 0.1 x volume of DNase inactivation reagent for 2 minutes at room temperature. Samples were then centrifuged at 12,000rpm for 1 minute and the DNA-free RNA supernatant transferred to a fresh tube.

2.3.3. RNA purification

RNA samples were subjected to an additional purification step to purify and concentrate RNA using the RNeasy® MinElute™ cleanup kit (Qiagen, UK). Briefly, samples were mixed with a guanidine salt buffer containing 0.01 x volume of β-mercapto-ethanol (β-ME) and 100% ethanol, and then passed through a centrifuge column containing a silica-gel membrane at 12,000 rpm for adsorption of RNA. Contaminants were washed away using 2 separate ethanol wash solutions in 30 second 12,000 rpm centrifuge steps prior to a 5 minute spin to dry the column and subsequent elution of RNA in 20 µl of RNA-free water. Sample purification was validated using 1 µl of pre and post-treated RNA on the Agilent 2100 Bioanalyzer using the Agilent RNA 6000 Nano-assay kit (Figure 2.2) and also on the NanoDrop® ND-1000 spectrophotometer (NanoDrop,UK).

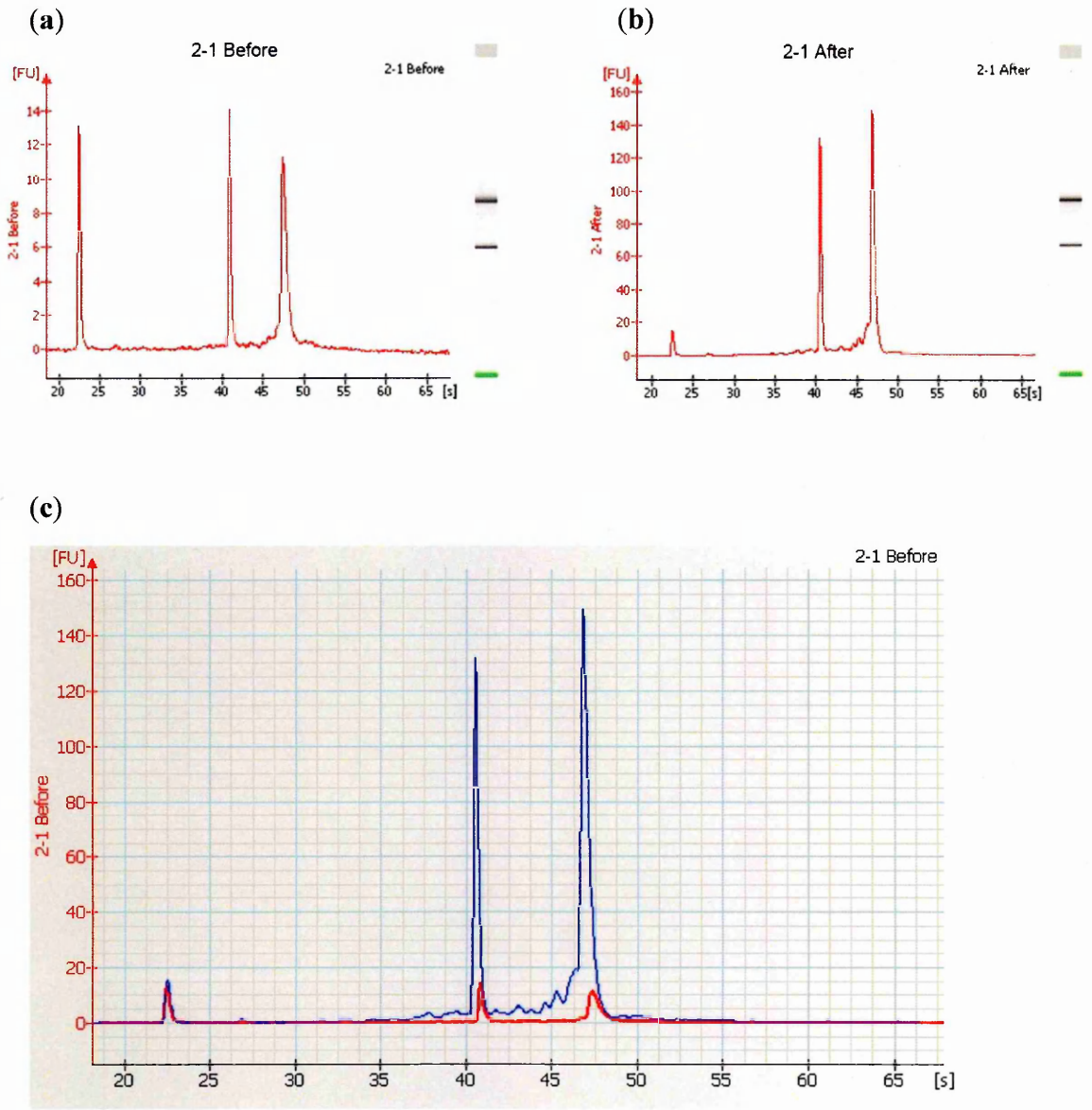

Figure 2.2. Typical bioanalyser analysis of RNA samples.

Figure shows RNA before (**a**), and after (**b**), purification with Qiagen MinElute kit. Peaks and bands represent 28s and 18s components of RNA. A typical overlap of RNA peaks pre- and post-purification is also represented (**c**).

Before purification

After purification

2.3.4. Reverse transcription

Purified RNA was reverse transcribed into complementary DNA (cDNA) using the Qiagen Omniscript® reverse transcription (RT) kit. Template RNA was combined with 10x buffer RT, 5 mM of 2'deoxy-nucleotide-5'-triphosphates (dNTPs), 4 U Omniscript® reverse transcriptase and RNase-free water (all Qiagen, UK components), along with 40 U RNase inhibitor (Ambion, UK) and 20 µg random primers (Promega,UK). The reaction mixture was incubated at 37°C for 60 minutes and cDNA stored at -20°C or processed immediately.

2.3.5. Relative quantitation of gene expression

All gene expression assays were acquired from Applied Biosystems (ABI) 'Assays-on-Demand' service and all samples were assayed in triplicate on the Taqman® 7000 machine using the protocol shown in Figure 2.3. Each gene expression assay consisted of a FAM™ dye labelled Taqman® minor groove binder (MGB) probe formulated at a final concentration of 250 nM, and two unlabelled PCR primers formulated at 900 nM concentration in a single 20x assay tube. The specifics of RT-PCR are detailed below in Figure 2.4. 18s eukaryotic RNA was used throughout as an endogenous control and relative quantitation of gene expression was calculated using the delta delta cycle threshold method ($2^{-\blacktriangle\blacktriangle ct}$) as described by Livak (Livak & Schmittgen, 2001). All samples were run in a final reaction volume of 25 µl comprising of 1.25 µl Taqman® gene expression assay (20x), 12.5 µl Taqman® universal PCR master mix, no AmpErase uracil-N-glycosylase (UNG), 9.25 µl of RT-PCR grade water and 2.0 µl cDNA sample, and all analyses were performed using ABI Prism 7000 sequence detection system (SDS) software (Figure 2.5).

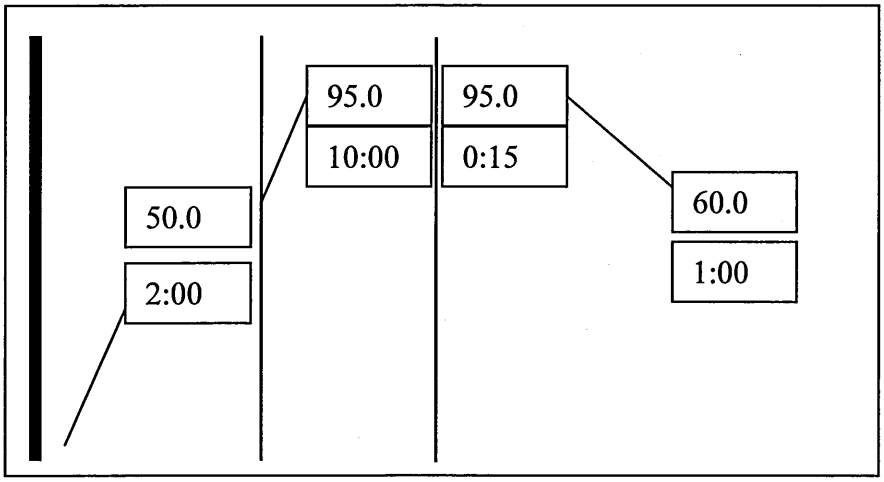

Stage:	1	2	3
Replicates:	1	1	40

Key: Temperature (°C) | Time (minutes)

Figure 2.3. Universal thermocycler PCR reaction programme: (Applied Biosystems 9600 Emulation).

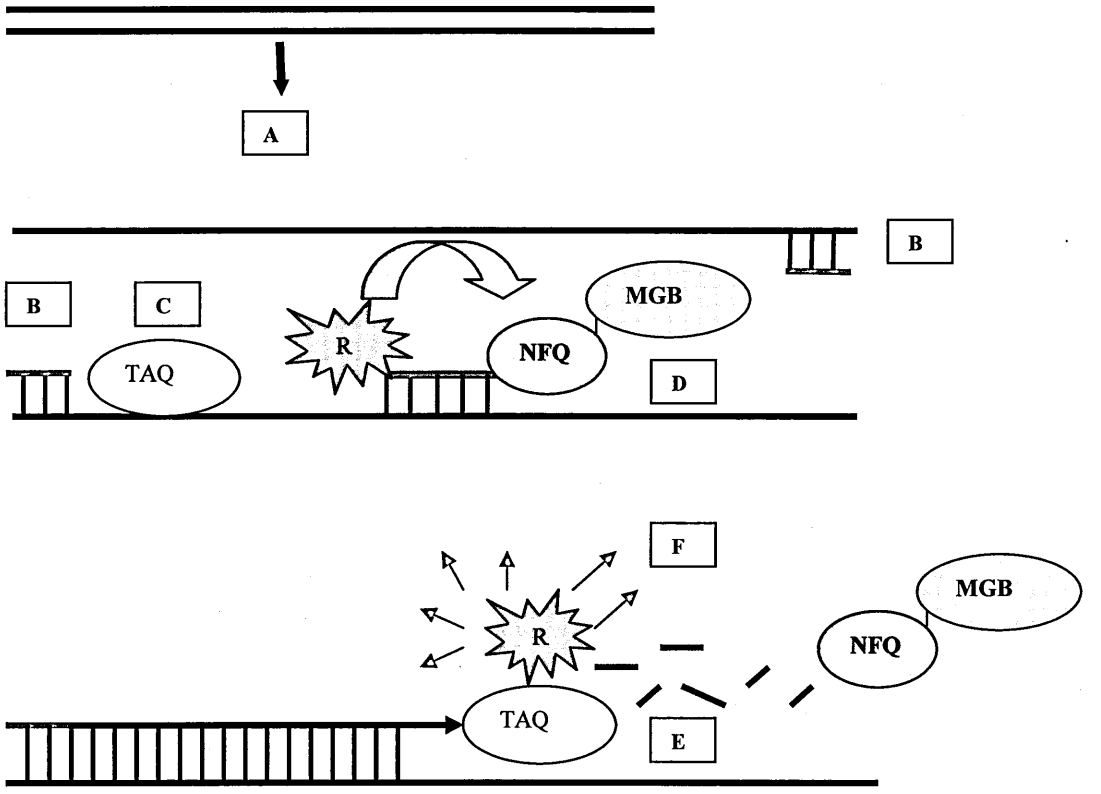

Figure 2.4. Real-time PCR and fluorescence resonance energy transfer (FRET) technology.

Following reverse transcription, double stranded cDNA is denatured (**A**) and acts as a template in the initial steps of the RT-PCR reaction. Forward and reverse primers at a final concentration of 900nM bind to the cDNA (**B**), along with an ABI AmpliTaqGold® (TAQ) DNA polymerase (**C**) and assay specific Taqman® minor groove binder (MGB) probe (**D**) featuring a 5' reporter (R) dye (such as 6-FAM) and non-fluorescent quencher dye (NFQ) at the 3' end. The 5' nuclease activity of TAQ allows cleavage of the Taqman® MGB probe (**E**) resulting in dissociation of the reporter dye from the quencher and subsequent increase of reporter fluorescence (**F**). Signal increases exponentially throughout the reaction as PCR products accumulate.

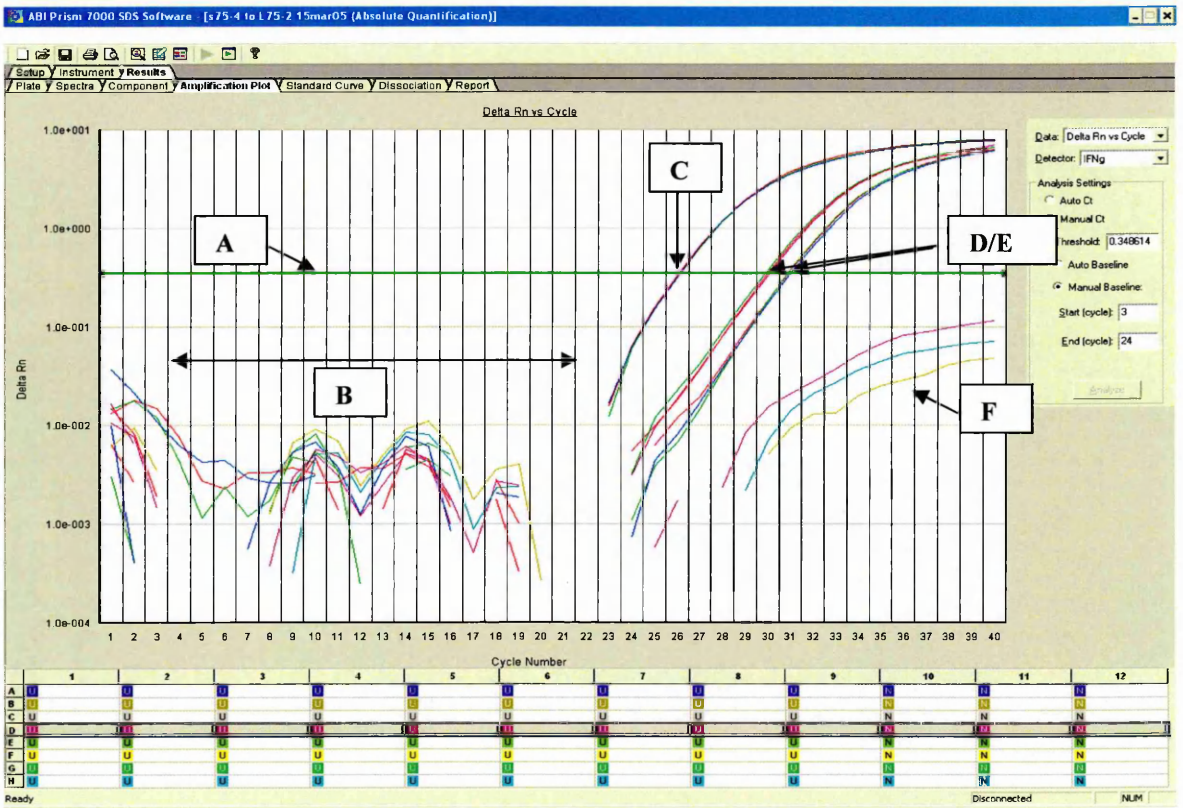

Figure 2.5. Detection of reporter signal by ABI Prism 7000 SDS software.

Relative quantitation of gene expression requires setting of a threshold level (**A**) during the exponential phase of the PCR reaction. A baseline level is set (**B**) to ignore non-specific detection of signal prior to specific gene amplification. An endogenous control gene such as 18sRNA (**C**) is included in each reaction and expression of target genes (**D/E**) are calculated relative to its cycle threshold (ct) value, obtained from the point at which its fluorescence crosses the threshold level. Sample wells with water and no cDNA template (**F**) are run as negative controls.

2.4. Cytokine analysis *via* protein detection

2.4.1. BD™ cytometric bead array (CBA)

Protein levels of specific cytokines were measured using BD™ cytometric bead array (CBA) technology on a BD™ FACScan flow cytometer. All samples were analysed using the BD™ mouse inflammation kit. Equal volumes of mouse inflammation capture beads (10 µl/test) specific for the inflammatory cytokines IL-12p70, IL-6, IL-10, CCL2, TNF-α and IFN-γ were pooled and a 50 µl cocktail combined with 50 µl of sample supernatant and 50 µl PE detection reagent in single 12x75 mm polypropylene tubes or 96-well plates. Samples were incubated for 2 hours at room temperature in the dark and were then washed in 300µl BD™ wash buffer, centrifuged for 5 minutes at 200g and resuspended in 300 µl BD™ wash buffer with 4% paraformaldehyde prior to analysis. Standard curves were run as a reference in each experiment ranging from 0-5000 pg/ml using 1 vial of reconstituted mouse inflammation standards (Figure 2.6). Relative concentrations of sample cytokine concentrations were determined using the BD CBA software.

2.4.2. IFN-α sandwich enzyme linked immunosorbent assay (ELISA)

Protein levels of mouse IFN-α were measured using a sandwich immunoassay using a mouse specific IFN-α kit obtained from PBL Biomedical Laboratories (USA). Mouse sera or tissue supernatants were obtained from whole blood or homogenised animal tissue following centrifugation at 10,000 rpm for 10 minutes. Samples were either frozen at -20°C or processed immediately. Microtitre plates (96-wells), pre-coated with IFN-α capture monoclonal antibody were supplied ready for use. Experimental samples were added in duplicate in 100 µl quantities alongside a reference standard curve (0-500 pg/ml) constructed using the National Institute of Health's (NIH)

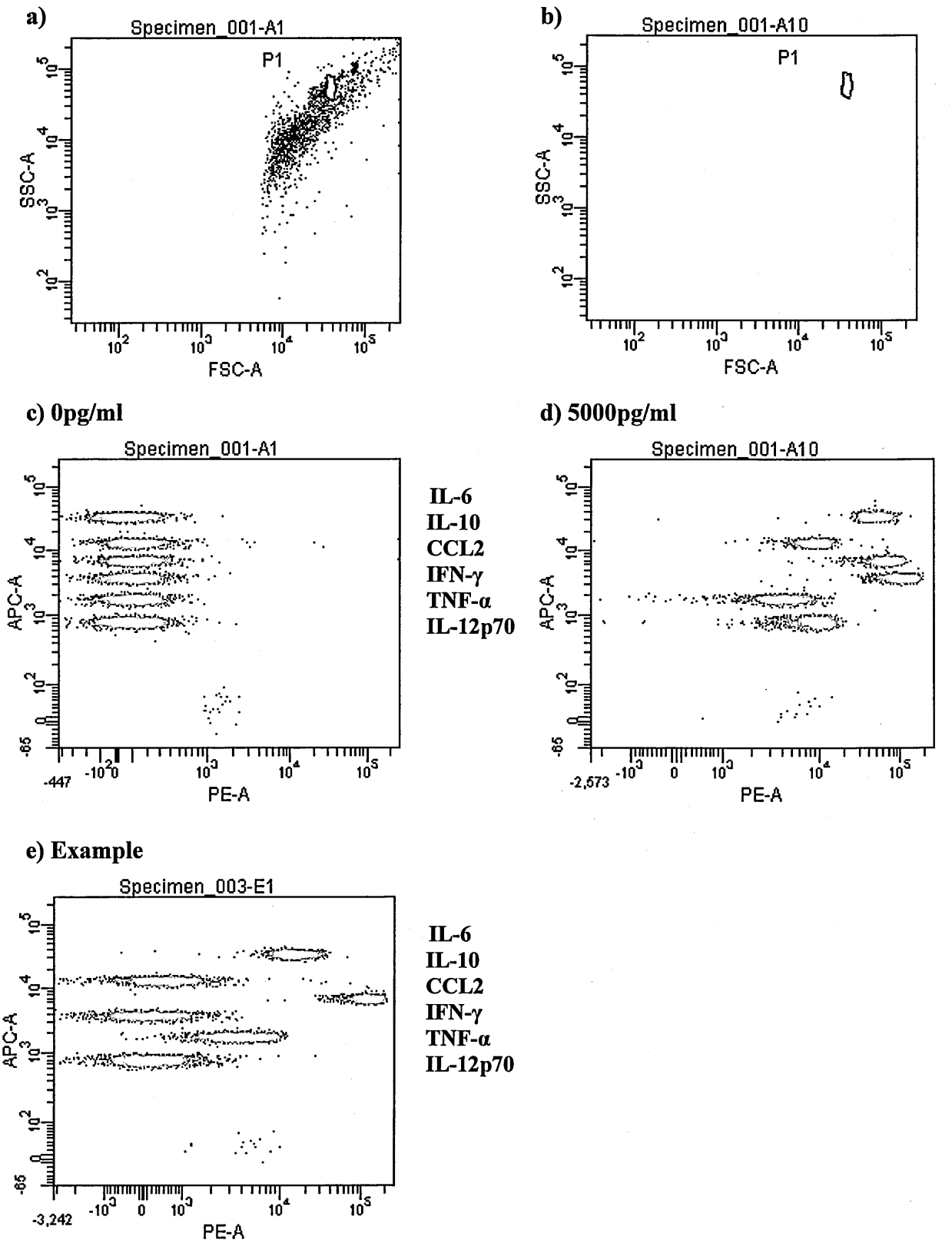

Figure 2.6. Cytokine quantification through CBA protein detection.
(a) Supernatant samples are run through a flow cytometer and cytokine specific capture beads identified using FSC:SSC. **(b)** Data is filtered using FCAP software and quantification determined using standards run from 0pg/ml **(c)** to 5000pg/ml **(d)**. Example specimen positive for IL-6, CCL2 and TNF-α **(e)**.

international reference standard for mouse IFN-α (Pestka, 1986) and dilution buffer containing 0.1 g/L thiomersal to act as a preservative. Plates were then sealed with a plastic cover and incubated at room temperature for 1 hour in a sealed container. Secondary antibody concentrate was then diluted 1:20 with dilution buffer as recommended by the manufacturer's instructions (50 µl into 950 µl) making a secondary antibody stock solution. This stock solution was used at a ratio of 12.5 µl stock solution per 1 ml dilution buffer as required (e.g. 25 µl antibody stock solution to 2 ml dilution buffer) to make a secondary antibody working solution. After 1 hour incubation, plates were washed once with wash solution, tapped dry onto absorbent lint-free paper and then incubated for 24 hours with 100 µl mouse IFN-α secondary antibody solution per well at room temperature in a sealed container. Plates were then washed three times with wash solution, tapped dry and each well incubated with 100 µl horseradish peroxidise (HRP) enzyme conjugate solution for 1 hour at room temperature and then washed four times with wash solution. Once dry, plates were incubated with 100 µl of tetramethyl-benzidine (TMB) as a substrate for 15 minutes at room temperature in the dark. This reaction was stopped by addition of 100 µl stop solution and read immediately on a Thermolab multiscan plate reader using Ascent software 2.4.2 (Thermolab systems, UK) at a wavelength of 450 nm. Concentration of mouse IFN-α in the samples was determined *via* extrapolation from the reference curve specific for each plate.

2.5. Flow cytometry

Cells obtained from mouse lung and tissue samples were analysed on either BD FACScan™ or BD FACSCanto™ II flow cytometers, using CellQuest Pro software or FACSDiva respectively. Organs were homogenised using a sterile sieve and

plunger with 1 ml of PBS into one well of a 6-well plate. Homogenised samples were then centrifuged at 4,000 rpm for 5 minutes to pellet cells. Supernatants were frozen at -20°C for analysis *via* ELISA or CBA. Pelleted cells were then resuspended in 5 ml flow buffer (PBS with 2% FCS), carefully layered over 3 ml of lymphocyte separation medium (LSM®, ICN/Cappel), then centrifuged at 800g for 30 minutes to separate red blood cells, mononuclear cells and plasma. Following centrifugation, the central lymphocyte layer was removed and made up to 10 ml with flow buffer. Samples were then centrifuged at 200g for 10 minutes to pellet cells then resuspended in flow buffer.

2.5.1. Antibody staining

Antibody specific for CD32/CD16 (BD Biosciences, UK) was added to each sample at a ratio of 2 µl per 10^6 cells to prevent non-specific binding of antibody to the common antibody chain receptors present on immune cells (BD fragment crystallisable (Fc) block™). After mixing, samples were incubated at 4°C for 5 minutes, then 100 µl sample was incubated for 30 minutes in 12x75 mm polypropylene tubes or 96-well plates at room temperature with appropriate antibody cocktails specific for cell identification and activation markers. After staining, cells were washed in 1 ml of flow buffer, centrifuged at 4000 rpm for 5 minutes, and resuspended in either flow buffer with 4% paraformaldehyde or BD fixation solution (containing 3% paraformaldehyde) to preserve antibody conjugations. Prior to analysis, cells were incubated overnight at 4°C. Isotype controls specific to each antibody isotype were run alongside each experiment along with unstained and single stained control samples. 50 µl of flow-count fluorospheres (Beckman Coulter, UK)

were added to each sample immediately before reading to allow determination of absolute cell counts whenever possible.

2.5.2. Apoptosis measurement

Macrophage cell-lines were assessed for apoptosis using a BD Pharmingen™ Annexin-V apoptosis kit. Briefly, macrophages were grown overnight in 6-well plates at a concentration of $1x10^6$/ml overnight at 37°C to allow cells to adhere. Cell supernatants were then removed and either replaced with fresh medium or stimulated with CpG at the desired concentration for 24 hours at 37°C. Cells were then washed twice in cold PBS and resuspended in calcium binding buffer (as per instructions) at a concentration of $1x10^6$/ml. A 100 µl aliquot ($1x10^5$ macrophages) was then incubated with 5 µl of Annexin-V antibody conjugated to PE and 5 µl of 7-Amino-Actinomycin D antibody conjugated to APC. Cells were incubated for 15 minutes at room temperature in the dark and then washed with 1 ml of PBS. Cells were resuspended in 400 µl of calcium binding buffer and read *via* flow cytometry immediately.

2.6. Animals and infection

2.6.1. Sources of animals

All animal experiments were conducted in accordance with the Scientific Procedures Act 1986, under both personal and project licences issued by the Home Office. Adult female Balb/C mice (6-8 weeks old) were obtained from Charles River laboratories (Kent, UK) and genetic B-cell knock-out mice on a Balb/C background were obtained from Taconic (USA), model number 001487-MM.

2.6.2. Infection with VACV strain IHD

Mice were infected with VACV strain IHD in 10 µl volume *via* the intranasal route according to experimental design. Previous studies in house had established the MLD of VACV to be $5x10^4$ pfu/ml. Mice were monitored daily at regular intervals throughout infection periods and clinical signs of infection recorded thoroughly. Humane endpoints were enforced throughout all experiments, as governed by a 30% decrease in body weight, blindness or severe respiratory distress as has been previously described (Pulford *et al.,* 2004).

2.6.3. CpG and PBS dosing

Mice were dosed with varying concentrations of CpG, made up in 50 µl volumes of PBS, *via* intramuscular, intranasal, sub-cutaneous or intra-peritoneal routes, according to experimental design. Control mice were given an equal volume of PBS *via* the same route.

2.6.4. Bronchoalveolar lavage collection and staining

Lung lavage samples were obtained from Balb/C as described by Maxeiner and colleagues (Maxeiner *et al.*, 2007). Five volumes of PBS (0.2 mls) were injected through mouse tracheal tubes using a syringe, recovered and placed in a glass vial and stored temporarily at 4°C. Macrophage purity of lavage samples was determined through immunohistological staining. Briefly, 0.5 ml of pooled lavage sample was centrifuged onto a microscope slide using a Shandon cytospin (Thermo Scientific, UK) for 10 minutes at 1800 rpm. Once dry, slides were placed into a mechanical rack and stained using the Hema 'Gurr' rapid staining set for haematology as detailed in

Table 2.2. Slides were then air-dried and analysed beneath a light microscope at either x 400 or x 1000 magnification.

2.6.5. Alveolar macrophage purification

Pooled lavage samples were centrifuged at 400g for 5 minutes and resuspended in 1ml of endotoxin-free RPMI 1640 medium with 2mM L-glutamine containing 10% FCS, 100 U/ml penicillin, and 100 μg/ml streptomycin. Cells were then placed into wells of a 96-well plate to allow cells to adhere overnight. The following morning, supernatants were removed and wells washed to remove any non-adherent cell types. Adherent cells were then stimulated with CpG or lysed using the method detailed in section 2.3.1 for isolation of total RNA.

2.6.6. Neutrophil ablation

Neutrophil ablation was achieved using the monoclonal antibody RB6-8C5 (RB6) (Chemicon Europe) that binds specifically to Gr-1. Prior to use, stock concentration of antibody was diluted to 1 mg/ml and 500 μg administered intraperitonealy one day prior to VACV infection. An IgG2b isotype control monoclonal antibody (Mac-5) was used alongside RB6 in the neutrophil ablation study as a non-specific control.

2.6.7. Technical assistance

All animal handling, infections and dissections throughout this thesis were conducted by trained colleagues and not in any part by me. As such, their invaluable assistance and help throughout, needs to be acknowledged.

Step	Solution	Task
1	Fixing solution (Buffered methanol)	5 x 1s dunk
2	Staining solution 1 (Buffered Eosin)	3 x 1s dunk
3	Staining solution 2 (Buffered Methylene Blue)	6 x 1s dunk
4	Buffer solution 7.2	45s

Table 2.2. The Hema Gurr rapid staining procedure. Samples fixed upon microscope slides were stained for haematological analysis.

* s – second(s)

2.7. Statistical Methods

Two statistical packages were used to analyse data obtained throughout this thesis. Two-way analysis of variants (ANOVAs) with Bonferroni's post-test corrections, and Kaplan-Meier log rank survival analyses were performed using GraphPad Prism® 4 software (GraphPad, USA). All other statistical tests employing three or four parameter general linear analysis, with Bonferroni's post-tests, were conducted using Minitab® Release 14. All mean values quoted or depicted graphically represent the geometric mean of samples unless otherwise stated.

Chapter 3: The prophylactic use of CpG-B 7909 against VACV

3.1. Introduction

The immunostimulatory properties of CpGs have led to their use in a variety of different therapeutic applications (section 1.2.7). An extensive number of studies have investigated CpGs against a range of different infectious diseases caused by bacterial, parasitic and viral pathogens. The results of these studies against infectious diseases have varied greatly with the type of CpG used, the route of administration, and also the timing of CpG delivery.

3.1.1. CpG prophylaxis and bacterial infection

CpG treatment against bacterial pathogens has achieved protection in a number of murine models resulting in the alleviation of clinical signs of disease and reduction in bacterial loads. For instance, intraperitoneal CpG treatment of mice prior to infection with *Francisella tularensis* live vaccine strain (LVS) and *Listeria monocytogenes* has been shown to confer complete protection against infection (Elkins *et al.*, 1999b). Here, mice treated with a single dose of CpG or bacterial DNA between 3 and 7 days prior to infection with lethal doses of bacteria all survived infection. Additionally, pre-treatment of mice with CpG 10 days and 14 days prior to infection with *Francisella tularensis* (LVS strain) was still able to confer 80% and 40% levels of protection respectively (Elkins *et al.*, 1999b). Following on, studies by Klinman and colleagues demonstrated that this level of protection could be maintained indefinitely against both *Francisella* and *Listeria* with repeated CpG dosing at regular 2-weekly intervals (Klinman *et al.*, 1999). Protection against *Burkholderia pseudomallei* has also been demonstrated using CpGs (Wongratanacheewin *et al.*, 2004). In these

studies, high levels of protection (90-100%) were observed when mice were pre-treated with CpG between 10 and 2 days prior to infection. These high levels of protection were associated with attenuated levels of the pro-inflammatory cytokine IFN-γ as well as significant reductions in bacterial burdens. Mice were still protected to a lesser extent (57%) when pre-treated 15 days beforehand with CpG. Interestingly, these results were obtained using an intramuscular dose of CpG against an intraperitoneal infection. Studies have also demonstrated protection against *Burkholderia mallei*, a close relative of *Burkholderia pseudomallei* (Waag *et al.*, 2006). This study investigated the effect of two different classes of CpGs (CpG-A and CpG-B) and demonstrated a clear difference in their protective capacity against aerosol infection with *Burkholderia mallei*. Intraperitoneal CpG administration with the B-class CpG-B 7909 two days prior to infection was shown to confer complete protection against lethality and restricted bacterial growth in both the lungs and spleens of infected mice. This level of protection dropped slightly to 90% when mice were treated on the day of infection but plummeted to 10% when treated 24 hours post-infection. The A-class CpG 2216 did not confer any protection against *Burkholderia mallei* (Waag *et al.*, 2006). Intratracheal CpG treatment of mice infected with *Klebsiella pneumoniae* has also proven effective with 80% of infected mice surviving lethal infection when pre-treated two days before bacterial infection (Deng *et al.*, 2004). This study reported rapid increases in neutrophil, NK cell and T-lymphocyte numbers in the lung and increases in a variety of type-1 cytokines including TNF-α, IL-12 and IFN-γ. Once again, administration of CpG resulted in significant reductions of bacterial burdens in key organs such as the lung and also reduced bacteraemia in the blood. Systemic administration of CpG has also been shown to have therapeutic value in pulmonary tuberculosis, reducing lung

inflammation and mycobacterial growth potentially *via* an IFN-γ dependent mechanism (Juffermans *et al.*, 2002).

3.1.2. CpG prophylaxis and parasitic infection

Protective responses have also been reported against parasitic infections. Treatment of mice with CpG-B 1826 up to 48 hours prior to challenge with *Plasmodium yoelii* sporozoites, a causative agent of murine malaria, conferred sterile protection against infection (Gramzinski *et al.*, 2001). These studies associated this sterility with early and rapid increases in levels of IFN-γ and IL-12. CpG administration 7 days prior to challenge was also able to prevent infection in 60% of cases whereas CpG treatment on the day of challenge failed to prevent infection. In contrast, treatment with CpG 2 hours prior and 10 hours after challenge with *Leishmania major* afforded long-term protection (up to 22 weeks) against disease (Zimmermann *et al.*, 1998b). CpG-mediated protection against parasitic infection may be due to the prevention of the Th-2 mediated disease profile associated with many parasitic infections. In this way, therapy possibly echoes that seen in the treatment of allergic responses which also benefit from the skewing of the immune response to a Th-1 profile.

3.1.3. CpG prophylaxis and viral infection

CpGs have also been assessed for their prophylactic or therapeutic value against a number of viral pathogens both *in vitro* and in a number of animal models. Many studies have utilised the adjuvant effects of CpGs in the treatment of viruses such as HBV (Halperin *et al.*, 2003), VACV (Belyakov *et al.*, 2006), lymphocytic choriomeningitis virus (LCMV) (Vabulas *et al.*, 2000) and influenza (Cooper *et al.*, 2004). CpGs have also been studied for their direct antiviral properties. Recent *in*

vitro studies have suggested CpGs may be effective against severe acute respiratory syndrome (SARS) (Bao *et al.*, 2006). In these studies, supernatants from human PBMCs stimulated with CpG were shown to significantly protect epithelial cells from SARS-CoV infection. Other *in vitro* studies have suggested that co-culture of PBMCs with CpGs can inhibit hepatitis B virus replication (Li *et al.*, 2006). In animal models, many studies using CpGs as a monotherapy have been able to demonstrate increased levels of protection. Studies in C57BL/6 mice have shown that intravaginal delivery of CpG prior to infection with HSV-2 can confer complete protection against lethality when given 24 hours prior to infection (Sajic *et al.*, 2003; Ashkar *et al.*, 2003) and confer 90% protection when given 48 hours before infection (Harandi *et al.*, 2003). These studies were all able to demonstrate significant reductions in viral titres and minimal vaginal pathology in pre-treated animals. Interestingly, altering the route of CpG delivery in these studies also resulted in a loss of protection, suggesting that the local delivery of CpG could be important against viral infection. In neonatal mice, studies have shown CpG administered on the day of infection was able to protect against a lethal challenge with the neurotrophic tacaribe arenavirus (TCAV) (Pedras-Vasconcelos *et al.*, 2006). Here, CpG-treated neonates were shown to have reduced viral titres in the brain following systemic administration of CpG. However, once again the level of protection afforded varied according to the route of CpG and virus delivery. This was evident from results showing that intraperitoneal CpG delivery conferred 52% protection against intraperitoneal virus infection, whereas intranasal dosing of CpG failed to confer any protection against intraperitoneal infection. Indeed, local delivery of the B-class CpG-B 7909 has been shown to protect against intranasal VACV infection in a Balb/C mouse model of infection (Rees *et al.*, 2005). Results from this study suggested that CpG-B 7909 administered up to 7 days prior to

infection could provide complete protection against lethality. This study also reported a reduction in viral titres in the brain, spleen and lungs of infected mice and an increase in the levels of chemokines such as RANTES and MIP-1β. In addition, this study also examined the use of CpG-A 1585 as a prophylactic against VACV and found that complete protection was also achieved if given by the intranasal route. This protection relied upon substanially higher doses of CpG and failed to reduce disease morbidity (measured by weight loss) as effectively as CpG-B (Rees *et al.,* 2005).

3.2. Aims of this chapter

The pre-treatment of mice prior to challenge with infectious pathogens has achieved success in a variety of bacterial, parasitic and viral infections. These include the use of both CpG-A 1585 and CpG-B 7909 against VACV. In these preliminarly studies with VACV, CpG-B 7909 proved most effective in conferring protection (Rees *et al.,* 2005). In addition, the early release of chemokines like RANTES and MIP-1β following CpG-B 7909 administraion suggest that components of the innate immune system play a key role in CpG mediated protection against VACV infection (Rees *et al.*, 2005). More detailed studies are therefore required to understand the roles and function of cells of the innate system during CpG-B mediated protection against VACV infection. In this chapter, an immunological analysis of the kinetics of the innate immune response, after local delivery of CpG is investigated.

3.3. Results

3.3.1. Experimental outline

The *in vivo* responses of animals pre-treated with the B-class CpG-B 7909 were compared against those given a control PBS dose. Two groups of six-eight week old female Balb/C mice were pre-treated with 75 μg CpG-B 7909 intranasally or PBS three days prior to intranasal infection with 10 MLD VACV. Groups of mice (n=4) from both treatment groups were humanely culled prior to infection on day 0, and thereafter on days +1, +3, +5, +7 and +9 post-infection, for comparative immune analyses. Cytokine analyses of lung, spleen and serum preparations for the pro-inflammatory cytokines TNF-α, IL-6, IFN-α and IFN-γ, along with the chemokine CCL2 and anti-inflammatory cytokine IL-10 were determined throughout the course of the experiment. The expression of key activation markers on macrophages, neutrophils, DCs, NK cells, B-cells and T-cells in the lungs and spleens of mice were enumerated by flow cytometry.

3.3.2. Cytokine responses in the lung

The levels of the pro-inflammatory cytokines and chemokines measured in the lungs of mice pre-treated with CpG-B 7909, all differed significantly from PBS control mice throughout the early stages of infection. Over the first 3 days of infection, levels of TNF-α (Figure 3.1a), IL-6 (Figure 3.1b), and IFN-α (Figure 3.1c) were all expressed in significantly higher quantities in the lungs of CpG-B 7909 treated mice ($p<0.001$). Levels of IFN-γ (Figure 3.1d) and CCL2 (Figure 3.1e) were also significantly greater in CpG-treated animals on days 0 and +1 ($p<0.001$) and day +3 (IFN-γ $p<0.01$; CCL2 $p<0.05$). By day +5, only pro-inflammatory TNF-α ($p<0.05$) and IFN-α ($p<0.05$) levels were significantly higher than those measured in the PBS

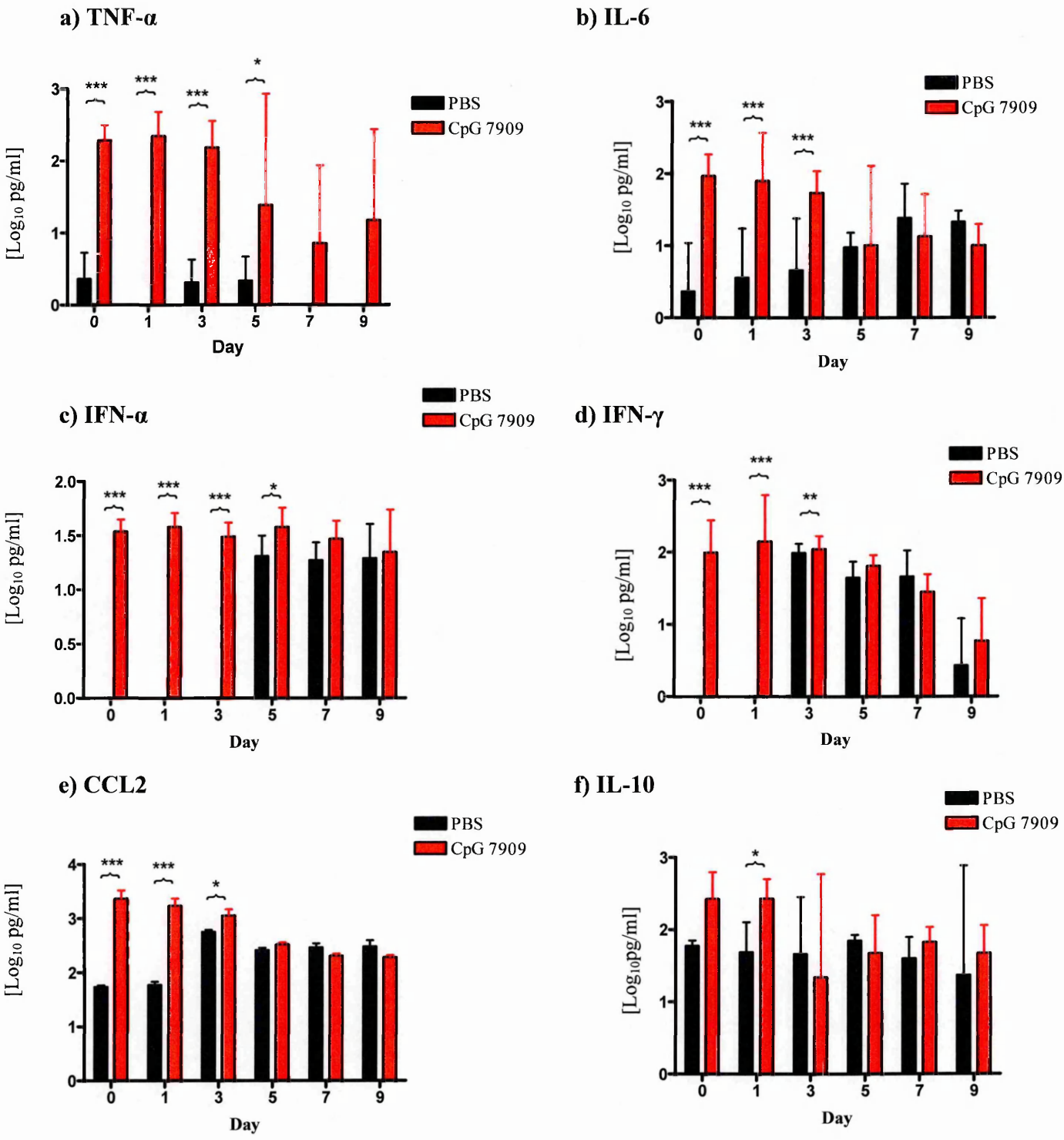

Figure 3.1. Measurement of lung cytokine levels in Balb/C mice pre-treated with either CpG-B 7909 or PBS throughout infection with VACV. Protein levels determined *via* CBA analysis or IFN-α elisa. Bars represent the geometric mean of four mice (Log_{10} pg/ml) and error bars indicate 95% confidence intervals for cytokines **(a)** TNF-α; **(b)** IL-6; **(c)** IFN-α; **(d)** IFN-γ; **(e)** CCL2; **(f)** IL-10. Statistical significance was determined using a two-way ANOVA and Bonferroni's post-tests. Significant findings between treatment groups are represented as * ($p<0.05$), ** ($p<0.01$) and *** ($p<0.001$).

control group. Beyond this, no significant differences between treatment groups were found in any of the cytokines or chemokines measured. The anti-inflammatory cytokine IL-10 was also elevated in the lungs of CpG-B 7909 pre-treated mice during the early stages of infection (Figure 3.1f). In contrast to the pro-inflammatory cytokines, levels of IL-10 only differed significantly from control levels on day +1 of infection ($p<0.05$).

3.3.3. Cellular responses in the lung

3.3.3.1. Lung macrophage responses

Antibody specific to the mouse macrophage cell marker F4/80 was used to label macrophages from lung cell suspensions. The activation status of macrophages at each time point was determined *via* the expression of CD54 and MHC class II molecules (IA/IE) on the surface of F4/80 positive cells.

Figure 3.2a shows the total number of $F4/80^+$ cells in the lungs of mice pre-treated with CpG-B 7909 and those pre-treated with PBS. Total macrophage numbers were significantly higher in CpG-treated individuals than in PBS treated mice throughout infection ($p<0.001$), but followed the same trend over time regardless of treatment group. The most significant difference in the level of macrophage numbers was seen 24 hours post infection ($p<0.001$). Increases in total macrophage cell numbers were accompanied by an increase in the number of activated cells as indicated by the number of macrophages expressing CD54 (Figure 3.2b) and macrophages expressing IA/IE (Figure 3.2c).

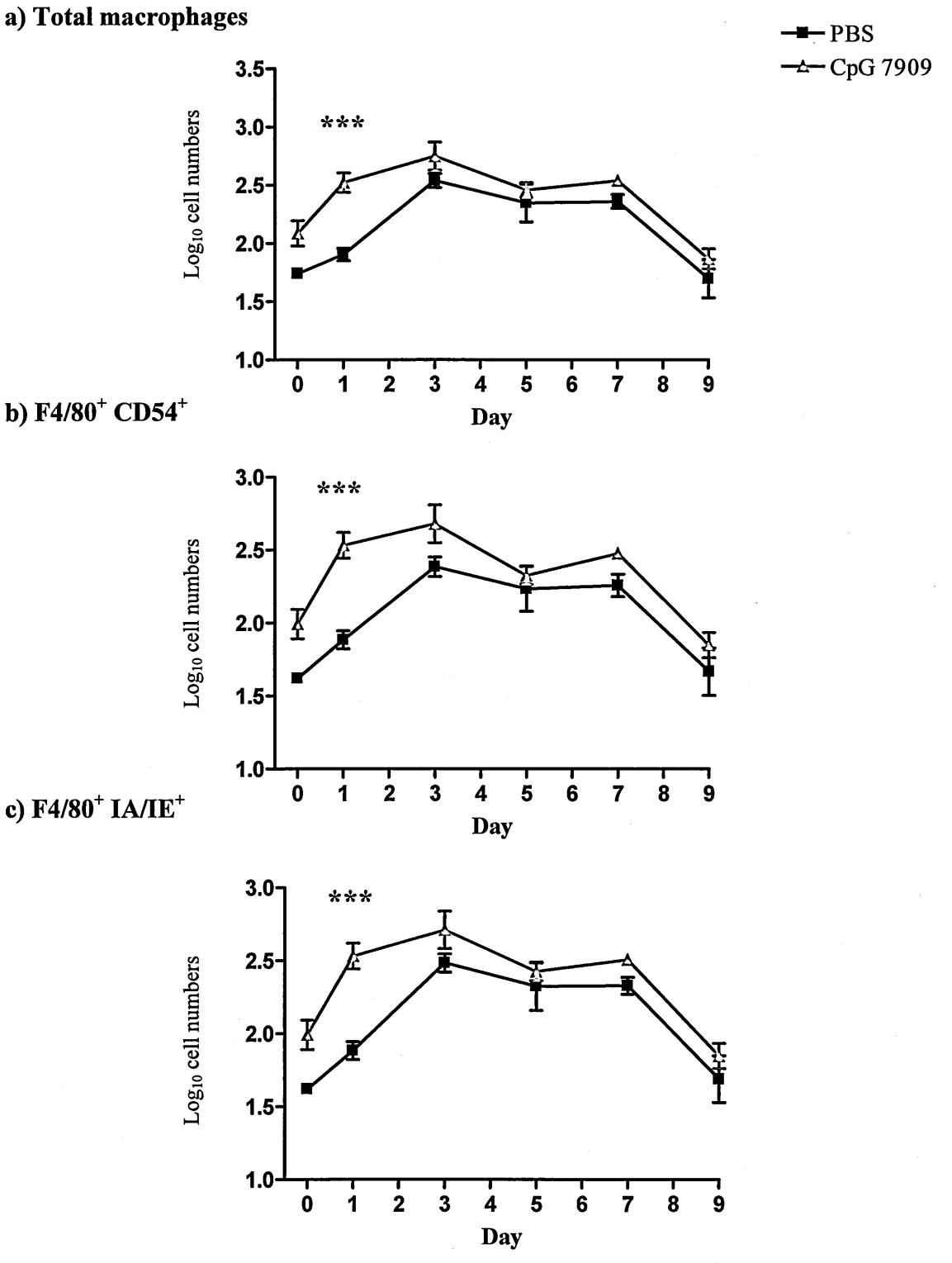

Figure 3.2. Lung macrophage numbers during VACV infection in CpG-B 7909 and PBS pre-treated groups. Mice were pre-treated with CpG on day -3 and exposed to VACV on day 0. The numbers of F4/80$^+$ macrophages in the lungs of infected mice were examined over days 0-9 using flow cytometry. Figure shows **(a)** total number of F4/80$^+$ macrophages; **(b)** macrophages expressing CD54; **(c)** macrophages expressing IA/IE. Graph represents geometric mean of four mice. Results shown include ± SEM. Statistical significance was determined using a two-way ANOVA and Bonferroni's post-tests. Significant findings between treatment groups are represented as *** ($p<0.001$).

An initial increase in the percentage of $CD54^+$ macrophages was observed in both treatment groups during the first 24 hours of infection (Figure 3.3a). This level of expression was maintained by macrophages from CpG-treated animals out to day +3, but not in PBS control mice, where expression levels fell significantly below those in the CpG-treated group ($p<0.05$). In CpG-treated mice, the percentage of macrophages expressing MHC II was significantly lower than that observed in the PBS treated group on the first day of infection ($p<0.01$). By day +3, the percentage of MHC II^+ macrophages was comparable between treatment groups and remained so throughout the duration of infection.

3.3.3.2. Lung neutrophil responses

Lung neutrophils were characterised by gating on granulocytic cells using forward scatter/side scatter dot plots and using a monoclonal antibody to Ly6G as a cell marker. Activation of neutrophils was determined by monitoring expression of the activation makers CD54 and CD11b on Ly6G positive cells.

Figure 3.4a illustrates the total number of lung neutrophils over the course of infection. On days 0 and +1, a significantly higher number of total lung neutrophils was observed in CpG-treated mice than in those treated with PBS ($p<0.001$). The numbers of activated cells were also significantly higher over this early stage, with higher numbers of CpG-treated neutrophils expressing CD54 (Figure 3.4b) on day 0 ($p<0.001$) and CpG activated neutrophils expressing CD11b (Figure 3.4c) on both days 0 and +1 ($p<0.001$). From day +3 onwards, the total numbers of neutrophils as well as the number of activated neutrophils were identical in both treatment groups.

a) % F4/80$^+$ CD54$^+$

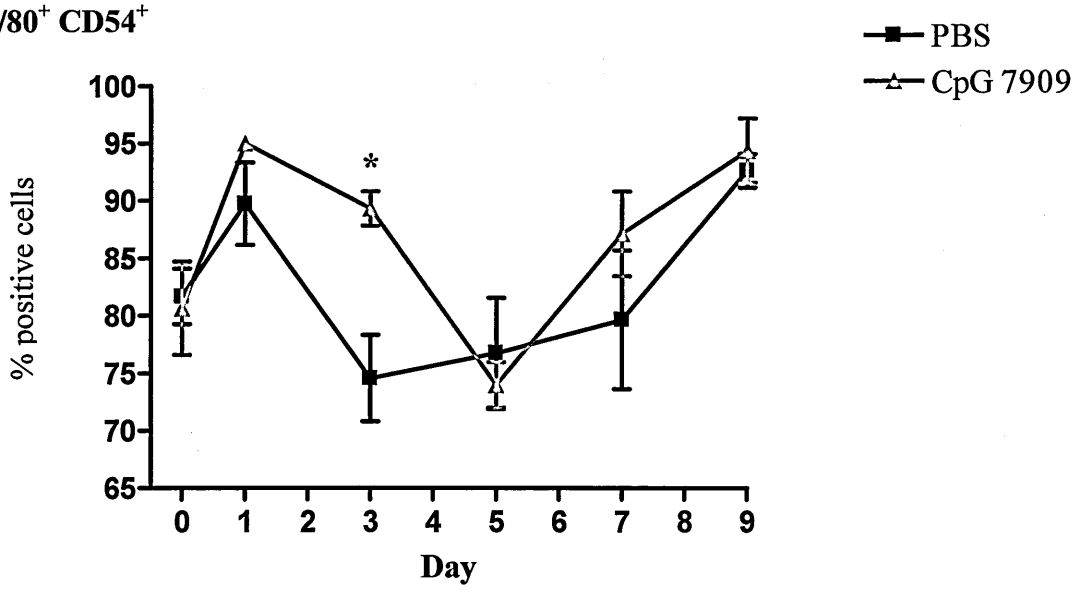

b) % F4/80$^+$ IA/IE$^+$

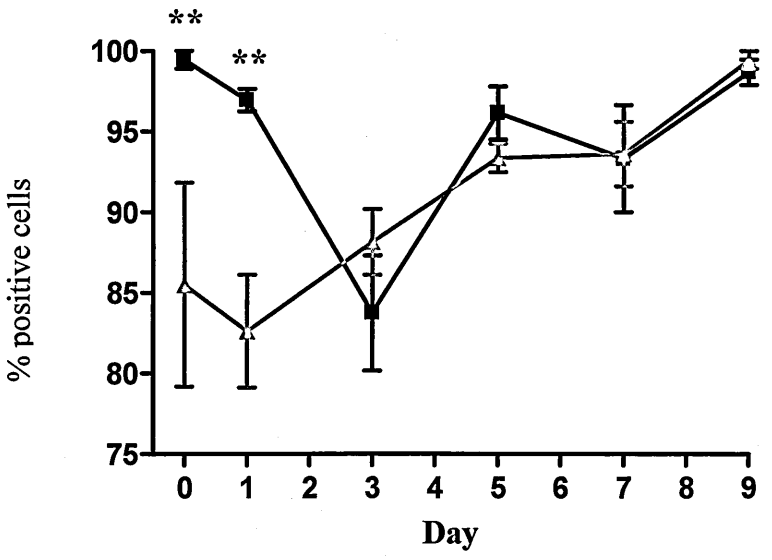

Figure 3.3. Activation of lung macrophages during VACV infection in CpG-B 7909 and PBS pre-treated groups. Lung macrophage activation was monitored by expression of activation marker CD54 (Figure 3.3a) and co-stimulation marker IA/IE (Figure 3.3b) over the course of infection using flow cytometry. Graph represents geometric mean of four mice. Error bars represent ± SEM. Statistical significance was determined using a two-way ANOVA and Bonferroni's post-tests. Significant findings between treatment groups are represented as * ($p<0.05$) and ** ($p<0.01$).

a) Total neutrophils

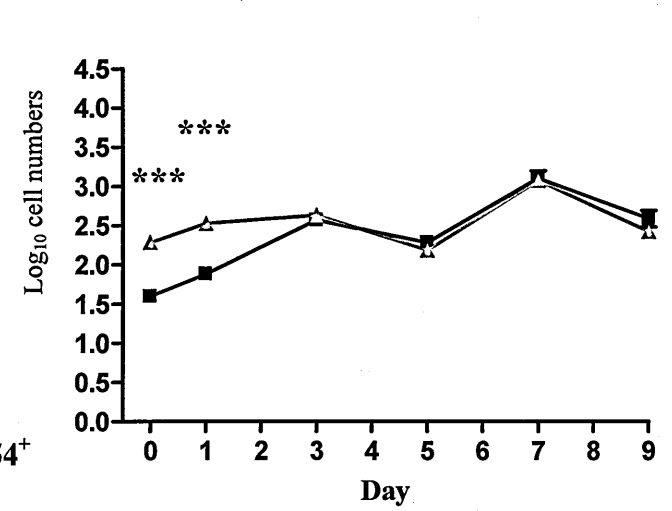

b) Ly6G$^+$ CD54$^+$

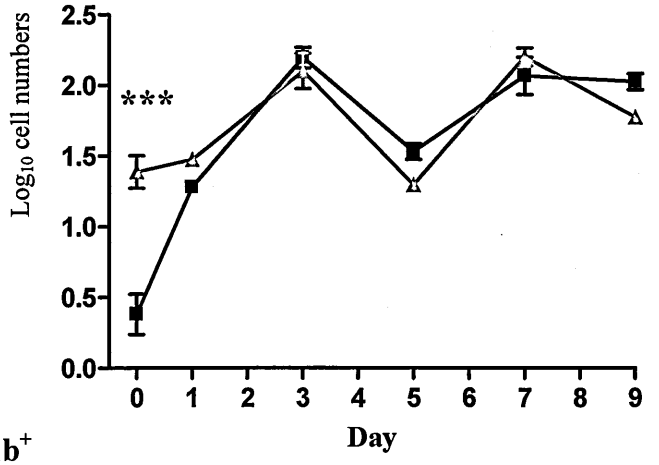

c) Ly6G$^+$ CD11b$^+$

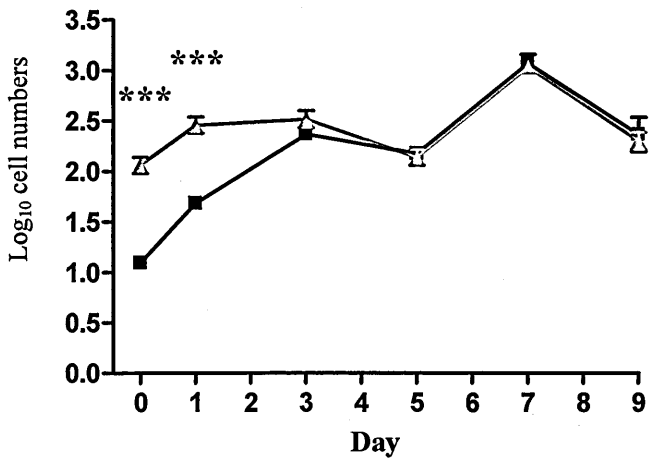

Figure 3.4. Lung neutrophil numbers during VACV infection in CpG-B 7909 and PBS pre-treated groups. Numbers of Ly6G$^+$ neutrophils in the lungs of infected mice were examined in both PBS and CpG-B 7909 animals pre-treated on day -3 over a nine day period using flow cytometry. Figure shows **(a)** total number of Ly6G$^+$ neutrophils; **(b)** neutrophils expressing CD54; **(c)** neutrophils expressing CD11b. Graph represents geometric mean of four mice. Results shown include ± SEM. Statistical significance was determined using a two-way ANOVA and Bonferroni's post-tests. Significant findings between treatment groups are represented as *** ($p<0.001$).

The percentage of neutrophils expressing CD54 fluctuated over the course of infection in both treatment groups as seen in Figure 3.5a. On day 0, the percentage of cells expressing CD54 was comparable between PBS and CpG pre-treated groups. On day +1 of VACV infection, the percentage of neutrophils expressing CD54 in CpG-treated mice was significantly lower than that observed in PBS treated mice ($p<0.01$). Beyond day +1, the percentage levels of $CD54^+$ neutrophils were comparable between treatment groups. The percentage of $CD11b^+$ neutrophils in CpG-treated mice was significantly higher than that in PBS mice on days 0 (p0.001) and +1 ($p<0.01$) (Figure 3.5b). CD11b expression levels remained significantly higher than PBS CD11b levels on day +3 ($p<0.05$) and day +9 ($p<0.05$).

3.3.3.3. Lung dendritic cell responses

Dendritic cell responses were characterised using the cell differentiation marker CD11c to identify lung DCs. The activation status of these cells was monitored *via* expression of MHC II (IA/IE) and the co-stimulation marker CD80.

The total numbers of dendritic cells in the lung increased significantly above pre-infection levels ($p<0.001$) after VACV infection in both CpG-B 7909 and PBS treated animals (Figure 3.6a). Dendritic cell numbers reached a peak on day +7 and total numbers only differed between treatment groups on day +9 where the lungs of PBS treated mice had significantly fewer DCs than in those treated with CpG-B 7909 ($p<0.01$). Whilst the total numbers of DCs were similar between treatment groups, mice pre-treated with CpG-B 7909 had significantly higher numbers of MHC II^+ DCs on day 0 ($p<0.001$) and day +1 ($p<0.05$) than mice pre-treated with PBS (Figure 3.6b). This same trend was also observed in DCs positive for the co-stimulation

a) % Ly6G$^+$ CD54$^+$

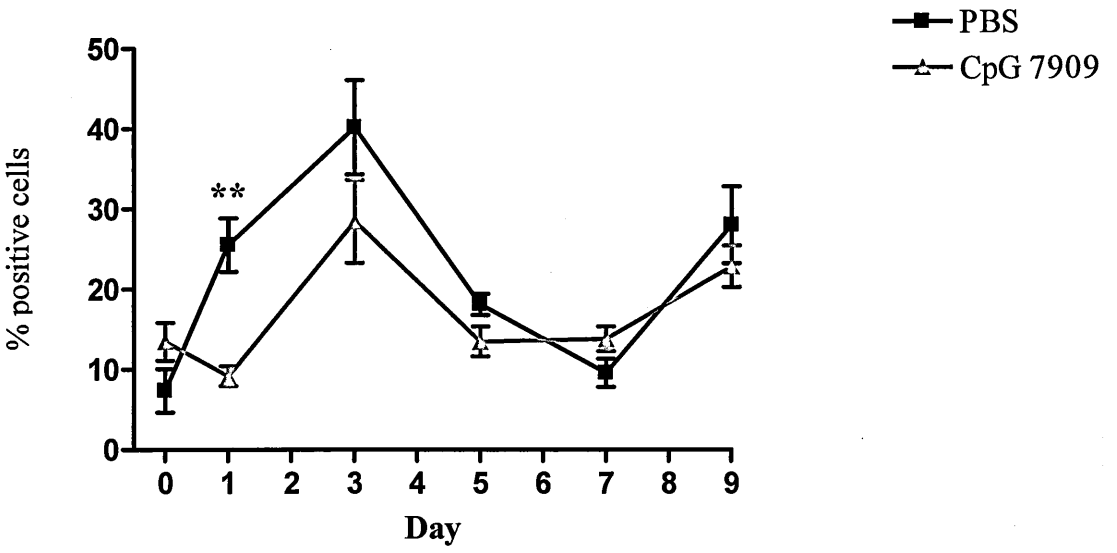

b) % Ly6G$^+$ CD11b$^+$

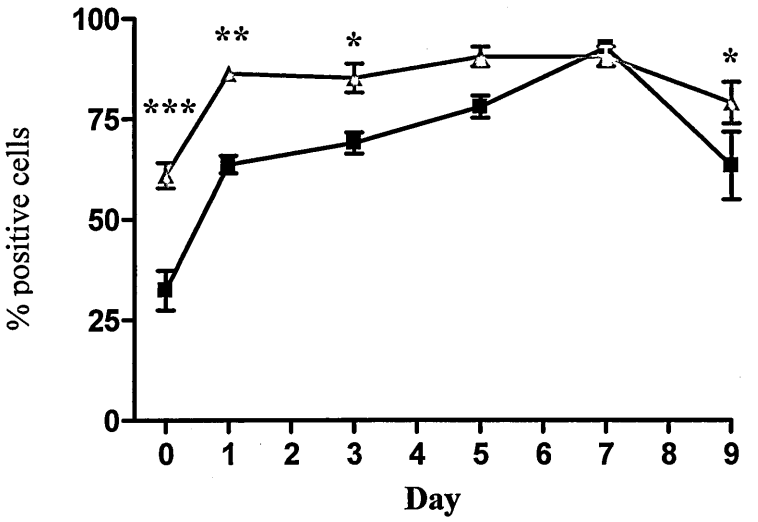

Figure 3.5. Activation of lung neutrophils during VACV infection in CpG-B 7909 and PBS pre-treated groups. Lung neutrophil activation was monitored by expression of activation marker CD54 (Figure 3.5a) and diapedesis marker CD11b (Figure 3.5b) over the course of infection using flow cytometry. Graph represents geometric mean of four mice. Error bars represent ± SEM. Statistical significance was determined using a two-way ANOVA and Bonferroni's post-tests. Significant findings between treatment groups are represented as * ($p<0.05$), ** ($p<0.01$) and *** ($p<0.001$).

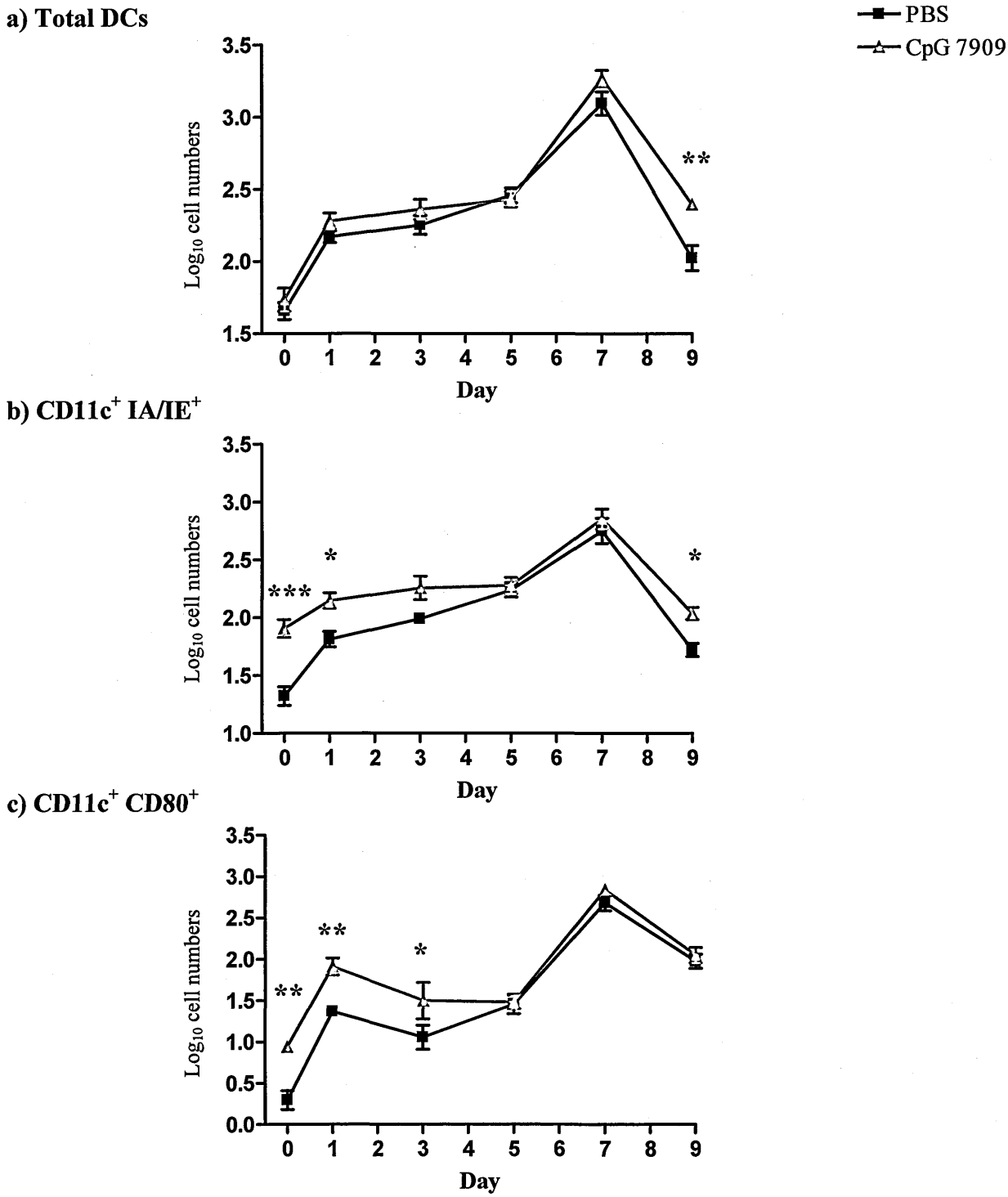

Figure 3.6. Lung dendritic cell numbers during VACV infection in CpG-B 7909 and PBS pre-treated groups. Numbers of $CD11c^+$ DCs in the lungs of infected mice were examined in both PBS and CpG-B 7909 animals pre-treated on day -3 over a nine day period using flow cytometry. Figure shows **(a)** total number of $CD11c^+$ DCs; **(b)** DCs expressing IA/IE; **(c)** DCs expressing CD80. Graph represents geometric mean of four mice. Results shown include ± SEM. Statistical significance was determined using a two-way ANOVA and Bonferroni's post-tests. Significant findings between treatment groups are represented as * ($p<0.05$), ** ($p<0.01$) and *** ($p<0.001$).

marker CD80 (Figure 3.6c). Here, CpG-treated mice had significantly higher numbers of $CD80^+$ DCs on day 0 ($p<0.01$), day +1 ($p<0.01$) and day +3 ($p<0.05$) of infection than mice pre-treated with PBS.

The percentage of DCs expressing MHC II in CpG-treated mice was significantly higher than those in PBS mice on days +1 ($p<0.01$) and +3 ($p<0.01$) (Figure 3.7a). In both treatment groups the percentage of MHC II^+ cells dropped from baseline levels post-infection. The percentage of $CD80^+$ DCs in CpG-treated mice was significantly higher than those in PBS mice on days 0 ($p<0.001$) and +1 ($p<0.001$) of infection but interestingly, were significantly below those in PBS mice by day +9 of infection ($p<0.001$) (Figure 3.7b).

3.3.3.4. Lung natural killer cell responses

The NK cell marker CD49b was used to distinguish NK cells in lung preparations. Activation of NK cells was determined using antibodies to CD54 and CD69.

NK cell numbers in CpG-treated mice remained constant throughout infection, but differed significantly from PBS NK cell numbers on days +1 and +9 ($p<0.001$) (Figure 3.8a). On each of these days, CpG-B 7909 treated mice had greater numbers of NK cells in their lungs. NK $CD54^+$ cells (Figure 3.8b) were only significantly elevated from PBS mice on day +9 of infection ($p<0.01$). In contrast, the number of NK cells expressing CD69 (Figure 3.8c) was significantly higher in CpG-B 7909 treated mice than in PBS during the early stages of infection on days 0 ($p<0.05$), and day +1 ($p<0.001$). As seen with NK $CD54^+$ cell numbers, CpG-treated NK $CD69^+$ cell numbers were significantly higher than PBS mice on day +9 of infection ($p<0.05$).

a) % CD11c$^+$ IA/IE$^+$

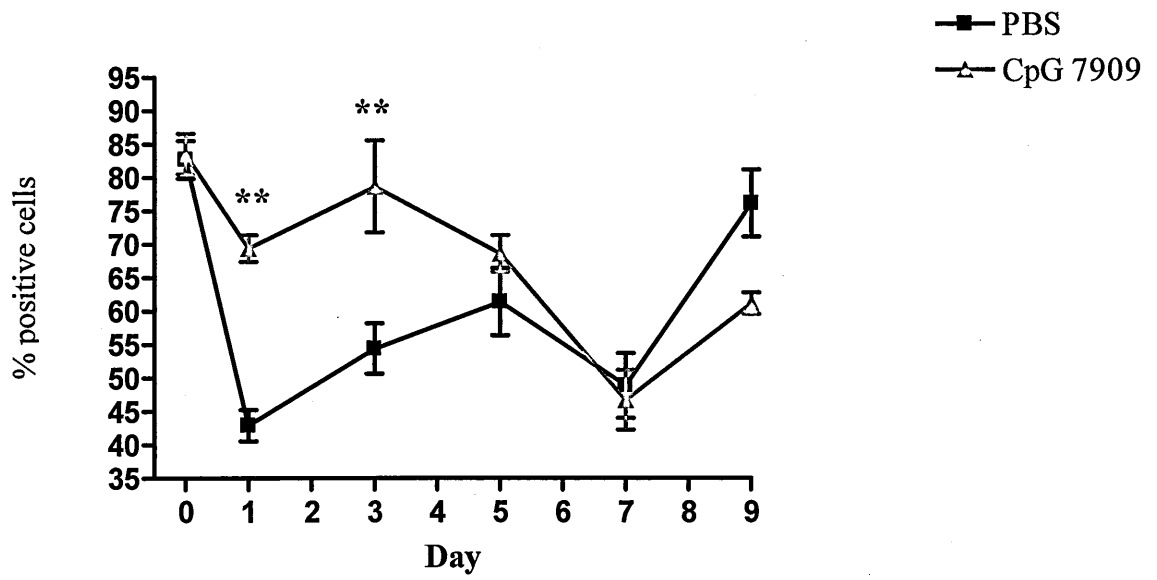

b) % CD11c$^+$ CD80$^+$

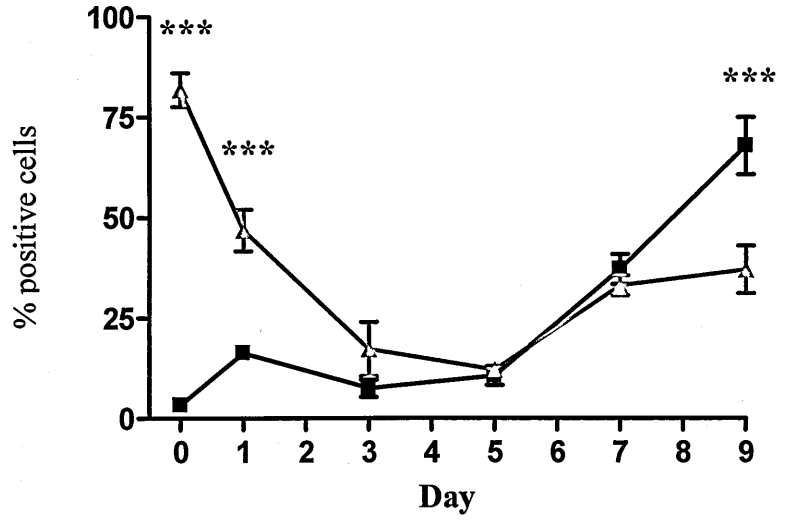

Figure 3.7. Activation of lung dendritic cells during VACV infection in CpG-B 7909 and PBS pre-treated groups. Lung DC activation was monitored by expression of co-stimulation markers IA/IE (Figure 3.7a) and CD80 (Figure 3.7b) over the course of infection using flow cytometry. Graph represents geometric mean of four mice. Error bars represent ± SEM. Statistical significance was determined using a two-way ANOVA and Bonferroni's post-tests. Significant findings between treatment groups are represented as ** ($p<0.01$) and *** ($p<0.001$).

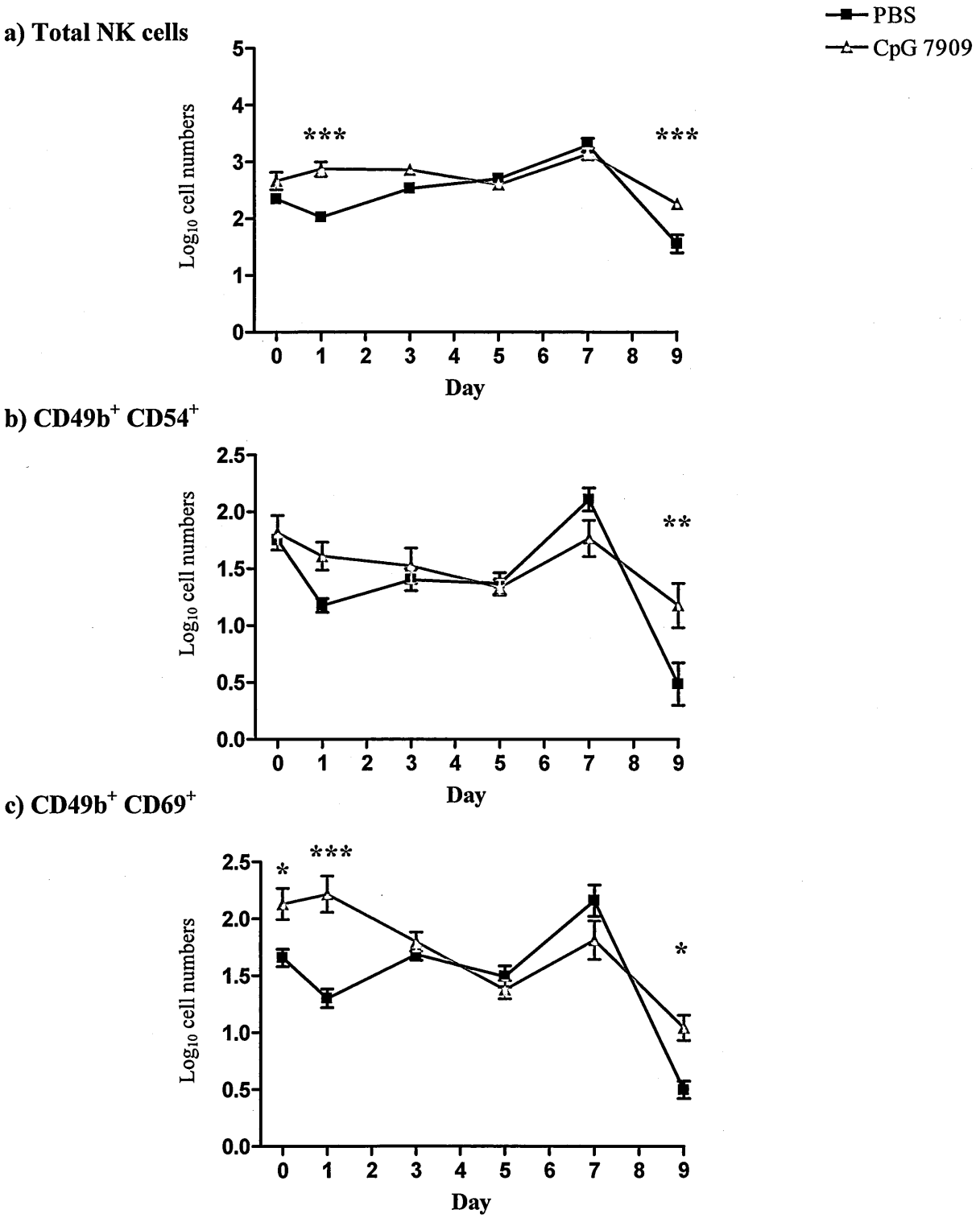

Figure 3.8. Lung natural killer cell numbers during VACV infection in CpG-B 7909 and PBS pre-treated groups. Numbers of CD49b$^+$ NK cells in the lungs of infected mice were examined in both PBS and CpG-B 7909 animals pre-treated on day -3 over a nine day period using flow cytometry. Figure shows **(a)** total number of CD49b$^+$ NK cells; **(b)** NK cells expressing CD54; **(c)** NK cells expressing CD69. Graph represents geometric mean of four mice. Results shown include ± SEM. Statistical significance was determined using a two-way ANOVA and Bonferroni's post-tests. Significant findings between treatment groups are represented as * ($p<0.05$), ** ($p<0.01$) and *** ($p<0.001$).

The percentage of activated NK cells followed the same trend in both treatment groups. Percentages of NK cells in both PBS and CpG-B 7909 treated mice expressing CD54 (Figure 3.9a) and CD69 (Figure 3.9b) dropped significantly over time ($p<0.001$) from their day 0 baseline levels. The percentage of $CD54^+$ NK cells in PBS mice was significantly higher than in CpG-treated mice on day 0 ($p<0.05$) but no other differences in percentage levels were seen between groups post infection.

3.3.3.5. Lung B-cell responses

Antibody specific to CD19 was used to label B-cells from cell suspensions. The activation status of B-cells at each time point was determined by staining of co-stimulatory molecules CD80 and CD86.

Total B-cell numbers on days 0 and +1 (Figure 3.10a) were significantly higher in mice pre-treated with CpG-B 7909 than those from the PBS control group ($p<0.05$). This was also observed in the number of B-cells expressing CD86 (day 0 $p<0.01$; day +1 $p<0.05$) (Figure 3.10b) and the number of B-cells expressing CD80 ($p<0.05$ on days 0 and +1) (Figure 3.10c). After day one of infection, neither total B-cell numbers nor activation marker specific B-cell numbers differed significantly between treatment groups.

No significant differences in the percentage of activated B-cells were observed between treatment groups until day +9 of infection. The percentage of CD19 $CD86^+$ cells (Figure 3.11a) and CD19 $CD80^+$ cells (Figure 3.11b) were both significantly higher in PBS mice than in those from mice that had been treated with CpG-B 7909.

a) % CD49b$^+$ CD54$^+$

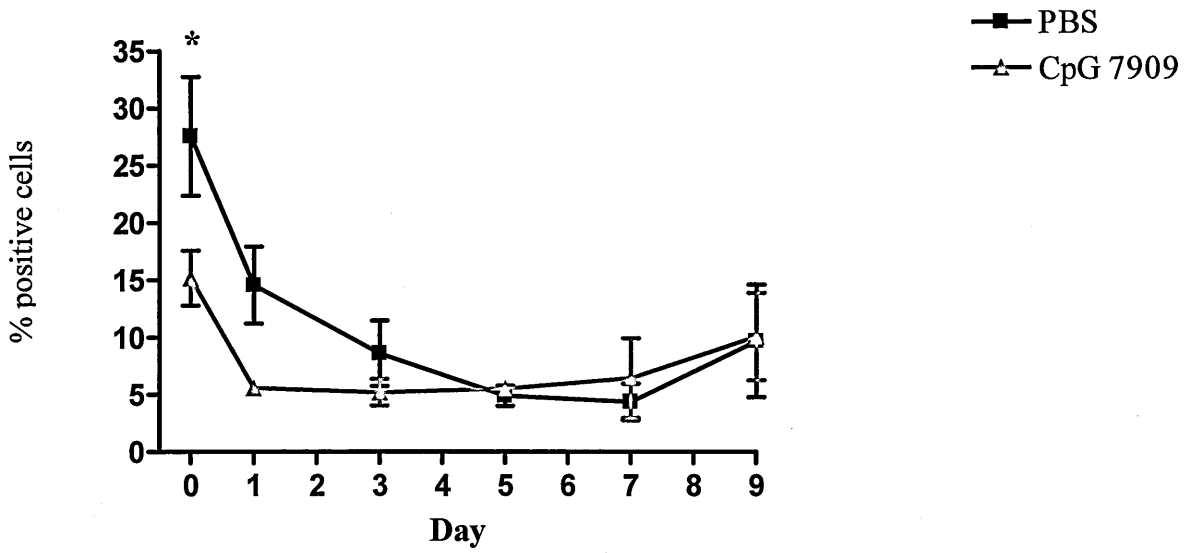

b) % CD49b$^+$ CD69$^+$

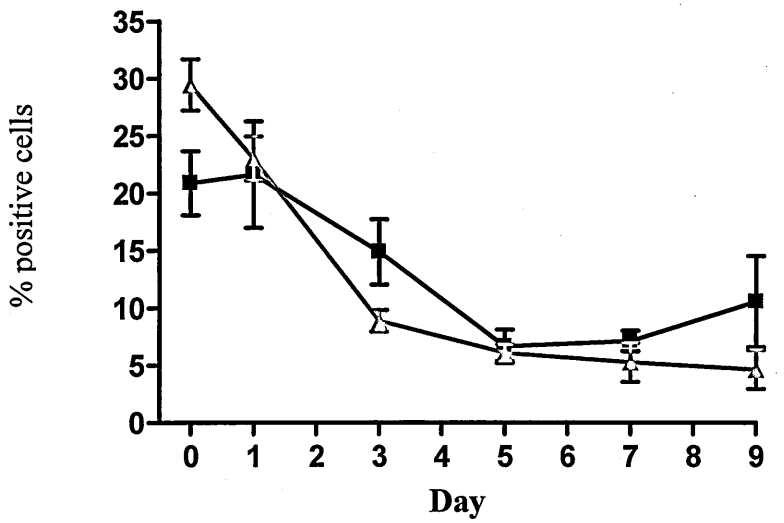

Figure 3.9. Activation of lung natural killer cells during VACV infection in CpG-B 7909 and PBS pre-treated groups. Lung NK cell activation was monitored by expression of activation markers CD54 (Figure 3.9a) and CD69 (Figure 3.9b) over the course of infection using flow cytometry. Graph represents geometric mean of four mice. Error bars represent ± SEM. Statistical significance was determined using a two-way ANOVA and Bonferroni's post-tests. Significant findings between treatment groups are represented as * ($p<0.05$).

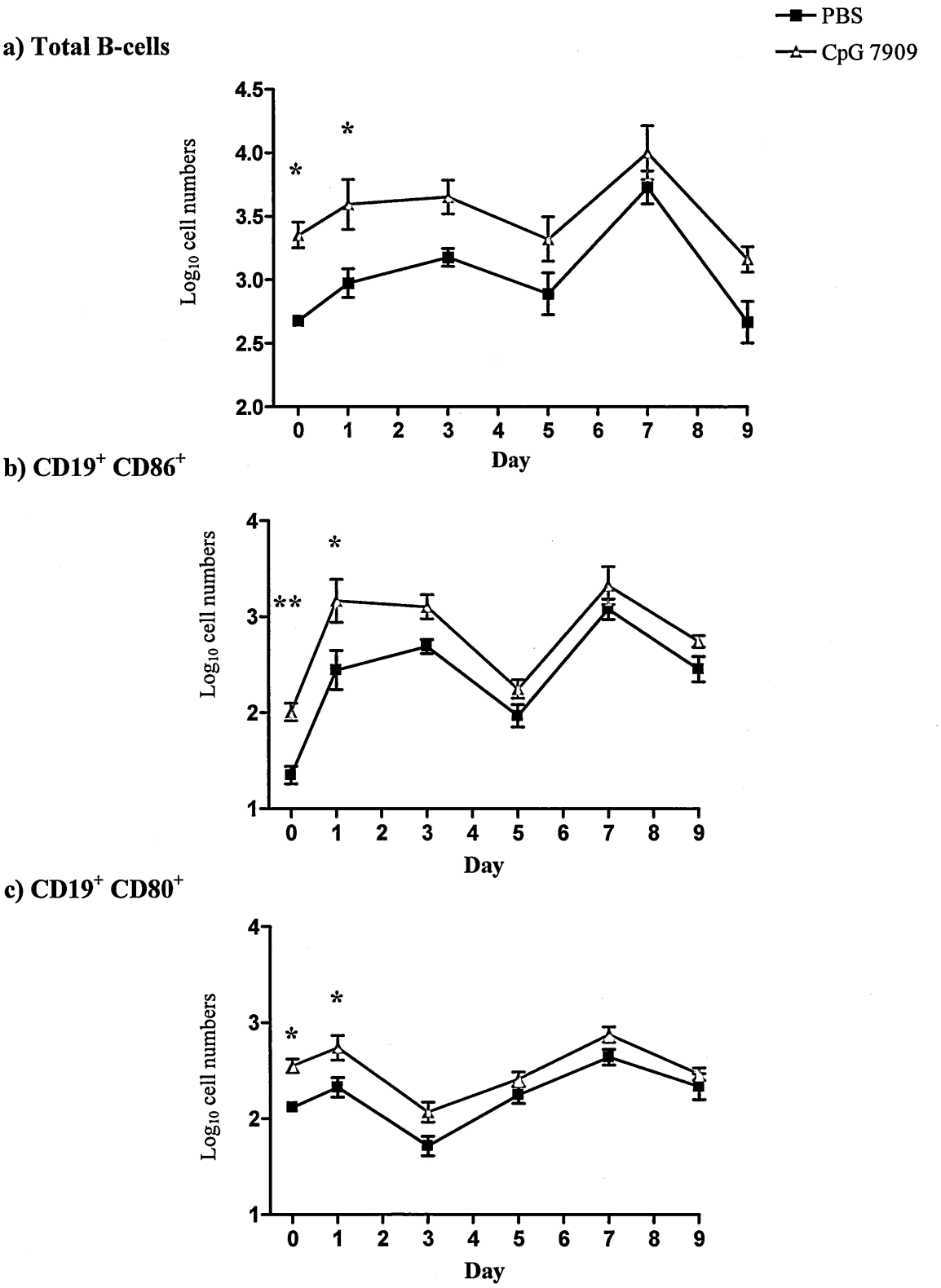

Figure 3.10. Lung B-cell numbers during VACV infection in CpG-B 7909 and PBS pre-treated groups. Numbers of $CD19^+$ B-cells in the lungs of infected mice were examined in both PBS and CpG-B 7909 animals pre-treated on day -3 over a nine day period using flow cytometry. Figure shows **(a)** total number of $CD19^+$ B-cells; **(b)** B-cells expressing CD86; **(c)** B-cells expressing CD80. Results shown include ± SEM. Statistical significance was determined using a two-way ANOVA and Bonferroni's post-tests. Significant findings between treatment groups are represented as * ($p<0.05$) and ** ($p<0.01$).

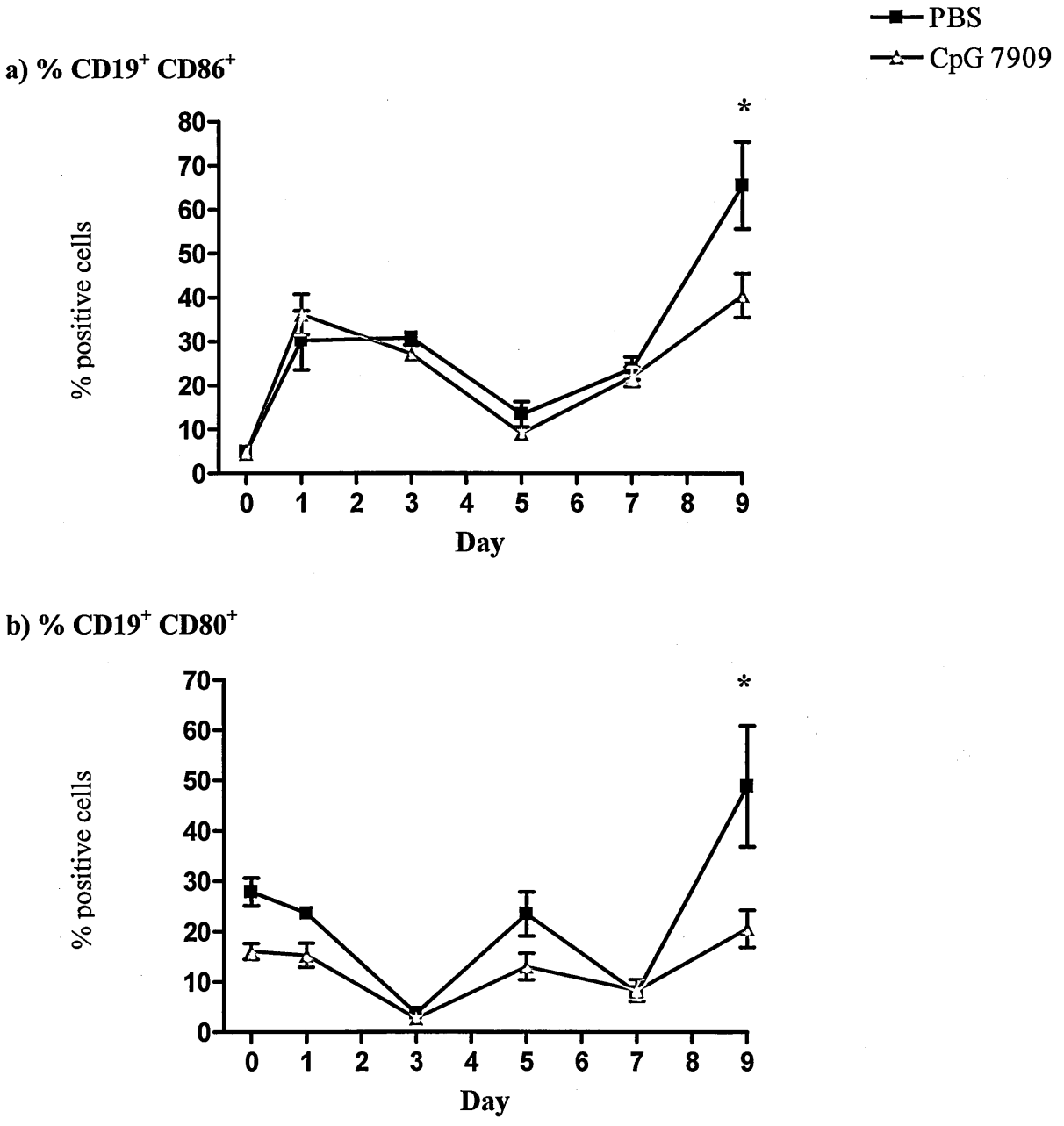

Figure 3.11. Activation of lung B-cells during VACV infection in CpG-B 7909 and PBS pre-treated groups. Lung B-cell activation was monitored by expression of activation markers CD86 (Figure 3.11a) and CD80 (Figure 3.11b) over the course of infection using flow cytometry. Graph represents geometric mean of four mice. Error bars represent ± SEM. Statistical significance was determined using a two-way ANOVA and Bonferroni's post-tests. Significant findings between treatment groups are represented as * ($p<0.05$).

3.3.3.6. Lung T-cell responses

Both CD4 and CD8 positive T-cells were monitored over the course of infection using CD3 as a pan T-cell marker. Lung $CD4^+$ T-cell responses are represented in Figure 3.12a. Throughout infection, the number of $CD4^+$ T-cells was higher in mice pre-treated with CpG-B 7909 than those given PBS, although only significantly so at the very start (day 0; $p<0.01$) and end (day +9; $p<0.001$) of the experiment. Lung $CD8^+$ T-cells followed the same pattern of influx and efflux regardless of treatment regimen and did not differ significantly throughout infection at any time-point (Figure 3.12b).

3.3.4. Cytokine responses in the spleen

Very few differences in the expression of cytokines and chemokines were identified between CpG-B 7909 and PBS control mice throughout infection. Protein levels of the pro-inflammatory cytokines TNF-α (Figure 3.13a), IL-6 (Figure 3.13b), and IFN-α (Figure 3.13c) were all expressed at similar quantities in the spleens of CpG-B 7909 treated mice and PBS control mice ($p>0.05$). Levels of IFN-γ (Figure 3.13d) did differ statistically between treatment groups at particular stages of infection. Mice pre-treated with CpG-B 7909 had significantly more IFN-γ detectable in their spleens on day 0 ($p<0.001$) and day +1 ($p<0.05$) compared to untreated comtrols. By day +3 post infection, the level of IFN-γ in PBS mice peaked at a level significantly above that seen in CpG-B 7909 mice ($p<0.001$). The expression of CCL2 (Figure 3.13e) and IL-10 (Figure 3.13f) did not differ between treatment groups throughout the course of infection at any time point ($p>0.05$). The levels of all cytokines measured were shown to vary significantly throughout infection ($p<0.05$).

a) $CD3^+$ $CD4^+$ T-cells

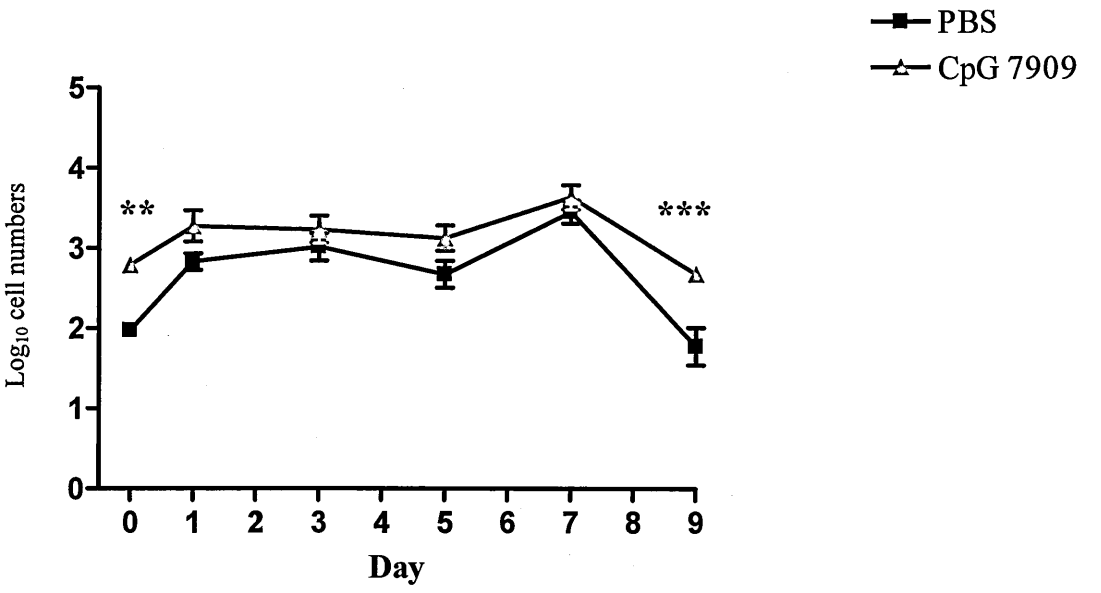

b) $CD3^+$ $CD8^+$ T-cells

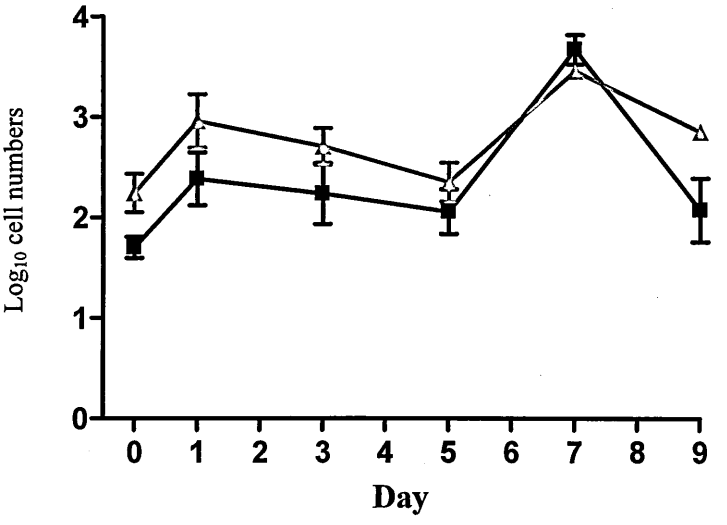

Figure 3.12. Lung T-cell numbers during VACV infection in CpG-B 7909 and PBS pre-treated groups. Numbers of $CD3^+$ T-cells in the lungs of infected mice were examined in both PBS and CpG-B 7909 animals pre-treated on day -3 over a nine day period using flow cytometry. Figure shows **(a)** total number of $CD4^+$ T-cells; **(b)** total number of $CD8^+$ T-cells. Graph represents geometric mean of four mice. Results shown include ± SEM. Statistical significance was determined using a two-way ANOVA and Bonferroni's post-tests. Significant findings between treatment groups are represented as ** ($p<0.01$) and *** ($p<0.001$).

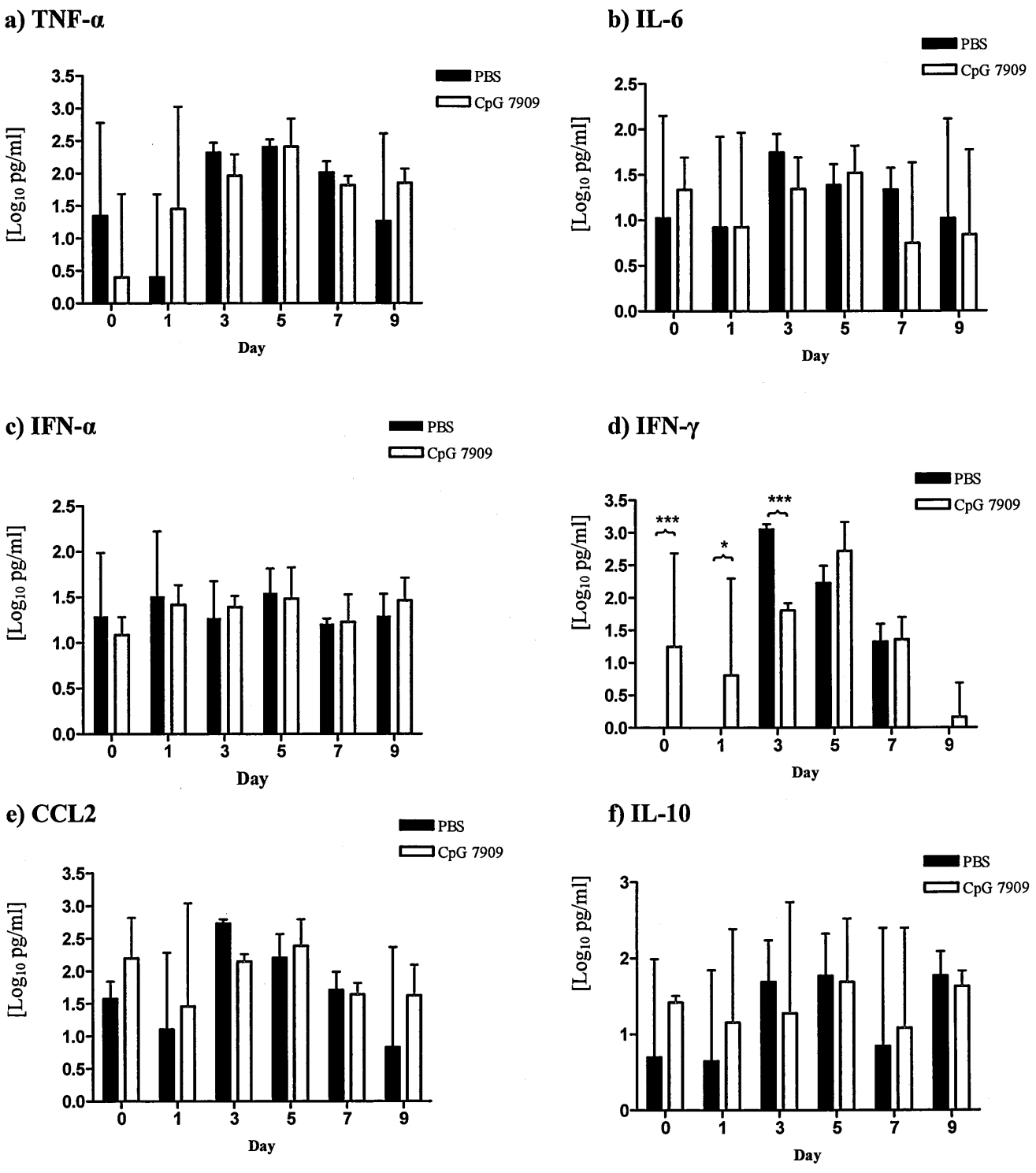

Figure 3.13. Measurement of spleen cytokine levels in Balb/C mice pre-treated with either CpG-B 7909 or PBS throughout infection with VACV. Protein levels determined *via* CBA analysis. Bars represent the geometric mean of four mice (Log_{10} pg/ml) and error bars indicate 95% confidence intervals for cytokines **(a)** TNF-α; **(b)** IL-6; **(c)** IFN-α; **(d)** IFN-γ; **(e)** CCL2; **(f)** IL-10. Statistical significance was determined using a two-way ANOVA and Bonferroni's post-tests. Significant findings between treatment groups are represented as * ($p<0.05$) and *** ($p<0.001$).

3.3.5. Cellular responses in the spleen

3.3.5.1. Spleen macrophage responses

Over the first five days of infection, no differences were observed between the numbers of macrophages from CpG-treated mice and those from control PBS mice ($p>0.05$). By day +7, the total number of macrophages in CpG-treated mice were significantly higher than those recorded in PBS mice ($p<0.01$). The numbers of macrophages in CpG-treated mice were also significantly higher on day +9 ($p<0.001$). The numbers of activated macrophages expressing CD54 (Figure 3.14b) and macrophages expressing MHC II (Figure 3.14c) mirrored this finding. MHC II^+ macrophages in CpG-treated mice were significantly higher on day +7 than those in control mice ($p<0.05$) and on day +9 both $CD54^+$ ($p<0.01$) and MHC II^+ ($p<0.001$) macrophage numbers were also significantly higher in CpG-treated animals.

The percentage of activated splenic macrophages varied significantly from baseline levels over time ($p<0.05$) but percentage levels of $CD54^+$ (Figure 3.15a) and MHC II^+ (Figure 3.15b) macrophages did not differ between treatment groups at any stage throughout infection ($p>0.05$).

3.3.5.2. Spleen neutrophil responses

The total numbers of neutrophils in both treatment groups fluctuated significantly over the course of infection ($p<0.001$) reaching a peak on day +7 before returning towards baseline levels on day +9 (Figure 3.16a). On day +9, mice treated with CpG-B 7909 retained a small but significantly greater number of neutrophils in their spleens compared to mice pre-treated with PBS. This trend was mirrored when examining the number of activated neutrophils expressing CD11b (Figure 3.16c).

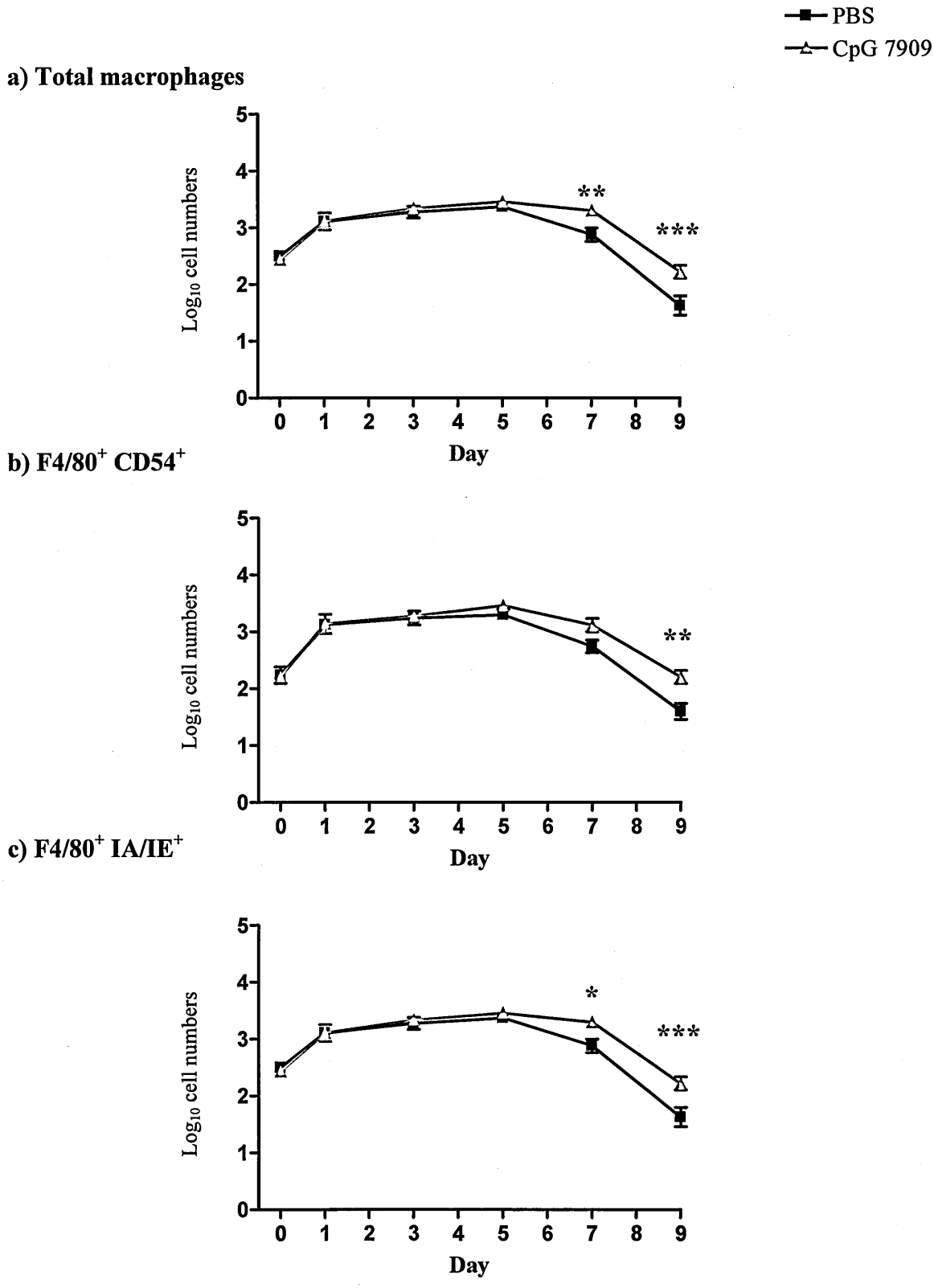

Figure 3.14. Spleen macrophage numbers during VACV infection in CpG-B 7909 and PBS pre-treated groups. Numbers of F4/80$^+$ macrophages in the spleens of infected mice were examined in both PBS and CpG-B 7909 animals pre-treated on day -3 over a nine day period using flow cytometry. Figure shows **(a)** total number of F4/80$^+$ macrophages; **(b)** macrophages expressing CD54; **(c)** macrophages expressing IA/IE. Graph represents geometric mean of four mice. Results shown include ± SEM. Statistical significance was determined using a two-way ANOVA and Bonferroni's post-tests. Significant findings between treatment groups are represented as * ($p<0.05$), ** ($p<0.01$) and *** ($p<0.001$).

a) % F4/80$^+$ CD54$^+$

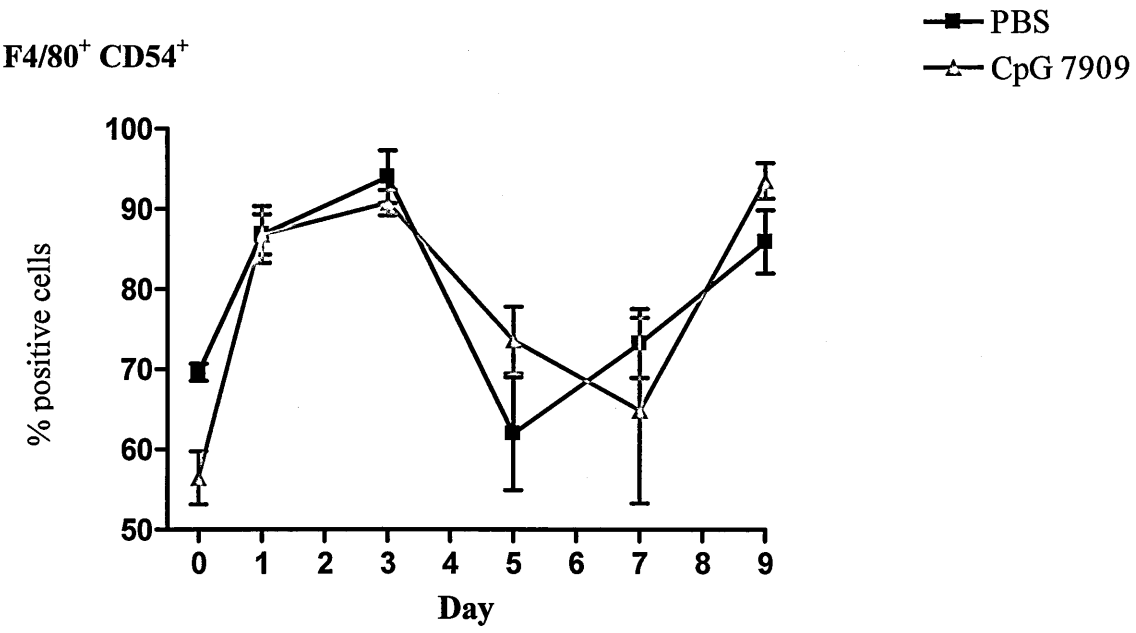

b) % F4/80$^+$ IA/IE$^+$

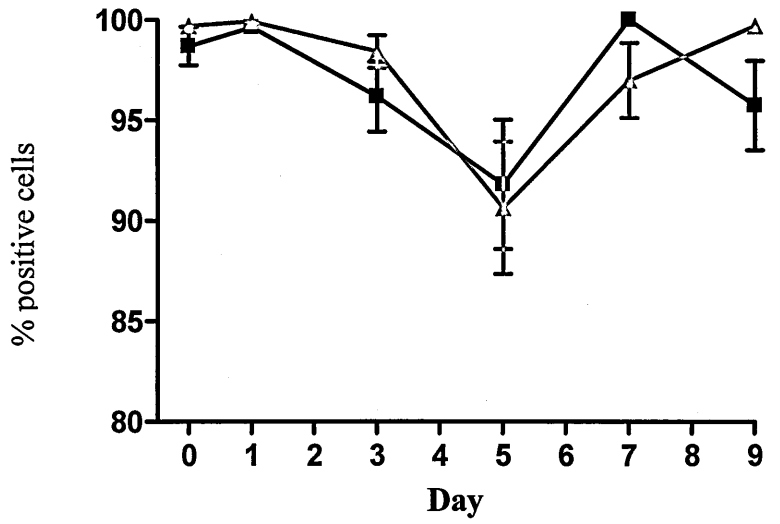

Figure 3.15. Activation of spleen macrophages during VACV infection in CpG-B 7909 and PBS pre-treated groups. Spleen macrophage activation was monitored by expression of activation marker CD54 (Figure 3.15a) and co-stimulation marker IA/IE (Figure 3.15b) over the course of infection using flow cytometry. Graph represents geometric mean of four mice. Error bars represent ± SEM. No statistical significance was determined using a two-way ANOVA and Bonferroni's post-tests.

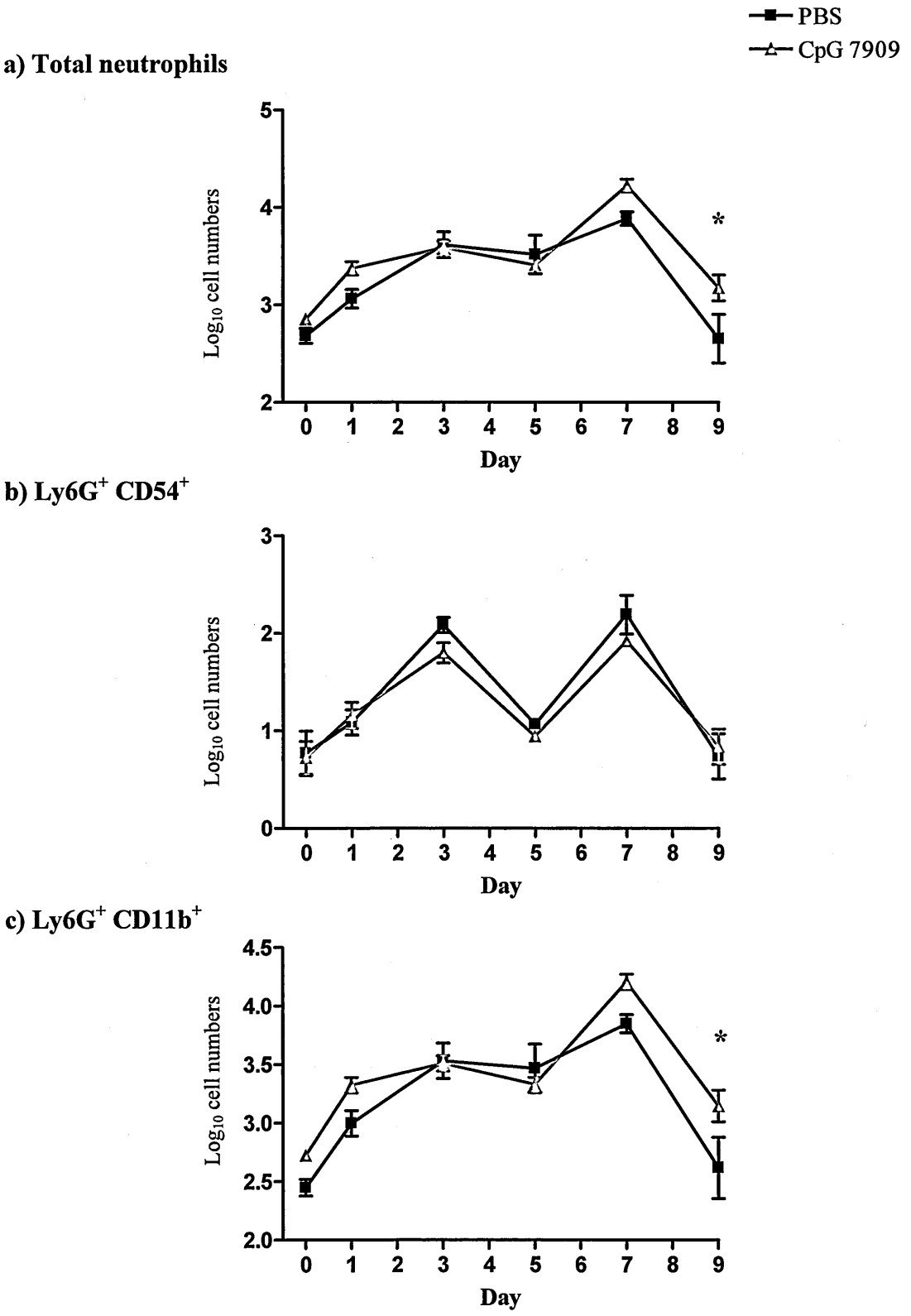

Figure 3.16. Spleen neutrophil numbers during VACV infection in CpG-B 7909 and PBS pre-treated groups. Numbers of $Ly6G^+$ neutrophils in the spleens of infected mice were examined in both PBS and CpG-B 7909 animals pre-treated on day -3 over a nine day period using flow cytometry. Figure shows **(a)** total number of $Ly6G^+$ neutrophils; **(b)** neutrophils expressing CD54; **(c)** neutrophils expressing CD11b. Graph represents geometric mean of four mice. Results shown include ± SEM. Statistical significance was determined using a two-way ANOVA and Bonferroni's post-tests. Significant findings between treatment groups are represented as * ($p<0.05$).

Here, significant differences between treatment groups were only determined on day +9 of infection where higher numbers of $CD11b^+$ neutrophils were found in CpG-treated mice ($p<0.05$). The number of neutrophils expressing CD54 (Figure 3.16b) did not vary between treatment groups at any stage throughout infection.

A very low percentage of neutrophils in the spleen were found to express CD54 and percentages values were seen to fluctuate significantly over time ($p=0.0011$) (Figure 3.17a). Whilst no significant differences between treatment groups were identified at any particular time-point, the effect of CpG treatment was found to have a significant overall effect on the percentage of neutrophils expressing CD54 ($p=0.0456$). In contrast, on day 0 the percentage of neutrophils expressing CD11b in CpG-treated mice was significantly higher than that observed in PBS treated mice ($p<0.001$) (Figure 3.17b). Beyond day 0, levels of CD11b increased relative to baseline in both treatment groups and Ly6G $CD11b^+$ percentage levels were not seen to differ significantly from each other at any further time-point.

3.3.5.3. Spleen dendritic cell responses

Time was seen to have a significant effect on the total numbers of DCs in the spleen ($p<0.001$) with numbers increasing gradually over the early stages of infection in both treatment groups (Figure 3.18a). Numbers of DCs peaked on day +7 in both treatment groups. On day +9, the total numbers of splenic DCs were significantly higher in CpG-B 7909 treated mice ($p<0.01$). This was also observed in the number of MHC II expressing DCs (Figure 3.18b) where numbers fluctuated in an almost identical fashion to that seen with total DC numbers. The numbers of CD11c $CD80^+$ cells also

a) % Ly6G$^+$ CD54$^+$

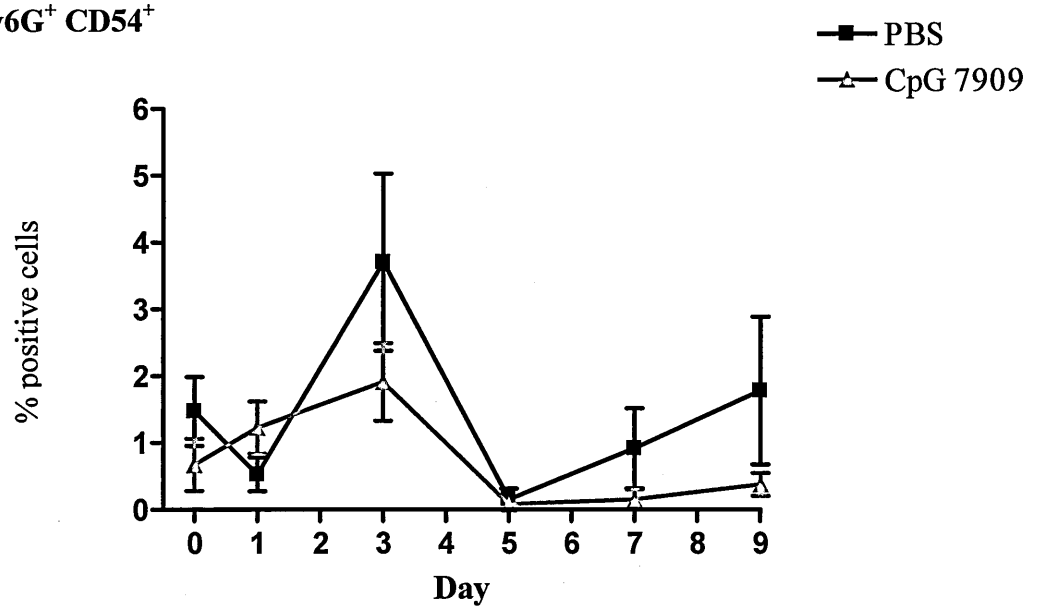

b) % Ly6G$^+$ CD11b$^+$

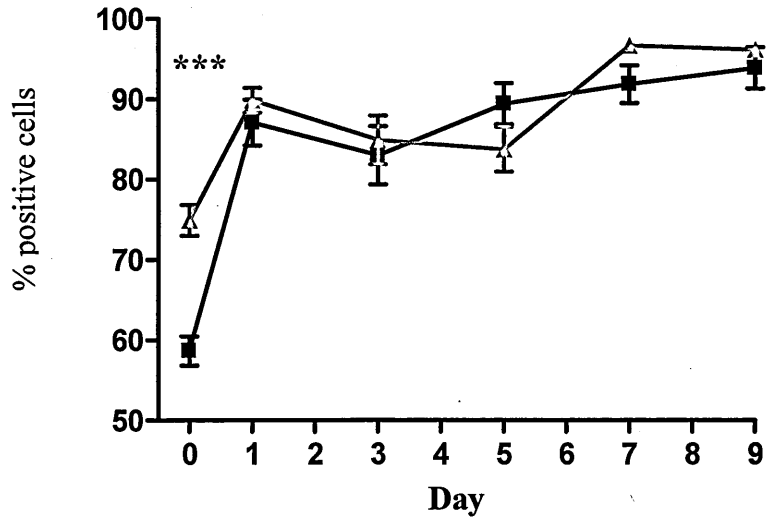

Figure 3.17. Activation of spleen neutrophils during VACV infection in CpG-B 7909 and PBS pre-treated groups. Spleen neutrophil activation was monitored by expression of activation marker CD54 (Figure 3.17a) and diapedesis marker CD11b (Figure 3.17b) over the course of infection using flow cytometry. Graph represents geometric mean of four mice. Error bars represent ± SEM. Statistical significance was determined using a two-way ANOVA and Bonferroni's post-tests. Significant findings between treatment groups are represented as *** ($p<0.001$).

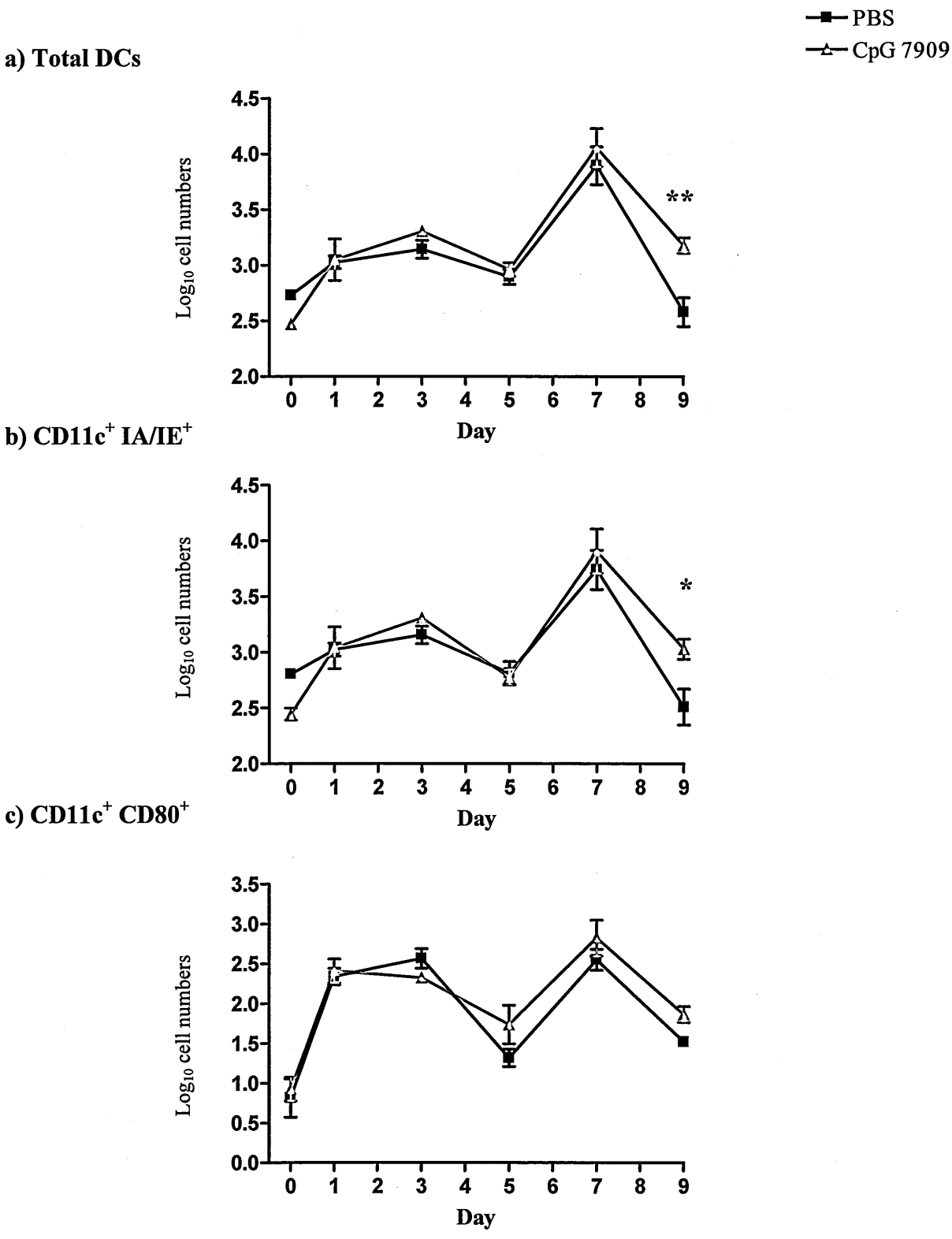

Figure 3.18. Spleen dendritic cell numbers during VACV infection in CpG-B 7909 and PBS pre-treated groups. Numbers of $CD11c^+$ DCs in the spleens of infected mice were examined in both PBS and CpG-B 7909 animals pre-treated on day -3 over a nine day period using flow cytometry. Figure shows **(a)** total number of $CD11c^+$ DCs; **(b)** DCs expressing IA/IE; **(c)** DCs expressing CD80. Graph represents geometric mean of four mice. Results shown include ± SEM. Statistical significance was determined using a two-way ANOVA and Bonferroni's post-tests. Significant findings between treatment groups are represented as * ($p<0.05$) and ** ($p<0.01$).

fluctuated over time (Figure 3.18c) but did not differ between treatment groups at any stage.

Almost all splenic DCs expressed MHC II constitutively (Figure 3.19a.). The high level of MHC II expression was seen in both treatment groups equally and percentage levels were only seen to dip significantly on day +7 ($p<0.001$) before returning to baseline levels on day +9. In contrast, the percentage levels of DCs expressing CD80 were very low in both treatment groups on day 0 (Figure 3.19b). Following infection, the percentage of DCs expressing CD80 increased significantly in both CpG-B 7909 and PBS mice ($p<0.001$). On day +3 of infection, percentage levels of CD11c $CD80^+$ cells in CpG mice dropped significantly below those seen in PBS mice ($p<0.001$). By day +5, percentage levels in both treatment groups returned towards baseline and thereafter remained comparable with each other until the end of the experiment.

3.3.5.4. Spleen natural killer cell responses

The total numbers of spleen NK cells did not differ significantly between treatment groups until day +9 of infection when mice that had received CpG-B 7909 prior to infection had significantly higher numbers of $CD49b^+$ cells (Figure 3.20a). Numbers of NK cells positive for CD54 (Figure 3.20b) or CD69 expression (Figure 3.20c) varied significantly over the course of infection ($p<0.001$) but no significant differences were seen between treatment groups at any point of infection for either activation marker.

The percentage of NK cells expressing CD54 (Figure 3.21a) fluctuated significantly over the course of infection in both treatment groups ($p<0.001$). At each time-point,

a) % CD11c$^+$ IA/IE$^+$

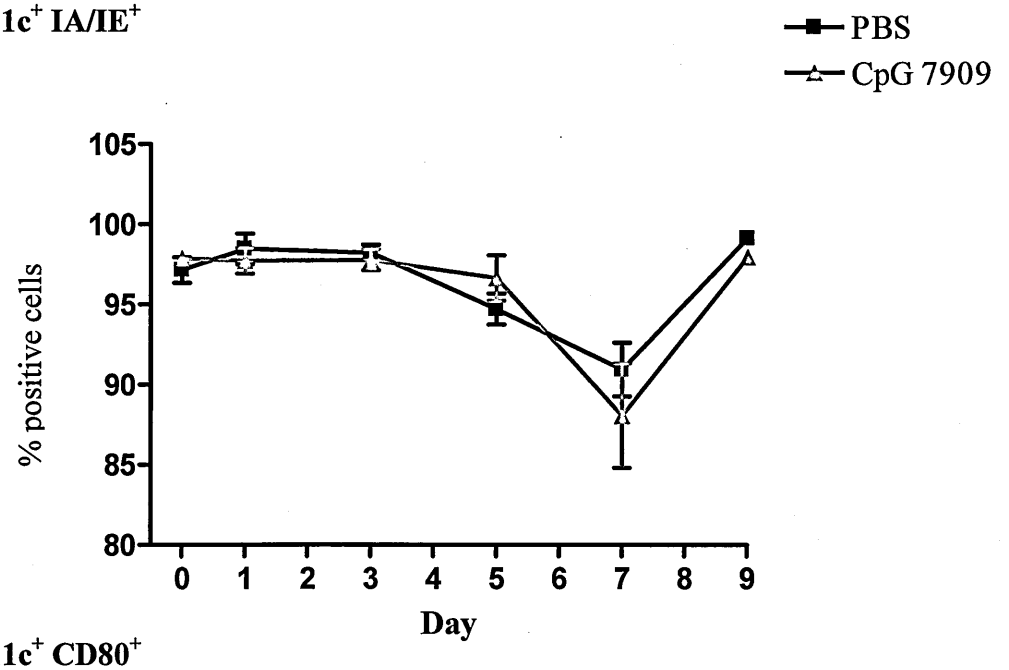

b) % CD11c$^+$ CD80$^+$

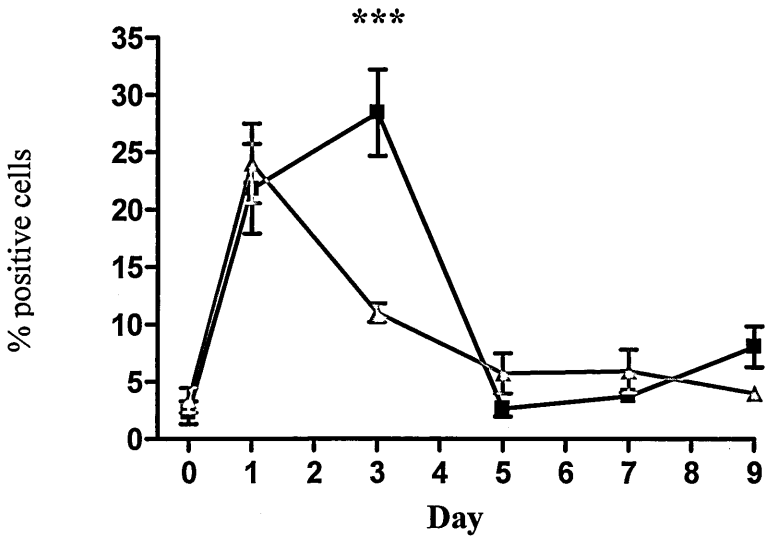

Figure 3.19. Activation of spleen dendritic cells during VACV infection in CpG-B 7909 and PBS pre-treated groups. Spleen DC activation was monitored by expression of co-stimulation markers IA/IE (Figure 3.19a) and CD80 (Figure 3.19b) over the course of infection using flow cytometry. Graph represents geometric mean of four mice. Error bars represent ± SEM. Statistical significance was determined using a two-way ANOVA and Bonferroni's post-tests. Significant findings between treatment groups are represented as *** ($p<0.001$).

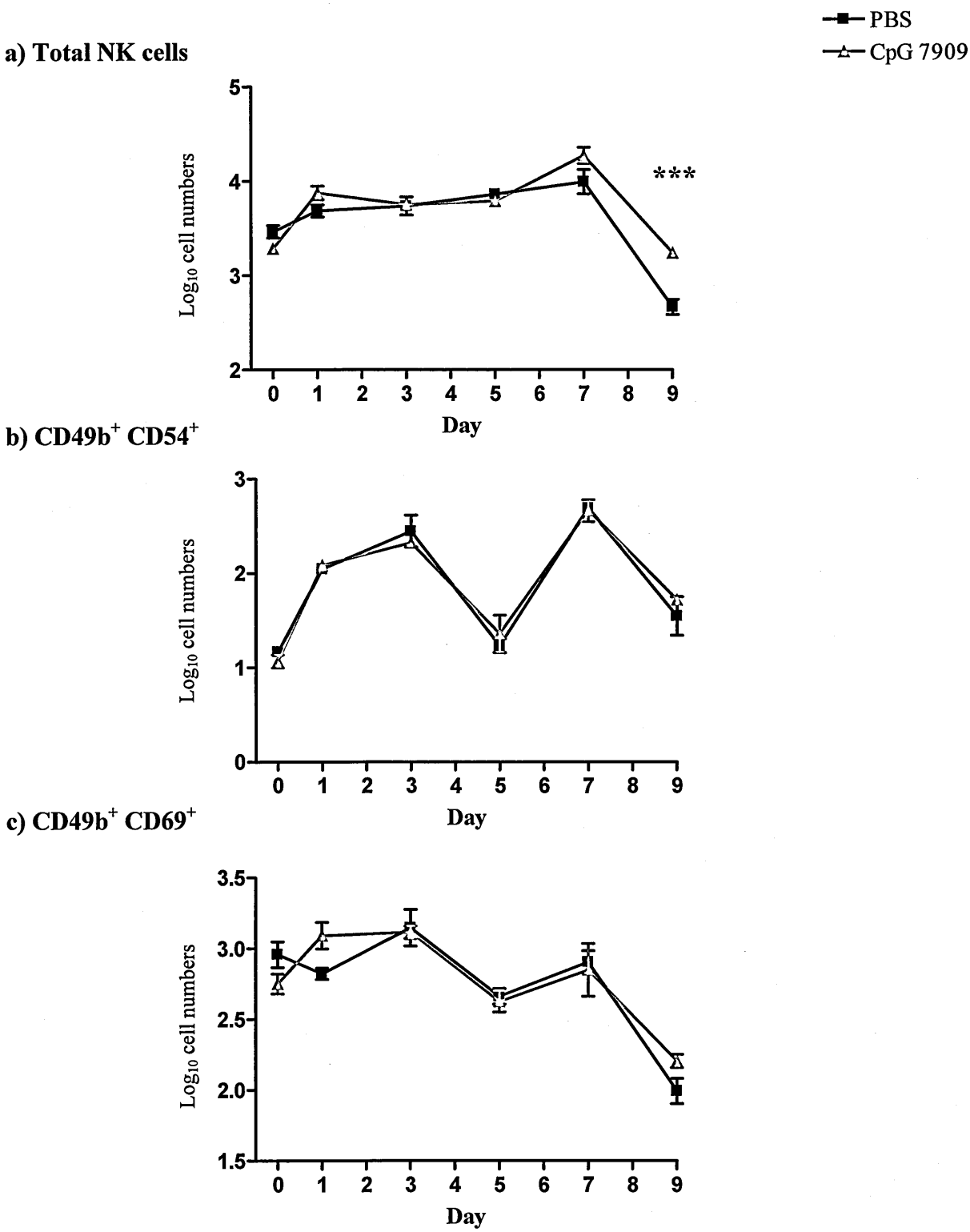

Figure 3.20. Spleen natural killer cell numbers during VACV infection in CpG-B 7909 and PBS pre-treated groups. Numbers of $CD49b^+$ NK cells in the spleens of infected mice were examined in both PBS and CpG-B 7909 animals pre-treated on day -3 over a nine day period using flow cytometry. Figure shows **(a)** total number of $CD49b^+$ NK cells; **(b)** NK cells expressing CD54; **(c)** NK cells expressing CD69. Graph represents geometric mean of four mice. Results shown include ± SEM. Statistical significance was determined using a two-way ANOVA and Bonferroni's post-tests. Significant findings between treatment groups are represented as *** ($p<0.001$).

a) % CD49b$^+$ CD54$^+$

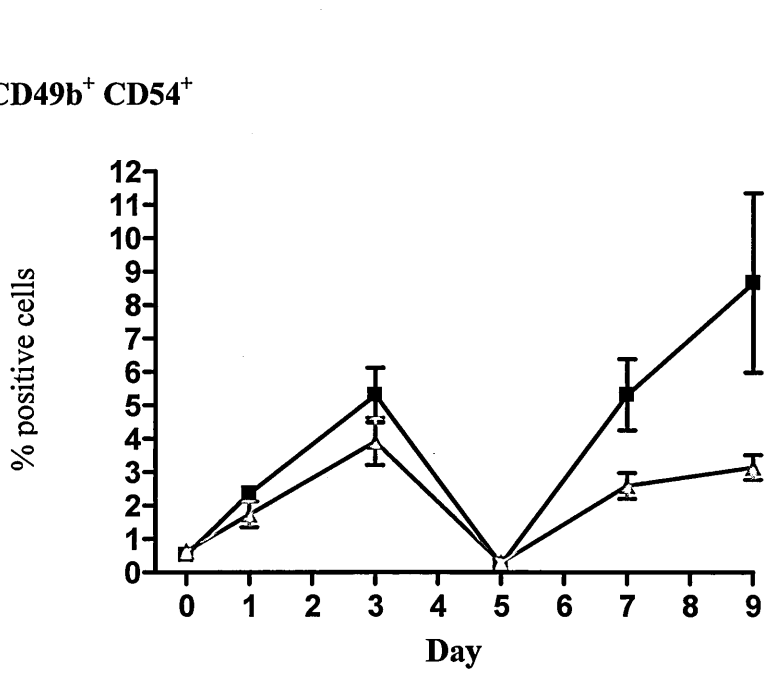

b) % CD49b$^+$ CD69$^+$

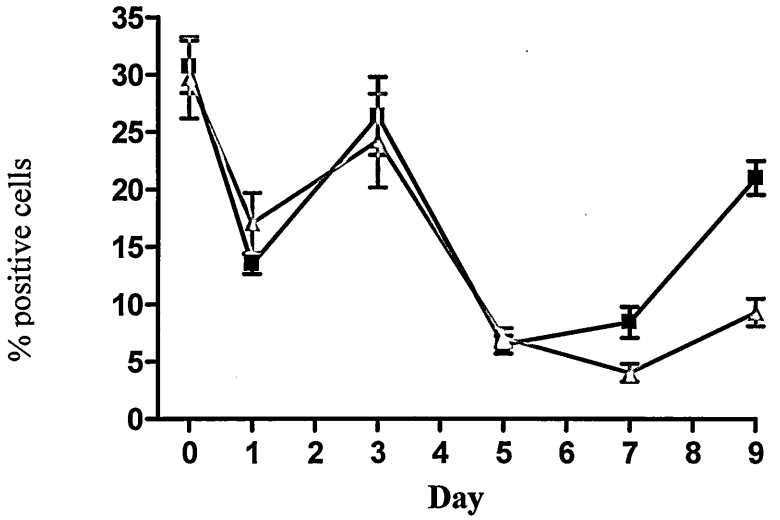

Figure 3.21. Activation of spleen natural killer cells during VACV infection in CpG-B 7909 and PBS pre-treated groups. Spleen NK cell activation was monitored by expression of activation markers CD54 (Figure 3.21a) and CD69 (Figure 3.21b) over the course of infection using flow cytometry. Graph represents geometric mean of four mice. Error bars represent ± SEM. No statistical significance was determined using a two-way ANOVA and Bonferroni's post-tests.

the percentage of NK cells expressing CD54 was lower in CpG-B 7909 pre-treated mice than that seen in control PBS mice. Although percentage levels at any one time-point did not differ significantly between treatment groups, pre-treatment with CpG-B 7909 did have a significant effect overall ($p=0.0004$). The percentage levels of NK cells expressing CD69 (Figure 3.21b) also varied significantly over time ($p<0.001$). Both treatment groups exhibited a similar trend throughout infection with percentage levels of $CD49b^+$ $CD69^+$ cells gradually falling over time. CpG-B 7909 pre-treatment did not significantly affect the percentage levels of NK cells expressing CD69, relative to control PBS levels, at any time-point individually during infection.

3.3.5.5. Spleen B-cell responses

Figure 3.22a shows the total number of B-cells present in the spleens of CpG-B 7909 and PBS pre-treated mice. Total B-cell numbers were significantly elevated on day 0 ($p<0.001$) and day +9 ($p<0.001$) in the spleens of CpG-treated mice compared to those given PBS. Levels of B-cell activation were comparable between treatment groups until day +9 of infection (Figures 3.22b and 3.22c) where activated B-cell numbers in control mice dropped significantly below those from CpG-treated mice ($p<0.001$).

On day 0, the percentages of B-cells expressing CD86 (Figure 3.23a) and CD80 (Figure 3.23b) were both significantly lower in the spleens of mice that had been pre-treated with CpG-B 7909 compared to control PBS mice ($p<0.001$). Upon infection, the percentage of B-cells expressing these co-stimulatory markers increased significantly ($p<0.001$). This resulted in comparable levels of CD80 and CD86 expression between treatment groups. Throughout the remainder of infection, the

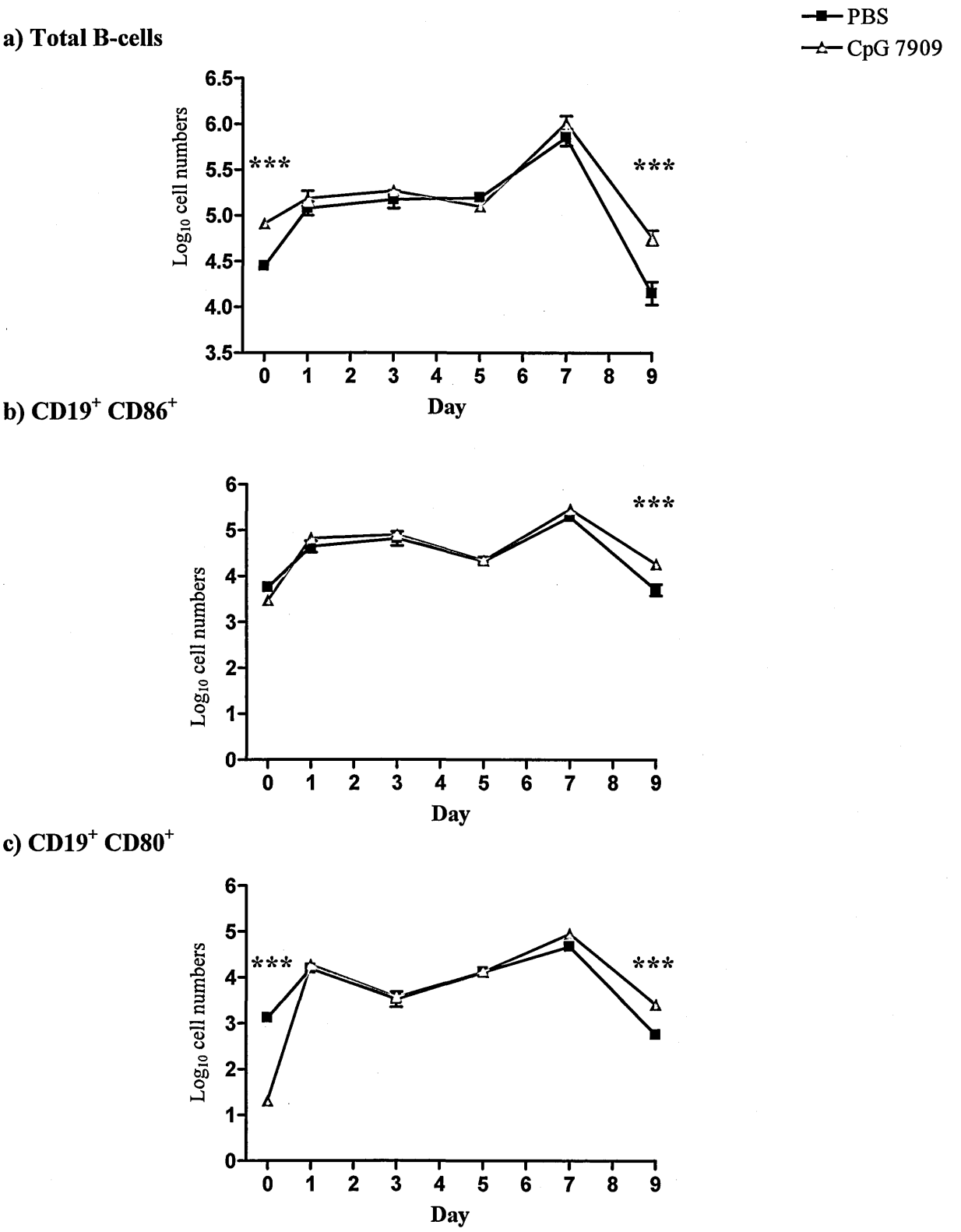

Figure 3.22. Spleen B-cell numbers during VACV infection in CpG-B 7909 and PBS pre-treated groups. Numbers of $CD19^+$ B-cells in the spleens of infected mice were examined in both PBS and CpG-B 7909 animals pre-treated on day -3 over a nine day period using flow cytometry. Figure shows **(a)** total number of $CD19^+$ B-cells; **(b)** B-cells expressing CD86; **(c)** B-cells expressing CD80. Results shown include ± SEM. Statistical significance was determined using a two-way ANOVA and Bonferroni's post-tests. Significant findings between treatment groups are represented as *** ($p<0.001$).

a) % CD19$^+$ CD86$^+$

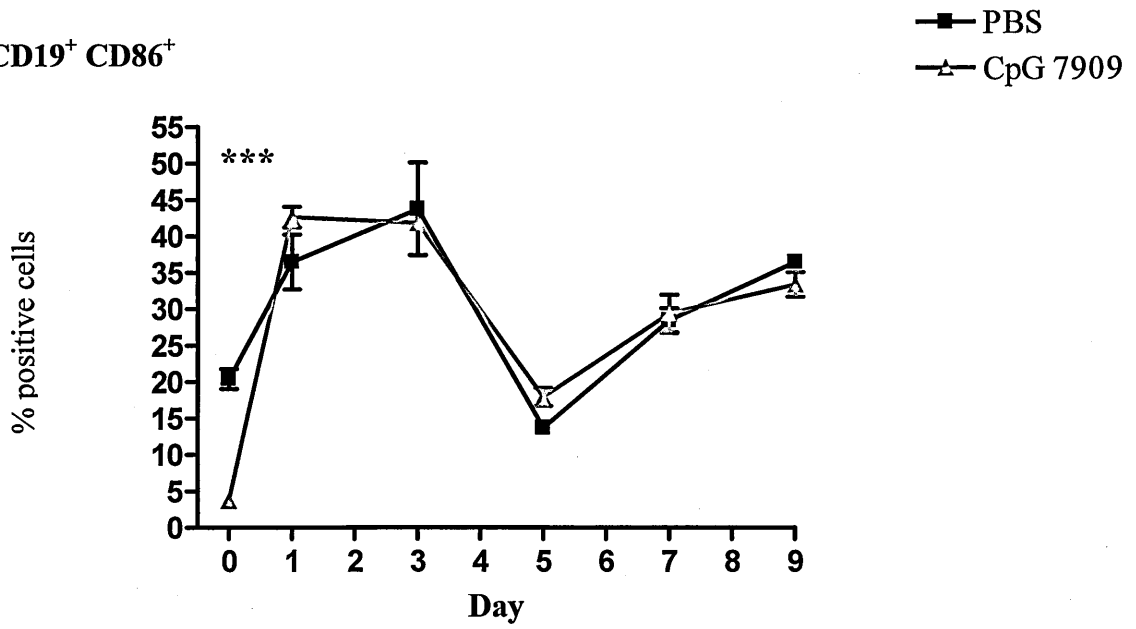

b) % CD19$^+$ CD80$^+$

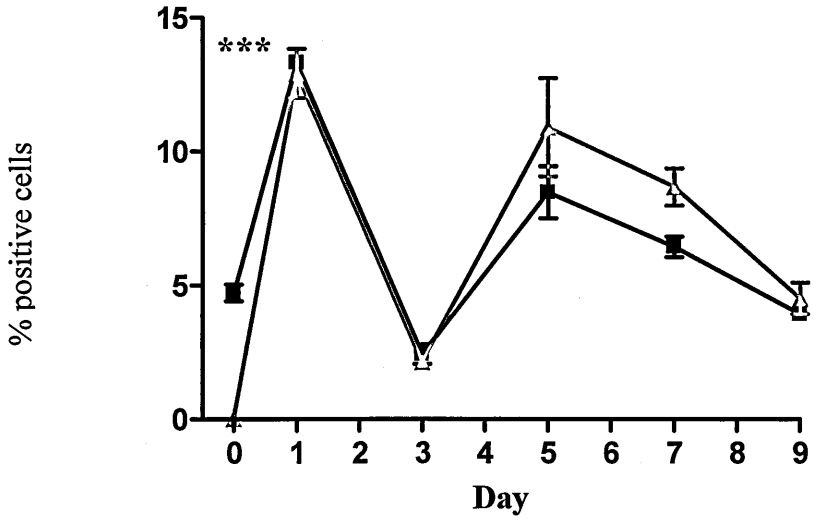

Figure 3.23. Activation of spleen B-cells during VACV infection in CpG-B 7909 and PBS pre-treated groups. Spleen B-cell activation was monitored by expression of activation markers CD86 (Figure 3.23a) and CD80 (Figure 3.23b) over the course of infection using flow cytometry. Graph represents geometric mean of four mice. Error bars represent ± SEM. Statistical significance was determined using a two-way ANOVA and Bonferroni's post-tests. Significant findings between treatment groups are represented as *** ($p<0.001$).

percentage levels of B-cells expressing CD86 or CD80 in both treatment groups, fluctuated with no significant difference between treatment groups.

3.3.5.6. Spleen T-cell responses

Cell numbers for $CD4^+$ (Figure 3.24a) and $CD8^+$ (Figure 3.24b) T-cells both altered significantly over the course of infection ($p<0.001$). $CD4^+$ T-cells increased more than $CD8^+$ T-cells relative to baseline. In both cases, no significant differences were seen in the number of T-cells in either treatment group until the final day of infection. On day +9, the number of $CD4^+$ and $CD8^+$ T-cells were both significantly higher in the spleens of mice that had been pre-treated with CpG-B 7909 than those from the control PBS group ($p<0.001$).

3.3.6. Cytokine responses in the sera

Levels of all cytokines were detectable in the serum of both CpG pre-treated and PBS treated mice albeit at substantially lower levels than that detected in the lungs or spleens. No significant differences between treatment groups were detected in the measurement of the vast majority of samples. The levels of pro-inflammatory cytokines TNF-α (Figure 3.25a), IL-6 (Figure 3.25b), IFN-α (Figure 3.25c) and IFN-γ (Figure 3.25d) were all detected at comparable levels in the sera of CpG-B 7909 treated mice and PBS control mice ($p>0.05$). Levels of the chemokine CCL2 (Figure 3.25e) did not differ significantly between treatment groups either. However, the anti-inflammatory cytokine IL-10 was seen to be significantly higher on day +1 of infection in CpG pre-treated mice ($p<0.001$) but at no other time throughout infection. The levels of all cytokines measured in the serum samples, varied significantly

a) $CD3^+$ $CD4^+$ T-cells

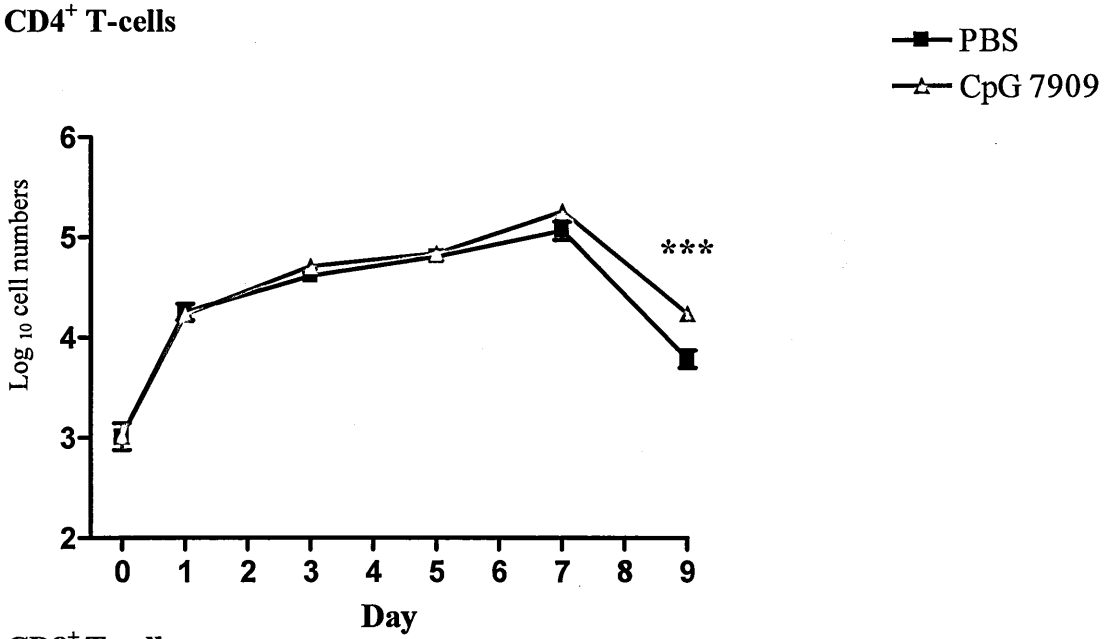

b) $CD3^+$ $CD8^+$ T-cells

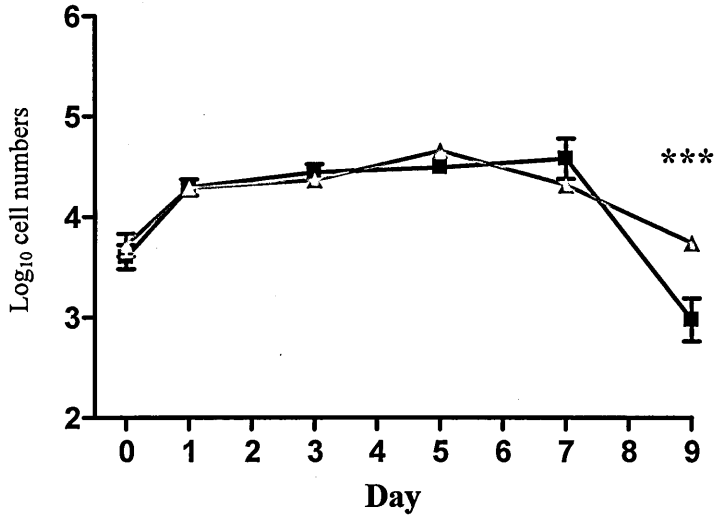

Figure 3.24. Spleen T-Cell numbers during VACV infection in CpG-B 7909 and PBS pre-treated groups. Numbers of $CD3^+$ T-cells in the spleens of infected mice were examined in both PBS and CpG-B 7909 animals pre-treated on day -3 over a nine day period using flow cytometry. Figure shows **(a)** total number of $CD4^+$ T-cells; **(b)** total number of $CD8^+$ T-cells. Graph represents geometric mean of four mice. Results shown include ± SEM. Statistical significance was determined using a two-way ANOVA and Bonferroni's post-tests. Significant findings between treatment groups are represented as *** ($p<0.001$).

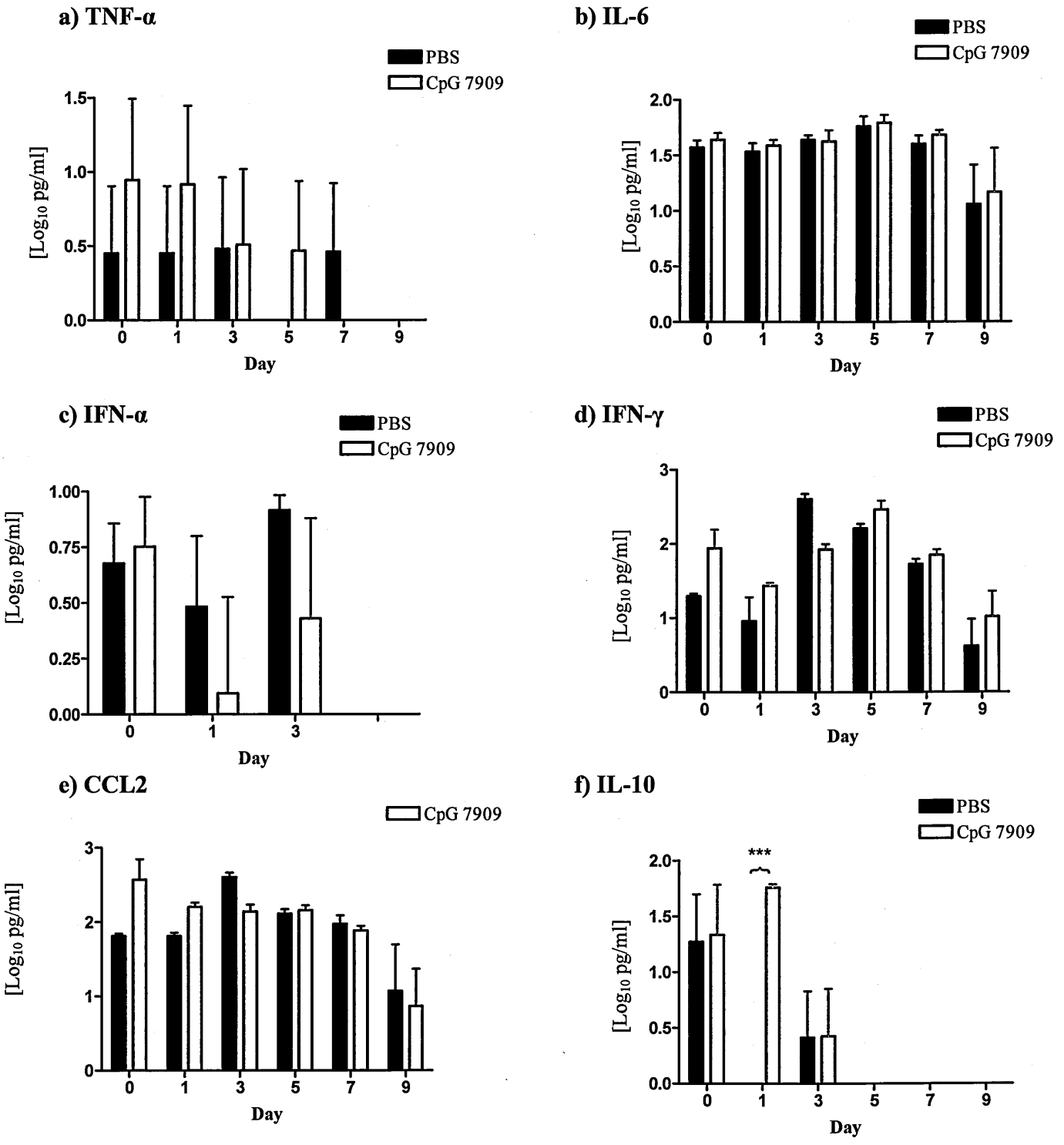

Figure 3.25. Measurement of serum cytokine levels in Balb/C mice pre-treated with either CpG-B 7909 or PBS throughout infection with VACV. Protein levels determined *via* CBA analysis or IFN-α elisa. Bars represent the geometric mean of four mice (Log_{10} pg/ml) and error bars indicate 95% confidence intervals for cytokines **(a)** TNF-α; **(b)** IL-6; **(c)** IFN-α; **(d)** IFN-γ; **(e)** CCL2; **(f)** IL-10. Statistical significance was determined using a two-way ANOVA and Bonferroni's post-tests. Significant findings between treatment groups are represented as *** ($p<0.001$).

throughout infection ($p<0.05$), with the exception of TNF-α (Figure 3.25a) and IFN-α (Figure 3.25c) ($p>0.05$).

3.3.7. The role of B-cells in CpG mediated VACV protection

The results detailed above show a prominent pro-inflammatory response in mice pre-treated with CpG-B 7909 compared to mice given PBS. The initiation of this response is likely to have been mediated through interaction of CpG and TLR9 expressing cells in the lung environment given the intranasal route of CpG delivery. B-class CpGs, such as CpG-B 7909, are known to exert their most potent stimulatory effects on B-cells (Krieg *et al.*, 1995). This suggests that B-cells may be crucial to the initiation of the protective response against VACV following CpG stimulation. In addition, the data presented here supports a role for B-cells in CpG-mediated protection against VACV, as indicated by the increased numbers of activated B-cells in the lungs of CpG-treated mice (Figure 3.10). Therefore, the role of B-cells in protection against VACV following CpG treatment was investigated using B-cell knock-out (KO) mice on a Balb/C background. Groups of wild-type and B-cell KO mice (n=8) were pre-treated with 75μg/ml CpG-B 7909 or PBS three days prior to challenge with 10 MLD VACV and monitored over a 14-day period. Results show that 75% of B-cell KO mice pre-treated with CpG survived infection (6/8) compared to 86% (6/7) of CpG-treated intact mice (Figure 3.26a). This figure also shows that 75% of PBS-treated immunocompetent mice survived infection compared to 38% (3/8) in B-cell KO that had been treated with PBS. A log-rank test on survival data failed to determine any significant difference between these treatment groups ($p=0.1970$). The severity of disease in treatment groups as determined by % weight loss, was found to differ significantly between treatment groups ($p=0.0146$). Here, intact mice receiving CpG-

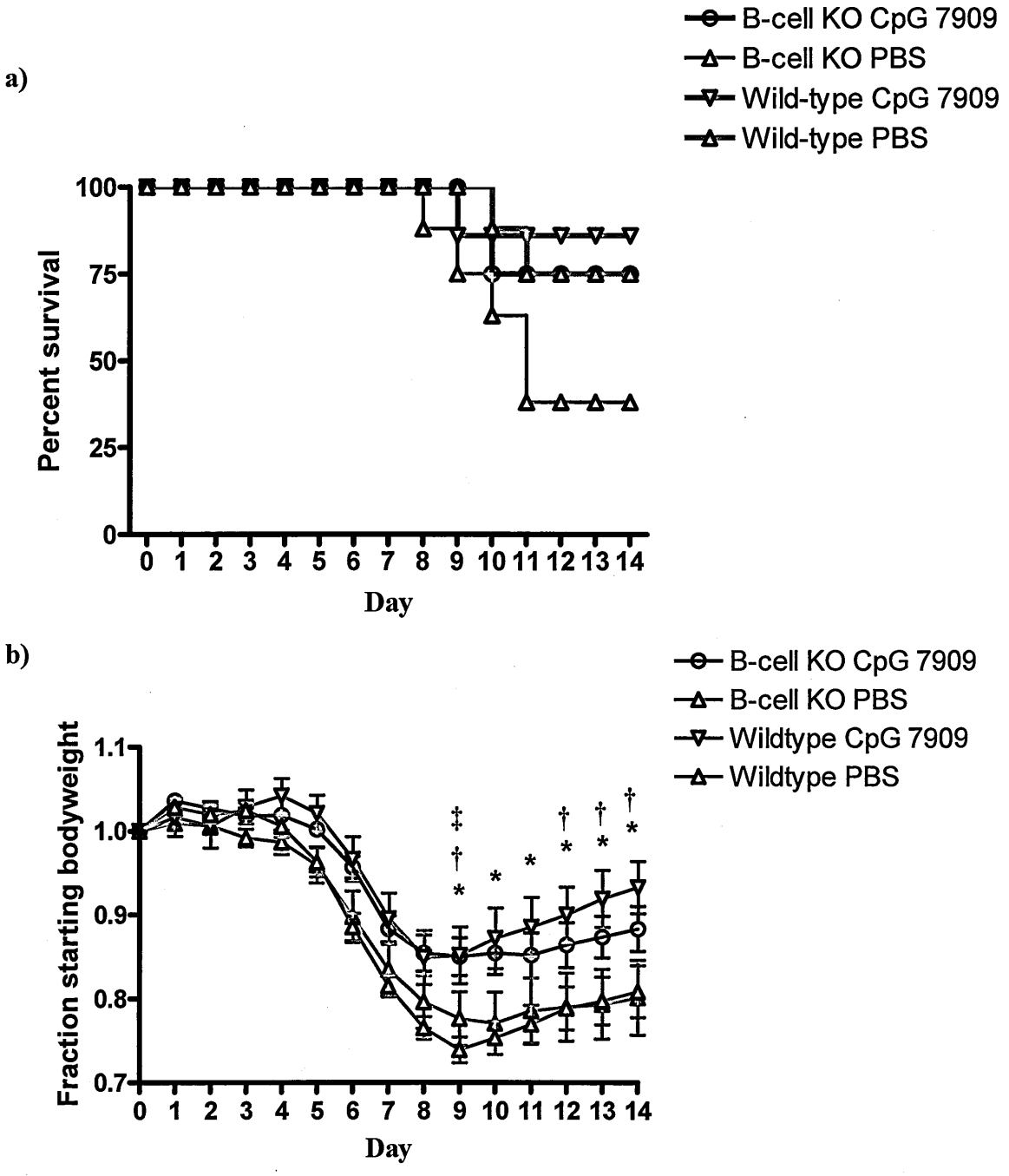

Figure 3.26. Effect of B-cell KO on CpG-mediated VACV protection. Groups of B-cell KO mice (n=8) were pre-treated with either 75μg CpG-B 7909 or PBS three days prior to challenge with 10 MLD VACV. Wild-type (Wt) mice were treated and challenged in parallel with 75μg CpG-B 7909 (n=7) or PBS (n=8). **(a)** Survival data: **(b)** Mean weight loss: Mice were weighed daily throughout the experiment, data points represent geometric mean weight per time-point ± SEM. Statistical significance was determined using a two-way ANOVA and Bonferroni's post-tests.

* *Wt CpG v Wt PBS ($p<0.05$);* † *Wt CpG v B KO PBS ($p<0.05$);* ‡ *Wt PBS v B KO CpG ($p<0.05$).*

B 7909 tolerated infection significantly better than intact PBS mice and B-cell KO PBS mice, particularly in the latter stages of infection (Figure 3.26b). Interestingly, B-cell KO mice treated with CpG-B 7909 also fared better than wild-type mice treated with PBS, with the average weight between treatment groups being significantly higher on day +9 of infection (Figure 3.26b). Treatment was also found to have a significant effect on the rate of the development of clinical signs of infection and recovery ($p=0.0005$) as measured by the kinetics of weight loss.

3.3.8. The role of neutrophils in CpG mediated VACV protection

Following intranasal delivery of CpG-B 7909 into the lung, the numbers of various pulmonary innate effector cells increased significantly compared to non-CpG-treated controls (Section 3.3.3). Amongst these, the numbers of activated neutrophils in CpG-treated mice were found to be significantly elevated compared to those pre-treated with PBS (Section 3.3.3.2). Neutrophils are potent phagocytic cells that are known to be amongst the first cell types recruited to the site of infection and have been shown to phagocytose VACV *in vitro* (West *et al.*, 1987). Therefore, the role of neutrophils in response to CpG stimulation in VACV challenged mice was investigated. A neutralising antibody (RB6-8C5) to a prevalent neutrophil marker Gr-1 was used to ablate neutrophil responses from the initial stages of infection. Groups of mice ($n=8$) were treated with 75μg/ml CpG-B 7909 or PBS three days prior to challenge with 10 MLD VACV. The day before challenge, mice were injected with 500μg of either the neutrophil ablating antibody RB-6 or a non-specific IgG2b isotype control antibody (Mac-5). Survival data for this experiment is represented in Figure 3.27a. Neutrophil depletion was found to have no significant protective effect on survival as determined by the Kaplan-Meier log-rank survival test ($p=0.4205$). However, disease severity was

a)

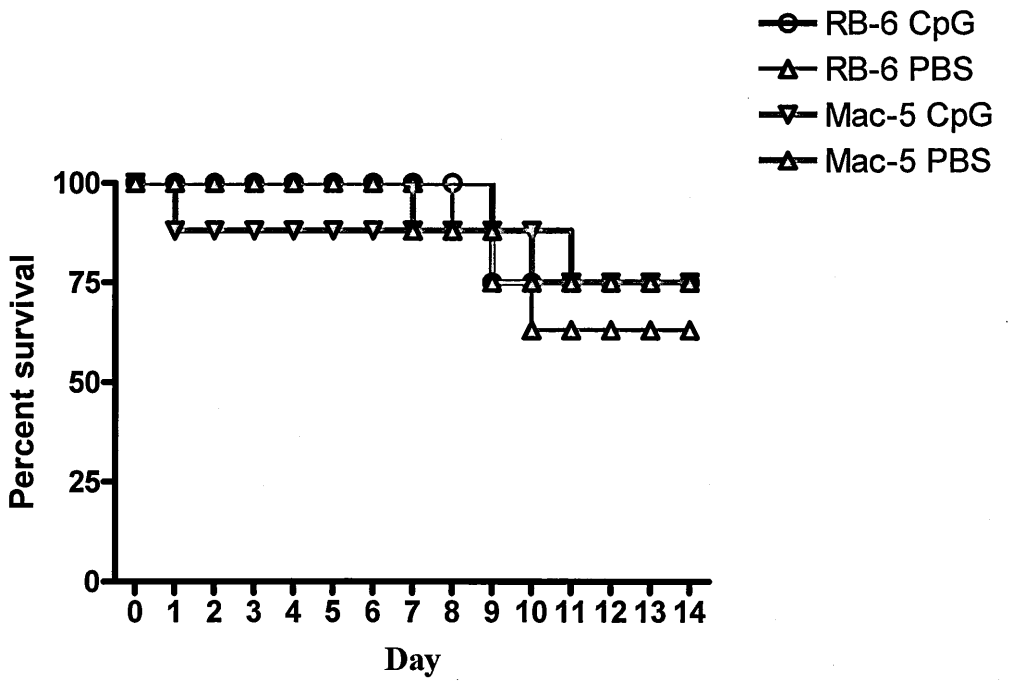

b)

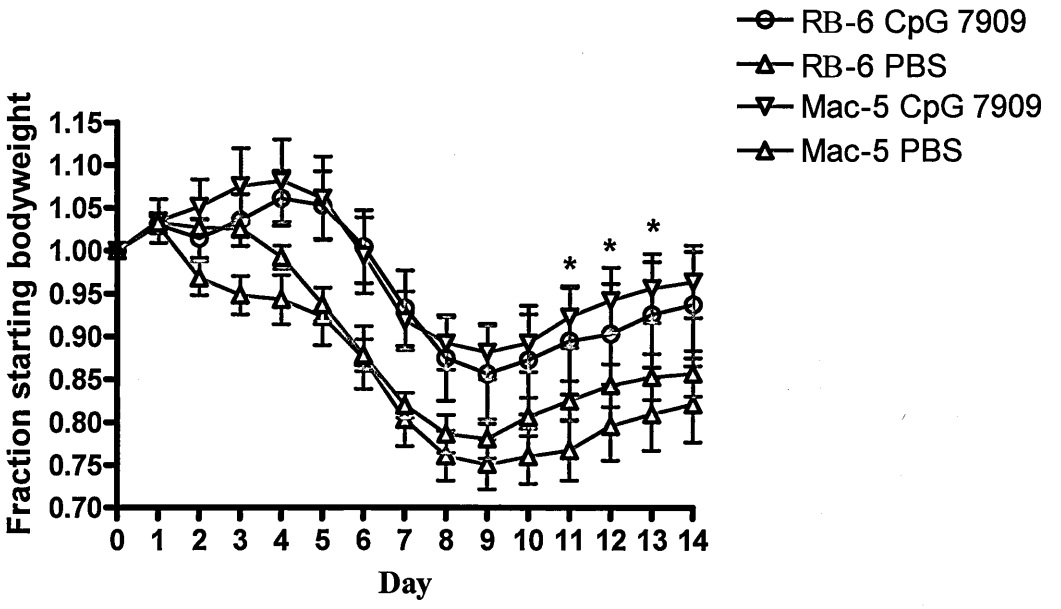

Figure 3.27. Effect of neutrophil depletion on CpG-mediated VACV protection. Groups of Balb/C mice (n=8) were treated with a neutrophil depleting antibody (RB-6) or an isotype control antibody (Mac-5) and then pre-treated with either 75μg/ml CpG-B 7909 or PBS three days prior to challenge with 10 MLD VACV. **(a)** Survival data: **(b)** Mean weight loss; Mice were weighed daily throughout the experiment, data points represent geometric mean weight per time-point ± SEM. Statistical significance was determined using a two-way ANOVA and Bonferroni's post-tests.

* *Denotes statistical significance ($p<0.05$) between RB-6 PBS and Mac-5 CpG treatment groups.*

found to vary significantly between treatment groups ($p=0.0238$) (Figure 3.27b). In addition, CpG treatment also had a significant effect on the rate of weight loss between groups ($p=0.0124$). Here, mice depleted of neutrophils and treated with PBS lost weight significantly quicker over the early stages of infection than neutrophil depleted mice treated with CpG ($p<0.0232$). Towards the end of infection on days +11, +12 and +13, the mean weights recorded for neutrophil depleted mice treated with PBS (RB-6 PBS) and control antibody mice treated with CpG-B 7909 (Mac-5 CpG) differed significantly ($p<0.05$) (Figure 3.27b).

3.4. Discussion

The use of CpGs as an immunotherapy has demonstrated success in a wide variety of studies when administered prior to challenge with an infectious pathogen. These have included studies into the protective effects of different classes of CpGs against a variety of bacterial, parasitic and viral pathogens (Elkins *et al.*, 1999b; Ashkar *et al.*, 2003; Krieg, 2006). To date, the use of CpGs as a prophylactic against orthopoxvirus infection has not been fully studied. Studies by colleagues here at Dstl have previously established that CpG-B 7909 can provide full protection against an intranasal challenge with VACV (Rees *et al.*, 2005). These studies established that CpG-B 7909 could be given up to seven days prior to challenge with VACV and still confer complete protection. Additionally, this preliminary work observed significant differences in the dissemination of VACV in CpG-treated and untreated groups and also noted an increase in the levels of the chemokines RANTES and MIP-1β in CpG-treated mice compared to un-treated control mice (Rees *et al.*, 2005). However, this study did not provide a comprehensive immunological investigation into other cytokines or cell-types that may prove vital to the protective response against VACV afforded by intranasal CpG delivery. Therefore, this chapter has re-examined the use of CpG as a prophylactic against VACV and presents a comprehensive analysis of the immunological effects of CpG-B 7909 when administered prior to intranasal challenge with VACV.

The immunomodulatory nature of CpGs results from their direct interaction with cells that express the pattern recognition receptor TLR9 (Hemmi *et al.*, 2000). In the lung, a range of different cell types express TLR9 and can respond directly to CpG stimulation. B-class CpGs such as CpG-B 7909 are predominantly recognised as

potent stimulators of B-cells by direct binding and stimulation of TLR9. This has been shown to result in cellular proliferation and the up-regulation of co-stimulatory molecules such as CD80, CD86 and CD40 (Krieg *et al.,* 1995). In the results presented in this chapter, flow cytometry analysis of lung samples identified significantly higher numbers of $CD80^+$ and $CD86^+$ B-cells in the lungs of CpG-treated mice on day 0 and +1 of infection compared to those from untreated animals. CD80 and CD86 are required for effective antigen presentation to T-lymphocytes and their up-regulation is indicative of B-cell maturation and activation (Suvas *et al.*, 2002). These increases in the numbers of activated B-cells in CpG-treated mice may have been a result of direct TLR9 stimulation. Other TLR9 expressing cells in the lung include myeloid and plasmacytoid dendritic cells and these cell-types can also be activated directly by CpG-B stimulation (Demedts *et al.*, 2006; Sparwasser *et al.*, 2000). CpG stimulation of DCs results in DC maturation and increased antigen presenting capability. In this study, the numbers of $CD11c^+$ DCs and percentages of activated dendritic cells (%$CD80^+$, %MHC II^+) were also significantly higher in the lungs of CpG-treated mice. Increases in the expression of CD80 and MHC II on DCs allow for more effective antigen presentation to T-lymphocytes and is a well documented response to CpG stimulation (Askew *et al.*, 2000; Sparwasser *et al.*, 2000). In addition, levels of IFN-α were significantly higher in CpG-treated animals than in those receiving PBS. The predominant cellular source of IFN-α are pDCs and its prominent release from activated pDCs has been shown by a variety of groups following CpG stimulation (Krug *et al.*, 2001). These differences in PBS and CpG-treated mice may all have been a direct result of CpG stimulation.

In addition to altering the phenotype of TLR9 expressing cells, direct stimulation of TLR9 results in the activation of transcription factors such as NF-κB and subsequent release of pro-inflammatory cytokines to promote a prominent Th-1 cytokine environment (Krieg *et al.*, 1995; Yi *et al.*, 1996b; Krug *et al.*, 2001; Klinman *et al.*, 1996). Once secreted, these cytokines exert a wide range of effects including the stimulation of other cell types that do not express TLR9. Thus, CpGs influence the kinetics and activation of a variety of cell types through both direct and indirect TLR9 stimulation. Collectively, these cytokines function to activate relevant cell types in the surrounding area and to recruit cells such as neutrophils and macrophages from the blood and surrounding tissues.

Expression of the type I and type II interferons, IFN-α and IFN-γ, were significantly increased in the lungs of mice that received CpG treatment compared to untreated control mice. These cytokines may play a variety of roles in inflammation. The release of IFN-α often initiates a potent antiviral response in the host, resulting in the activation of many other interferon-related genes including IFN-γ (Takaoka & Yanai, 2006). The release of IFN-γ following CpG stimulation has typically been observed from activated NK cells (Ballas *et al.*, 1996; Sivori *et al.*, 2006; Marshall *et al.*, 2006). In this study, significantly elevated numbers of activated NK cells expressing the early activation marker CD69 were observed in the lung early in infection, correlating with the observed increases in pulmonary IFN-γ levels. The antiviral properties of the interferons are well established. Together, interferons create an antiviral state that restricts the replication of viruses within host cells (Platanias, 2005; Katze, He, & Gale, 2002). Many other studies have examined the prophylactic effect of CpG treatment prior to viral challenge and these studies have reported reduced pathology

and viral titres in CpG-treated animals compared to control groups (Ashkar *et al.*, 2003; Li *et al.*, 2006; Harandi *et al.*, 2003; Sajic *et al.*, 2003). In many cases, protection in these studies has relied upon strong IFN-γ responses, as seen in the effective treatment of HSV-2 infection with another B-class CpG 1826 (Harandi, Eriksson, & Holmgren, 2003). Here, mice deficient in IFN-γ, IL-12 or IL-18 failed to confer any significant protection against virus infection.

In addition to its direct antiviral properties, IFN-γ has also been shown to stimulate macrophages to release TNF-α and promote the release of other pro-inflammatory cytokines such as IL-6 from B-cells (Yi *et al.*, 1996a). It is of note that levels of both IL-6 and TNF-α were significantly elevated in the lungs of CpG-treated mice in this study. IL-6 is a potent pro-inflammatory cytokine with pyrogenic properties that is thought to play a role in the recruitment of monocytes to the site of infection and modulation of other cellular functions (Kaplanski *et al.*, 2003; Morales-Montor, 2005). Importantly, IL-6 plays a fundamental role in the immune response against VACV as IL-6 knock-out (KO) mice fail to control virus replication efficiently (Kopf *et al.*, 1994). TNF-α is a pleiotropic pro-inflammatory cytokine with a variety of diverse immunological functions which can promote cellular proliferation and activation, apoptosis or contribute to the onset of septic shock if over-expressed (Rahman & McFadden, 2006). TNF-α has been shown to have powerful pro-inflammatory effects and many viruses, including VACV, encode TNF receptor homologues to combat its effects (Saraiva & Alcami, 2001; Rahman & McFadden, 2006; Lidbury *et al.*, 1995). Other studies have also observed increases in IL-6 and TNF-α following intranasal CpG stimulation, with increased cytokine expression being detectable in the BAL of treated mice within 4 hours (Schwartz *et al.*, 1997).

Levels of CCL2, a monocytic chemoattractant protein, were also significantly higher in the lungs of mice pre-treated with CpG-B 7909, as has been reported in previous studies involving CpGs (Edwards *et al.*, 2005). This chemokine acts as a chemoattractant to recruit monocytes and macrophages along a concentration gradient to the site of inflammation. Macrophages have been shown to respond to CpG stimulation both *in vivo* and *in vitro* with activation enhancing both phagocytic and anti-microbicidal activity in addition to pro-inflammatory cytokine and chemokine release (Utaisincharoen *et al.*, 2002; Utaisincharoen *et al.*, 2003; Huang *et al.*, 2005). Macrophage numbers in this study were significantly elevated in the lungs of CpG-treated mice compared to control groups (Figure 3.2). In addition, macrophage expression of MHC II was found to be significantly lower in CpG-treated animals than in PBS mice (Figure 3.3b), a response that has also been documented in other studies (Chu *et al.*, 1999). It is possible that the reduction of MHC II on macrophages enhances antigen presentation by other professional antigen presenting cells such as dendritic cells to promote a more effective specific immune response (Chu *et al.*, 1999). The expression of TLR9 on alveolar macrophages has been reported in a number of studies (Huang *et al.*, 2005), although other studies have suggested that TLR9 on alveolar macrophages may be non-functional (Suzuki *et al.*, 2005). Therefore, the activation of macrophages in the lung may have been a result of cytokine stimulation (e.g. by IFN-γ) or a direct consequence of TLR9 stimulation.

Neutrophil responses in the lung were also found to be significantly different between treatment groups. Neutrophils are key phagocytic cells that kill pathogens through release of lytic enzymes, reactive oxygen species or through release of extracellular

chromatin nets (Nathan, 2006). Here, CpG-treated mice were found to have increased numbers of activated neutrophils compared to PBS mice over the first few days of infection. Neutrophils are not generally thought to express TLR9 although direct CpG stimulation of human neutrophils has been reported (Hayashi, Means, & Luster, 2003). This makes the indirect stimulation of neutrophils more likely to account for the increases in neutrophil activation. Increases in CD11b expression are typically indicative of cellular egress and in this data, maybe a sign of recent recruitment of neutrophils to the site of stimulation. Interestingly, the percentage of $CD54^{+}$ neutrophils was significantly lower on day +1 of infection in CpG-treated mice than in control mice. Expression of CD54, also known as intracellular adhesion molecule-1 (ICAM-1), can be down-regulated by anti-inflammatory cytokines such as IL-10 and this down-regulation may prevent neutrophils leaving the site of infection (Tomioka *et al.*, 2000).

Levels of the anti-inflammatory cytokine IL-10 were observed as being significantly higher on day +1 of infection in CpG-treated animals than untreated controls. Given the extent of cytokine stimulation in CpG-treated animals, increased levels of IL-10 may act to help balance the immune response to prevent a detrimental immune response in the host. However, it has been suggested that IL-10 may serve a dual role in inflammation by enhancing NK activity (Lauw *et al.*, 2000). Therefore, it is possible that the increased activation of NK cells in CpG-treated animals may be linked to these increased levels of IL-10. This in turn may contribute to the high levels of IFN-γ observed throughout the early stages of infection.

Although thought to be transient in their expression, all cytokine levels were first determined three days after CpG delivery on the day of challenge (day 0) and remained significantly above control levels throughout the first three days of VACV infection. As a result it is unclear whether the levels of cytokines detected in the lungs of CpG-treated mice were at their peak levels, in a plateau phase or had reduced in the days following CpG delivery. It is likely that elevated levels of pro-inflammatory cytokines such as those described above, may have contributed significantly to the protective response against VACV through the presence of a fully activated and primed immune response at the time of infection.

The patterns of immune stimulation seen in the lungs of CpG stimulated mice were not mirrored in the spleens. However, other significant differences were observed between treatment groups suggesting that CpGs can result in significant immune effects at sites distal from their original point of delivery. Here, levels of pro-inflammatory cytokines such as IFN-α, TNF-α, and IL-6 in CpG-treated mice were comparable with control mice throughout the course of infection. Levels of IFN-γ in the spleens of PBS treated mice on day +3 of infection were significantly higher than in those that received CpG-B 7909. In previous work, dissemination of VACV to the spleens of PBS mice also occurred on day +3 of infection (Rees *et al.,* 2005). In contrast, mice pre-treated with CpG-B 7909 did not have peak titres of VACV in the spleen until day +4 of infection. Viral titres were not obtained throughout this study because lung and spleen cell suspensions were preserved for analysis by flow cytometry. However, it is of note that peak IFN-γ levels in PBS treated mice in this study correlate with the arrival of VACV on day +3 in the Rees study. Likewise, peak IFN-γ levels in CpG-treated mice in this study occurred on day +4 which matches the

arrival of virus in the spleens of CpG-treated mice in the Rees study (Rees *et al.*, 2005). In addition, Rees and colleagues also observed significantly lower viral titres in the lungs of CpG-treated mice in the early stages of infection. It is possible that the release of high levels of IFN in the lung along with extensive cellular activation during the early stages of infection may have played a significant role in delaying dissemination of VACV to the spleen.

Cellular activation data in the spleen identified a number of significant differences between treatment groups. On day 0 of infection, significantly higher numbers of activated macrophages and B-cells were present in CpG-treated animals. It is unclear whether these cells were directly activated by CpG through TLR9 stimulation despite being reported to express TLR9 (Krieg *et al.*, 1995; Suzuki *et al.*, 2005). For this to happen, CpG-ODN would either have to cross the mucosal barrier of the lung to gain access to the blood for systemic transportation, or alternatively, CpGs may need to have been transported in phagocytic cells such as neutrophils to the spleen and then be released upon cellular necrosis or apoptosis. This is plausible given the significant increase in the number of $CD11b^{+}$ expressing neutrophils in CpG-treated animals observed on day 0. However, it is also possible that the observed differences may be a result of these cell-types being stimulated in the lung and then having migrated to the spleen. Given the lack of cytokines detectable in the serum of CpG treated mice, it is also doubtful that these cell-types were activated as a result of systemic cytokine activation. Of particular interest is the prevalence of significant differences between treatment groups on days +7 and +9 of infection. In the animal model used throughout these studies, mice receiving CpG treatment typically begin to recover around this period of infection (day +7 to +9). Interestingly, all significant differences at these

latter time-points revealed elevated numbers or increased activation in CpG-treated mice compared to those mice treated with PBS. This may be indicative of CpG-treated mice developing an appropriate immune response or a more sustained innate response. Alternatively, CpG-treatment may promote a more rapidly formed adaptive immune response as indicated by increased numbers of B and T-lymphocytes in the spleen.

The immunological differences described above in the lungs and spleens of VACV infected mice point towards a very significant role for the local lung environment in conferring CpG-mediated protection. Table 3.1 summarises the significant cellular differences between CpG-treated and untreated mice in the lung. These results show a large number of significant differences between treatment groups, particularly on day 0 and day +1 of infection. Throughout this 24 hour period, the lungs of CpG-treated mice had higher numbers of activated macrophages, neutrophils, dendritic cells, NK cells, B-cells and $CD4^+$ T-cells than untreated mice. In addition, significantly higher levels of pro-inflammatory and antiviral cytokines were present in CpG-treated mice during this time. In contrast, very few differences between CpG-treated and untreated mice were identified in the spleen during early infection (Table 3.2). This finding may emphasise the importance of local lung inflammation at the time of VACV challenge. The arrival of activated or primed effector cells into the lungs of CpG-treated mice prior to VACV challenge is likely to be one of the key contributors to CpG-mediated protection. Collectively, these cytokine and cellular responses are likely to attack VACV at the source, restricting its replication in the lung and severely hindering its ability to establish infection. This in turn may restrict local lung pathology and delay viral dissemination around the body. Significant differences between treatment groups

	Day						
	0	+1	+3	+5	+7	+9	CpG-B 7909 Treatment
Total macrophages		+++					+++
$F4/80^+$ $CD54^+$		+++					
$F4/80^+$ IA/IE^+		+++					+++
% $CD54^+$			+				+
% IA/IE^+	++	++					+
Total neutrophils	+++	+++					+++
$Ly6G^+$ $CD54^+$	+++						+
$Ly6G^+$ $CD11b^+$	+++	+++					+++
% $CD54^+$		++					+
% $CD11b^+$	+++	++	+			+	+++
Total dendritic cells						++	+++
$CD11c^+$ IA/IE^+	+++	+				+	+++
$CD11c^+$ $CD80^+$	++	++	+				+++
% IA/IE^+		++	++				+++
% $CD80^+$	+++	+++				+++	++
Total NK cells		+++				+++	+++
$CD49b^+$ $CD54^+$						++	+
$CD49b^+$ $CD69^+$	+	+++				+	+++
% $CD54^+$	+						+
% $CD69^+$							
Total B-cells	+	+					+++
$CD19^+$ $CD86^+$	++	+					+++
$CD19^+$ $CD80^+$	+	+					+++
% $CD86^+$						+	
% $CD80^+$						+	+++
Total $CD4^+$ T-cells	++					+++	+++
Total $CD8^+$ T-cells							++

Table 3.1. Significant differences between CpG-B 7909 and PBS treatment groups in the lungs of mice during VACV infection. Significant differences are recorded for each immune cell type investigated *via* flow cytometry in the lungs of VACV infected mice. Differences between total and activated cell numbers are reported along with differences between the % of activated cell-types for days 0, +1, +3, +5, +7 and +9 post-infection. The overall effect of CpG treatment is also reported. Significance between treatment groups determined *via* two-way ANOVA with Bonferroni's post-tests and represented as: + $p<0.05$; ++ $p<0.01$; +++ $p<0.001$.

	Day						
	0	+1	+3	+5	+7	+9	CpG-B 7909 Treatment
Total macrophages					++	+++	++
$F4/80^+$ $CD54^+$						++	++
$F4/80^+$ IA/IE^+					+	+++	++
% $CD54^+$							
% IA/IE^+							
Total neutrophils						+	++
$Ly6G^+$ $CD54^+$							
$Ly6G^+$ $CD11b^+$						+	++
% $CD54^+$							+
% $CD11b^+$	+++						++
Total dendritic cells						++	
$CD11c^+$ IA/IE^+						+	
$CD11c^+$ $CD80^+$							
% IA/IE^+							
% $CD80^+$			+++				
Total NK cells						+++	++
$CD49b^+$ $CD54^+$							
$CD49b^+$ $CD69^+$							
% $CD54^+$							+++
% $CD69^+$							
Total B-cells	+++					+++	
$CD19^+$ $CD86^+$						+++	
$CD19^+$ $CD80^+$	+++					+++	
% $CD86^+$	+++						
% $CD80^+$	+++						
Total $CD4^+$ T-cells						+++	++
Total $CD8^+$ T-cells						+++	

Table 3.2. Significant differences between CpG-B 7909 and PBS treatment groups in the spleens of mice during VACV infection. Significant differences are recorded for each immune cell type investigated *via* flow cytometry in the spleens of VACV infected mice. Differences between total and activated cell numbers are reported along with differences between the % of activated cell-types for days 0, +1, +3, +5, +7 and +9 post-infection. The overall effect of CpG treatment is also reported. Significance between treatment groups determined *via* two-way ANOVA with Bonferroni's post-tests and represented as: + $p<0.05$; ++ $p<0.01$; +++ $p<0.001$.

were also found on day +9 of infection in both the lung and spleens of infected mice (Table 3.1 and Table 3.2). Here, higher numbers of activated cell types were present in mice treated with CpG-B 7909 than in control mice. Of particular interest are differences in numbers and activation status of T and B-lymphocytes. This implies that during the latter stages of infection, both the lung and the spleen may contribute significantly to the resolution of infection in CpG-treated mice, potentially through initiation of an adaptive response.

The role of B-cells and neutrophils in CpG mediated protection were investigated using B-cell KO mice and a neutralising antibody to a neutrophil cell marker. Results from the B-cell KO study revealed that B-cells were not fundamental in the protection elicited by CpGs against VACV as there was no significant difference in the survival of intact and B-cell KO mice treated with CpG ($p=0.1970$). In addition, no significant differences were determined between the average weights of wild-type and B-cell KO mice that received CpGs ($p>0.05$). This suggests that in an acute VACV infection, CpG-B 7909 is able to directly stimulate cell types other than B-cells and this stimulation is sufficient to generate a protective response. This is further suggested by the observation that both B-cell KO mice and wild-type mice that received CpG-B 7909 tolerated infection equally, but significantly better than their equivalent PBS control groups (Figure 3.26b). These observations question the role of VACV specific antibody in the resolution of acute VACV infection in CpG mediated protection. Antibody secretion follows the recognition of antigen by receptors on B-cells and their subsequent differentiation into plasma cells. The generation of specific antibody is not possible in the absence of B-cells. In untreated intact mice, antibody is thought to play a significant role in the resolution of acute VACV infection through direct

neutralisation and opsonisation of virus particles (Belyakov *et al.*, 2003). In this present study, untreated B-cell KO mice were most susceptible to virus infection (Figure 3.26a). In addition, other studies have examined the role of B-cells in protection against VACV and suggested that mice deficient in B-cells fail to clear infection (Xu *et al.*, 2004; Chaudhri *et al.*, 2006). These observations support a role for antibody production in protection. However, in CpG-treated B-cell KO mice, it is possible that the strength of the Th-1 response generated by CpG-B 7909 compensates for the lack of neutralising antibody. Redundancy in the immune response is well reported and has been seen in studies where antibody to VACV was essential in $CD4^+$ and $CD8^+$ deficient mice, but not required when these cell-types were present (Belyakov *et al.*, 2003). B-cell KO mice have also been used to study immunity to vaginal HSV-2 infection (Parr & Parr, 2000). In this study, the lack of B-cells did not significantly affect levels of protection, as has been reported here. However, the kinetics of the immune response and control of viral titres were found to differ between wild-type and B-cell KO mice suggesting that B-cells may still play a role in controlling viral infection. In other studies, B-cells have also been reported to be important in controlling secondary *Francisella* infection in a manner that does not involve antibody (Elkins *et al.*, 1999a). These studies suggest that antibody may not always be required to confer protection against pathogens and that B-cells may provide significant contributions to the immune response in other ways.

The high expression of the cell surface marker Gr-1 on neutrophils enables *in vivo* depletion of neutrophils with the monoclonal antibody RB6-8C5 and has been used extensively to study the role of neutrophils in infection (Nathan, 2006). Neutrophils

have previously been shown to play a significant role in HSV-1 and HSV-2 virus protection (Tumpey *et al.*, 1996; Milligan, 1999) and have also been shown to phagocytose VACV particles (West *et al.,* 1987). In this study, neutrophils were depleted on day -1 of challenge, i.e 24 hours prior to VACV challenge but 48 hours after CpG stimulation. Neutrophils were only depleted at this time-point to ensure neutrophils were not present during the initial infection with VACV. Survival analysis on CpG-treated and untreated groups found no significant differences between neutrophil depleted and neutrophil replete groups. These results initially suggest the absence of neutrophils at the time of VACV challenge does not affect CpG mediated VACV protection. However, this raises three clear points for discussion. Firstly, neutrophil numbers are constantly regenerated over time due to their short lifespan. Consequently, it is not known for certain at which point neutrophil numbers returned to baseline levels. In this data, the rate of weight loss in RB6-PBS mice over the first few days of VACV infection was greater than for other groups. This may suggest an important early role for neutrophils in the resolution of VACV infection and not necessarily a role in CpG-mediated protection. Regeneration of neutrophil numbers and subsequent activation after this point could explain the temporary stabilisation of weight loss seen between days +3 to +5 and ultimately contribute to the resolution of infection. Secondly, in addition to phagocytosis and release of lytic enzymes and reactive oxygen species into the surrounding areas, neutrophils also influence the behaviours of other cell types. For instance, neutrophils secrete chemotactic signals such as cathepsin-G, which attracts monocytes, and chemerin which attracts both immature DCs and pDCs to the site of inflammation (Bennouna *et al.*, 2003; Chertov *et al.*, 1997; Wittamer *et al.*, 2005). In addition, neutrophils can also influence the properties of differentiated macrophages through secretion of cytokines such as TNF-

α and IFN-γ (Ethuin *et al.*, 2004). Since neutrophils were present at the time of treatment in all groups, it is unclear whether they play an important role prior to VACV challenge. Thirdly, an unfortunate consequence of using the RB6 antibody is that Gr-1 is also expressed to a lesser extent on other cell types (Geissmann *et al.*, 2003; Matsuzaki *et al.*, 2003). These include Gr-1^{+} CD8^{+} T-cells and some monocytes. The extent of unwanted cellular depletion was not determined in these studies and thus the effect of losing other Gr-1 expressing cells types in the early stages of infection cannot be accounted for. Other studies have suggested that up to 85% of these additional Gr-1 expressing cell sub-sets may be depleted (Easton *et al.*, 2007). As expected, neutrophil depleted PBS mice were found to be most susceptible to infection and experienced the most severe weight loss of all groups tested (Figure 3.27). Given the data obtained in this study, it is possible that neutrophils could be significant contributors to CpG mediated protection against VACV but may not be the main contributors to protection.

In conclusion, this chapter has sought to address the immunological basis behind the successful pre-treatment of mice with CpG-B 7909 prior to VACV infection. The results presented within this chapter demonstrate that intranasal delivery of the B-class CpG-B 7909 elicits a powerful immunological response in the local lung environment at the time of infection and that this response correlates strongly with protection. This response includes the secretion of pro-inflammatory cytokines such as IFN-α, IFN-γ, TNF-α and IL-6 and the recruitment and activation of key effector cell types such as dendritic cells, macrophages, neutrophils and NK cells. Consequently, at the time of VACV challenge, the lung environment is loaded with elevated numbers of key effector cells that are primed for infection and are potentially

already in an antiviral state. Immune responses in the lungs and spleens of CpG-treated mice in the latter stages of infection may both play a significant part in virus clearance and alleviation of clinical signs of disease. This work has also suggested that B-cells and neutrophils may not be crucial cell types in protecting against VACV infection following CpG-B 7909 prophylaxis.

The ability of CpG-B 7909 to protect in this pre-exposure model correlates with its ability to induce a strong, local Th-1 inflammatory response. Whether CpG-B 7909 can confer similar levels of protection when administered concomitantly with VACV challenge or post-challenge is currently unknown. The next chapter in this thesis will address this question and examine whether the immunological response generated by CpG-B 7909 is equally as effective when given after virus exposure.

Chapter 4: The use of CpG-B 7909 as a post-exposure therapeutic against VACV

4.1. Introduction

The timing of CpG delivery in the treatment against infectious disease has proven to be one of the most crucial aspects of CpG mediated therapy. The majority of studies reporting the successful use of CpGs as a monotherapy have involved a dosing regimen that begins prior to pathogen challenge. For instance, studies against intracellular bacteria such as *Francisella tularensis* and *Listeria monocytogenes* have achieved full protection when mice were pre-dosed with CpG up to 7 days before infection and partial protection when administered as early as 14 days prior to infection (Elkins *et al.*, 1999b). Similar levels of protection have also been seen in CpG pre-treatment of *Burkholderia pseudomallei* infection where 100% protection against lethality was obtained when CpGs were administered up to 10 days prior to infection, and 57% protection was obtained when CpGs were given 15 days prior to infection (Wongratanacheewin *et al.*, 2004). However, CpG treatment on the day of infection saw protection drop to 33% in these studies and granted no protection at all if given 24 hours after challenge. Similarly low levels of protection (10%) were also reported in studies using *Burkholderia mallei* when CpGs were administered 24 hours post-challenge (Waag *et al.*, 2006). In contrast, treatment with CpG 48 hours prior to *B.mallei* challenge was able to confer full protection and provide 90% protection if treated at the time of challenge (Waag *et al.*, 2006). CpGs used as a post-exposure treatment for *Mycobacterium tuberculosis* have yielded more positive results. Here, CpGs administered to mice two weeks post-infection resulted in a significant drop in the number of bacteria in the lungs of infected mice and an increase in the IFN-γ

production by splenocytes when measured three weeks post-treatment (Juffermans *et al.*, 2002). Significant improvements in tuberculosis disease progression were also seen when CpGs were first given 2 hours pre- and then 6 hours post-challenge (Juffermans *et al.*, 2002).

The effective post-exposure treatment of parasitic infection has also been reported by Zimmermann and colleagues. Single doses of CpG to mice infected with *Leishmania major* proved curative when given during the first 8 days of infection but failed to elicit protection if given as a single dose thereafter (Zimmermann *et al.*, 1998b). However, three consecutive doses of CpG were shown to control infection with *L.major*, starting as late as day +20 of infection (Zimmermann *et al.*, 1998b). Protection against the intracellular parasite *Toxoplasma gondii* has also been achieved using CpGs. Here, a single injection of CpG at the time of challenge was sufficient to confer long-term survival against toxoplasmosis (Zimmermann *et al.*, 1998a). This same study reported that CpG treatment was also able to reduce disease severity in mice given a sub-lethal dose of *T.gondii* by reducing the number of cysts found in the brain.

Against viral infection, successful CpG-mediated protection has been mostly reported when administered prior to or at the same time of infection, as has been seen in mouse models of HSV-2 (Harandi *et al.*, 2003; Sajic, *et al.*, 2003; Ashkar, *et al.*, 2003), VACV (Rees *et al.*, 2005) (Chapter 3) and TCAV (Pedras-Vasconcelos *et al.*, 2006). However, some viruses have also been successfully treated using CpGs post-challenge. For instance, although pre-treatment of HSV-2 48 hours prior to infection with CpG was shown to confer 80% protection in a murine model (Harandi *et al.*,

2003), treatment given 4 hours after challenge was still able to confer 66% protection against lethal infection. In another model of virus infection, CpG treatment +4, +9 and +14 days after infection with FLV in animal models has been shown to significantly increase disease recovery from 6% in control mice to 74% in mice treated with CpG (Olbrich *et al.*, 2002).

4.2. Aims of this chapter

The pre-treatment of VACV infection with the B-class CpG-B 7909 has been shown to afford high levels of protection against VACV (Rees *et al.*, 2005). However, the ability of the same CpG to confer protection when given post-challenge is unclear. This chapter examines the use of CpG-B 7909 as a post-exposure therapy following intranasal challenge with VACV and assesses the immunological impact of delayed treatment in mouse models of infection.

4.3. Results

4.3.1. Selection of day and dose for post-exposure CpG delivery

Previous work by colleagues within Dstl and through personal communication with our collaborator AM Krieg, highlighted concerns over the toxicity of administration of high doses of CpG-B 7909 concurrent with VACV challenge. Consequently, an experiment was designed to examine the effect of lower doses of CpG-B 7909 than those used in the published pre-exposure model (Rees *et al.*, 2005), following intranasal challenge with VACV. Given the previous success of treating VACV in the pre-exposure model, the intranasal route was again selected as the preferred route of treatment for post-exposure CpG-B 7909 delivery. Groups of mice (n=5) were challenged intranasally with 10 MLD VACV and then treated intranasally with PBS, or 15μg, 30μg or 50μg of CpG-B 7909 on day +1 or day +2 of challenge (Figure 4.1). Mice receiving either the 15μg or 50μg dose of CpG-B 7909 on day +1 were not protected from VACV challenge (Figure 4.1a). In contrast 60% of mice treated with 30μg of CpG on day +1 survived infection. No protection was observed when treatment with CpG-B 7909 was withheld until day +2 of infection, regardless of dose used (Figure 4.1b).

4.3.2. Effect of multiple doses of CpG-B 7909 *via* the intranasal route

The previous experiment had demonstrated that a single 30μg dose of CpG-B 7909 could provide protection against lethal VACV infection. The use of a second dose of CpG-B 7909 to improve protection further in the challenge model was examined. Groups of mice (n=4) were challenged intranasally with 10 MLD VACV and subsequently treated intranasally on day +1 and day +2, day +1 and day +3, or day +2 and day +3 with 30μg of CpG-B 7909. Control mice were given PBS on the day of

a) Day +1

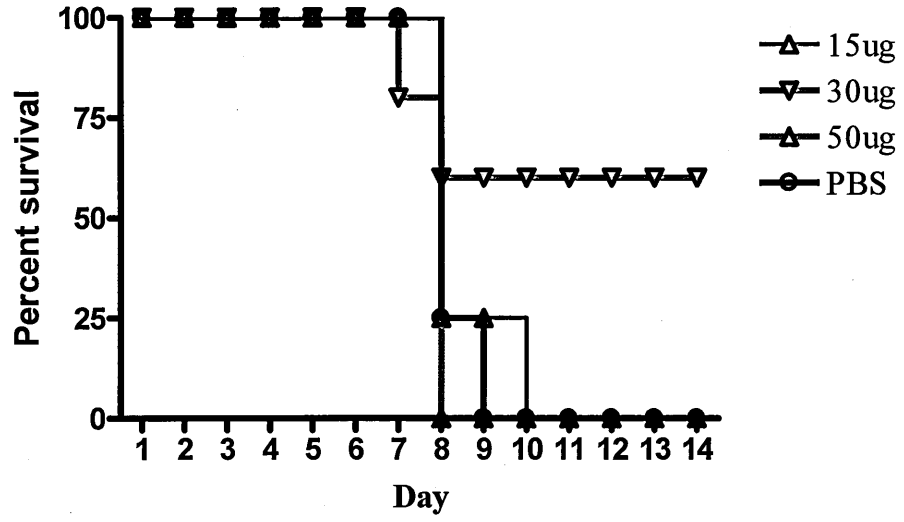

b) Day +2

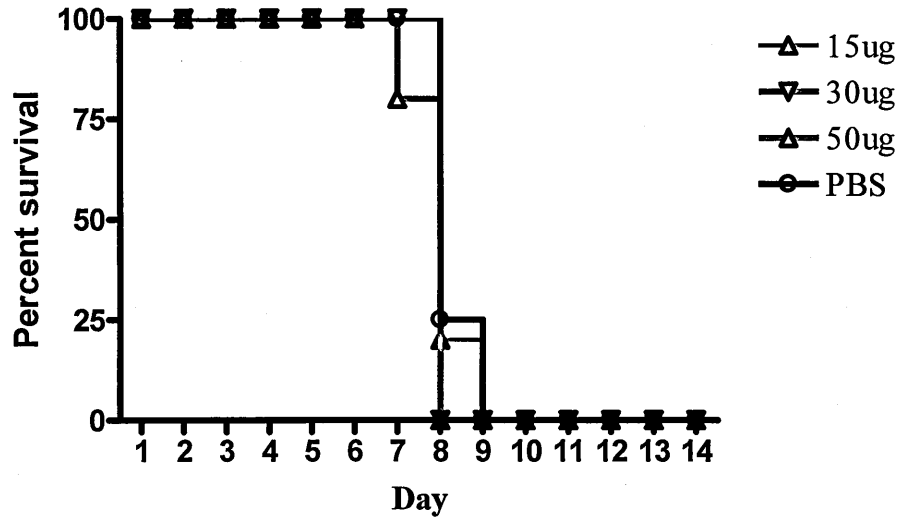

Figure 4.1. Different intranasal doses of CpG-B 7909 as a post-exposure treatment in mice infected with VACV. Graphs show survival data of mice (n=5) challenged intranasally on day 0 with 10 MLD VACV. Mice were treated intranasally on **(a)** day +1 or **(b)** day +2 with varying doses of CpG-B 7909 or PBS.

challenge or 75μg CpG-B 7909 six days prior to challenge. In this experiment, 25% mice treated with CpG-B 7909 survived infection regardless of dosing regimen (Figure 4.2). Interestingly, all control mice survived infection, suggesting that all groups of mice may have received a sub-lethal dose of VACV (Figure 4.2). Regardless, these results suggest that the multiple dosing of mice with CpG-B 7909 post-exposure using any of the regimens in this study, does not improve upon the levels of protection seen following a single treatment of CpG-B 7909.

4.3.3. Immunological impact of post-exposure CpG-B 7909 delivery

4.3.3.1. Experimental outline

The use of a single 30μg dose of CpG-B 7909 was selected for further immunological investigation *in vivo*. This experiment was run in parallel to that described in section 3.3.1 to reduce the numbers of control mice required. Briefly, two groups of Balb/C mice were challenged intranasally with 10 MLD VACV. All mice receiving CpG-B 7909 were treated on day +1 of infection with a single 30μg intranasal dose. All control mice were given 10μl of PBS 3 days prior to challenge. Groups of mice (n=4) from both treatment groups were humanely culled following infection on days +3, +5 and +7, for comparative immune analyses. Cytokine analyses of lung and spleen preparations and sera, allowed for the pro-inflammatory cytokines TNF-α, IL-6, IFN-α and IFN-γ, along with the chemokine CCL2 and anti-inflammatory cytokine IL-10 to be determined throughout the course of the experiment. Flow cytometric analysis of mouse spleen and lung samples allowed for enumeration of macrophages, neutrophils, DCs, NK cells, B-cells and T-cells, along with characterisation of key cellular markers for particular cell types.

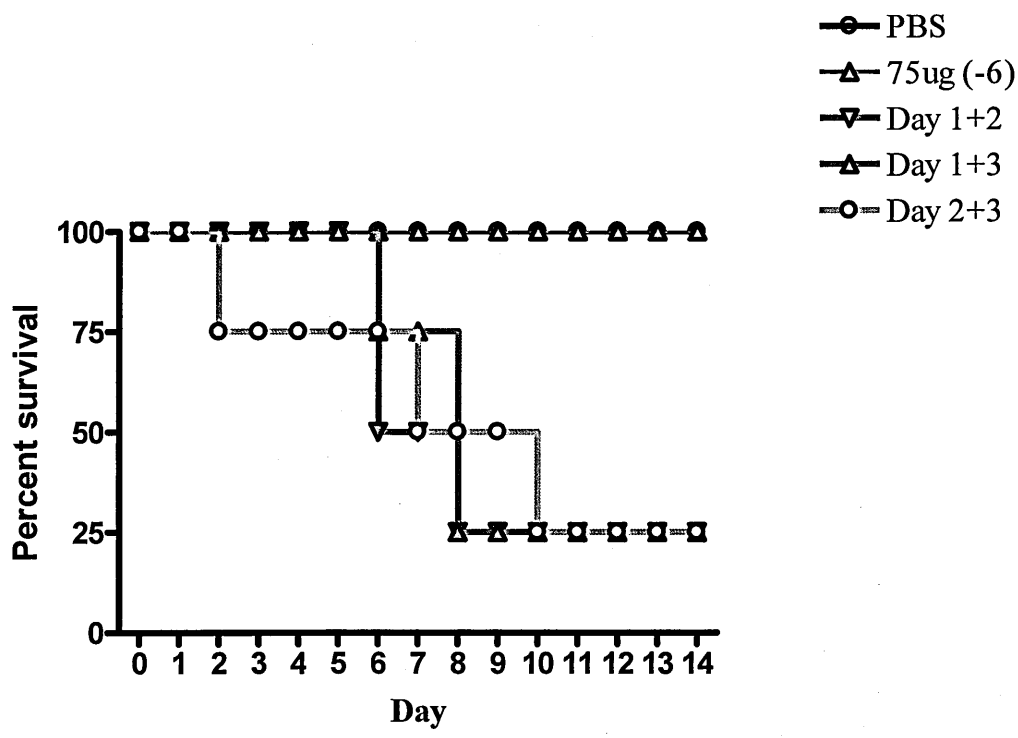

Figure 4.2. Effect of multiple dosing with CpG-B 7909 as a post-exposure treatment in mice infected with VACV. Graph shows survival data of mice (n=4) challenged on day 0 with 10 MLD VACV. Mice were treated intranasally post-infection with 30μg doses of CpG-B 7909 or PBS as shown.

4.3.3.2. Cytokine responses in the lung

The levels of all pro-inflammatory cytokines and chemokines measured in the lungs of mice treated 24 hours post intranasal VACV challenge were shown to differ significantly from PBS treated mice at some time throughout the infection time-course (Figure 4.3). On day +3 post infection, levels of TNF-α (Figure 4.3a), IL-6 (Figure 4.3b), IFN-α (Figure 4.3c), IFN-γ (Figure 4.3d), CCL2 (Figure 4.3e), and IL-10 (Figure 4.3f), were all significantly higher ($p<0.001$) in CpG-B 7909 treated animals. By day +5, levels of IFN-γ and IL-10 were no longer significantly different from PBS treated animals ($p>0.05$) whilst levels of TNF-α ($p<0.01$), IL-6 ($p<0.05$), CCL2 ($p<0.01$) and IFN-α ($p<0.01$) remained significantly elevated in CpG-B 7909 treated mice. Thereafter on day +7, only levels of TNF-α ($p<0.05$) and IFN-α ($p<0.001$) remained significantly higher in CpG-treated mice than in those given PBS.

4.3.3.3. Cellular responses in the lung

4.3.3.3.1. Lung macrophage responses

Antibody specific to the mouse macrophage cell marker F4/80 was used to label macrophages from lung cell suspensions. The activation status of macrophages at each time point was determined using monoclonal antibodies to monitor changes in the cellular expression of the activation marker CD54 and the expression of MHC class II molecules (IA/IE) on the surface of F4/80 positive cells.

Figure 4.4 shows the numbers of $F4/80^+$ cells in the lungs of mice treated with PBS or treated with CpG-B 7909 post intranasal VACV challenge. Total macrophage numbers in CpG-B 7909 treated mice were at their highest on day +3 and were elevated at each time point as shown in Figure 4.4a. Although total macrophage

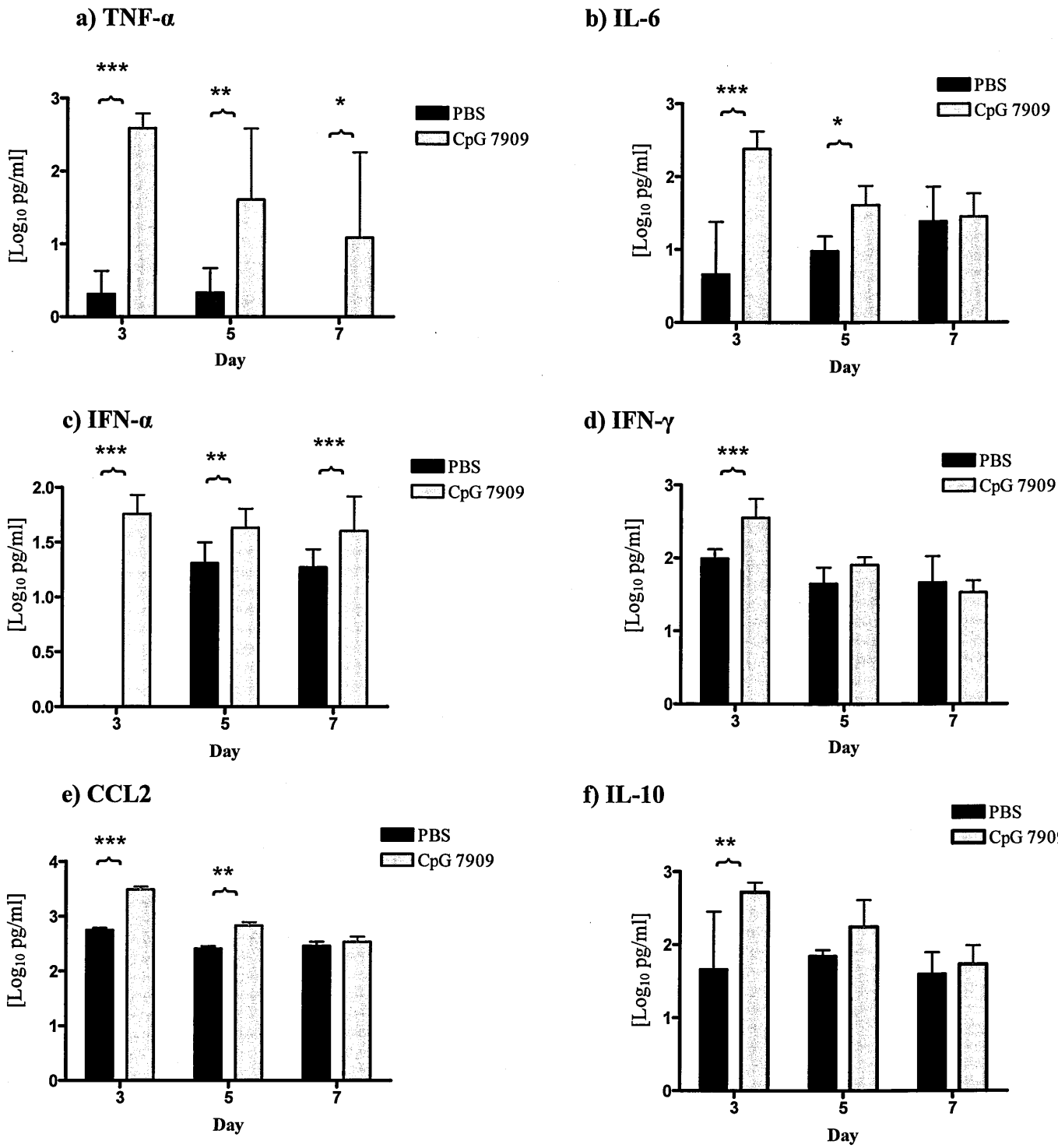

Figure 4.3. Measurement of lung cytokine levels in Balb/C mice treated with CpG-B 7909 or PBS post-infection with VACV. Mice were either treated on day +1 post infection with CpG-B 7909 or pre-treated with PBS. Protein levels determined *via* CBA analysis or IFN-α elisa. Bars represent the geometric mean of four mice (Log_{10} pg/ml) and error bars indicate 95% confidence intervals for cytokines **(a)** TNF-α; **(b)** IL-6; **(c)** IFN-α; **(d)** IFN-γ; **(e)** CCL2; **(f)** IL-10. Statistical significance was determined using a two-way ANOVA and Bonferroni's post-tests. Significant findings between treatment groups are represented as * ($p<0.05$), ** ($p<0.01$) and *** ($p<0.001$).

a) Total macrophages

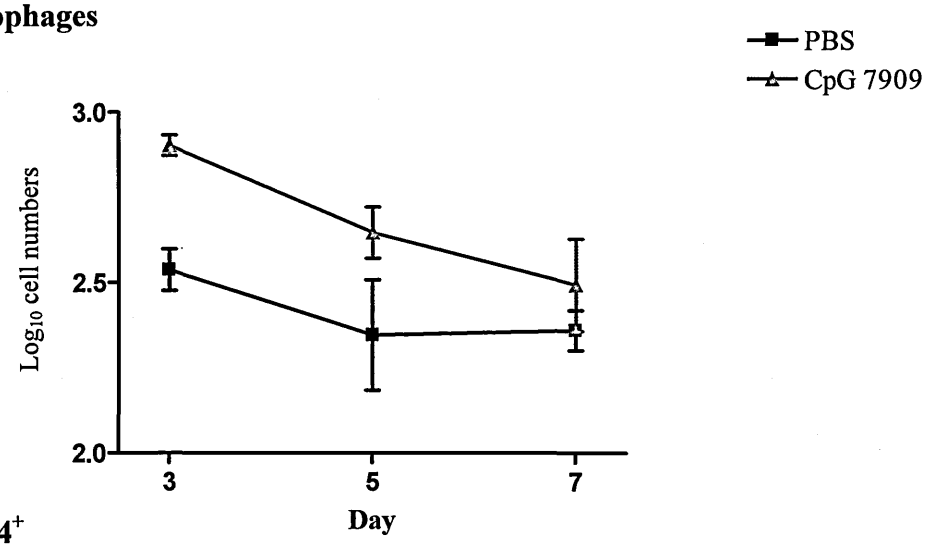

b) F4/80$^+$ CD54$^+$

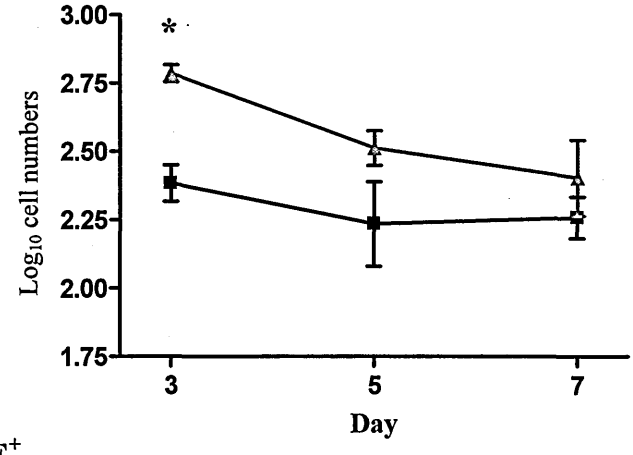

c) F4/80$^+$ IA/IE$^+$

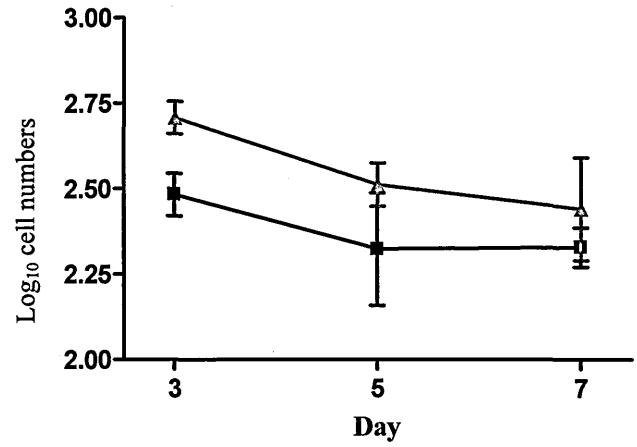

Figure 4.4. Lung macrophage numbers during VACV infection in CpG-B 7909 and PBS treated groups. Numbers of F4/80$^+$ macrophages in the lungs of infected mice were examined over a seven day period in mice either pre-treated with PBS or treated on day +1 with CpG-B 7909 using flow cytometry. Figure shows **(a)** total number of F4/80$^+$ macrophages; **(b)** macrophages expressing CD54; **(c)** macrophages expressing IA/IE. Graph represents geometric mean of four mice. Results shown include ± SEM. Statistical significance was determined using a two-way ANOVA and Bonferroni's post-tests. Significant findings between treatment groups are represented as * ($p<0.05$).

numbers never differed significantly at any individual time-point, CpG-B 7909 treatment was found to have a significant effect on total macrophage numbers over the course of infection by two-way ANOVA ($p<0.01$). Similarly, the number of macrophages expressing CD54 was also found to be significantly increased over the course of the infection by CpG-B 7909 treatment ($p<0.01$), with $CD54^+$ macrophages in CpG-B 7909 treated mice significantly higher ($p<0.05$) on day +3 (Figure 4.4b). Despite the apparent increase in IA/IE^+ macrophage cell numbers in mice treated with CpG-B 7909 (Figure 4.4c), these levels failed to reach statistical significance ($p>0.05$). Throughout, total macrophage numbers and numbers of activated macrophages were at their highest on day +3 of infection. By day +5, significant differences between CpG-treated and control treated mice in the total number and $CD54^+$ cells were lost.

The percentages of macrophages expressing CD54 are represented in Figure 4.5a. Here, no significant differences were observed between CpG and PBS treated groups on any day ($p>0.05$). In contrast, the percentage of macrophages expressing the co-stimulation marker MHC II, were significantly lower ($p<0.001$) on day +3 in CpG-treated mice (Figure 4.5b). By day +5, the percentage of cells expressing MHC II had increased in CpG-B 7909 treated animals to levels comparable to control groups.

4.3.3.3.2. Lung neutrophil responses

Neutrophils were characterised using a monoclonal antibody to Ly6G as a cell marker. Activation of neutrophils was determined by monitoring expression of the activation makers CD54 and CD11b on Ly6G positive cells and through gating on neutrophil-rich areas on forward/side scatter plots.

a) % F4/80$^+$ CD54$^+$

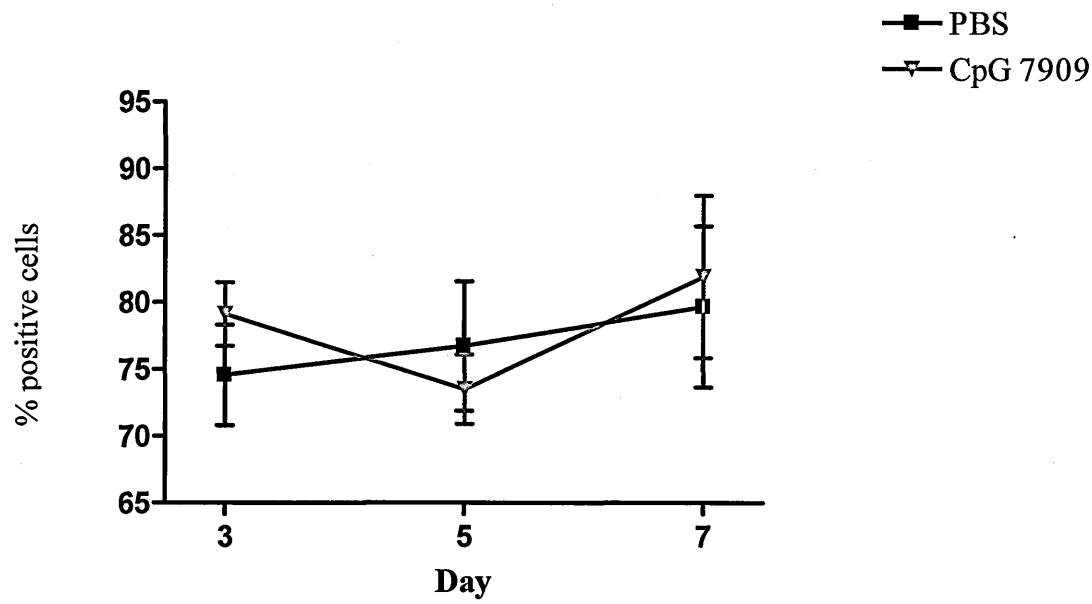

b) % F4/80$^+$ IA/IE$^+$

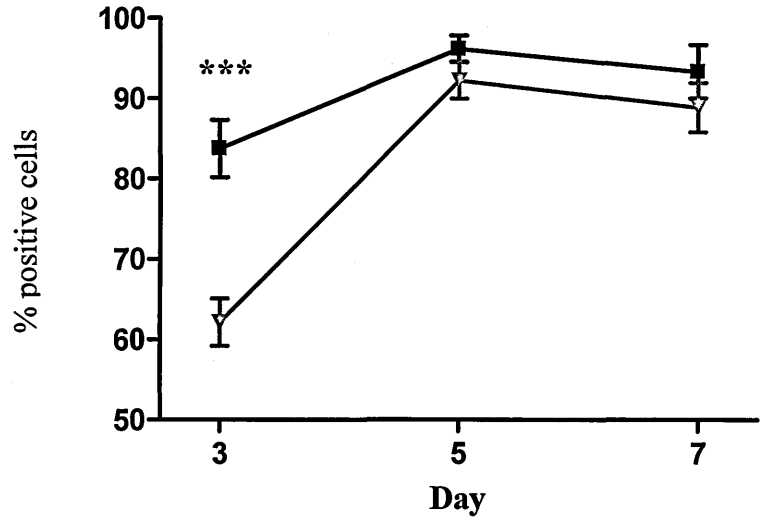

Figure 4.5. Activation of lung macrophages during VACV infection in CpG-B 7909 and PBS treated groups. Lung macrophage activation was monitored by expression of activation marker CD54 (Figure 4.5a) and co-stimulation marker IA/IE (Figure 4.5b) over the course of infection using flow cytometry. Graph represents geometric mean of four mice. Error bars represent ± SEM. Statistical significance was determined using a two-way ANOVA and Bonferroni's post-tests. Significant findings between treatment groups are represented as *** ($p<0.001$).

Lung neutrophil numbers are represented in Figure 4.6. Total neutrophil numbers (Figure 4.6a), as well as the number of neutrophils expressing either CD54 (Figure 4.6b) or CD11b (Figure 4.6c) were not found to differ significantly between treatment groups at individual time-points post-infection ($p>0.05$). In contrast, neutrophil numbers were found to alter significantly over the time course of infection ($p<0.001$). Whilst the actual number of neutrophils was not found to differ between treatment groups, significant differences in the percentage of cells expressing these activation markers were found. Specifically, the percentage of neutrophils expressing CD54 in mice treated with CpG-B 7909 post challenge were significantly lower ($p<0.05$) than PBS control mice on day +3 of infection (Figure 4.7a). In contrast, the percentage of neutrophils expressing CD11b was significantly higher in CpG-treated groups than PBS groups on days +3 and +5 post challenge (Figure 4.7b). The percentage levels of both $CD54^+$ neutrophils and $CD11b^+$ neutrophils altered significantly in different directions over the course of infection ($p<0.001$). This may suggest a role for activated neutrophils throughout VACV infection.

4.3.3.3.3. Lung dendritic cell responses

Dendritic cell responses were characterised using the cell differentiation marker CD11c to identify lung DCs and the activation status of cells was monitored *via* expression of MHC II (IA/IE) and the co-stimulation marker CD80.

Dendritic cell numbers altered significantly ($p<0.001$) over the course of infection. The total numbers of dendritic cells in both treatment groups did not differ significantly from each other, with total numbers in both groups climbing steadily over the course of infection (Figure 4.8a). Similar trends were also observed in the

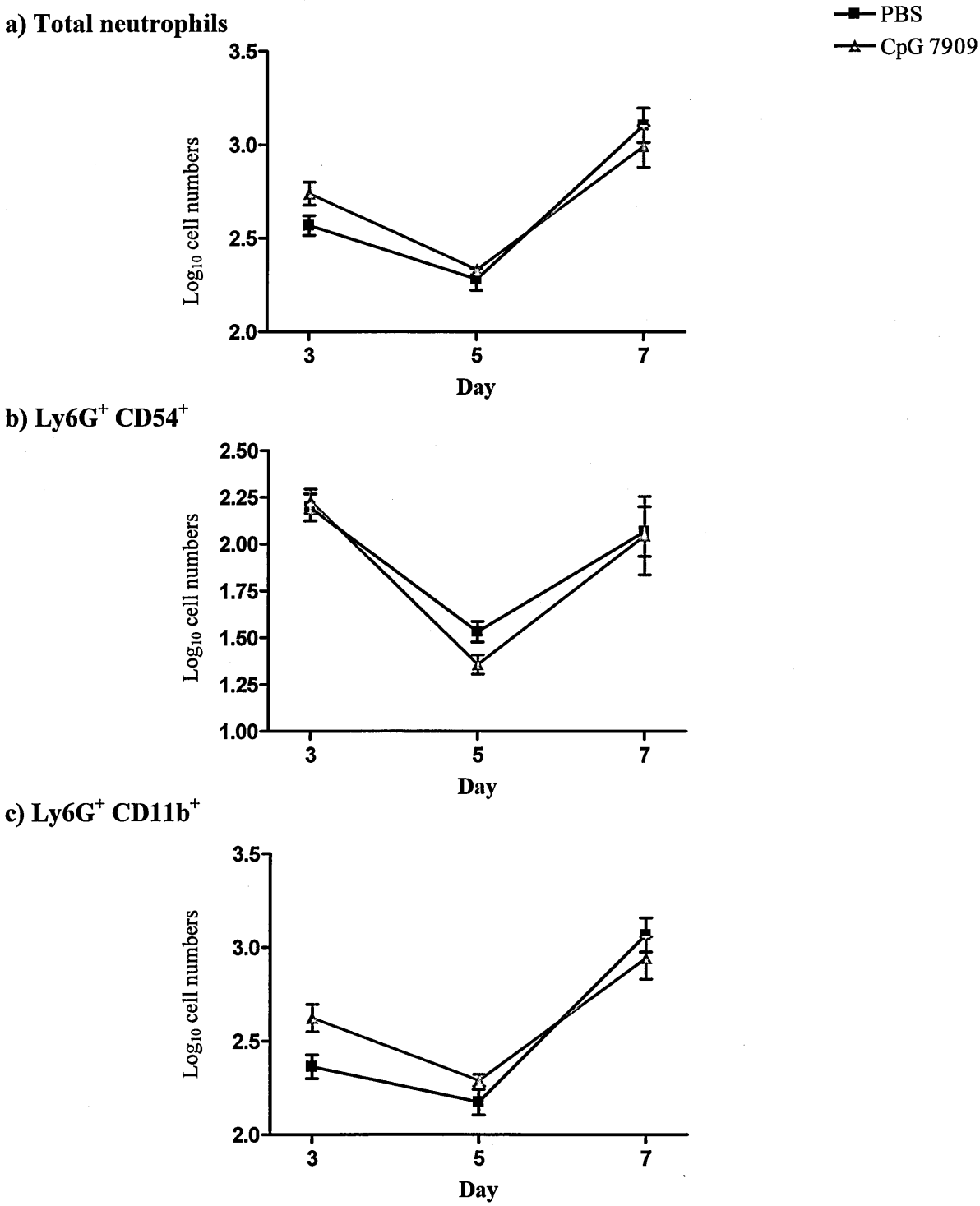

Figure 4.6. Lung neutrophil numbers during VACV infection in CpG-B 7909 and PBS treated groups. Numbers of Ly6G$^+$ neutrophils in the lungs of infected mice were examined over a seven day period in mice either pre-treated with PBS or treated on day +1 with CpG-B 7909 using flow cytometry. Figure shows **(a)** total number of Ly6G$^+$ neutrophils; **(b)** neutrophils expressing CD54; **(c)** neutrophils expressing CD11b. Graph represents geometric mean of four mice. Results shown include ± SEM. No statistical significance was determined using a two-way ANOVA and Bonferroni's post-tests.

a) % Ly6G$^+$ CD54$^+$

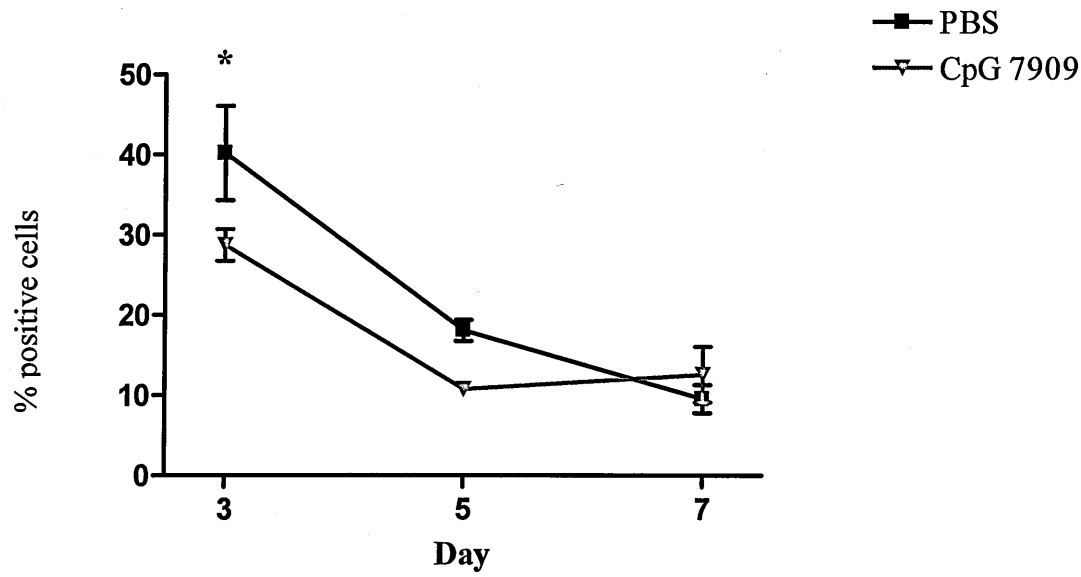

b) % Ly6G$^+$ CD11b$^+$

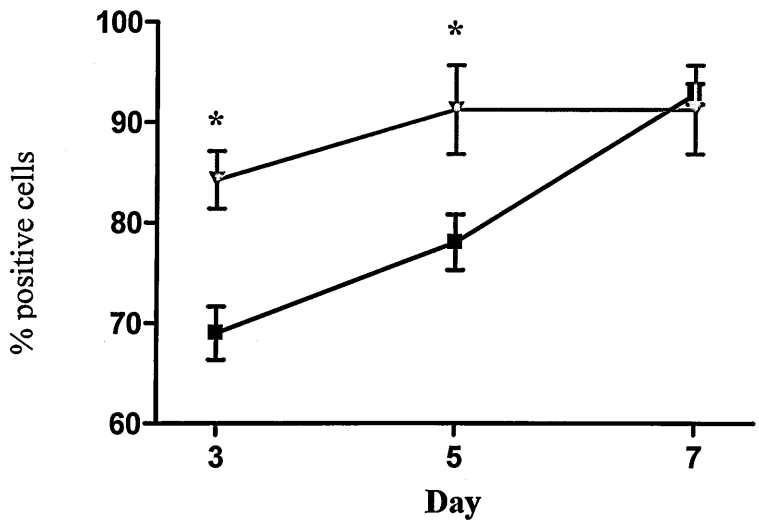

Figure 4.7. Activation of lung neutrophils during VACV infection in CpG-B 7909 and PBS treated groups. Lung neutrophil activation was monitored by expression of activation marker CD54 (Figure 4.7a) and diapedesis marker CD11b (Figure 4.7b) on days +3, +5 and +7 of infection using flow cytometry. Graph represents geometric mean of four mice. Error bars represent ± SEM. Statistical significance was determined using a two-way ANOVA and Bonferroni's post-tests. Significant findings between treatment groups are represented as * ($p<0.05$).

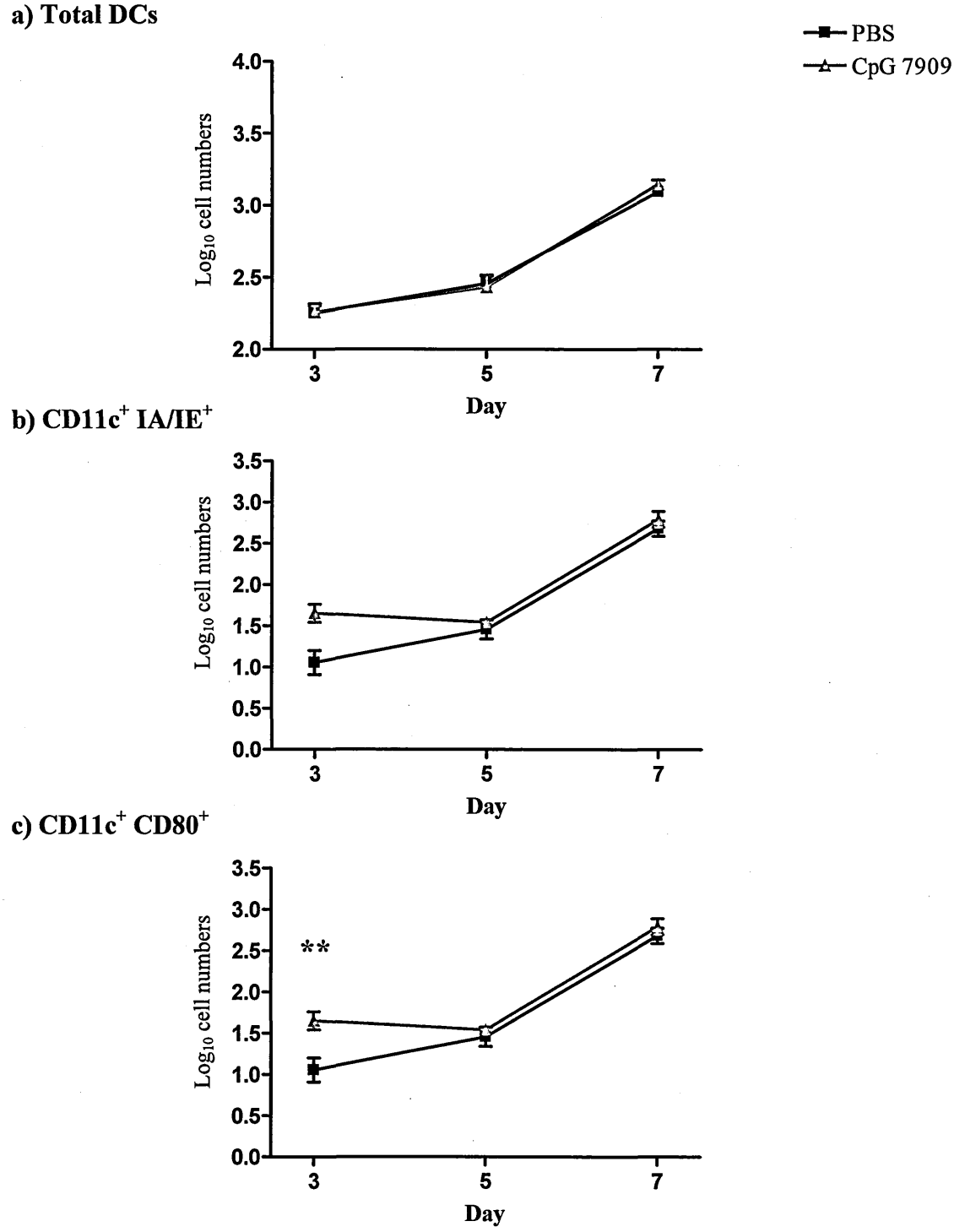

Figure 4.8. Lung dendritic cell numbers during VACV infection in CpG-B 7909 and PBS treated groups. Numbers of $CD11c^+$ DCs in the lungs of infected mice were examined over a seven day period in mice either pre-treated with PBS or treated on day +1 with CpG-B 7909 using flow cytometry. Figure shows **(a)** total number of $CD11c^+$ DCs; **(b)** DCs expressing IA/IE; **(c)** DCs expressing CD80. Graph represents geometric mean of four mice. Results shown include ± SEM. Statistical significance was determined using a two-way ANOVA and Bonferroni's post-tests. Significant findings between treatment groups are represented as ** ($p<0.01$).

number of DCs expressing the co-stimulation markers MHC II (Figure 4.8b) and those expressing CD80 (Figure 4.8c). However, on day +3 of infection, the numbers of DCs expressing CD80 were significantly higher ($p<0.01$) in mice that had been treated with CpG-B 7909 than in controls (Figure 4.8c).

The percentage of DCs expressing MHC II also altered significantly over the course of infection ($p<0.01$) but no significant differences were found between treatment groups ($p>0.05$) (Figure 4.9a). The percentage of DCs positive for CD80 also fluctuated significantly over time ($p<0.001$) with the percentage of $CD11c^+$ $CD80^+$ DCs being significantly higher on day +3 in CpG-B 7909 treated mice compared with controls (Figure 4.9b).

4.3.3.3.4. Lung NK cell responses

The NK cell marker CD49b was used to distinguish NK cells in lung preparations. Activation of NK cells was determined using antibodies to CD54 and CD69.

Total NK cell numbers were significantly higher ($p<0.01$) on day +3 of infection in CpG-B 7909 treated mice than controls (Figure 4.10a). The number of NK cells positive for CD54 altered significantly throughout the infection time-course ($p<0.001$) but at no time-point were numbers significantly different between treatment groups (Figure 4.10b). The numbers of NK cells expressing CD69 differed significantly between treatment groups on day +3 as represented in Figure 4.10c where the lungs of CpG-B 7909 treated mice contained higher numbers of $CD69^+$ NK cells ($p<0.01$).

a) % CD11c$^+$ IA/IE$^+$

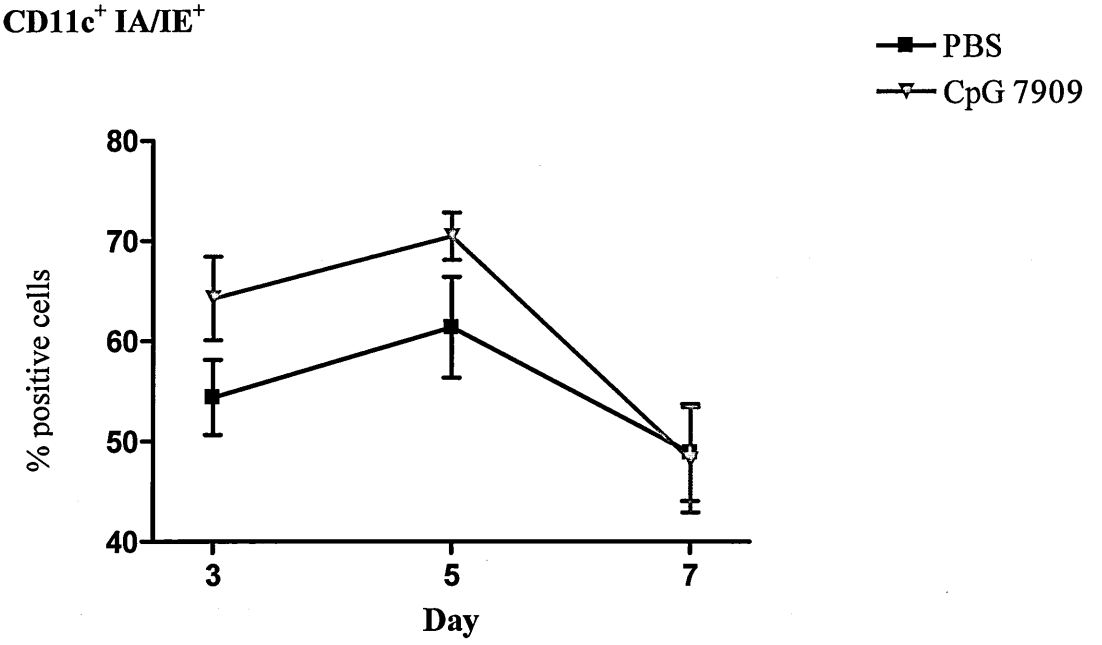

b) % CD11c$^+$ CD80$^+$

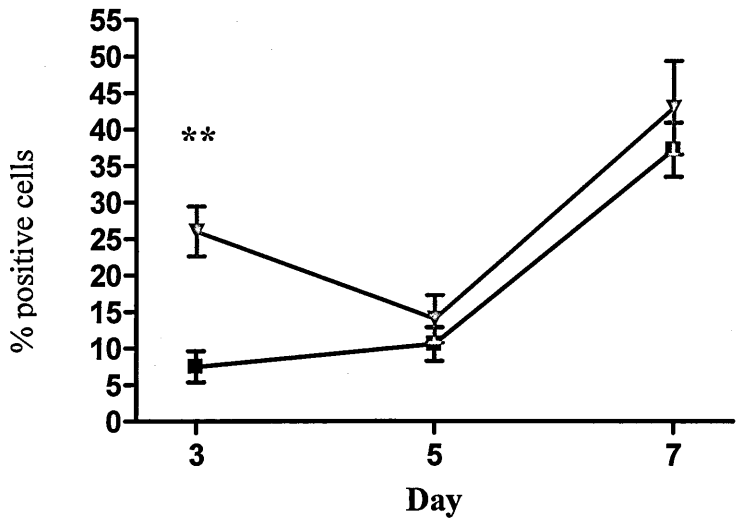

Figure 4.9. Activation of lung dendritic cells during VACV infection in CpG-B 7909 and PBS treated groups. Lung DC activation was monitored by expression of co-stimulation markers IA/IE (Figure 4.9a) and CD80 (Figure 4.9b) over the course of infection using flow cytometry. Graph represents geometric mean of four mice. Error bars represent ± SEM. Statistical significance was determined using a two-way ANOVA and Bonferroni's post-tests. Significant findings between treatment groups are represented as ** ($p<0.01$).

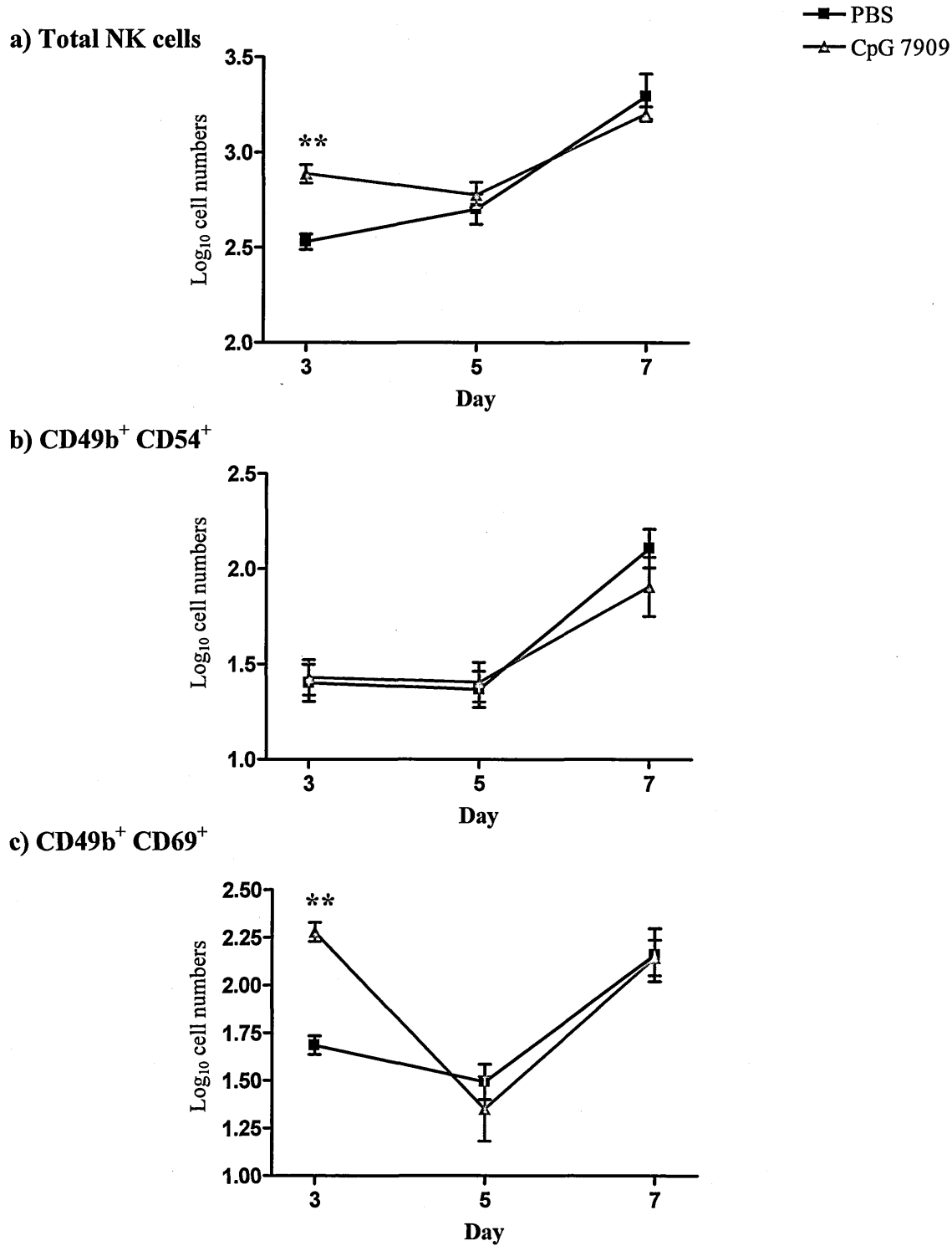

Figure 4.10. Lung natural killer cell numbers during VACV infection in CpG-B 7909 and PBS treated groups. Numbers of CD49b$^+$ NK cells in the lungs of infected mice were examined in mice either pre-treated with PBS or treated on day +1 with CpG-B 7909 over a seven day period using flow cytometry. Figure shows **(a)** total number of CD49b$^+$ NK cells; **(b)** NK cells expressing CD54; **(c)** NK cells expressing CD69. Graph represents geometric mean of four mice. Results shown include ± SEM. Statistical significance was determined using a two-way ANOVA and Bonferroni's post-tests. Significant findings between treatment groups are represented as ** ($p<0.01$).

The percentage of activated NK cells expressing CD54 did not differ between treatment groups at any time nor did percentage levels alter significantly over the course of infection in either group (Figure 4.11a). In contrast, the percentage of cells expressing the early activation marker CD69 were significantly different between treatment groups on day +3 (Figure 4.11b). Thereafter, by day +5, the percentage of $CD69^+$ NK cells had dropped significantly ($p<0.001$) in CpG-B 7909 treated mice to levels comparable with control mice.

4.3.3.3.5. Lung B-Cell responses

Antibody specific to CD19, a pan B-cell marker was used to label B-cells in suspensions. The activation status of B-cells at each time point was determined *via* changes in the cellular expression of co-stimulatory molecules CD80 and CD86.

Total B-cell numbers in the lungs of control and CpG-B 7909 treated mice varied significantly ($p<0.01$) over the course of infection but did not differ significantly between one another at any time point (Figure 4.12a). Likewise, the numbers of activated B-cells expressing CD86 (Figure 4.12b) or those expressing CD80 (Figure 4.12c) also fluctuated over the course of infection ($p<0.001$). Interestingly, numbers of $CD19^+$ $CD86^+$ cells appeared to dip on day +5 before returning to day +3 levels whereas the number of $CD19^+$ $CD80^+$ steadily increased over time. Throughout infection, increased numbers of activated B-cells were detected in all mice treated with CpG-B 7909. Consequently, whilst the differences in B-cell numbers did not differ significantly at any one time point, this overall trend resulted in a significant difference being found between treatment groups ($p<0.05$). No significant differences

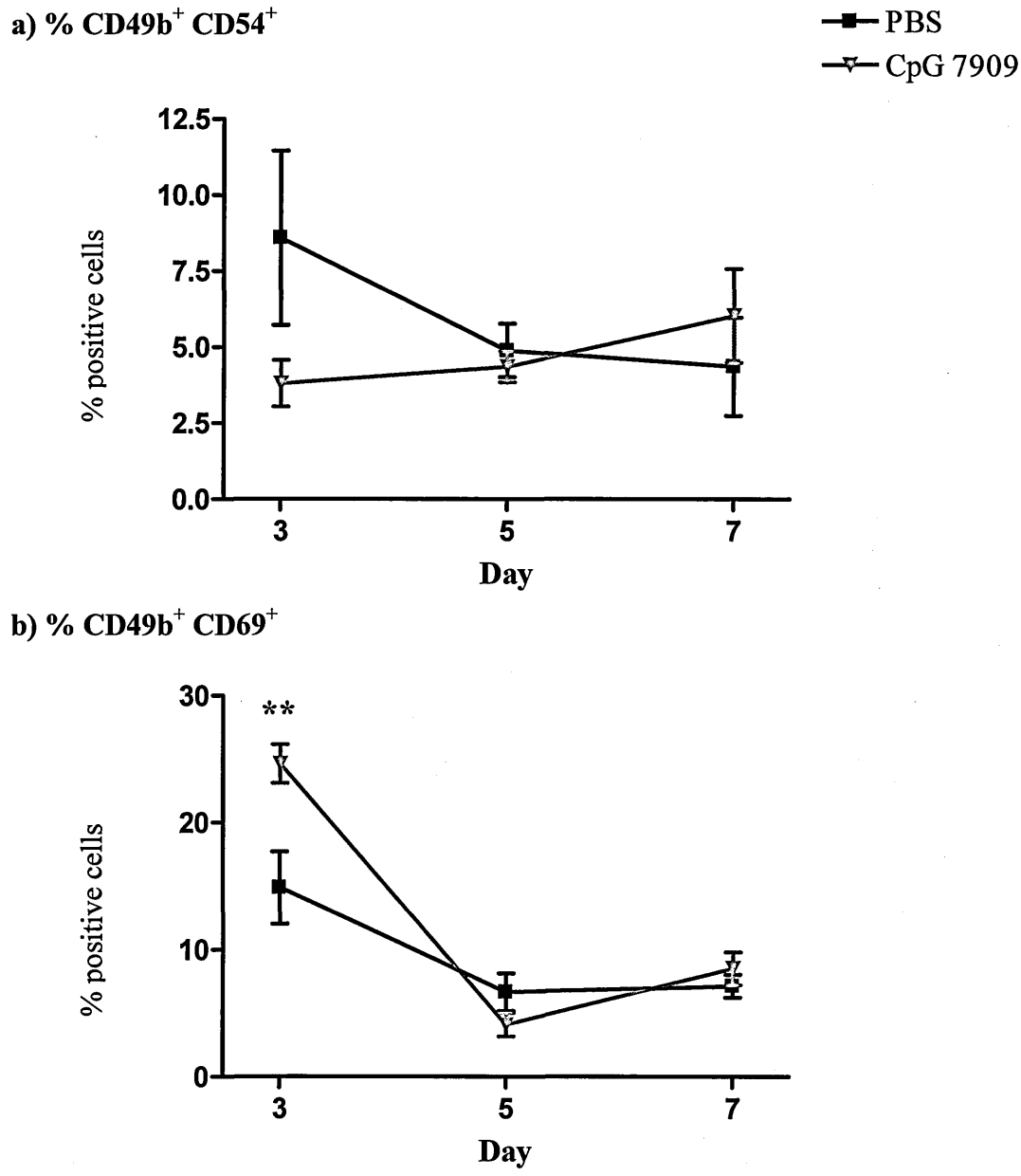

Figure 4.11. Activation of lung natural killer cells during VACV infection in CpG-B 7909 and PBS treated groups. Lung NK cell activation was monitored by expression of activation markers CD54 (Figure 4.11a) and CD69 (Figure 4.11b) over the course of infection using flow cytometry. Graph represents geometric mean of four mice. Error bars represent ± SEM. Statistical significance was determined using a two-way ANOVA and Bonferroni's post-tests. Significant findings between treatment groups are represented as ** ($p<0.01$).

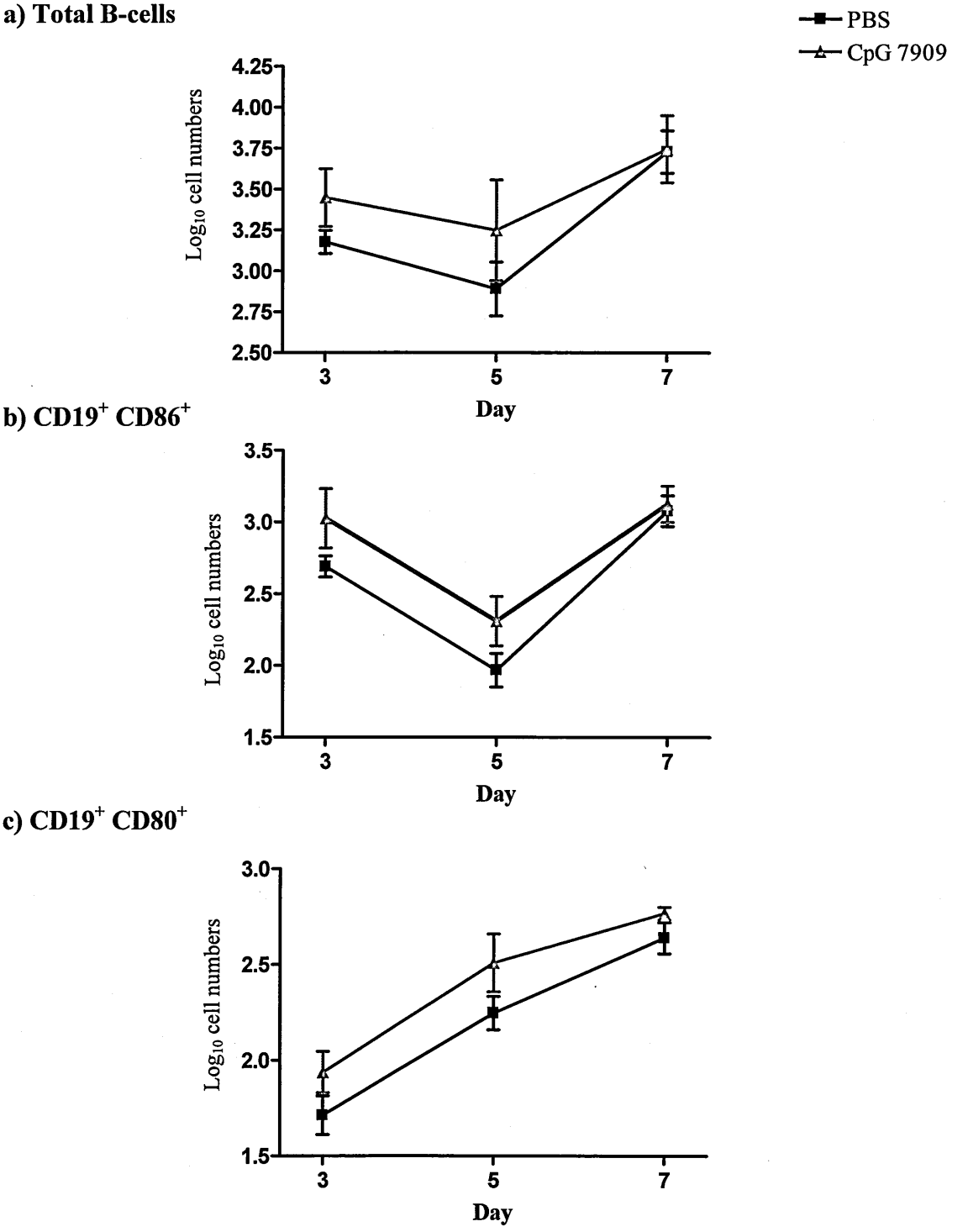

Figure 4.12. Lung B-cell numbers during VACV infection in CpG-B 7909 and PBS treated groups. Numbers of $CD19^+$ B-cells in the lungs of infected mice were examined in mice either pre-treated with PBS or treated on day +1 with CpG-B 7909 over a seven day period using flow cytometry. Figure shows **(a)** total number of $CD19^+$ B-cells; **(b)** B-cells expressing CD86; **(c)** B-cells expressing CD80. Results shown include ± SEM. No statistical significance was determined using a two-way ANOVA and Bonferroni's post-tests.

in the percentage of activated B-cells (Figure 4.13) were observed between treatment groups throughout infection ($p>0.05$).

4.3.3.3.6. Lung T-Cell responses

Antibody specific to CD3, a pan T-cell marker was used to identify T-cells in suspensions, whilst anti-CD4 and anti-CD8 antibodies distinguished between the two major T-cell sub-sets.

Lung $CD4^+$ T-cell responses are represented in Figure 4.14a and lung $CD8^+$ T-cells in Figure 4.14b. Throughout infection, the numbers of $CD4^+$ and $CD8^+$ T-cells were constantly higher in mice treated with CpG-B 7909 post VACV infection, than those given PBS. However, this observed increase failed to reach a level of statistical significance ($p>0.05$) which makes it unlikely to be a real effect of CpG treatment. Time was shown to have a significant effect on T-cell numbers, independent of CpG-B 7909 treatment, with both $CD4^+$ T-cells and $CD8^+$ T-cells significantly increasing between days +5 and +7 of infection ($p<0.01$ and $p<0.001$ respectively).

4.3.3.4. Cytokine responses in the spleen

Levels of all cytokines measured in the spleens of control and CpG-B 7909 treated mice are represented in Figure 4.15. With the exception of IFN-γ, the levels of all pro- and anti-inflammatory cytokines and chemokines measured were not significantly affected by CpG-B 7909 treatment at any time-point. The exception to this was in the levels of IFN-γ on day +3, which were found to be significantly lower ($p<0.001$) in CpG-B 7909 treated mice than those found in controls (Figure 4.15d).

a) % CD19$^+$ CD86$^+$

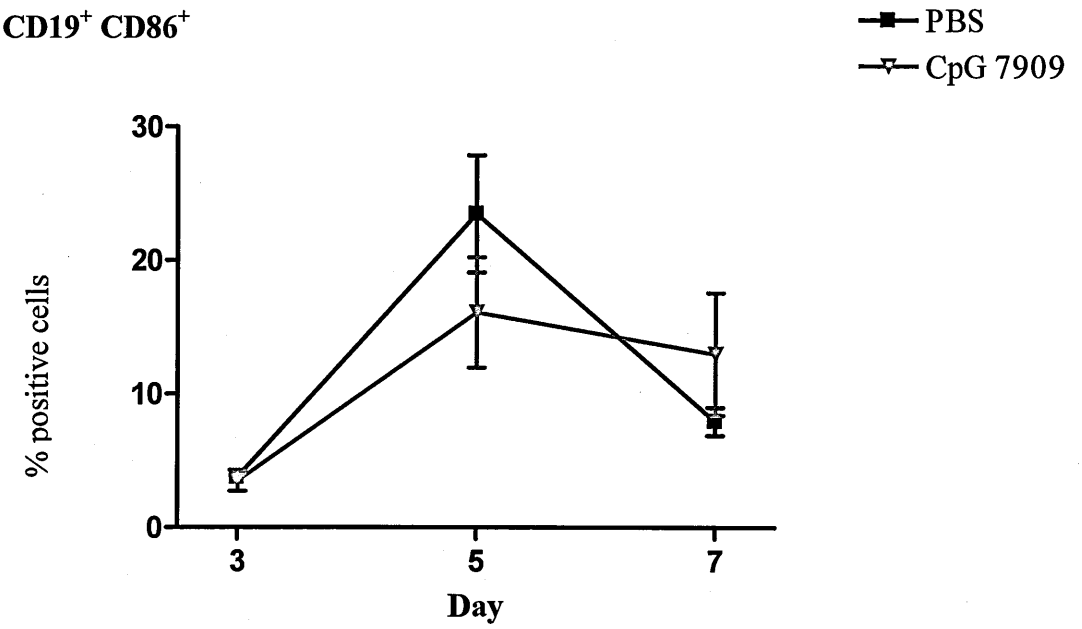

b) % CD19$^+$ CD80$^+$

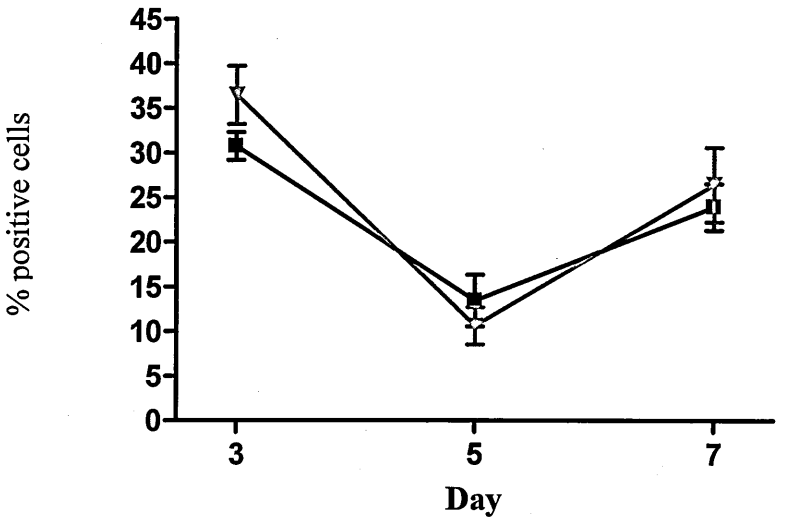

Figure 4.13. Activation of lung B-cells during VACV infection in CpG-B 7909 and PBS treated groups. Lung B-cell activation was monitored by expression of activation markers CD86 (Figure 4.13a) and CD80 (Figure 4.13b) over the course of infection using flow cytometry. Graph represents geometric mean of four mice. Error bars represent ± SEM. No statistical significance was determined using a two-way ANOVA and Bonferroni's post-tests.

a) $CD3^+$ $CD4^+$ T-cells

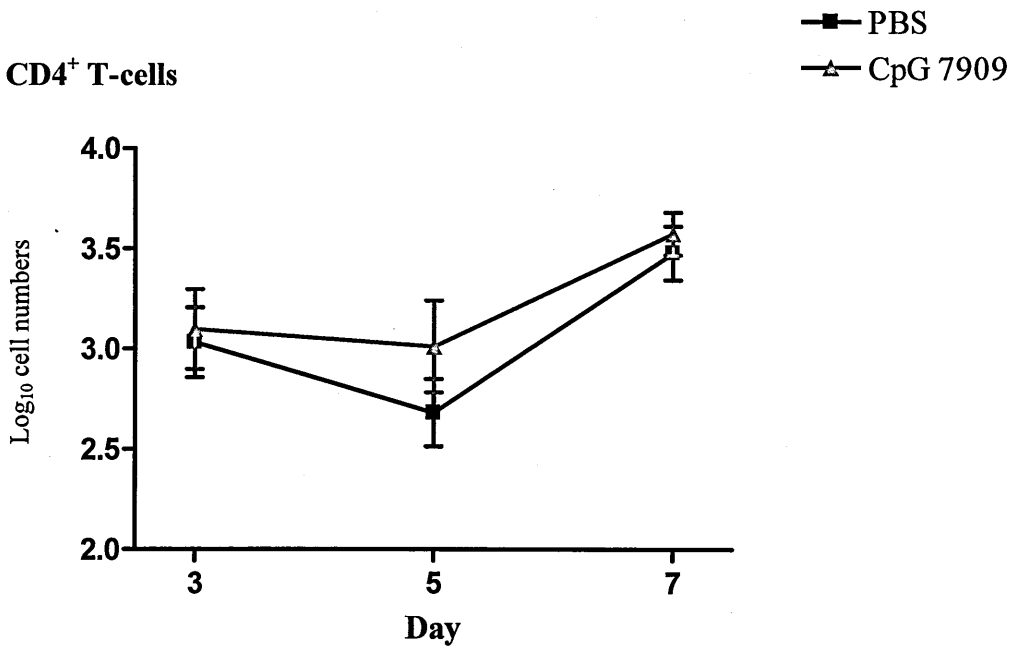

b) $CD3^+$ $CD8^+$ T-cells

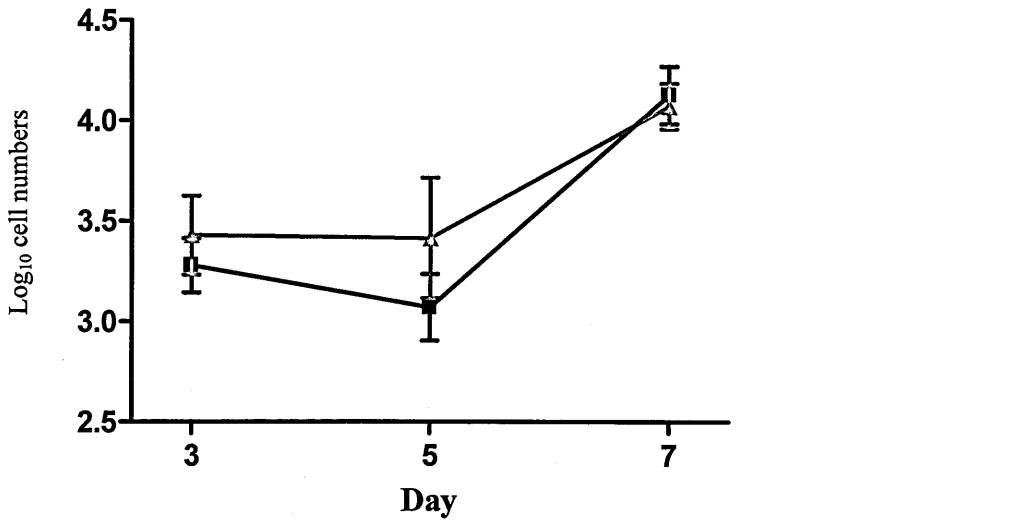

Figure 4.14. Lung T-cell numbers during VACV infection in CpG-B 7909 and PBS treated groups. Numbers of $CD3^+$ T-cells in the lungs of infected mice were examined over a seven day period in mice either pre-treated with PBS or treated on day +1 with CpG-B 7909 using flow cytometry. Figure shows **(a)** total number of $CD4^+$ T-cells; **(b)** total number of $CD8^+$ T-cells. Graph represents geometric mean of four mice. Results shown include ± SEM. No statistical significance was determined using a two-way ANOVA and Bonferroni's post-tests.

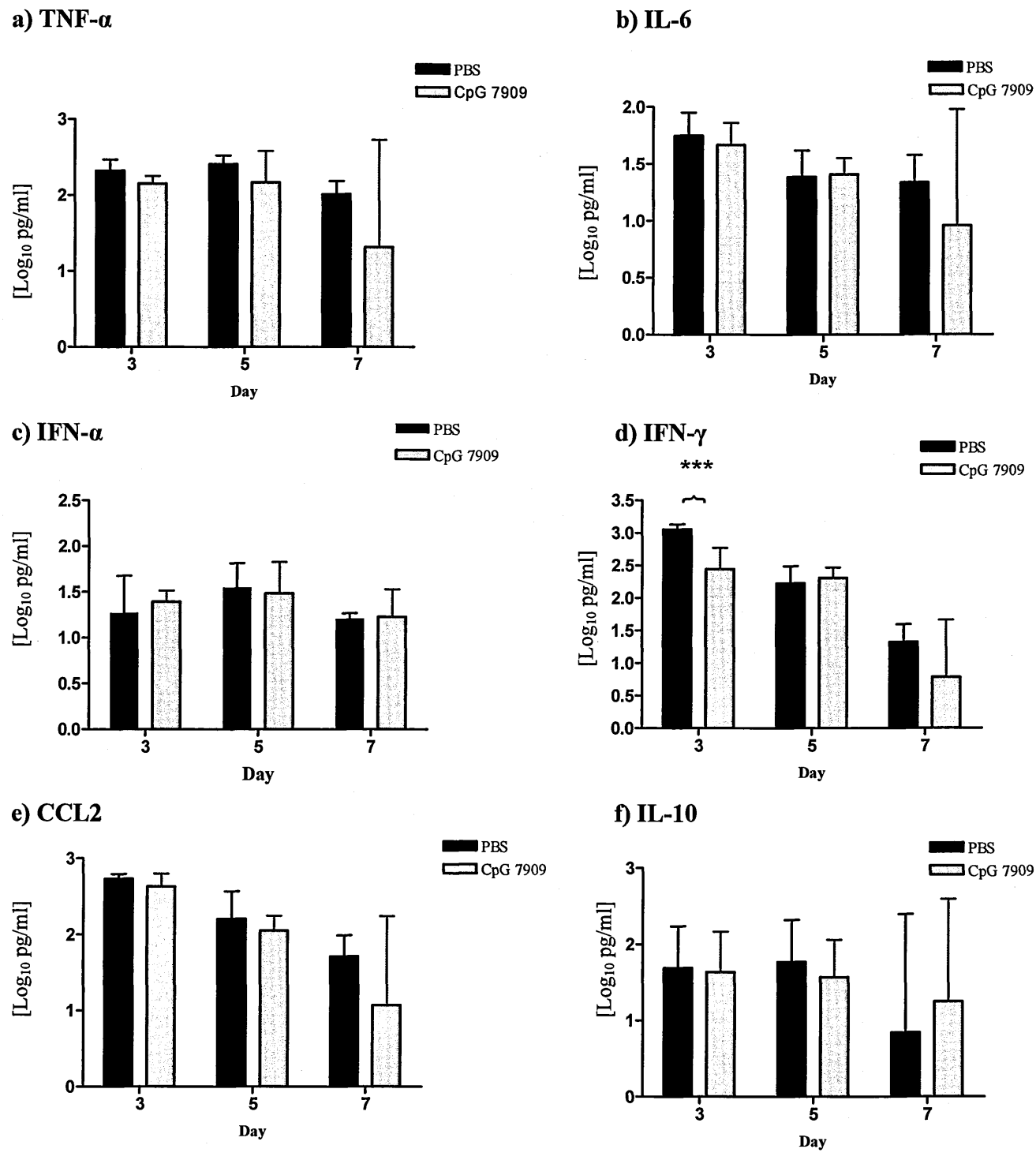

Figure 4.15. Measurement of spleen cytokine levels in Balb/C mice treated with CpG-B 7909 or PBS post-infection with VACV. Mice were either treated on day +1 post infection with CpG-B 7909 or pre-treated with PBS. Protein levels determined *via* CBA analysis or IFN-α elisa. Bars represent the geometric mean of four mice (Log_{10} pg/ml) and error bars indicate 95% confidence intervals for cytokines **(a)** TNF-α; **(b)** IL-6; **(c)** IFN-α; **(d)** IFN-γ; **(e)** CCL2; **(f)** IL-10. Statistical significance was determined using a two-way ANOVA and Bonferroni's post-tests. Significant findings between treatment groups are represented as * ($p<0.05$), ** ($p<0.01$) and *** ($p<0.001$).

4.3.3.5. Cellular responses in the spleen

4.3.3.5.1. Spleen macrophage responses

Total macrophage numbers in the spleen altered significantly between day +3 and day +7 post-infection ($p<0.01$) (Figure 4.16a). No significant effects of CpG-B 7909 treatment on macrophages expressing CD54 (Figure 4.16b) or MHC II (Figure 4.16c) were determined between control mice and CpG-B 7909 mice over the course of infection. This suggests that the macrophage egress observed in the spleen may be a consequence of VACV infection rather than CpG stimulation. Likewise, the percentages of activated macrophages (Figure 4.17) were not significantly different between treatment groups ($p>0.05$) but were significantly affected by time ($p<0.01$).

4.3.3.5.2. Spleen neutrophil responses

Total neutrophil numbers (Figure 4.18a) in the spleens of CpG-B 7909 treated mice were not significantly different from those in control PBS mice throughout the course of infection ($p>0.05$). Similarly, the numbers of activated neutrophils expressing either CD54 (Figure 4.18b) or CD11b (Figure 4.18c) did not differ between treatment groups. Neutrophil numbers fluctuated significantly over the course of infection ($p<0.001$) in both treated and untreated mice, presumably in response to VACV infection. The percentages of neutrophils expressing activation markers also varied significantly throughout infection but again, this happened irrespective of CpG-B 7909 treatment as no significant differences between treatment groups were determined throughout (Figure 4.19).

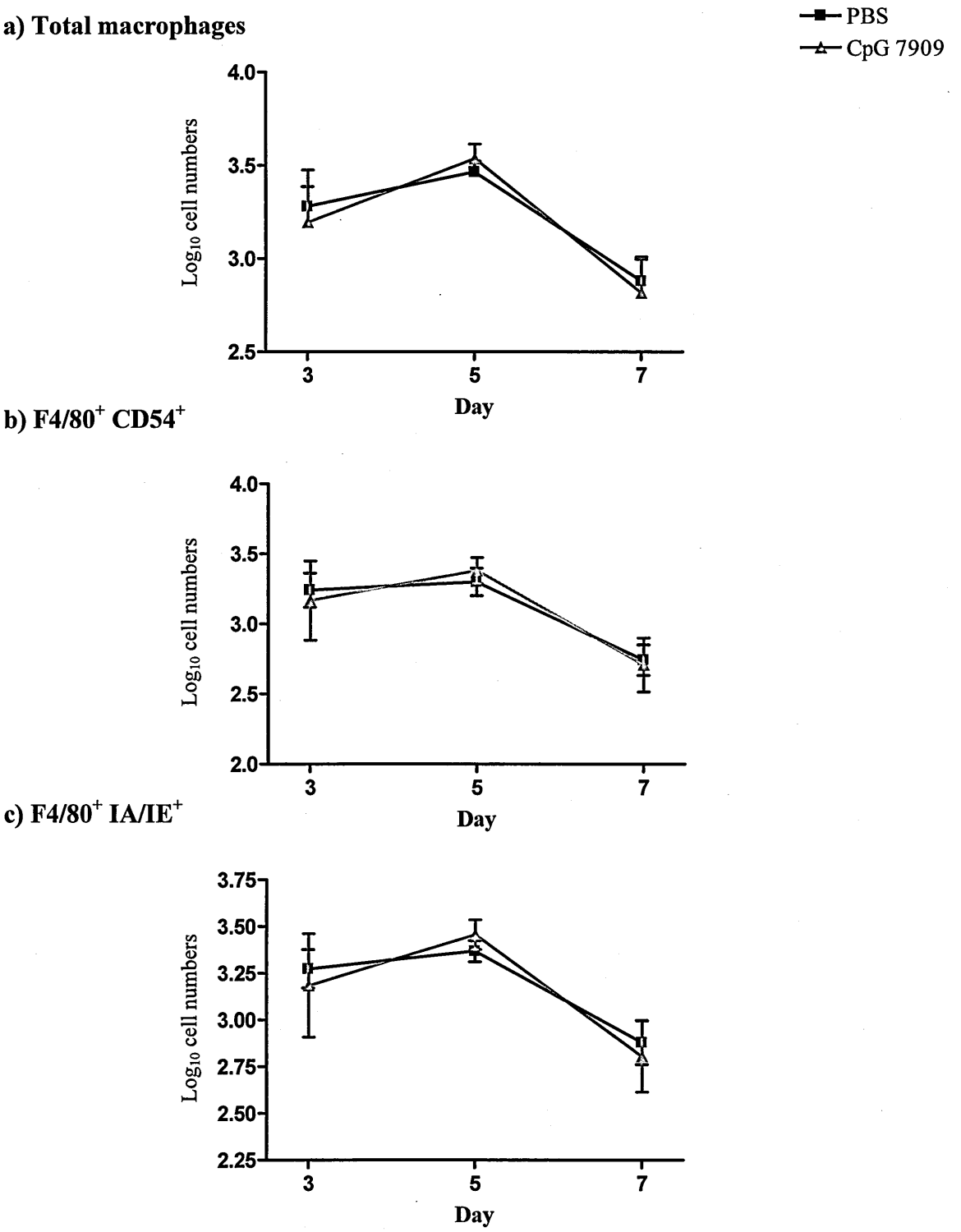

Figure 4.16. Spleen macrophage numbers during VACV infection in CpG-B 7909 and PBS treated groups. Numbers of F4/80$^+$ macrophages in the spleens of infected mice were examined over a seven day period in mice either pre-treated with PBS or treated on day +1 with CpG-B 7909 using flow cytometry. Figure shows **(a)** total number of F4/80$^+$ macrophages; **(b)** macrophages expressing CD54; **(c)** macrophages expressing IA/IE. Graph represents geometric mean of four mice. Results shown include ± SEM. No statistical significance was determined using a two-way ANOVA and Bonferroni's post-tests.

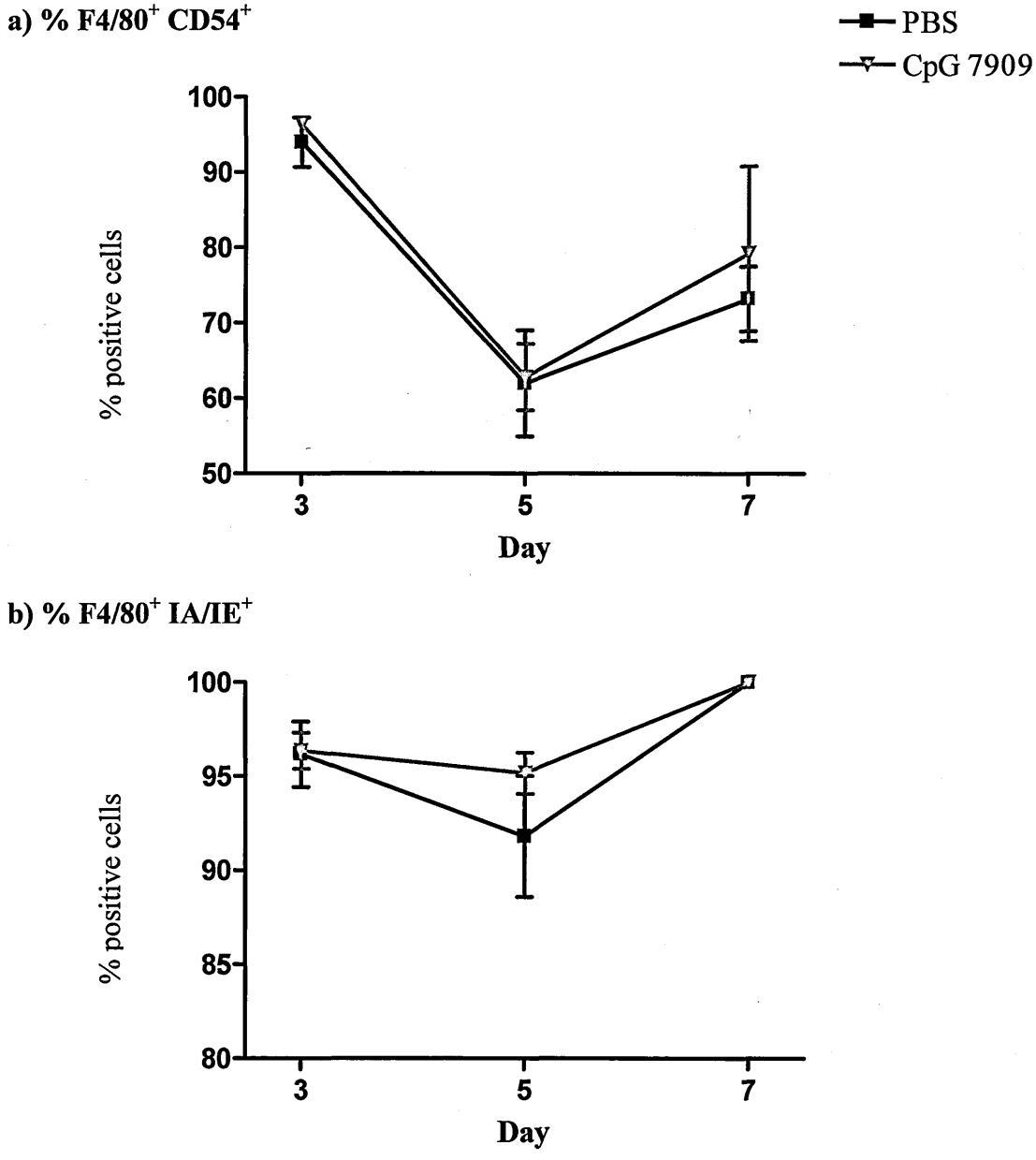

Figure 4.17. Activation of spleen macrophages during VACV infection in CpG-B 7909 and PBS treated groups. Spleen macrophage activation was monitored by expression of activation marker CD54 (Figure 4.17a) and co-stimulation marker IA/IE (Figure 4.17b) over the course of infection using flow cytometry. Graph represents geometric mean of four mice. Error bars represent ± SEM. No statistical significance was determined using a two-way ANOVA and Bonferroni's post-tests.

a) Total neutrophils

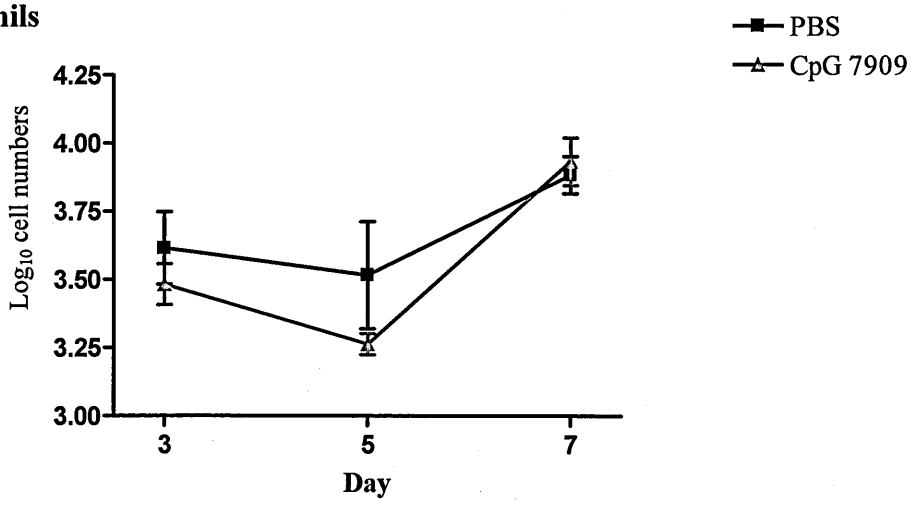

b) Ly6G$^+$ CD54$^+$

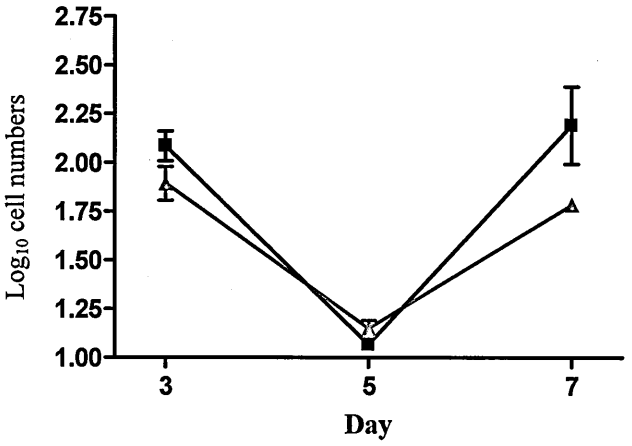

c) Ly6G$^+$ CD11b$^+$

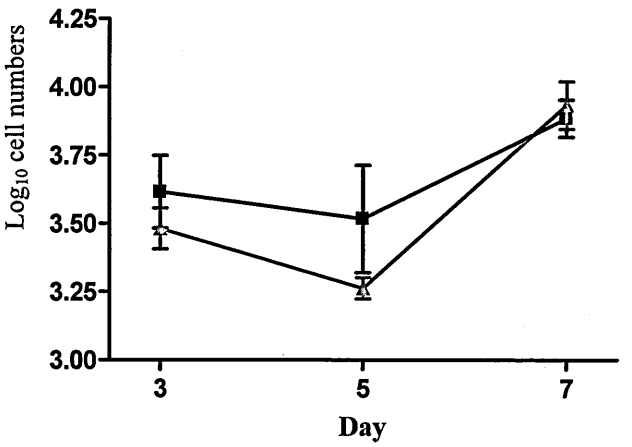

Figure 4.18. Spleen neutrophil numbers during VACV infection in CpG-B 7909 and PBS treated groups. Numbers of Ly6G$^+$ neutrophils in the spleens of infected mice were examined over a seven day period in mice either pre-treated with PBS or treated on day +1 with CpG-B 7909 using flow cytometry. Figure shows **(a)** total number of Ly6G$^+$ neutrophils; **(b)** neutrophils expressing CD54; (c) neutrophils expressing CD11b. Graph represents geometric mean of four mice. Results shown include ± SEM. No statistical significance was determined using a two-way ANOVA and Bonferroni's post-tests.

a) % Ly6G$^+$ CD54$^+$

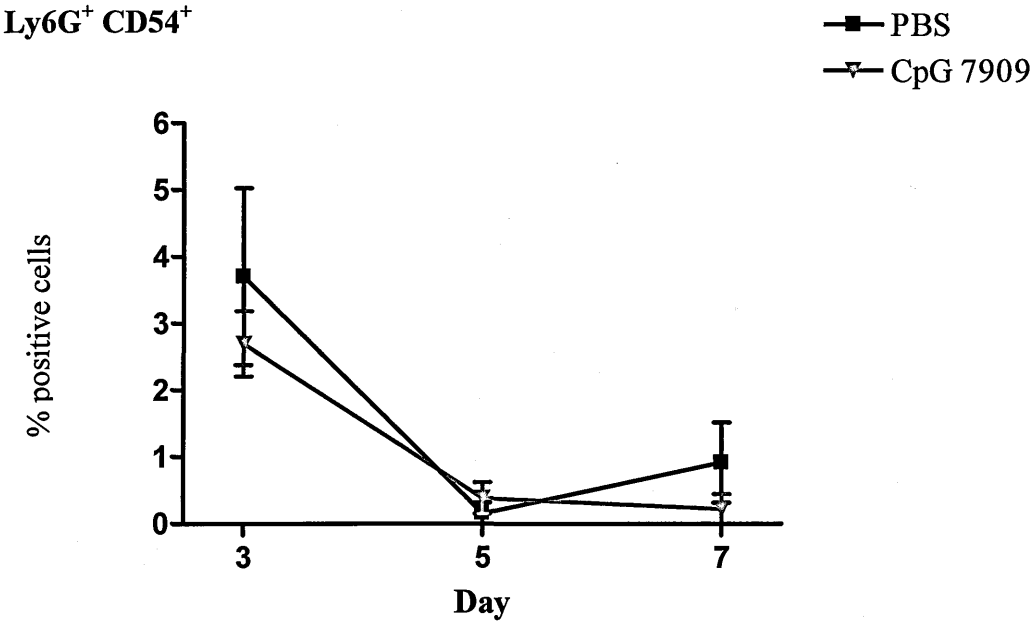

b) % Ly6G$^+$ CD11b$^+$

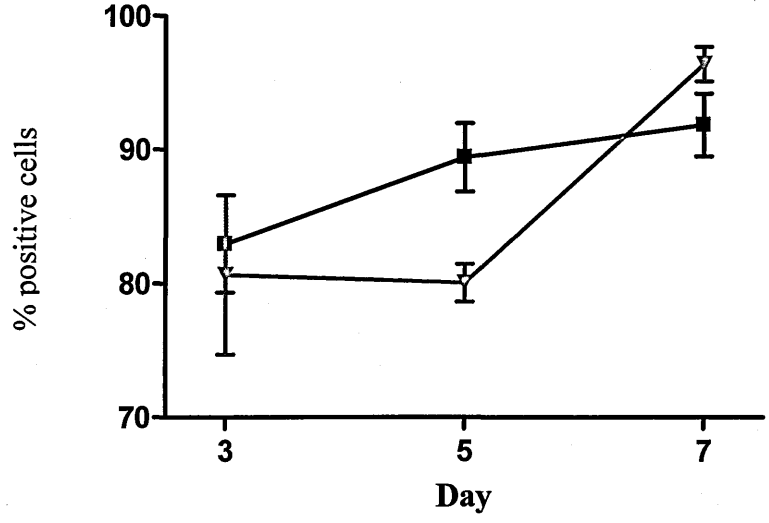

Figure 4.19. Activation of spleen neutrophils during VACV infection in CpG-B 7909 and PBS treated groups. Spleen neutrophil activation was monitored by expression of activation marker CD54 (Figure 4.19a) and diapedesis marker CD11b (Figure 4.19b) over the course of infection using flow cytometry. Graph represents geometric mean of four mice. Error bars represent ± SEM. No statistical significance was determined using a two-way ANOVA and Bonferroni's post-tests.

4.3.3.5.3. Spleen dendritic cell responses

Figure 4.20 represents the numbers of DCs in the spleens of VACV-infected mice treated with either PBS or CpG-B 7909. No significant differences between treatment groups were found in the total number of DCs present (Figure 4.20a), nor in the number of DCs expressing MHC II (Figure 4.20b) or CD80 (Figure 4.20c). Dendritic cell numbers were found to alter significantly ($p<0.001$) over the course of infection independent of CpG-B 7909 treatment. The percentage of DCs expressing MHC II was also seen to alter throughout infection as seen in Figure 4.21a where levels decreased steadily over time in both PBS and CpG-B 7909 treated mice. This happened irrespective of CpG-B 7909 treatment as no significant differences were determined between treatment groups. In contrast, the percentage of DCs expressing CD80 in CpG-B 7909 on day +3 was significantly higher ($p<0.05$) than that found in PBS treated mice (Figure 4.21b). In both treatment groups, the percentage of DCs expressing CD80 decreased significantly ($p<0.001$) between days +3 and +5 to baseline levels.

4.3.3.5.4. Spleen NK cell responses

No significant differences in the total number or number of activated NK cells were determined between treatment groups at any stage throughout the infection time course (Figure 4.22). NK cell numbers altered significantly over the duration of infection but once again, as no significant effect of CpG-B 7909 was determined, this appeared to be a consequence of virus infection. Whilst the numbers of NK cells in the spleen appeared to be uneffected by CpG treatment, the actual percentage of NK cells expressing the early activation marker CD69 was significantly different ($p<0.01$) between treatment groups on day +3 (Figure 4.23b). By day +5, the percentage of

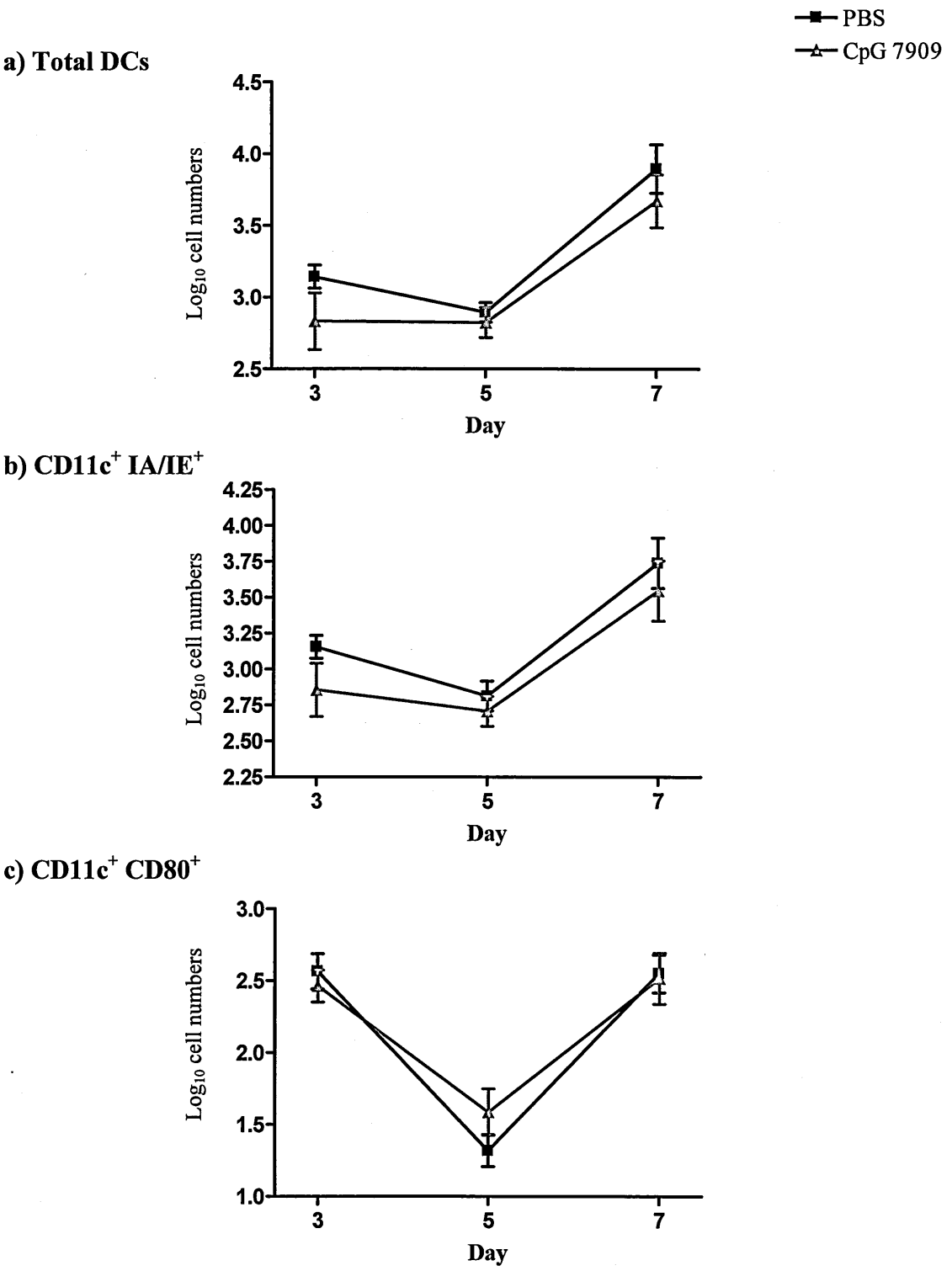

Figure 4.20. Spleen dendritic cell numbers during VACV infection in CpG-B 7909 and PBS treated groups. Numbers of $CD11c^+$ DCs in the spleens of infected mice were examined over a seven day period in mice either pre-treated with PBS or treated on day +1 with CpG-B 7909 using flow cytometry. Figure shows **(a)** total number of $CD11c^+$ DCs; **(b)** DCs expressing IA/IE; **(c)** DCs expressing CD80. Graph represents geometric mean of four mice. Results shown include ± SEM. No statistical significance was determined using a two-way ANOVA and Bonferroni's post-tests.

a) % CD11c$^+$ IA/IE$^+$

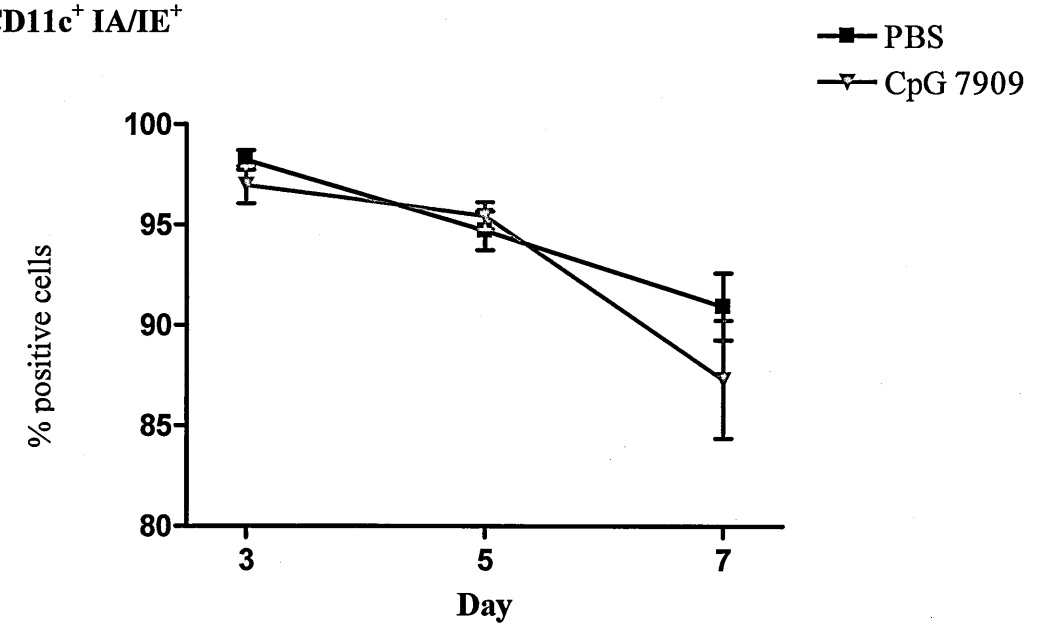

b) % CD11c$^+$ CD80$^+$

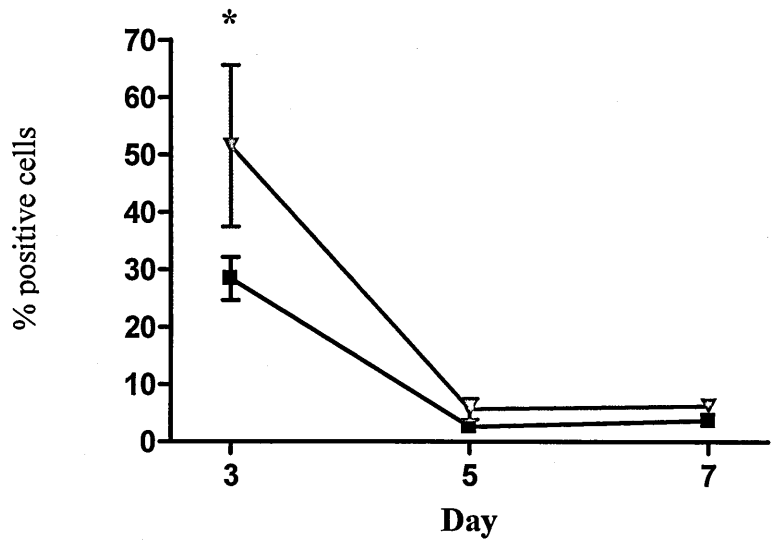

Figure 4.21. Activation of spleen dendritic cells during VACV infection in CpG-B 7909 and PBS treated groups. Spleen DC activation was monitored by expression of co-stimulation markers IA/IE (Figure 4.21a) and CD80 (Figure 4.22b) over the course of infection using flow cytometry. Graph represents geometric mean of four mice. Error bars represent ± SEM. Statistical significance was determined using a two-way ANOVA and Bonferroni's post-tests. Significant findings between treatment groups are represented as * ($p<0.05$).

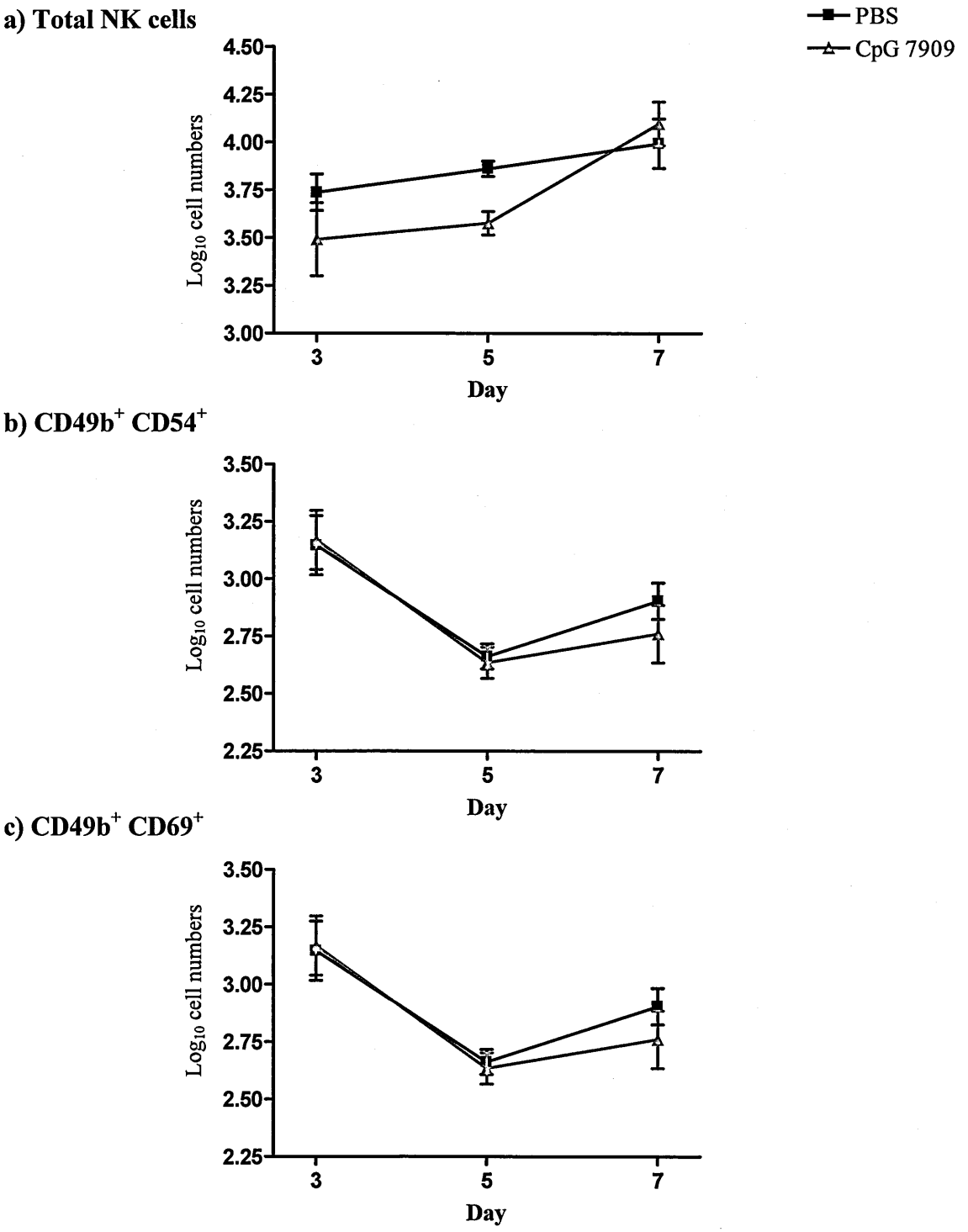

Figure 4.22. Spleen natural killer cell numbers during VACV infection in CpG-B 7909 and PBS treated groups. Numbers of CD49b$^+$ NK cells in the spleens of infected mice were examined over a seven day period in mice either pre-treated with PBS or treated on day +1 with CpG-B 7909 using flow cytometry. Figure shows **(a)** total number of CD49b$^+$ NK cells; **(b)** NK cells expressing CD54; **(c)** NK cells expressing CD69. Graph represents geometric mean of four mice. Results shown include ± SEM. No statistical significance was determined using a two-way ANOVA and Bonferroni's post-tests.

a) % CD49b$^+$ CD54$^+$

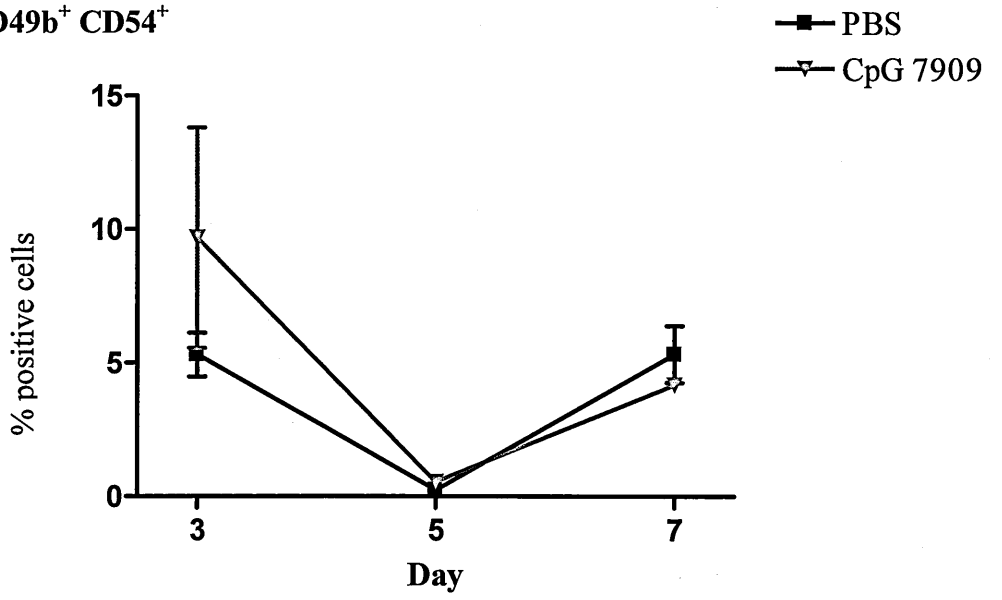

b) % CD49b$^+$ CD69$^+$

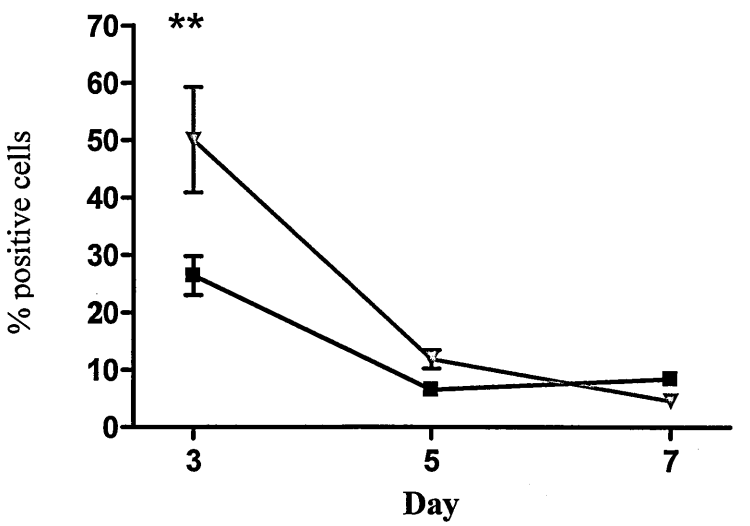

Figure 4.23. Activation of spleen natural killer cells during VACV infection in CpG-B 7909 and PBS treated groups. Spleen NK cell activation was monitored by expression of activation markers CD54 (Figure 4.23a) and CD69 (Figure 4.23b) over the course of infection using flow cytometry. Graph represents geometric mean of four mice. Error bars represent ± SEM. Statistical significance was determined using a two-way ANOVA and Bonferroni's post-tests. Significant findings between treatment groups are represented as ** ($p<0.01$).

$CD69^+$ NK cells in CpG-B 7909 treated mice dropped to levels seen in control mice and these remained comparable between groups for the remainder of the infection. The percentage of NK cells expressing CD54 did not differ significantly between treatment groups (Figure 4.23a).

4.3.3.5.5. Spleen B-cell responses

Total and activation marker-specific B-cell numbers are represented in Figure 4.24. B-cell numbers fluctuated significantly over time ($p<0.001$). However, no significant differences were observed between treatment groups in the total number of B-cells in the spleen (Figure 4.24a) or in the number of B-cells expressing the co-stimulation marker CD86 (Figure 4.24b). The numbers of B-cells expressing CD80 (Figure 4.24c) were significantly higher on day +7 in the spleens of mice that had been treated with CpG-B 7909 than in controls ($p<0.05$). Closer examination on day +7 revealed that the percentage of B-cells expressing CD80 in CpG-B 7909 treated mice was also significantly higher ($p<0.01$) than in control PBS mice (Figure 4.25b). In contrast, no significant differences were found between the percentages of B-cells expressing CD86 in CpG-B 7909 and PBS treated mice (Figure 4.25a).

4.3.3.5.6. Spleen T-cell responses

The number of CD4 positive T-cells in control and CpG-treated groups did not differ significantly from each other at any time-point (Figure 4.26a). However, there was a significant influence ($p<0.05$) of CpG treatment on $CD4^+$ T-cell numbers over the time-course of infection. Similarly, the numbers of $CD8^+$ T-cells were significantly lower in mice receiving CpG-B 7909 throughout the course of infection ($p<0.01$). In

a) Total B-cells

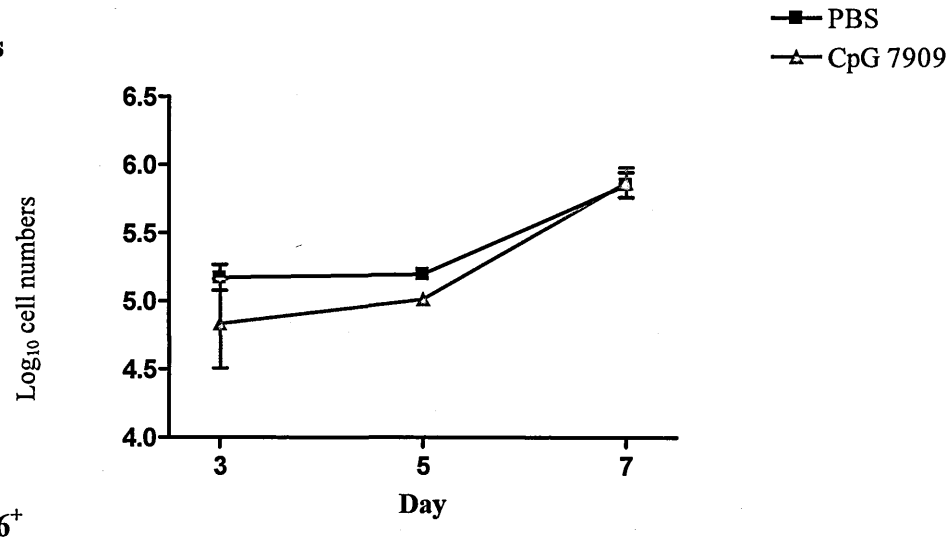

b) CD19$^+$ CD86$^+$

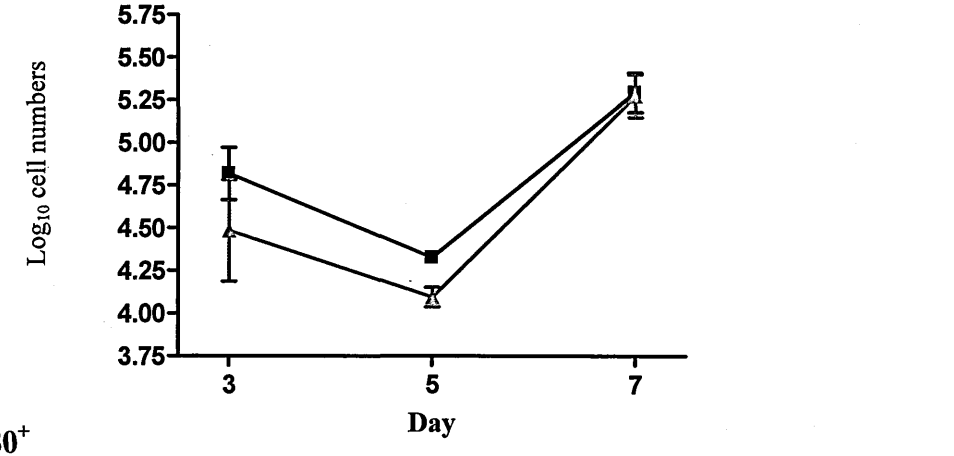

c) CD19$^+$ CD80$^+$

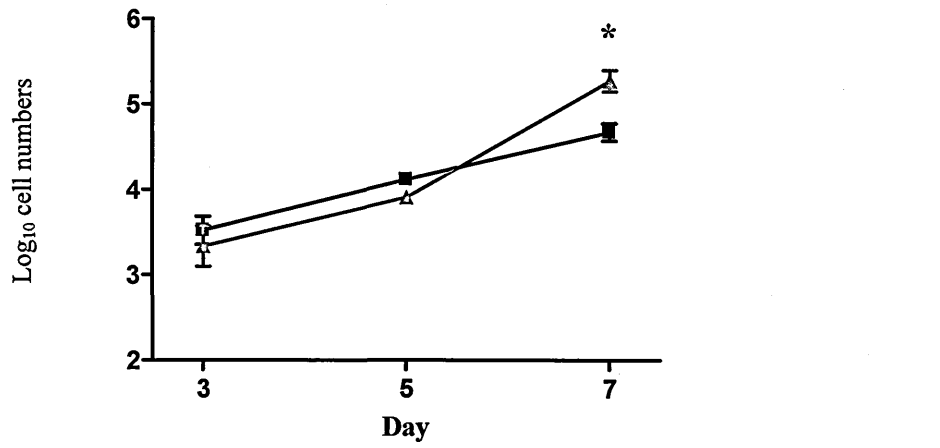

Figure 4.24. Spleen B-cell Numbers during VACV infection in CpG-B 7909 and PBS treated groups. Numbers of CD19$^+$ B-cells in the spleens of infected mice were examined over a seven day period in mice either pre-treated with PBS or treated on day +1 with CpG-B 7909 using flow cytometry. Figure shows **(a)** total number of CD19$^+$ B-cells; **(b)** B-cells expressing CD86; **(c)** B-cells expressing CD80. Results shown include ± SEM. Statistical significance was determined using a two-way ANOVA and Bonferroni's post-tests. Significant findings between treatment groups are represented as * ($p<0.05$).

a) % $CD19^+$ $CD86^+$

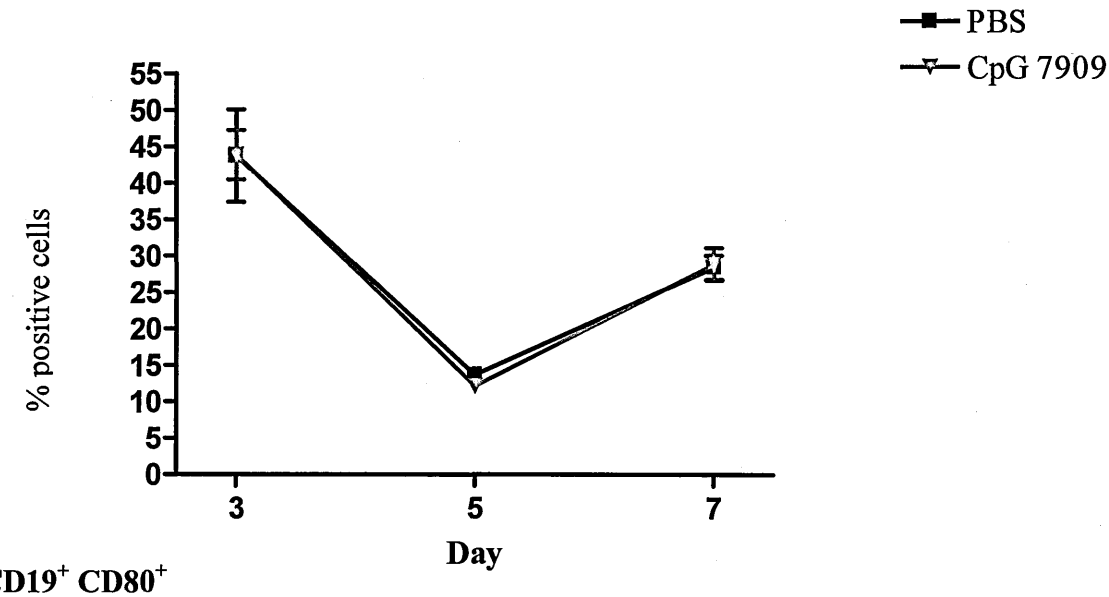

b) % $CD19^+$ $CD80^+$

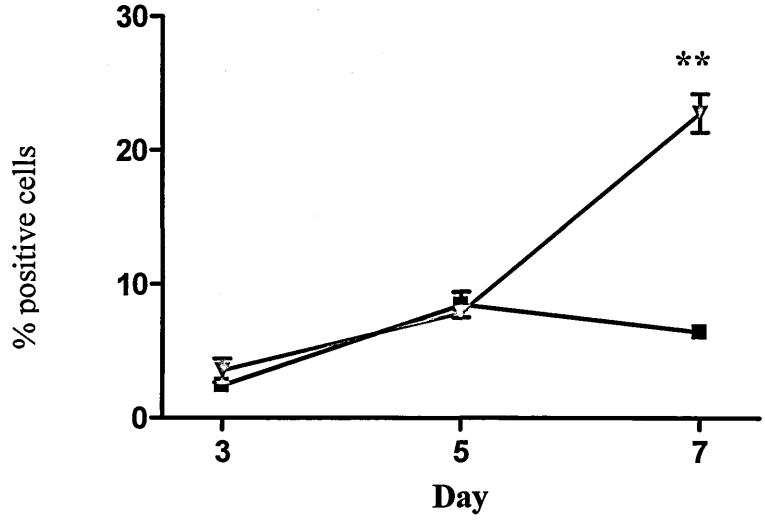

Figure 4.25. Activation of spleen B-cells during VACV infection in CpG-B 7909 and PBS treated groups. Spleen B-cell activation was monitored by expression of activation markers CD86 (Figure 4.25a) and CD80 (Figure 4.25b) over the course of infection using flow cytometry. Graph represents geometric mean of four mice. Error bars represent ± SEM. Statistical significance was determined using a two-way ANOVA and Bonferroni's post-tests. Significant findings between treatment groups are represented as ** ($p<0.01$).

a) $CD3^+$ $CD4^+$ T-cells

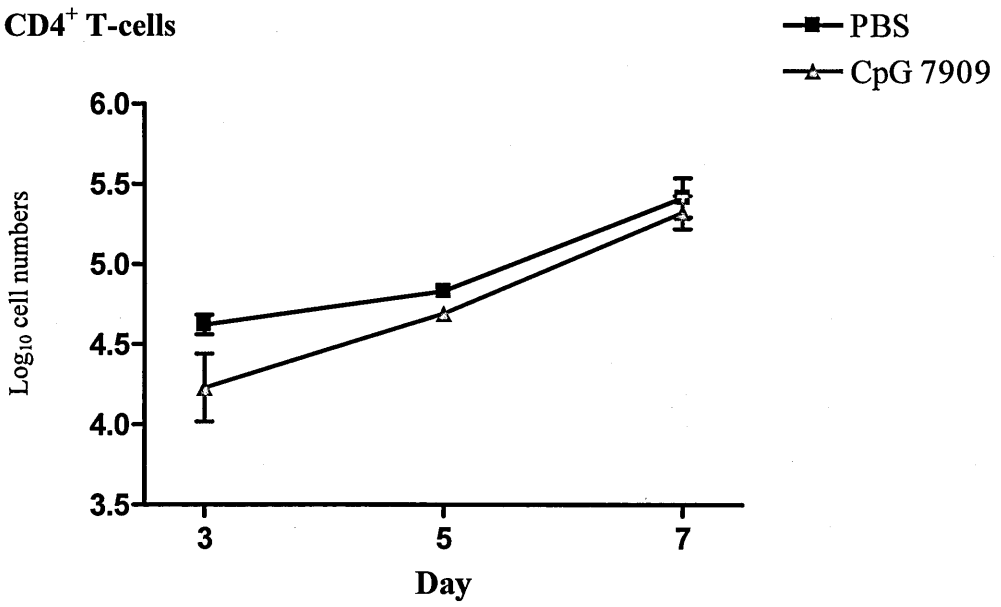

b) $CD3^+$ $CD8^+$ T-cells

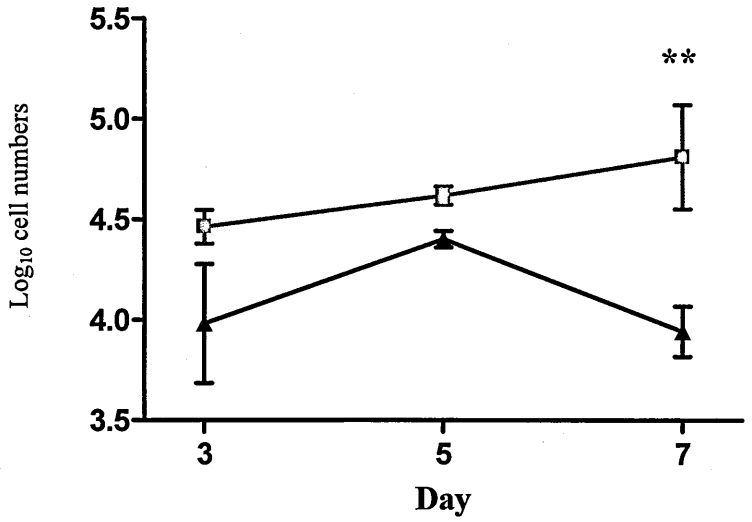

Figure 4.26. Spleen T-cell numbers during VACV infection in CpG-B 7909 and PBS treated groups. Numbers of $CD3^+$ T-cells in the spleens of infected mice were examined in mice either pre-treated with PBS or treated on day +1 with CpG-B 7909 over a seven day period using flow cytometry. Figure shows **(a)** total number of $CD4^+$ T-cells; **(b)** total number of $CD8^+$ T-cells. Graph represents geometric mean of four mice. Results shown include ± SEM. Statistical significance was determined using a two-way ANOVA and Bonferroni's post-tests. Significant findings between treatment groups are represented as ** ($p<0.01$).

particular, numbers of $CD8^+$ cells in PBS control mice were significantly higher ($p<0.01$) than CpG-treated mice on day +7 (Figure 4.26b).

4.3.3.6. Cytokine responses in the sera

Cytokine and chemokine levels detectable in the sera of mice from both treatment groups are represented in Figure 4.27. No significant differences in the serum levels of pro-inflammatory cytokines TNF-α, IL-6 or IFN-γ were seen between treatment groups throughout infection (Figure 4.27a, 4.27b, 4.27d), or for the chemokine CCL2 (Figure 4.27e). Serum levels of the anti-inflammatory cytokine IL-10 were found to be significantly higher ($p<0.05$) in CpG-B 7909 treated mice than in control groups on day +3 of infection only (Figure 4.27f). Levels of IFN-α from both CpG-B 7909 and PBS groups were only determined on day +3 of infection due to loss of sample. These samples did not differ significantly from each other (Figure 4.27e). Once again, serum levels of cytokines were substantially below those found in the lungs and spleens.

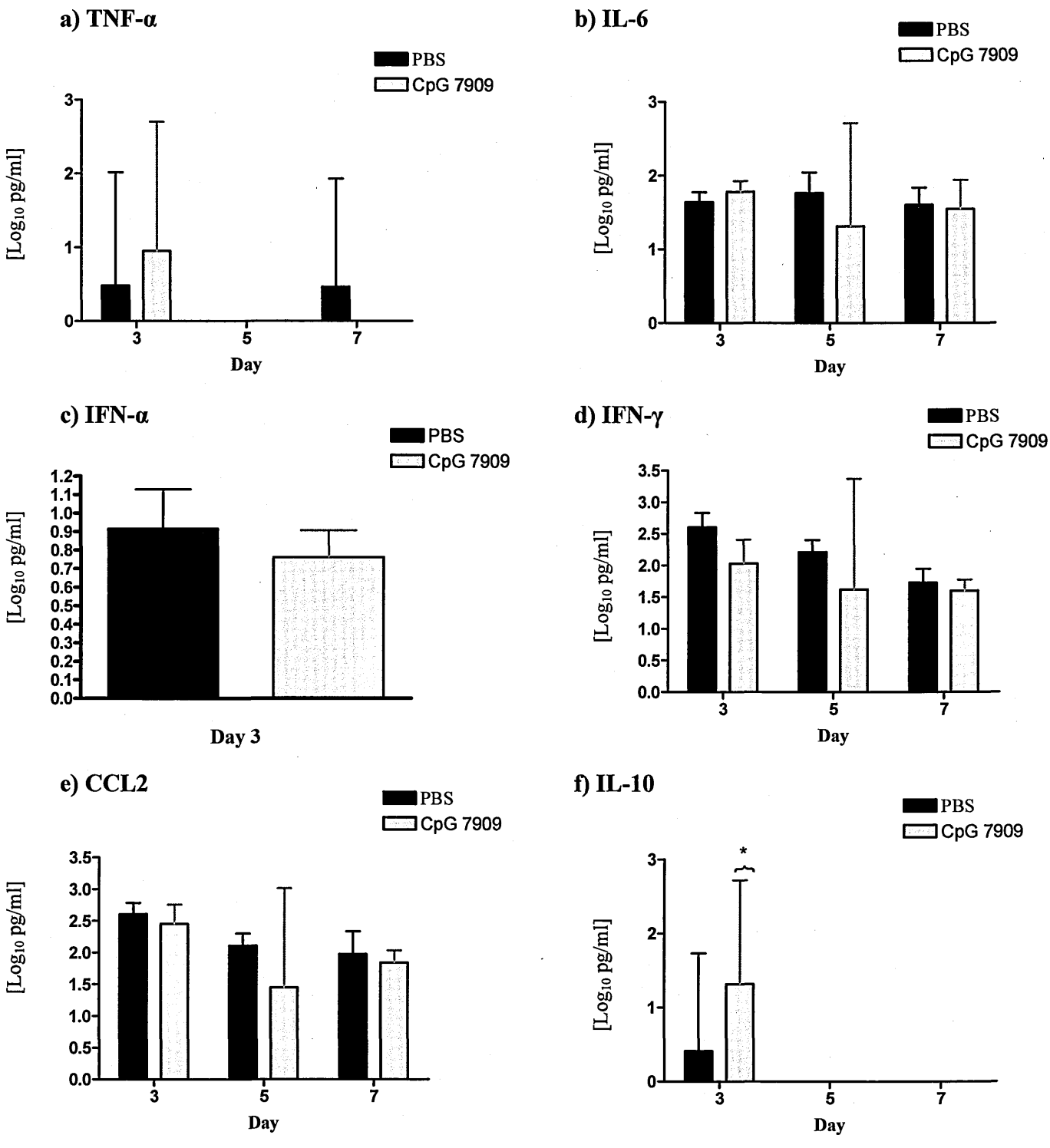

Figure 4.27. Measurement of serum cytokine levels in Balb/C mice treated with CpG-B 7909 or PBS post-infection with VACV. Protein levels determined *via* CBA analysis or IFN-α elisa. Bars represent the geometric mean of four mice (Log_{10} pg/ml) and error bars indicate 95% confidence intervals for cytokines **(a)** TNF-α; **(b)** IL-6; **(c)** IFN-α; **(d)** IFN-γ; **(e)** CCL2; **(f)** IL-10. Statistical significance was determined using a two-way ANOVA and Bonferroni's post-tests. Significant findings between treatment groups are represented as * ($p<0.05$).

4.4. Discussion

In this chapter, the protective effects of CpG-B 7909 have been examined when administered as a post-exposure therapy for intranasal infection with VACV. Previous work has suggested that CpG-B 7909 can be extremely effective at providing complete protection against VACV infection, if given up to 7 days prior to VACV challenge, (Rees *et al.*, 2005). However, historically the effectiveness of CpGs as a post-exposure monotherapy has yielded mixed results as detailed in a variety of studies (Waag *et al.,* 2006; Wongratanacheewin *et al.*, 2004; Olbrich *et al.,* 2002). The use of CpG-B 7909 has not previously been tested as a potential post-exposure antiviral to poxvirus infection. Therefore, this work has attempted to address whether the protective immunomodulating properties induced by CpG-B 7909 in a pre-exposure model, are similarly as effective when given after VACV challenge.

In initial studies, the local administration of a single 30μg dose of CpG-B 7909 protected 60% of mice when administered one day after intranasal challenge with VACV. This level of protection proved significant ($p<0.05$), although it was less effective than CpG-B 7909 given prior to virus exposure where full protection has been obtained (Chapter 3) (Rees *et al.*, 2005). This dose of CpG-B 7909 was more protective than the 15μg and 50μg CpG doses which failed to confer any protection. This may be a consequence of the 15μg dose failing to stimulate a sufficient immune response to combat the ongoing VACV infection. In contrast, the failure of the 50μg dose to protect may have been a result of over-stimulation of the immune response resulting in a hastened time to death. The fact that the 30μg dose sits in the middle of this scale may suggest it causes an appropriate level of immune stimulation that is able to afford some protection from VACV infection.

The drop in protection seen between CpG-B 7909 prophylaxis and post-exposure therapy of VACV infection is consistent with that seen by other groups in a variety of infection models. For instance, systemic delivery of CpG prior to intraperitoneal *B.pseudomallei* infection provided 100% protection against lethality, whereas only 33% protection, or no protection has been observed if CpGs are given at the time of challenge or on day +1 respectively (Wongratanacheewin *et al.,* 2004). Similarly, systemic CpG-B 7909 treatment prior to intranasal *B.mallei* infection afforded 90% protection, but only 10% if given 24 hours after challenge (Waag *et al.,* 2006). Protection has also been completely abrogated in a pulmonary *Klebsiella* model of infection when CpGs were administered at the time of infection, whereas treatment 48 hours prior to challenge resulted in 80% protection (Deng *et al.*, 2004).

Reduced levels of protection have also been documented against viral infection by numerous groups. Pre-treatment intravaginally with CpG 1826 has given 100% protection against lethal HSV-2 infection but only 20% or 13% if given either 24 hours or 72 hours post-challenge, respectively (Sajic *et al.*, 2003). Other groups have also reported reduced protection after post-exposure CpG treatment for HSV-2 (Harandi *et al.*, 2003) although, in this study, CpG administration came 4 hours after challenge resulting in a drop from 80% protection in pre-exposure models to 66%. In all of these studies, the introduction of CpGs prior to viral challenge significantly restricted viral titres compared to control groups over the course of the experiments. However, delayed treatment with CpG failed to reduce viral titres in all of the post-exposure models. For instance, HSV-2 viral titres in mice treated with CpG 24 or 72 hours post-infection were no different from control mice and significantly higher than those seen in mice treated 4 hours post infection with CpG (Sajic *et al.*, 2003). The

failure of CpGs in these models to limit the spread of infection correlates with disease severity and a loss of protection and has been linked to the timing of CpG delivery. In this current study, viral titres in post-exposure CpG-B 7909 treated mice could not be ascertained because lung and spleen cell suspensions were preserved for analysis by flow cytometry. However, as pre-treatment of mice with CpG-B 7909 has been shown to reduce VACV viral titres in the lungs, brain and spleen (Rees *et al.*, 2005), it would be interesting to see how CpG-B 7909 treatment post-exposure affected the dissemination and growth of virus in this model. It is certainly possible that the drop in protection seen in this post-exposure virus model may also be due to the failure of the infected host to limit the spread of VACV during the early stages of infection. Indeed, experiments performed by colleagues here at Dstl investigating a 50μg dose of CpG-B 7909 given on day +2 of VACV infection, found no differences in viral titres between untreated and CpG-treated groups (Personal communication).

The results in this chapter suggest that the administration of CpG-B 7909 to the lung post VACV infection can induce significant changes to an already activated inflammatory response initiated by viral infection. In the pre-exposure model, protection correlated with a prominent immunological response to CpG treatment, characterised by the rapid release of pro-inflammatory cytokines and increased cellular traffic into the lung prior to VACV infection (Chapter 3). Here, CpG-B 7909 treatment induced significant increases in the pulmonary levels of pro-inflammatory cytokines including TNF-α, IL-6, IFN-γ and IFN-α. Once again, the exact origins of these cytokines are unknown although macrophages, dendritic cells, and NK cells are likely candidates as these cell types have all been shown to release these cytokines following CpG stimulation (Ballas, Rasmussen, & Krieg, 1996; Platz *et al.*, 2004;

Demedts *et al.*, 2006; Katze, He, & Gale, 2002). Moreover, each of these cell-types expressed an activated phenotype on day +3 of infection. Consistent with direct CpG stimulation *via* TLR9, both the number and percentage of dendritic cells in the lung expressing the co-stimulatory marker CD80 were significantly higher in CpG-treated animals on day +3 of infection. Interestingly, given CpG-B 7909 is predominantly thought to activate B-cells, no significant differences were detected in either B-cell numbers or the percentages of activated B-cells at the site of CpG administration. This may be due to CpG stimulation being extremely rapid and inducing only transient effects on B-cells, as has been documented previously (Krieg *et al.*, 1995). Likewise, the pro-inflammatory cytokine IL-12 which drives expression of IFN-γ is also transient and is released rapidly following stimulation of dendritic cells and macrophages. This may also account for the lack of detectable levels of IL-12 throughout infection as the first sample was taken 48 hours after CpG treatment.

Indirect CpG stimulation may account for the observed increases in the percentages of lung neutrophils expressing CD11b on days +3 and +5 of infection. Increases in CD11b expression are typically indicative of cellular egress and in this instance, may be a sign of recent recruitment of neutrophils to the site of stimulation (Ley *et al.*, 2007). Interestingly, the percentage of $CD54^{+}$ neutrophils was significantly lower on day +3 of infection in CpG-treated mice than in control mice. Down-regulation of CD54 on neutrophils by anti-inflammatory cytokines such as IL-10 may be a strategy to retain neutrophils in the lung (Tomioka *et al.*, 2004). NK cell activation after CpG stimulation has been well documented despite the absence of TLR9 which may emphasise the importance of indirect stimulation in CpG mediated protection (Sivori *et al.*, 2006; Marshall *et al.*, 2006). The total numbers of NK cells in the lung, along

with those expressing the early activation marker CD69, were also significantly higher in the lungs of CpG-treated mice. Additionally, pulmonary levels of the chemokine CCL2 were significantly elevated in mice treated with CpG-B 7909 and this increase has also been reported in previous studies involving CpGs (Edwards *et al.,* 2005). Consistent with CCL2 release, CpG-treated mice had a significantly higher number of activated macrophages in the lung as determined by $CD54^+$ expression compared with control mice. Similar to that seen in Chapter 3, CpG stimulation appeared to reduce the percentage of macrophages expressing MHC II on day +3 in the lung, as has also been seen by other groups (Chu *et al.,* 1999). Pulmonary levels of IL-10 were significantly higher on day +3 in CpG- treated mice. These increases in IL-10 may promote NK cell activity as has been previously described (Lauw *et al.,* 2000), or may counter-balance the inflammatory effects of other pro-inflammatory cytokines. It may be that the immune profiles reported here in this post-exposure system result from the host's accommodation of the temporal nature of treatment and infection. Collectively, the immune responses at the site of infection may be crucial for protection against VACV.

In the spleens of infected mice, no differences between treatment groups were observed in the splenic levels of cytokines or chemokines measured over the course of infection. However, significant increases in the numbers and percentages of particular cell-types were found between treated and untreated groups suggesting that CpGs can have significant immunological effects at sites distal to their site of delivery. Specifically, increases in the percentages of $CD80^+$ dendritic cells, $CD69^+$ NK cells, and increased numbers of $CD80^+$ B-cells were determined. The lack of enhanced cytokine production in CpG-treated mice, suggests that cytokine stimulation of cells

alone is unlikely to account for these increases in CpG-treated mice. This opens the question as to whether the observed differences in CpG-treated mice may be a result of direct CpG stimulation *via* TLR9, particularly since DCs and B-cells are predominantly the cells activated. As described in Chapter 3, it is perhaps more likely that the observed differences may be a result of these cell-types being stimulated in the lung and then having migrated to the spleen where viral titres are likely to be high (Rees *et al.*, 2005).

The immunological differences between CpG-treated and untreated mice in the lungs and spleens of VACV infected mice provide insight into the protective nature of CpG-mediated therapy. As observed with CpG prophylaxis, a strong local inflammatory response in the lungs of mice receiving CpG treatment may be key to protection. Following intranasal CpG-B 7909 delivery, levels of pro-inflammatory cytokines and innate effector cells in the lung such as macrophages, neutrophils, dendritic cells and NK cells are significantly boosted (Table 4.1). In contrast, very little effect of CpG stimulation is evident in the spleen throughout early infection (Table 4.2). The increases in the number of innate cells in the lung and the changes in their activation state may aid the ongoing immunological response to VACV infection. If so, additional recruitment and activation of cells such as macrophages, dendritic cells and NK cells may slow down the replication of VACV and give the immune system an opportunity to fight infection more effectively. This may also provide sufficient time for the adaptive response to form and resolve infection. Indeed, lymphocyte responses in the spleen of mice on day +7 reveal significant differences between CpG-treated and untreated mice (Table 4.2). Here, increased numbers of $CD8^+$ T-cells and activated B-cells are present in CpG treated mice which may be indicative of the

	Day			Overall	
	+3	+5	+7	CpG-B 7909 Treatment	Time
Total macrophages				++	+
$F4/80^+$ $CD54^+$	+			++	+
$F4/80^+$ IA/IE^+					
% $CD54^+$					
% IA/IE^+	+++			+++	+++
Total neutrophils					+++
$Ly6G^+$ $CD54^+$					+++
$Ly6G^+$ $CD11b^+$					+++
% $CD54^+$	+			+	+++
% $CD11b^+$	+	+		++	+++
Total dendritic cells					+++
$CD11c^+$ $CD80^+$	++			++	+++
$CD11c^+$ IA/IE^+					+++
% $CD80^+$	++			++	+++
% IA/IE^+					++
Total NK cells	++				+++
$CD49b^+$ $CD54^+$					+++
$CD49b^+$ $CD69^+$	++				+++
% $CD54^+$					
% $CD69^+$	++			+	+++
Total B-cells					++
$CD19^+$ $CD86^+$				+	+++
$CD19^+$ $CD80^+$					+++
% $CD86^+$					+++
% $CD80^+$					+++
Total $CD4^+$ T-cells					++
Total $CD8^+$ T-cells					+++

Table 4.1. Significant differences between CpG-B 7909 and PBS treatment groups in the lungs of mice during VACV infection. Differences between total and activated cell numbers are reported along with differences between the percentages of activated cell-types for days +3, +5 and +7 post-infection. The overall effect of CpG-B 7909 treatment for each parameter is also reported. Additionally, the overall significance of the variation between days for each parameter is reported under Time. Significance between treatment groups determined by two-way ANOVA using Bonferroni's post-tests and represented as: + $p<0.05$; ++ $p<0.01$; +++ $p<0.001$.

	Day			Overall	
	+3	+5	+7	CpG-B 7909 Treatment	Time
Total macrophages					++
$F4/80^+$ $CD54^+$					++
$F4/80^+$ IA/IE^+					++
% $CD54^+$					+++
% IA/IE^+					++
Total neutrophils					+++
$Ly6G^+$ $CD54^+$					+++
$Ly6G^+$ $CD11b^+$					+++
% $CD54^+$					+++
% $CD11b^+$					++
Total dendritic cells					+++
$CD11c^+$ $CD80^+$					+++
$CD11c^+$ IA/IE^+					+++
% $CD80^+$	+				+++
% IA/IE^+					+++
Total NK cells					++
$CD49b^+$ $CD54^+$					+++
$CD49b^+$ $CD69^+$					+++
% $CD54^+$					++
% $CD69^+$	++			+	+++
Total B-cells					+++
$CD19^+$ $CD86^+$					+++
$CD19^+$ $CD80^+$			+		+++
% $CD86^+$					+++
% $CD80^+$			+++	+++	+++
Total $CD4^+$ T-cells				+	+++
Total $CD8^+$ T-cells			++	++	

Table 4.2. Significant differences between CpG-B 7909 and PBS treatment groups in the spleens of mice during VACV infection. Differences between total and activated cell numbers are reported along with differences between the percentages of activated cell-types for days +3, +5 and +7 post-infection. The overall effect of CpG-B 7909 treatment for each parameter is also reported. Additionally, the overall significance of the variation between days for each parameter is reported under Time. Significance between treatment groups determined by two-way ANOVA using Bonferroni's post-tests and represented as: + $p<0.05$; ++ $p<0.01$; +++ $p<0.001$.

formation of a VACV specific adaptive response. This implies that as with CpG prophylaxis, the immediate response of cells in the lung to CpG delivery and the latter involvement of cells in the spleen may be crucial to CpG-mediated protection.

A significant factor of VACV infection is the wealth of immunomodulatory proteins available at its disposal to disrupt the host response to infection (Haga & Bowie, 2005) (Section 1.3.2). Many of these genes are synthesised early during the VACV lifecycle making the delayed administration of immunomodulatory CpGs less likely to work. Collectively, these proteins could contribute significantly to the drop in protection observed in the post-exposure model of infection. Many VACV proteins such as A46R and A52R, function to disrupt TLR signaling (Stack *et al.*, 2005) and their presence prior to CpG delivery may severely dampen the ability of CpGs to stimulate cells through TLR9. Other immunomodulatory proteins such as VACV IFN-γR or TNF-α receptors (crmB-E) may bind these cytokines and prevent them from stimulating receptors on their intended target cells. The potential of these individual VACV proteins to limit the protective efficacy of CpG-B 7909 was not addressed during this work and remains to be elucidated in this post-exposure model.

The use of multiple doses of CpG treatment post-exposure has been successful in the treatment of pathogens in a number of model systems such as FLV, *L.monocytogenes* and *F.tularensis* (Olbrich *et al.,* 2002; Klinman *et al.*, 1999). However, against VACV, multiple doses of CpG-B 7909 seemed to exacerbate infection. This was evident from the observations showing mice that received two separate doses of CpG succumbed to infection before the control group and rapidly showed signs of intolerance to CpG treatment (Figure 4.2). In addition to the cytopathic effects caused

by poxvirus infection, a role for excessive inflammation in the pathogenesis of disease has long been cited as a significant contributor to disease pathology (Stanford *et al.*, 2007). Consequently it is possible that multiple doses of CpG during a pre-established acute poxvirus infection could provoke a pro-inflammatory immune response leading to exacerbated disease pathology and a hastened time to death. This may also explain why lower doses of CpG-B 7909 (30μg) prove more protective than higher doses in a post-exposure system.

Currently, CpG treatment administered at the time of challenge or post infection has only been successful in the control of slower growing pathogens that establish chronic infection. For instance, treatment of *M.tuberculosis* at the time of infection or even 2 weeks after infection significantly reduces bacterial loads in the lung and causes a reduction in lung pathology (Juffermans *et al.*, 2002). CpG treatment five days after intranasal infection with *C.neoformans* has also been shown to be effective, preventing bacterial dissemination and reducing lung eosinophilia (Edwards *et al.*, 2005). In a viral model, CpG post-exposure treatment of mice infected with FLV was also able to reduce viral titres with 74% mice not going on to develop leukaemia (Olbrich *et al.*, 2002). In this instance, the onset of disease recovery was not apparent until after the final treatment with CpG and was suggested to be highly reliant on the generation of specific $CD8^+$ T-cells. Therefore, in the more acute models of infection, like VACV, the delayed use of CpGs in a post-exposure therapy may be severely restricted in providing protection.

In summary, the use of CpG-B 7909 as a post-exposure therapy can provide a significant degree of protection if administered 24 hours after an otherwise lethal dose

of VACV. Intranasal delivery of CpG was shown to induce significant changes to the immune response in both the lungs and spleens of infected mice. In particular, CpG treatment resulted in significant changes to lung macrophages, neutrophils, dendritic cells and NK cells and resulted in elevated levels of TNF-α, IL-6, IFN-α and IFN-γ. In the spleens of infected mice, fewer significant changes in the numbers of cells or expression of cellular activation markers were observed following CpG treatment. Here, significant differences were determined later during infection with increases in B and T-lymphocyte numbers. Additionally, only levels of IFN-γ in the spleen were found to differ significantly between treatment groups with control mice having higher levels than CpG-treated mice. Collectively, these changes are likely to have contributed to the partial protection observed in mice treated with CpG. The failure of CpGs to provide complete protection against VACV, as has been observed in pre-exposure systems, may be a combination of allowing the virus to replicate to high titres, the release of immunomodulatory proteins, and the establishment of a firm foothold prior to administration of CpG therapy. In addition, it is also possible that the administration of CpGs during an already established VACV infection may result in overwhelming levels of inflammatory cytokines such as IL-1β which were not examined in this work. Together, each of these factors may play a role in limiting the efficacy of CpG treatment in the post-exposure model.

Chapter 5: Macrophage responses to different classes of CpG

5.1. Introduction

5.1.1. Defences at the lung surface

The previous chapters have assessed the host response to VACV *in vivo* in conjunction with CpG-B 7909 prophylaxis or therapy. These results have suggested that protection correlates with a prominent pro-inflammatory response, resulting in the activation and recruitment of a variety of innate immune cell types in the lung. CpG treatment against VACV has proven most effective when administered prior to challenge, making the cell-types that respond to CpG stimulation key to understanding how protection is conferred. B-cells, the cell-type thought most responsive to CpG-B stimulation, are present in the lung in low numbers, and results presented in 3.3.8 using B-cell KO mice suggest that B-cells may not be crucial in conferring CpG-B mediated protection against VACV. Similarly, protection against VACV was still conferred by CpG-B 7909 stimulation in neutrophil depleted Balb/C mice (3.3.9). This makes understanding the lung environment and the initial interactions between CpGs and other TLR9-expressing cells in the lung extremely important.

The lungs of air-breathing animals are constantly bombarded with antigenic material and need to be maintained by a variety of innate immune mechanisms. The mucosal lining of the lung epithelium provides a first-line of defence against inhaled antigens. Here, ciliated and non-ciliated epithelial cells, basal cells and goblet cells provide a mechanical barrier to particles, and secrete soluble constituents that comprise the airway surface fluid that covers the respiratory epithelium (Fokkens & Scheeren,

2000). This airway surface fluid is rich in complex glycoproteins called mucins and antimicrobial compounds such as lysozymes (Dajani *et al.*, 2005), β-defensins (Lehrer, 2004), and lactoferrin (Kruzel *et al.*, 2006) that prevent the colonisation of the epithelial surfaces by invading organisms. Bacteria and virus particles that are carried towards the alveolar surface also interact with opsonising components of the alveolar fluids such as IgG, and complement (Martin & Frevert, 2005), and surfactant/surfactant-associated proteins (SPs) such as SP-A and SP-D (Woodworth *et al.*, 2007). Micro-organisms may also be neutralised by IgA secreted mainly from the bronchial–associated lymphoid tissue (BALT) (Pilette *et al.*, 2001). Organisms that are able to bypass these defences are then met by cells of the immune system that reside in the alveolar space. These cell types may include T-cells, B-cells, neutrophils, eosinophils, mast cells and dendritic cells, but by far the most predominant cell type found in the alveolar spaces are the alveolar macrophages (AMs) (Bingisser & Holt, 2001). AMs account for approximately 95% of leukocytes in the alveolar spaces, making them the sentinel phagocytic cell in the lung and the first cell type to encounter foreign antigens (Sibille & Reynolds, 1990). Consequently, this also makes them very likely to be one of the first TLR9 expressing immune cells that encounter CpGs after intranasal delivery.

5.1.2. The role of alveolar macrophages

Alveolar macrophages are thought to play a dual role in maintaining lung homeostasis. Beyond their potent phagocytic capability, they are known to express a wide range of PRRs permitting recognition of foreign antigen and processing of danger signals leading to NF-κB activation and pro-inflammatory gene transcription (Oshikawa & Sugiyama, 2003). This has been demonstrated through TLR-mediated

release of pro-inflammatory cytokines such as IL-6, IL-1, IL-12 and TNF-α (Ogle *et al.*, 1994) and chemokine release of IL-8 resulting in rapid neutrophil recruitment into the alveolar spaces (Holt, 1986). The release of leukotrienes and reactive oxygen intermediates such as nitric oxide (NO) has also been well documented (Bingisser & Holt, 2001) and the expression of immunoglobulin receptors (f_cR), complement and mannose receptors, as well as a range of scavenger receptors and antigenic markers have also been well characterised (Laskin *et al.*, 2001). These data suggest AMs possess a number of mechanisms for direct pathogen killing to complement their ability to promote cellular recruitment from the pulmonary vasculature and clearance of infectious material. However, the lung has been shown to be a predominantly immunosuppressive environment that prevents over-zealous inflammatory responses to inhaled antigen (Bonfield *et al.*, 1995). AMs have been implicated in the down-regulation of the immune response through suppression of pulmonary DC APC function (Holt *et al.*, 1993) and through regulation of T-cell functions (Strickland *et al.*, 1993). These studies suggest AMs function poorly as accessory cells for T-cell activation and also modulate the presentation of antigen through dendritic cells to prevent an inflammatory response.

5.1.3. Varieties of lung macrophages and heterogeneity

A number of studies have shown the macrophage to be an extremely heterogeneous cell population (Gordon & Taylor, 2005). Differences relating to morphology, expression of surface markers and the release of specific products such as enzymes and cytokines have all been cited between macrophages that are found in different tissues (Laskin *et al.*, 2001; Dorger *et al.*, 2001). Within the lung itself, clear functional and morphological differences have been reported between alveolar and

interstitial macrophages in both murine (Crowell *et al.*, 1992) and human (Fathi *et al.*, 2001) tissues. Interstitial macrophages are found in the connective tissues of the lung, are not exposed to airborne particles (unlike AMs) and are thought to comprise about 40% of total macrophage numbers in the lung (Crowell *et al.*, 1992). These macrophages combat organisms that colonise or infiltrate the epithelial surfaces and secrete a diverse array of soluble mediators in the immediate vicinity of the lung matrix and pulmonary connective tissues. Studies also report the presence of another type of lung macrophage, the pulmonary macrophage, which differs from its alveolar and interstitial counterparts, adhering tightly to the lung endothelial cells to remove bacteria from the lung (Dehring & Wismar, 1989). Alveolar macrophages exhibit sub-populations (Sandron *et al.*, 1986) and studies show certain sub-populations are more prevalent during particular disease states. This is clear when comparing the phenotypes of AMs during acute and chronic infections, with the former having a prevalence of smaller, less mature 'monocyte-like' macrophages compared to a larger, more mature macrophage phenotype found in the latter (Brannen & Chandler, 1988). Likewise, interstitial macrophages exhibit considerable heterogeneity with respect to antigen expression, morphology and function (Kobzik *et al.*, 1988). These findings suggest that the response of macrophages during infection depends significantly on the type of macrophage encountered by the invading organism. Likewise, macrophage responses to therapeutic agents such as CpG could also vary according to the type of macrophage stimulated.

5.1.4. Macrophage responses to CpG

As described in Chapter 1, macrophages possess a variety of PRRs to facilitate a rapid response to pathogens. Macrophages have been shown to ingest, and be activated by,

bacterial DNA (Stacey *et al.*, 1996) and the expression of TLR9 on murine macrophages and their response to CpG stimulation has been investigated by several groups *in vitro*. CpG activation of macrophages alters the expression of a wide variety of genes (Gao *et al.*, 2002) and induces a prominent pro-inflammatory effect, governed by NF-κB activation, cytokine release and up-regulation of TLRs including TLR9 (An *et al.*, 2002). TLR9 stimulation on both peritoneal and alveolar macrophages through CpG has been shown to inhibit signaling through the IL-10R and to negate the effect of IL-10 stimulation (Fernandez *et al.*, 2004). Other studies have reported that CpGs enhance mouse macrophage uptake of *Burkholderia pseudomallei*, *Salmonella enterica* serovar *Typhi* and *E.Coli* (Utaisincharoen *et al.*, 2003) and promote the survival of bone marrow-derived macrophages in a TLR9 and PI3-K-Akt dependant manner (Sester *et al.*, 2006). The expression of chemokines including MIP-1α, MIP-1β, RANTES, and IP-10 have all been shown to be upregulated by the murine macrophage cell line RAW 264.7 and macrophages isolated from spleen and lung tissue fractions following CpG stimulation (Takeshita *et al.*, 2000). CpGs have also been shown to release pro-inflammatory cytokines and induce the production of NO and the inducible nitric oxide synthase (iNOS) enzyme in RAW 264.7 cells (Utaisincharoen *et al.*, 2002). Additionally, both NO and IL-1β mRNA synthesis has been observed in avian macrophages in a sequence specific manner following CpG stimulation (He *et al.*, 2003). Other studies also suggest that the degree of macrophage activation by CpG may vary according to the class of CpG used and the chemical content of the ODN backbone (Roberts *et al.*, 2005). Collectively, all these studies indicate the macrophage can be directly activated by CpGs to release a multitude of inflammatory factors.

5.1.5. Viral infections in the lung

Viral infections of the upper respiratory tract and lung are extremely common with a wide variety of viruses being able to colonise the lung surfaces. The positioning and prevalence of macrophages throughout the lung, along with their repertoire of PRRs, make them key cell-types in the initiation of the anti-viral response (Malmgaard *et al.*, 2004). Recently, AMs have been identified as the primary source of IFN-α following infection with the RNA virus Newcastle disease virus in a RIG-I dependent manner (Kumagai *et al.,* 2007). Interestingly, removal of AMs led to pDCs becoming the dominant IFN-α producers further suggesting that AMs typically suppress the functions of other cell-types (Kumagai *et al.,* 2007). Still, the role of AMs in viral infection may vary according to the virus itself and the interaction between viral PAMPs and PRRs. In addition, differences in the virus' ability to fuse to host cells, replicate and counteract the immune response may also affect the role of AMs (Van Reeth & Adair, 1997). This is supported by studies that find AMs promote inflammation when infected with influenza A virus (Lehmann *et al.*, 1996) and adenovirus (Zsengeller *et al.*, 2000) whereas they may act to suppress the immune response to VACV strain WR (Rivera *et al.*, 2007). HSV-2 infected macrophages can be activated through TLR-dependent and independent pathways and studies show active viral replication inside the cell boosts the IFN-α/β response (Malmgaard *et al.*, 2004). This work suggests that interactions between the virus and the cell surface of macrophages may not be enough to induce a full inflammatory response and thus the role of the AM may also vary due to virus cell tropism. Studies have not shown the role of the AM during infection with VACV strain IHD, nor examined how intranasal delivery of CpGs may affect the function of AMs prior to infection with VACV. However, studies have suggested that mice depleted of macrophages are unable to

control VACV infections due to impaired virus clearance and antigen presentation (Karupiah *et al.*, 1996).

5.1.6. CpG-B 7909 and CpG-B 10103

The *in vivo* studies detailed in Chapters 3 and 4 of this thesis were all conducted using the B-class CpG-B 7909. However, the progression of CpG-B 7909 into phase III clinical trials for cancer research in September 2005 resulted in the withdrawal of CpG-B 7909 from the majority of these studies. Consequently, CpG-B 10103 was used as an alternative B-class CpG throughout the *in vitro* work detailed in this chapter.

5.2. Aims of this chapter

The intranasal delivery of CpG in the VACV model has had a marked protective effect. As alveolar macrophages are one of the first cell types to encounter inhaled material, their response to the delivery of CpGs may be key to the initiation of this protective response. This chapter examines the effect of CpG stimulation on different macrophage populations using both primary cells and *in vitro* cell lines and different classes of CpGs. In addition, the growth of VACV in two macrophage cell lines is investigated in the context of pre-stimulation with CpGs.

5.3. Results

5.3.1. TLR9 is present on primary macrophages

To assess whether TLR9 is present on mouse AMs, bronchoalveolar lavage samples from Balb/C mice were obtained using the protocol detailed in section 2.6.4. In an initial experiment, BAL samples from 2 mice were taken and analysed separately for the presence of TLR9. Briefly, lavage samples were aliquoted onto a 96-well plate and left to adhere overnight in RPMI medium supplemented with 10% (x volume) FCS and 1% (x volume) PSG. The following morning, supernatants were carefully removed to leave only adherent cells. These remaining cells were processed for RT-PCR. Results from this experiment revealed that TLR9 transcript was clearly detectable in both mouse samples (Figure 5.1).

In a follow-up experiment to re-affirm expression of TLR9 on primary alveolar macrophages, BAL samples were taken from 4 Balb/C mice and then pooled. A small aliquot of crude BAL was then taken away for immunohistological staining using the Hema 'Gurr' rapid stain set which suggested that approximately 90% of cells recovered were alveolar macrophages (Figure 5.2a; Figure 5.2b). The remainder of the BAL sample was plated onto a 96-well plate, supplemented with medium and incubated overnight at 37°C. The following morning, any non-adherent cells were removed to leave only macrophages, and wells replenished with either fresh medium or stimulated in triplicate with 75 μg/ml CpG-B 10103 or 75 μg/ml CpG-sC 10109 for five hours. After five hours stimulation, supernatants were removed and cells analysed for expression of TLR9 and TNF-α *via* RT-PCR. Expression of TLR9 was once again clearly detected (Figure 5.3a) and interestingly, the expression of TNF-α was found to differ between unstimulated and CpG-stimulated samples (Figure 5.3b).

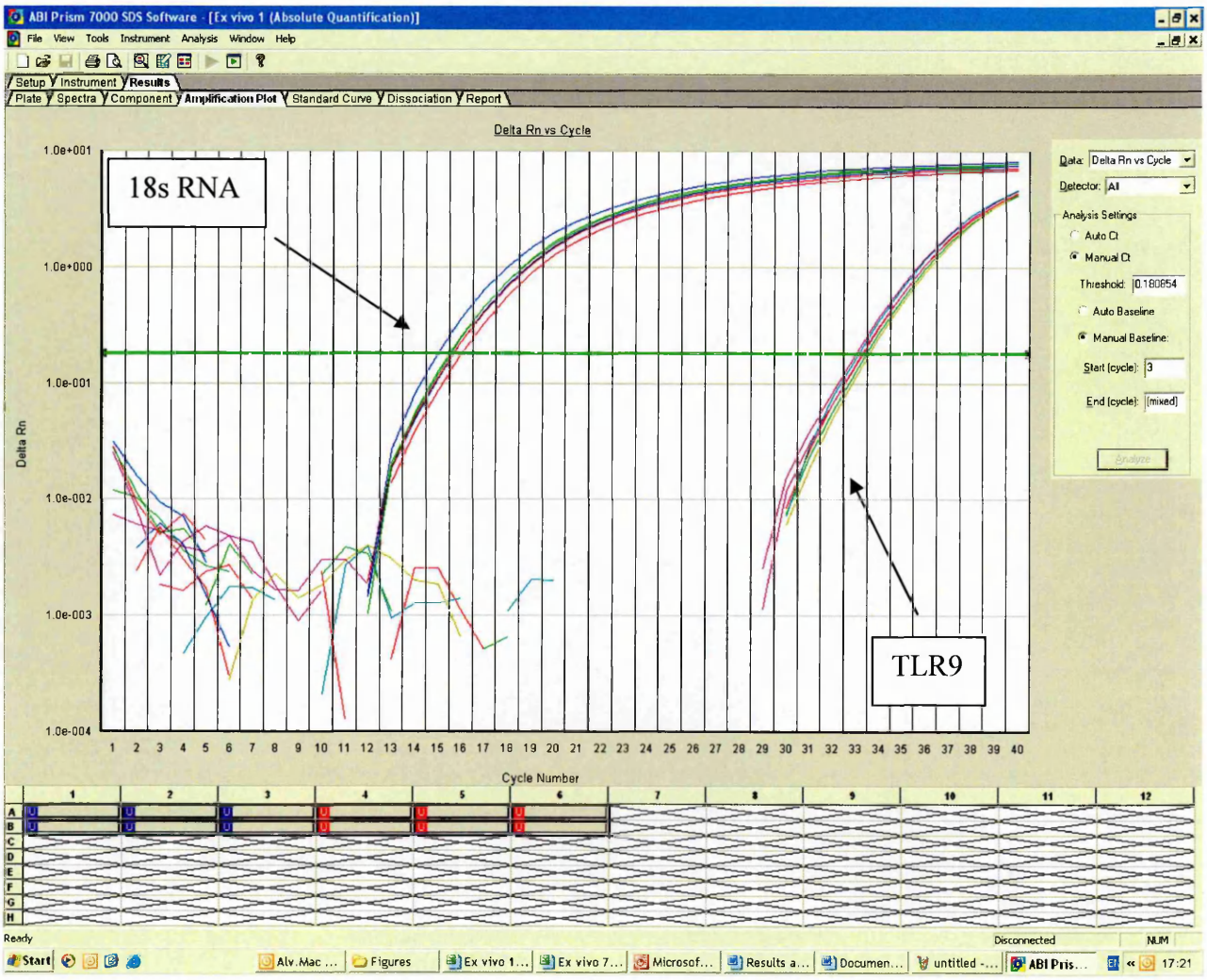

Figure 5.1. Expression of TLR9 on primary alveolar macrophages. Figure illustrates the expression of TLR9 and the endogenous control gene 18s RNA, analysed *via* RT-PCR on an ABI Taqman 7000 machine. Samples analysed in triplicate from two separate BAL samples obtained from Balb/C mice.

a)

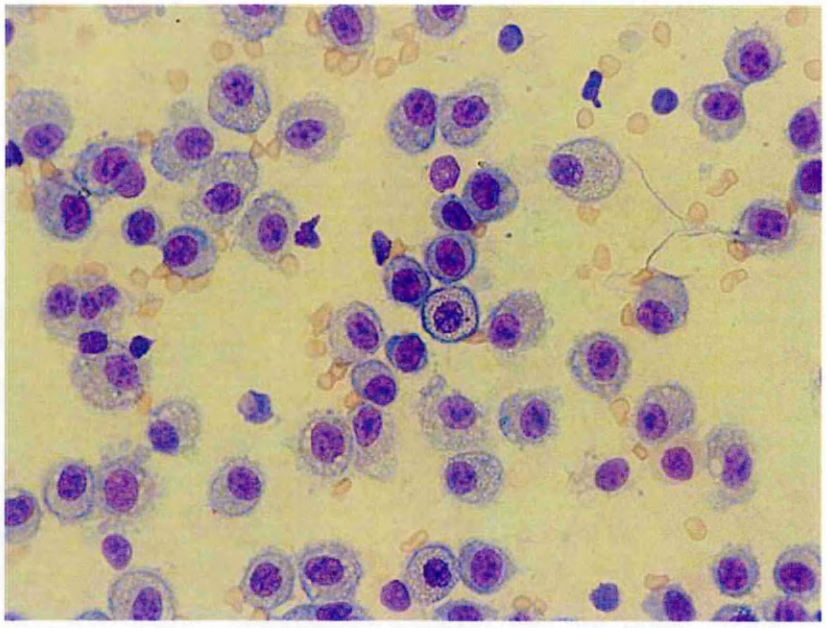

b)

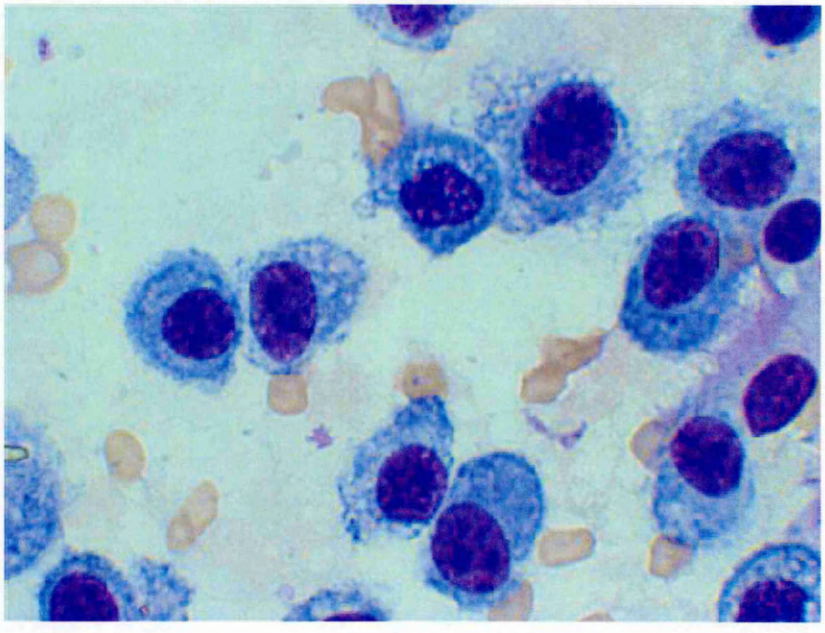

Figure 5.2. Immunohistological staining of BAL samples. Crude lavage preparations were stained using eosin and methylene blue. Approximately 90% of cells were assessed as being alveolar macrophages. **(a)** x400 **(b)** x1000 magnification.

a)

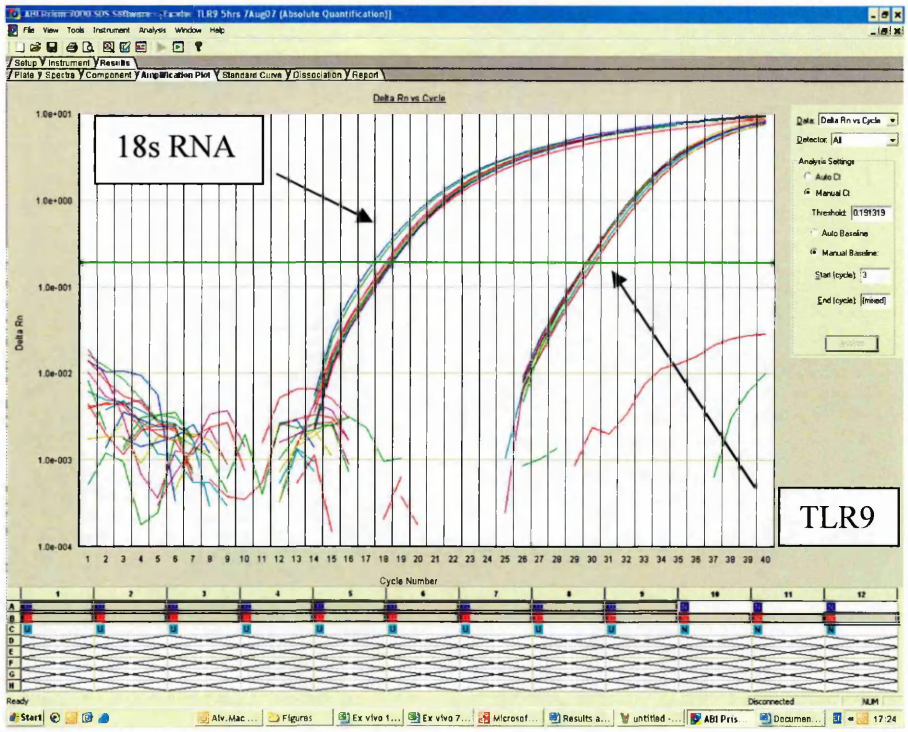

b)

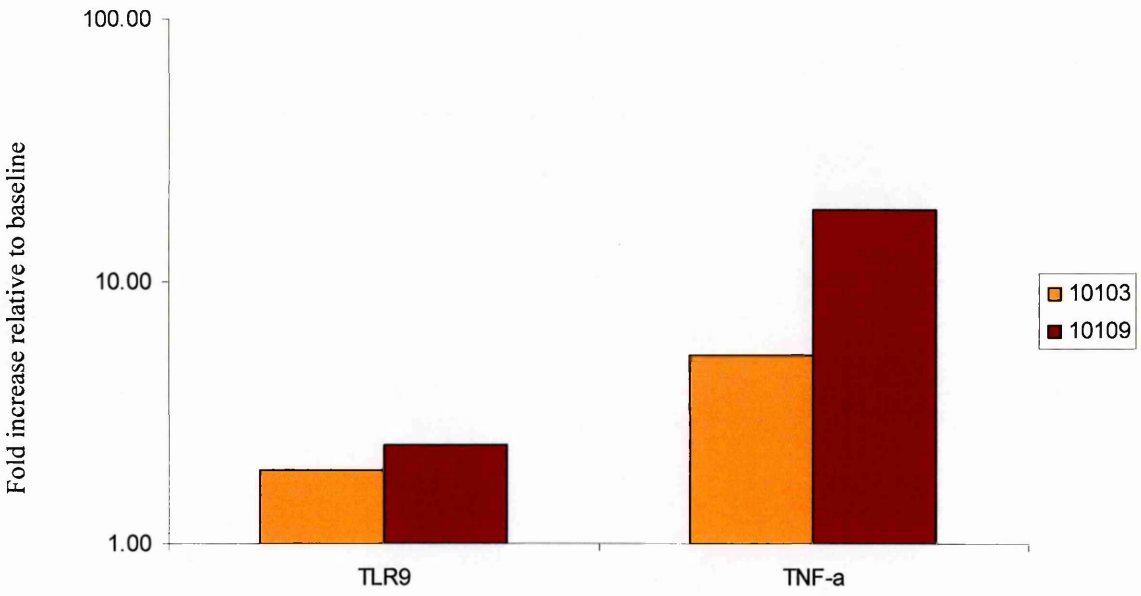

Figure 5.3. Primary alveolar macrophages are responsive to CpG. (a) TLR9 was detectable on primary alveolar macrophages from pooled Balb/C mouse BAL samples *via* RT-PCR analysis. **(b)** Expression of both TLR9 and TNF-α were found to increase relative to unstimulated controls (baseline) after 5 hours stimulation with 75μg/ml CpG-B 10103 and CpG-sC 10109.

Here, CpG-B 10103 was able to induce a five-fold increase in the expression of TNF-α relative to medium control wells, whilst CpG-sC induced more than an 18-fold increase in expression relative to medium. This suggested the administration of CpGs to primary AM cultures could induce a pro-inflammatory response. In addition, the expression of TLR9 on these cells differed from unstimulated samples, so that cells stimulated with CpG-10109 induced an approximate 2-fold increase in TLR9 expression (Figure 5.3b).

5.3.2. TLR9 expression in MH-S and J774 macrophage cell-lines upon stimulation with CpG

The difficulty of obtaining high numbers of AMs from BAL preparations resulted in the testing of two *in-vitro* cell-lines as potential models for *ex-vivo* AMs. Two different cell-lines, an alveolar macrophage cell-line (MH-S), and a blood monocyte/macrophage cell-line (J774), were obtained from ECACC (HPA, UK). Initially, the expression of TLR9 on these two cell-lines was examined *via* RT-PCR. MH-S and J774 macrophages were seeded onto 96-well plates at a concentration of $1x10^6$/ml, incubated overnight and stimulated in triplicate with a variety of different classes of CpG. Total RNA was extracted from cells after 1, 2, 5 and 24 hours stimulation with 75 μg/ml CpG. This experiment was then repeated twice, giving a total of three separate experiments for each time-point. RT-PCR analysis of samples confirmed the expression of TLR9 on both cell-lines. Results also suggested that expression of TLR9 was unaffected by CpG stimulation at any individual time-point (Figure 5.4). Interestingly, statistical analysis suggested that expression of TLR9 did vary significantly between time-points ($p<0.05$). However, since expression never

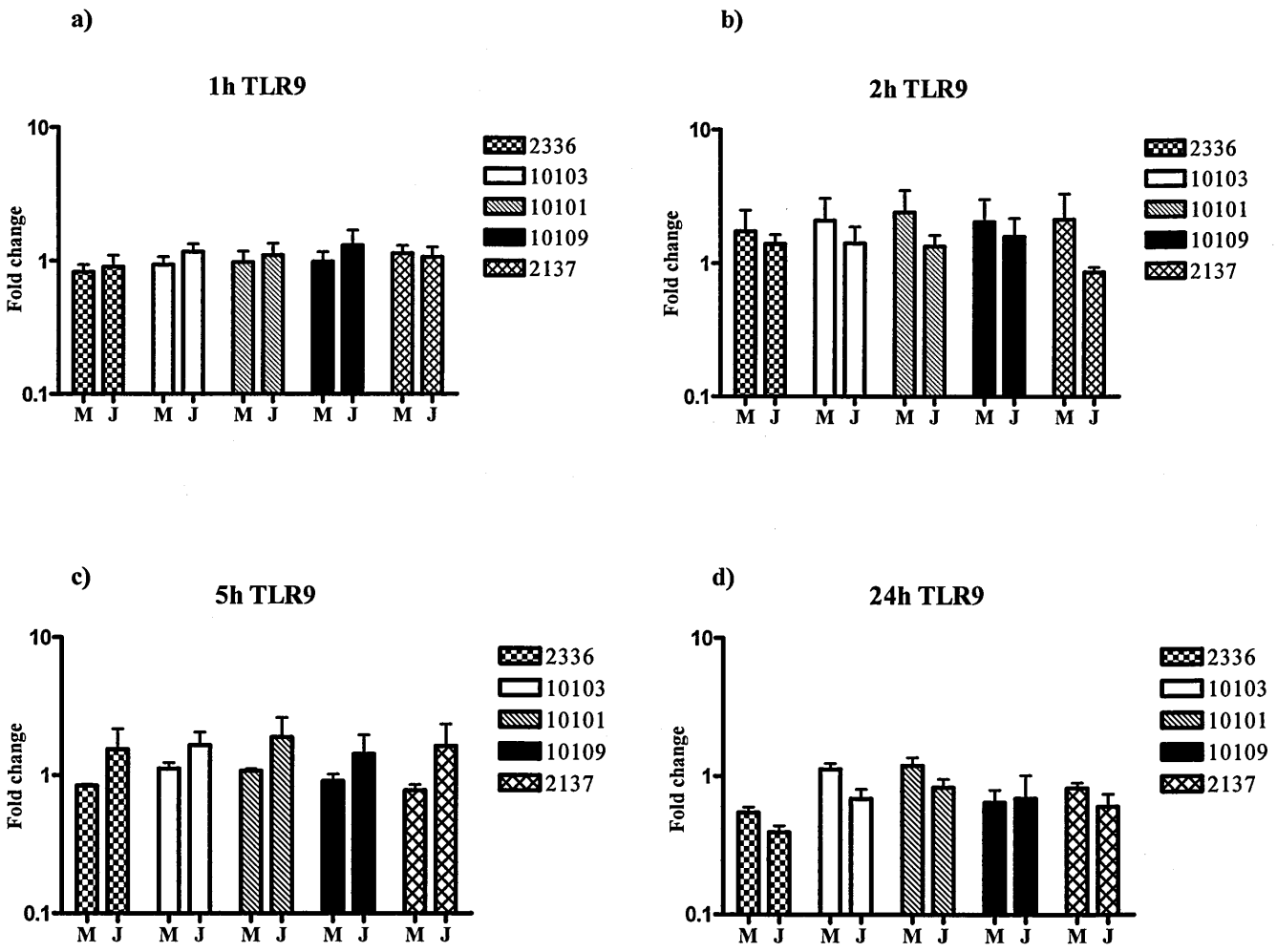

Figure 5.4. Changes in expression of TLR9 mRNA. MH-S (M) and J774 (J) macrophages were stimulated with 75μg/ml CpG and analysed *via* RT-PCR. Graphs show changes in TLR9 gene expression relative to unstimulated medium control wells after **(a)** 1 hour **(b)** 2 hours **(c)** 5 hours **(d)** 24 hours CpG stimulation. Experiments performed in triplicate, values represent geometric mean of three separate experiments. Error bars ± SEM.

No significant differences between CpGs and cell-line specific non-CpG 2137 determined by three-way ANOVA with Bonferroni's post-tests.

shifted more than 2-fold in either direction relative to unstimulated samples, the biological significance of this variance is uncertain.

Having established both *in vitro* macrophage cell-lines possessed transcripts for TLR9, the physical expression of TLR9 protein on these cell-lines was investigated. Intracellular expression of TLR9 was assessed *via* flow cytometry using a polyclonal FITC conjugated antibody for TLR9 and a rat IgG2a isotype control. Both MH-S and J774 cells were stimulated in 24-well plates for 24 hours with the two different CpGs, CpG-B 10103 or CpG-sC 10109. Results confirmed expression of TLR9 protein and failed to show any noticeable shift in TLR9 expression following CpG stimulation (Figure 5.5a-b). Expression of CD54 on both cell-lines was examined during these experiments as a positive control for cellular activation. Stimulation with either CpG resulted in a prominent shift in CD54 fluorescence consistent with cellular activation (Figure 5.5c-d).

5.3.3. The *in vitro* stimulatory properties of CpG-B 7909 are comparable to CpG-B 10103

The expression of TLR9 on both MH-S and J774 macrophage cell-lines suggested that these cells may be suitable for modelling the response of primary macrophages to CpG stimulation. To examine whether the properties of CpG-B 10103 were comparable to CpG-B 7909, a comprehensive analysis of cytokine/chemokine expression and NO release from both MH-S and J774 macrophages was undertaken. Results suggested that CpG-B 7909 and CpG 10103 stimulated macrophages equally as determined by RT-PCR, CBA and NO release ($p>0.05$). Statistical interaction plots for the analysis of cytokine data obtained from RT-PCR and CBA are represented in

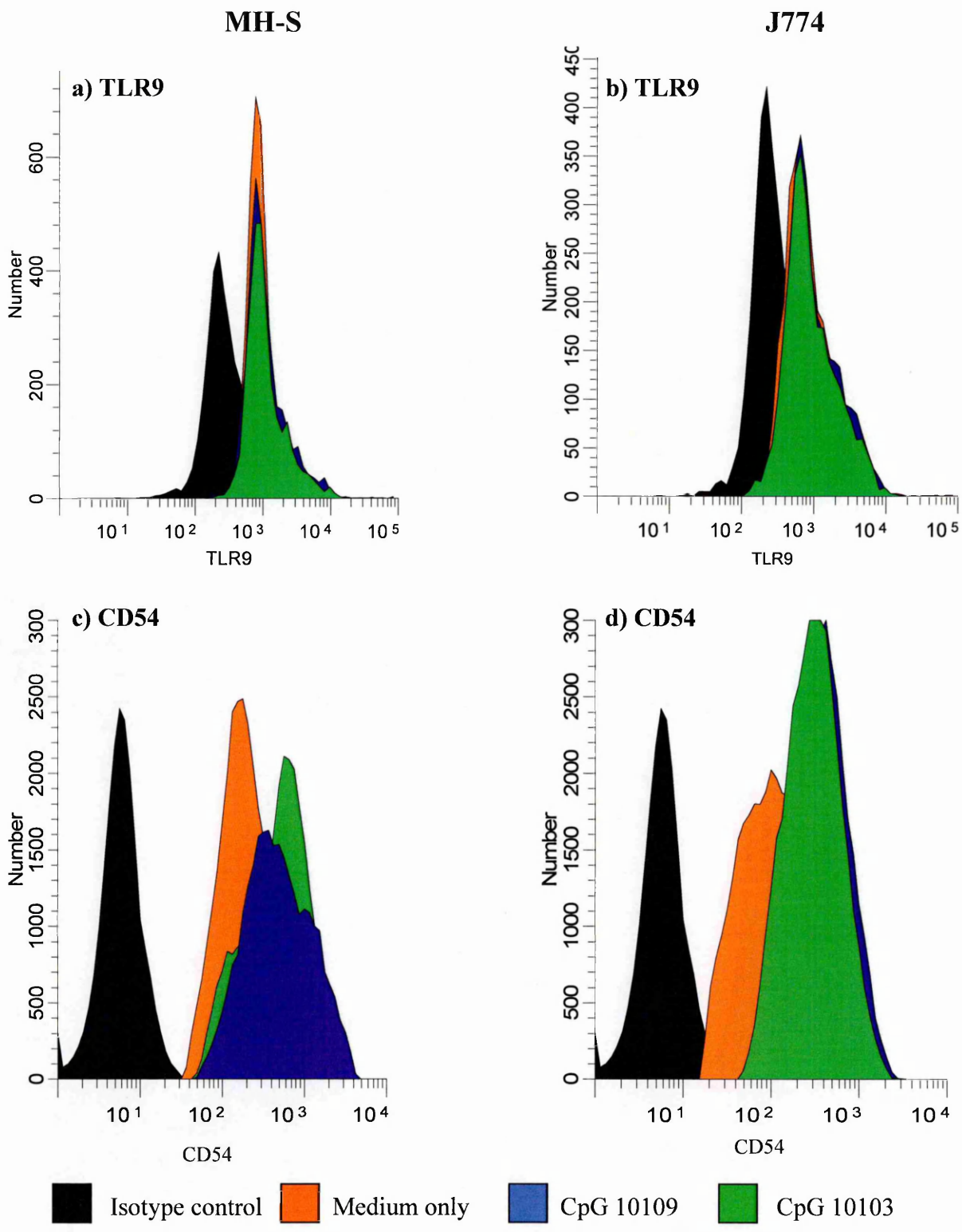

Figure 5.5. Expression of TLR9 on MH-S and J774 macrophages. Expression determined by intracellular flow cytometry at 24 hours in **(a)** MH-S macrophages **(b)** J774 macrophages. Cells stimulated with 75µg/ml CpG-B 10103, CpG-sC 10109 or replenished with fresh medium. Stimulation of cells confirmed by shift in CD54 expression on **(c)** MH-S and **(d)** J774 macrophages. Histograms are representative of three separate experiments.

Figure 5.6. Here, average values obtained from MH-S and J774 macrophages following CpG-B 10103 or CpG-B 7909 stimulation are seen to overlap almost completely indicating very close similarity between them. Similarly, Figure 5.7 illustrates the near identical effects of CpGs 7909 or 10103 on NO output from MH-S and J774 macrophages. Collectively, these results suggest that CpG 10103 is a suitable substitute for examining the stimulatory effects of CpG-B 7909 on macrophages *in vitro*.

5.3.4. Release of NO by MH-S and J774 macrophages following stimulation with CpG

The release of oxygen intermediates and nitrogen derivatives such as NO, are well characterised killing mechanisms employed by macrophages. Following activation, NO is released into the local environment and is readily detectable by quantification of nitrite levels as detailed in section 2.1.2. MH-S and J774 macrophages were seeded onto 96-well plates at a concentration of $1x10^6$/ml, incubated overnight and stimulated in triplicate with a variety of different classes of CpG at a range of concentrations (5-100 μg/ml). Measurements of NO were taken at 24, 48 and 72 hour time-points. This experiment was then repeated twice, giving a total of three separate experiments for each time-point.

5.3.4.1. A-class and semi-soft C-class CpGs stimulate greater NO responses than B-class and C-class CpGs in MH-S but not J774 macrophages

MH-S and J774 macrophages were stimulated with different CpGs and analysed for NO release 24 hours post-stimulation *via* Griess reaction (Figure 5.8). CpG-A (2336) and CpG-sC (10109) induced significantly more NO in MH-S macrophages than

a)

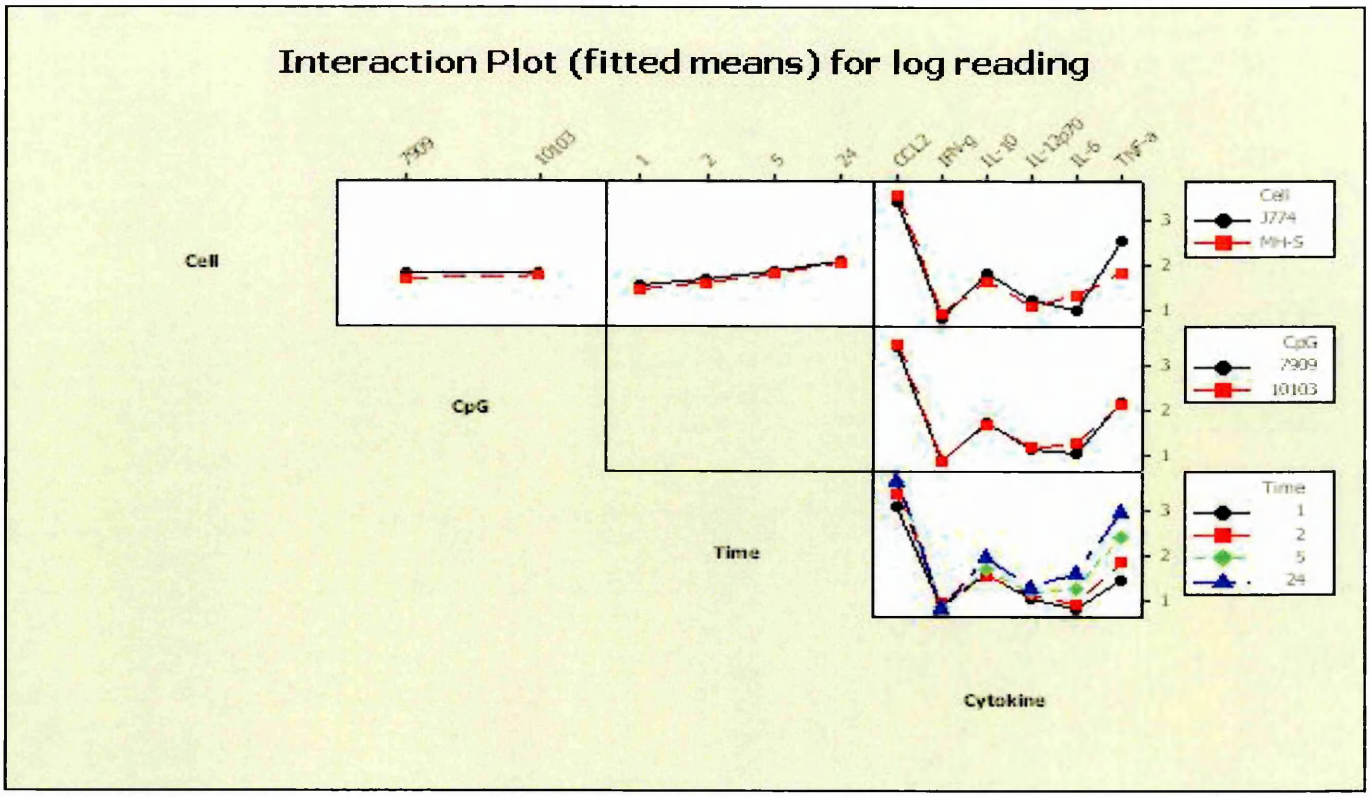

b)

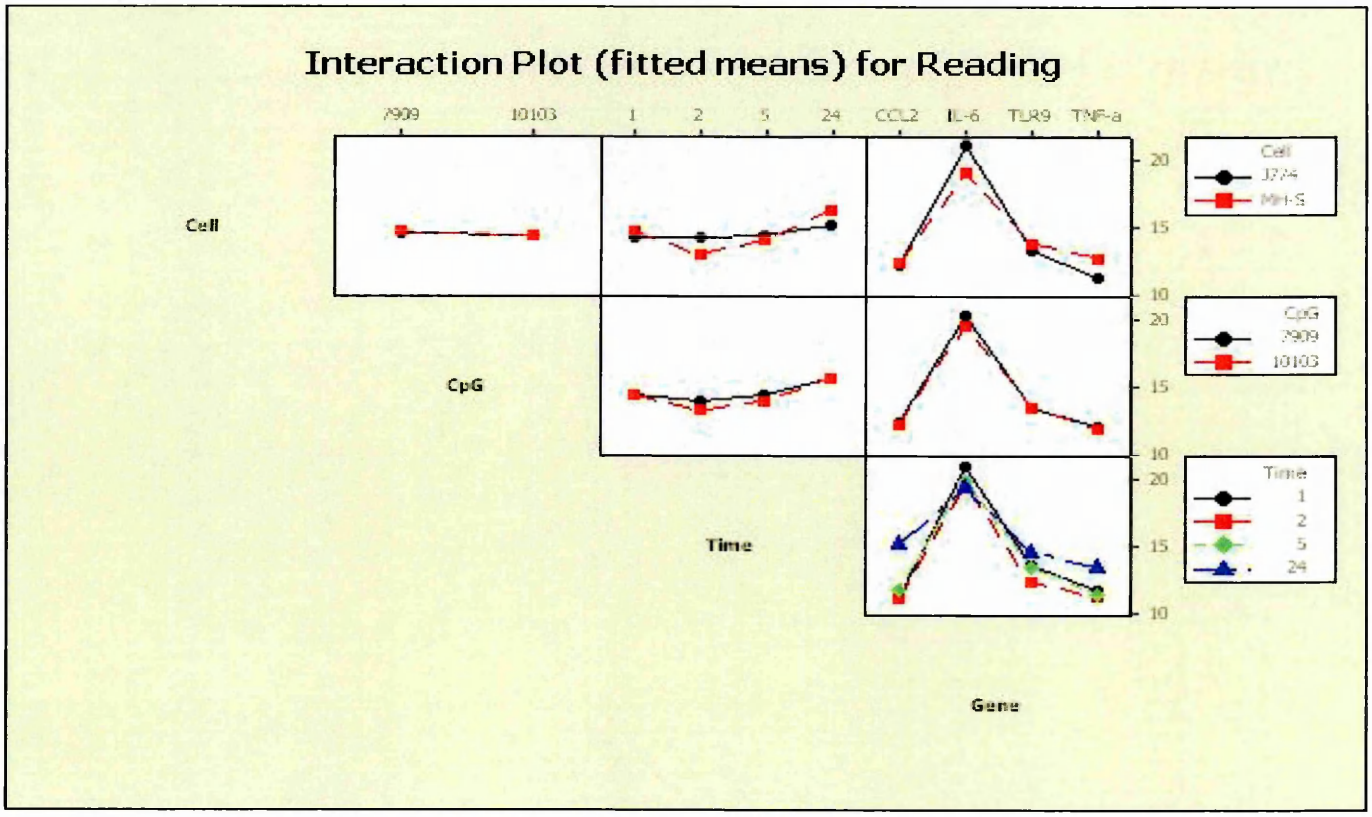

Figure 5.6. B-class CpGs 10103 and 7909 induce comparable cytokine responses in macrophages. Macrophage cell-lines MH-S and J774 were treated with either CpG 10103 or CpG-B 7909 and assessed for cytokine output via: **(a)** CBA **(b)** RT-PCR.

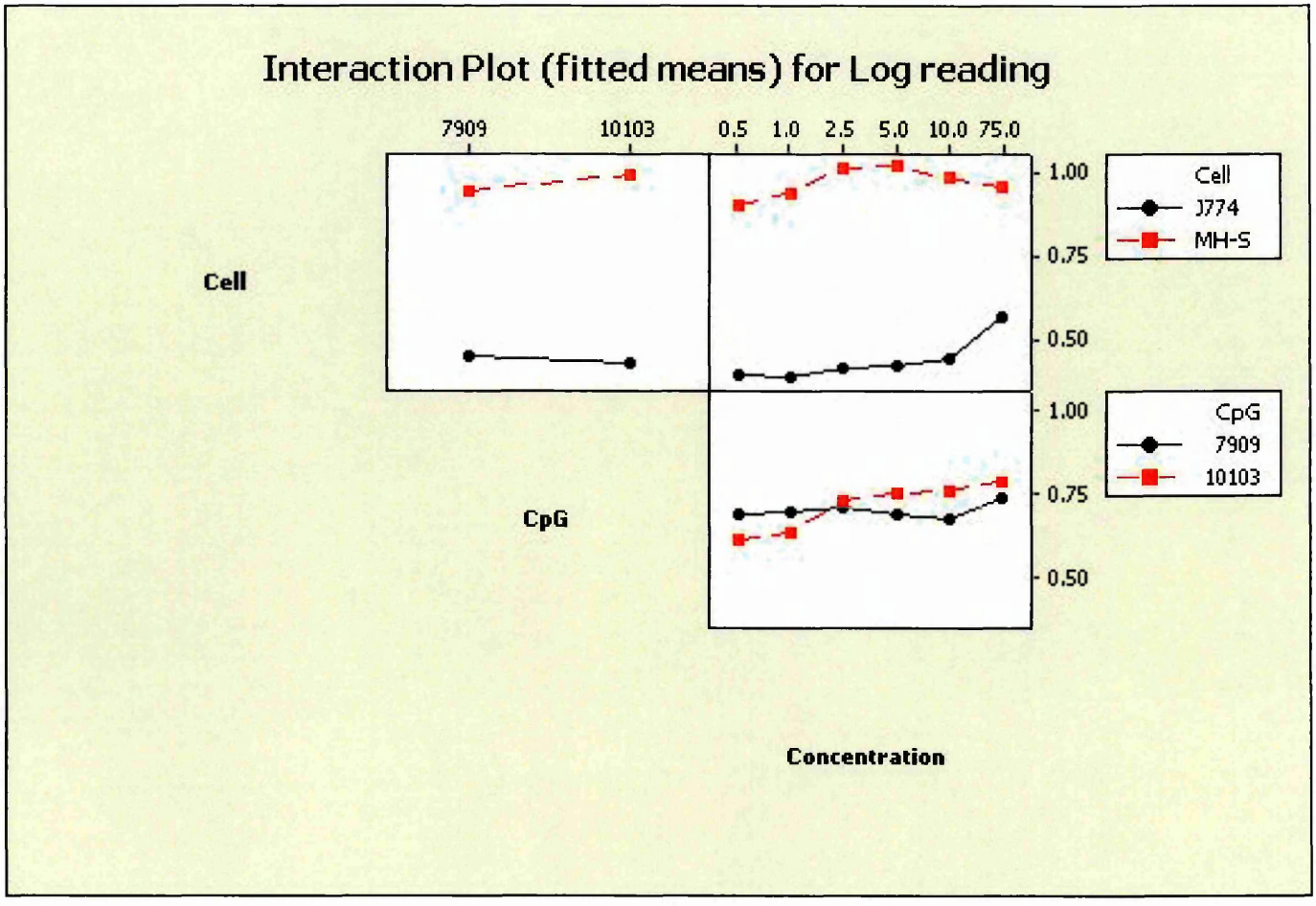

Figure 5.7. B-class CpGs 10103 and 7909 induce comparable NO responses in macrophages: Macrophage cell-lines MH-S and J774 were treated with either CpG-B 10103 or CpG-B 7909 and assessed for NO release *via* Griess reaction.

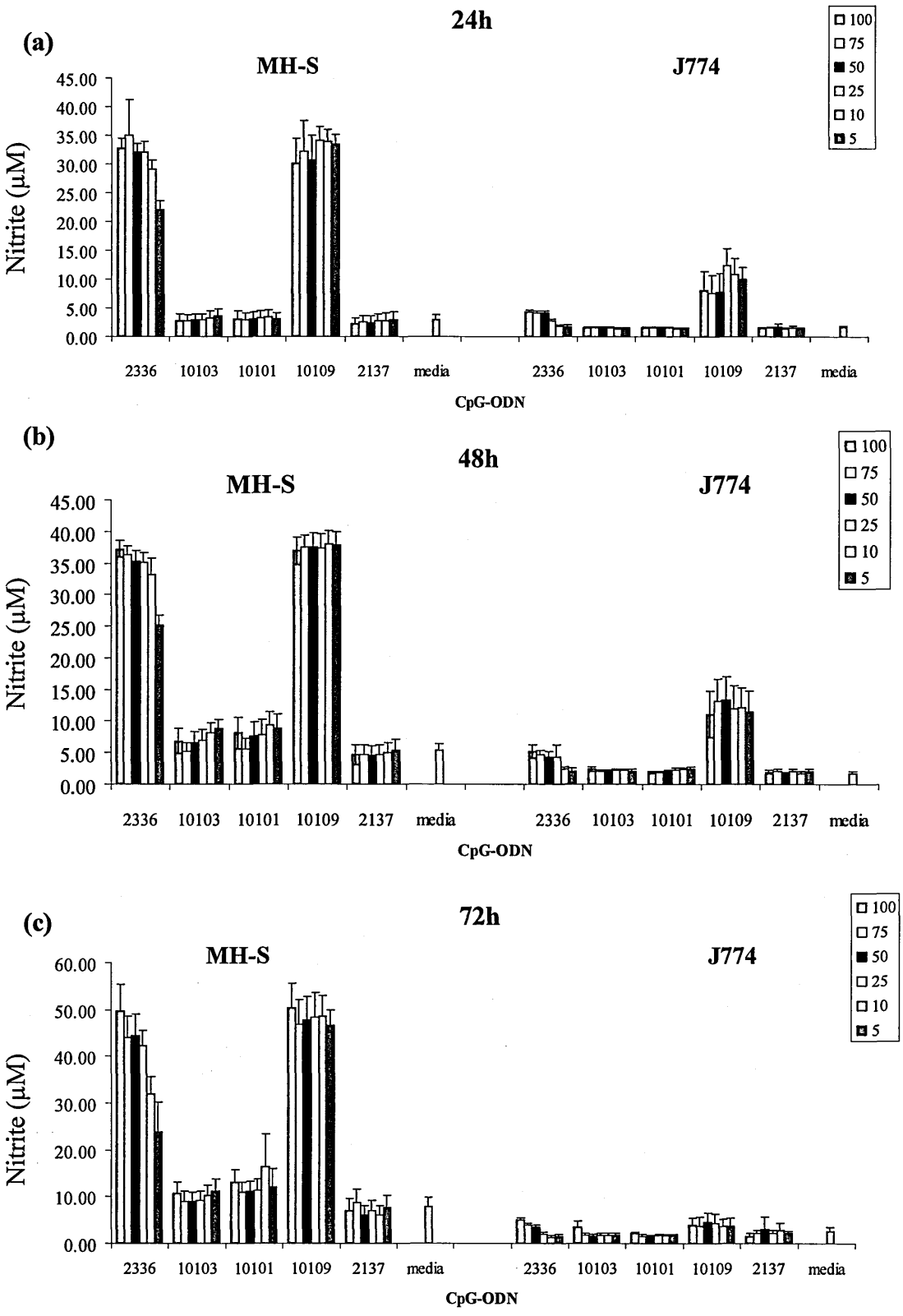

Figure 5.8. Release of NO as determined by nitrite measurement using the Griess reaction. Graph shows release of NO by MH-S and J774 macrophage cell lines **(a)** 24 hours **(b)** 48 hours **(c)** 72 hours after stimulation with 100-5 µg/ml CpG-A 2336, CpG-B 10103, CpG-C 10101, CpG-sC 10109, control non-CpG 2137 and non-stimulated medium control wells. Error bars ± 95% CI.

CpG-C (10101) and CpG-B (10103) and non-CpG control 2137 ($p<0.001$) (Figure 5.8a). Levels of NO induced by ODNs CpG-B, CpG-C and non-CpG 2137 were comparable with un-stimulated medium control wells. Maximum release of NO in these experiments was achieved irrespective of CpG concentration for all CpGs with the exception of CpG-A 2336 which induced maximum NO at higher concentrations. J774 macrophages did not share the same profile of NO production following CpG stimulation as that seen in MH-S macrophages. A-class CpG 2336 failed to induce significantly more nitric oxide than 10101, 10103 or 2137. However, 10109 was still able to induce modest levels of NO production, albeit significantly less than that produced by MH-S macrophages ($p<0.001$). This pattern was identical in experiments left to run for 48 hours (Figure 5.8b) and 72 hours (Figure 5.8c).

5.3.4.2. Lower concentrations of CpG do not induce higher concentrations of NO

Some classes of CpG have been reported to stimulate cells in a concentration dependent manner resulting in a bell-shaped response curve (Jurk *et al.*, 2004). Therefore, lower concentrations (75 μg/ml-0.625 μg/ml) of CpG were investigated using NO as a measurement of macrophage stimulation. Lower concentrations of CpG did not result in any enhanced NO production (Figure 5.9). These findings also confirmed results seen in earlier experiments that saw greater responses induced by CpG-A 2336 and CpG-sC 10109 in MH-S macrophages. The prominent release of NO induced by CpG-A and CpG-sC in earlier experiments prompted the inclusion of an additional control non-CpG 2243 which unlike control-ODN 2137, contains a mixed phosphorothioate-phosphodiester backbone. Previous studies have observed a non-specific stimulatory effect of oligonucleotide backbone chemistry on the activation of macrophages (Roberts *et al.*, 2005). No NO response was induced by

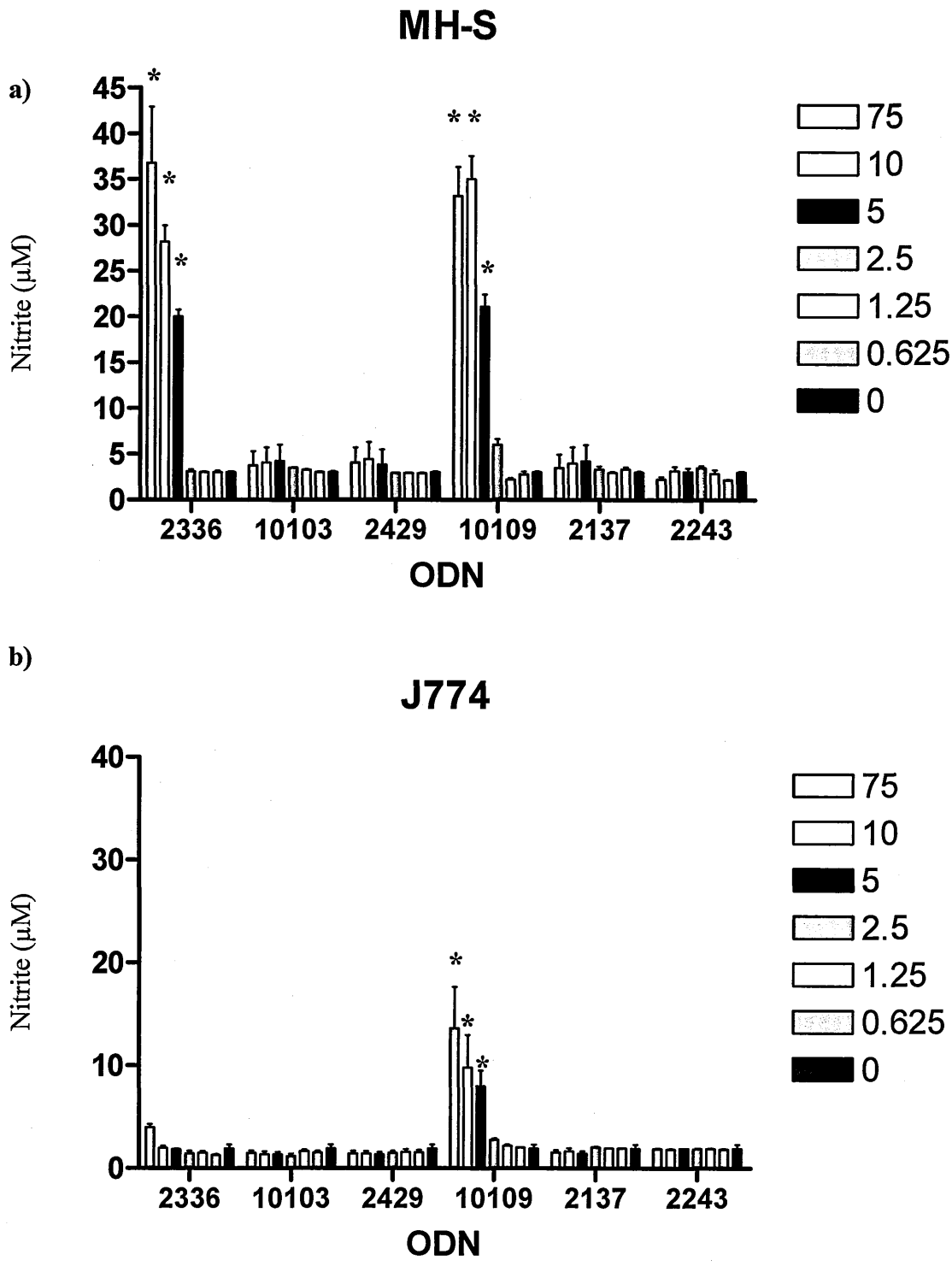

Figure 5.9. Release of NO by MH-S and J774 macrophages following stimulation with low concentrations of CpG. Macrophage cell lines **(a)** MH-S and **(b)** J774 were stimulated *in vitro* with varying concentrations (75-0.625 μg/ml) of different classes of CpG-ODNs. Fresh medium was used as a negative control. Non-CpG control ODNs 2137 and 2243 were assessed against CpGs to determine the non-specific effect of ODN backbone chemistry. Assays performed in triplicate and graphs represent an average of at least 2 experiments. Error bars ± 95% CI. *Significance ($p<0.001$) between CpG-ODNs and control non-CpG 2243.

control non-CpG 2243 in either MH-S or J774 cells suggesting the responses initiated by CpG-A 2336 and CpG-sC 10109 were not due to the chemical composition of the oligonucleotide backbone.

5.3.5. Chemokine and cytokine production by MH-S and J774 macrophage cell-lines after stimulation with different classes of CpGs

The activation of macrophages can be characterised by the secretion of pro-inflammatory cytokines and chemokines (Sibille & Reynolds, 1990). This experiment studied the mRNA synthesis and secretion of the chemokine CCL2, as well as the pro-inflammatory cytokines TNF-α and IL-6 *in vitro* in MH-S and J774 macrophage cell-lines following stimulation with CpG. Cells were grown to a concentration of $1x10^6$ cells/ml, incubated overnight and stimulated in triplicate with different classes of CpG at a concentration of 75 μg/μl. At times 1, 2, 5 and 24 hours, supernatants for each time-point were merged and frozen for analysis of protein by CBA. Total RNA was extracted immediately from cells as detailed in Section 2.3.1 for analyses by RT-PCR. This experiment was then repeated twice, giving a total of three separate experiments.

5.3.5.1. CCL2

Expression of CCL2 mRNA in MH-S cells and J774 cells after CpG stimulation is represented in Figure 5.10. Here, CCL2 mRNA was found to be significantly upregulated over time relative to un-stimulated control wells in both MH-S and J774 cells ($p<0.001$). Stimulation with CpG-A 2336 or CpG-sC 10109 resulted in the most prominent induction of CCL2 expression ($p<0.001$), inducing a rapid up-regulation of CCL2 as seen at the 2 hour and 5 hour time-points (Figure 5.10b and 5.10c). No

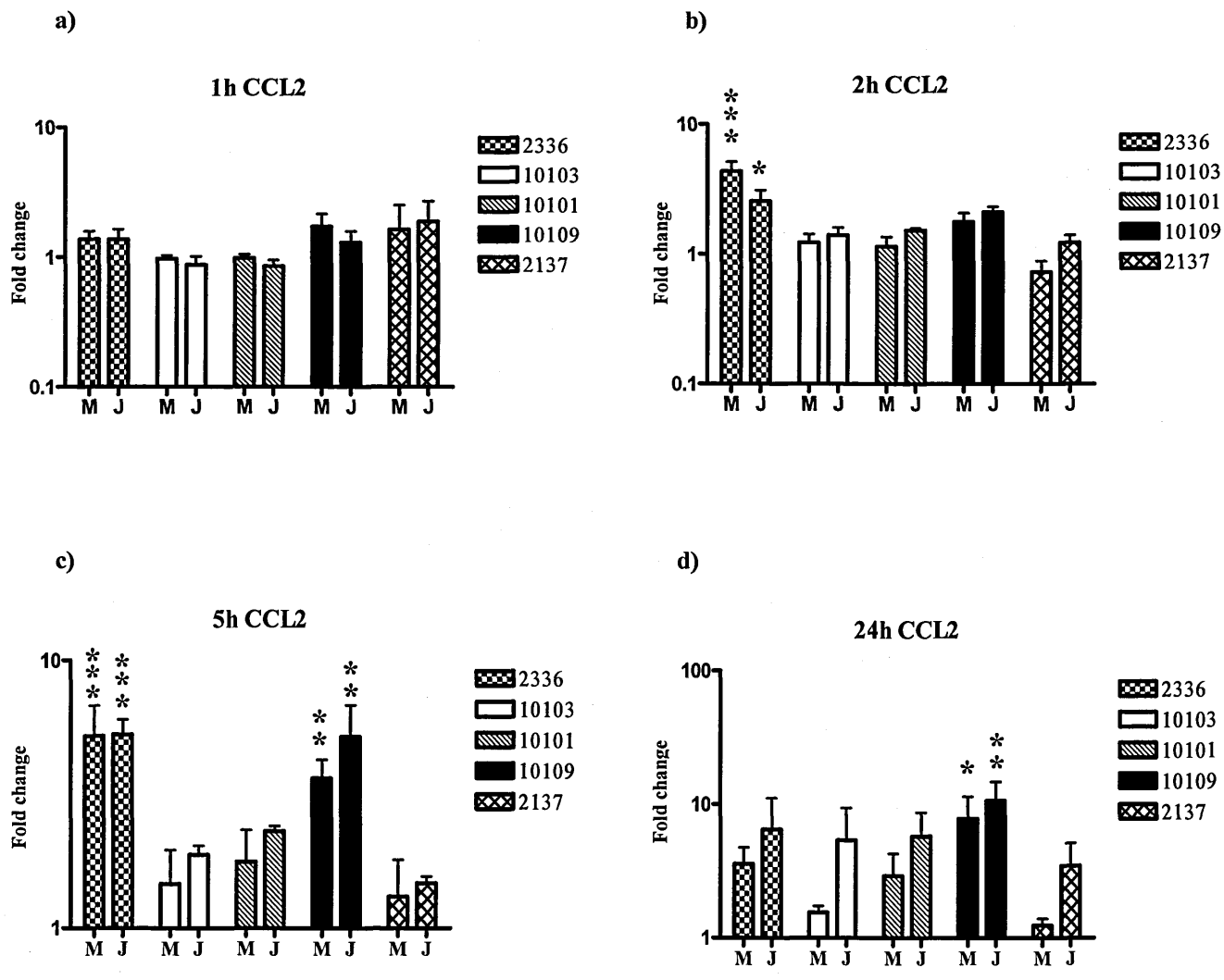

Figure 5.10. Changes in chemokine CCL2 mRNA expression. MH-S (M) and J774 (J) macrophages were stimulated with 75μg/ml CpG and analysed *via* RT-PCR. Graphs show changes in gene expression relative to unstimulated medium control wells after **(a)** 1 hour **(b)** 2 hours **(c)** 5 hours and **(d)** 24 hours CpG stimulation. Experiments performed in triplicate, values represent geometric mean of three separate experiments. Error bars ± SEM.

Significant differences between CpGs and cell-line specific non-CpG 2137 determined by three-way ANOVA with Bonferroni's post-tests and represented as:

** $p<0.05$, ** $p<0.01$, *** $p<0.001$.*

significant difference in the synthesis of CCL2 was found between the two cell-lines in response to CpG stimulation ($p>0.05$).

Figure 5.11 illustrates the levels of CCL2 protein in the supernatants from CpG stimulated MH-S macrophages and J774 macrophages as determined by CBA analysis. Both cell-lines secreted very high levels of CCL2 and no significant difference between the amounts of CCL2 produced was determined statistically ($p=0.487$). Macrophages stimulated with CpGs 2336 or 10109 did not secrete more CCL2 than any other CpG as was seen at the level of mRNA transcription. Unstimulated medium control released equivalent amounts of CCL2 as CpG stimulated macrophages. This suggests macrophages do not require stimulation with CpG to secrete CCL2 *in vitro*.

5.3.5.2. TNF-α

Changes in the expression of TNF-α mRNA in MH-S cells and J774 cells following stimulation with CpG can be seen in Figure 5.12. Expression of TNF-α altered significantly over time ($p=0.017$) with CpGs 2336 or 10109 increasing the expression of TNF-α mRNA most significantly throughout the first 5 hours of stimulation (Figure 5.12 a-c). The effects of CpG stimulation on TNF-α expression were comparable between MH-S cells and J774 cell-lines ($p=0.627$).

Figure 5.13 illustrates the detection of TNF-α protein levels in MH-S and J774 macrophages. These results show clear differences between MH-S and J774 secretion of TNF-α with J774 cells secreting significantly more TNF-α over time ($p<0.001$).

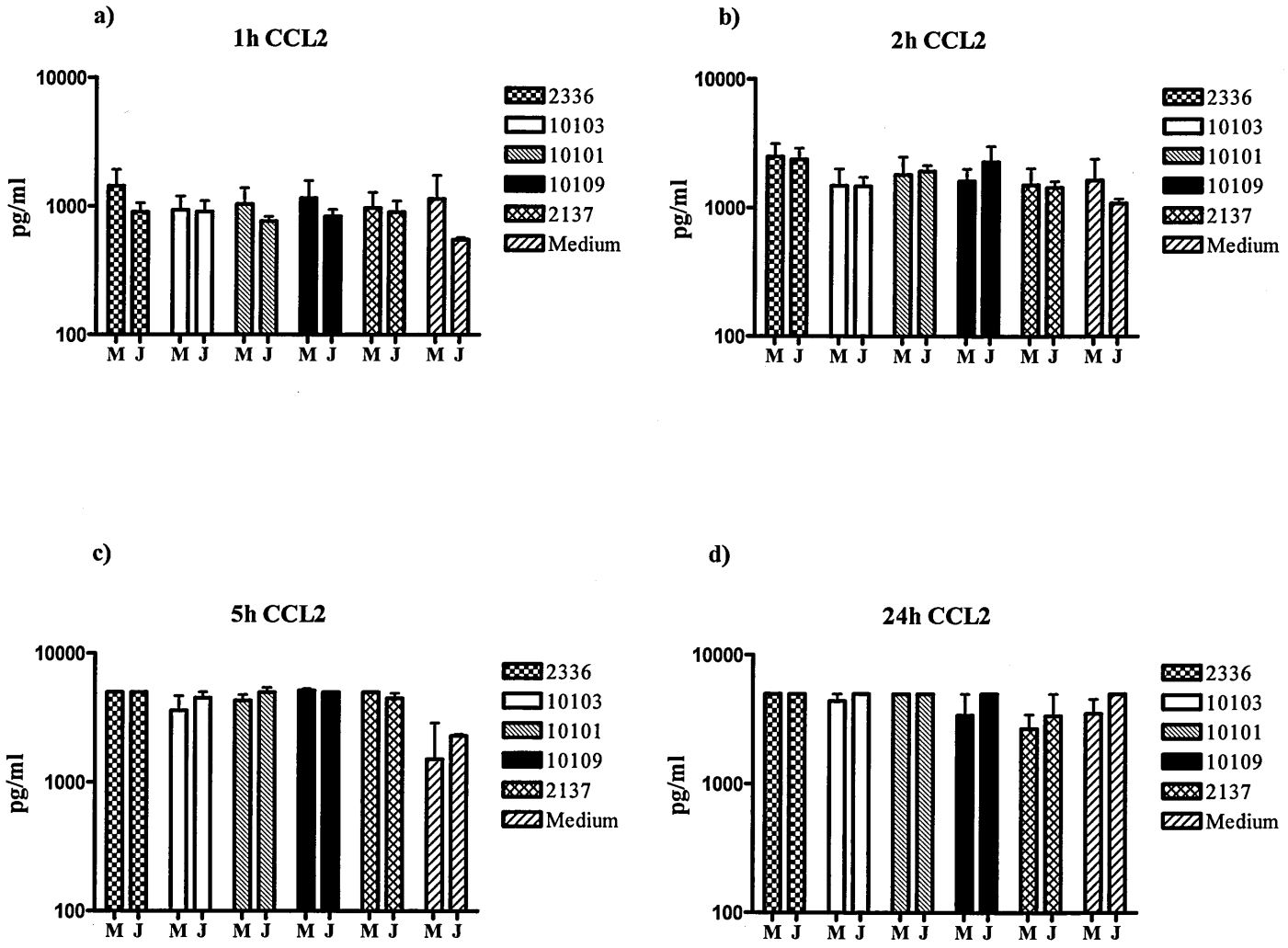

Figure 5.11. Changes in chemokine CCL2 protein release. MH-S (M) and J774 (J) macrophages were stimulated with 75μg/ml CpG and analysed *via* CBA. Graphs show levels of CCL2 (pg/ml) in supernatants of macrophage wells stimulated with CpGs 2336, 10103, 10101, 10109 and 2137 alongside unstimulated medium control wells after **(a)** 1 hour **(b)** 2 hours **(c)** 5 hours **(d)** 24 hours stimulation. Experiments performed in triplicate, values represent geometric mean of three separate experiments. Error bars ± SEM.

No significant differences between CpGs and cell-line specific non-CpG 2137 determined by three-way ANOVA with Bonferron'si post-tests.

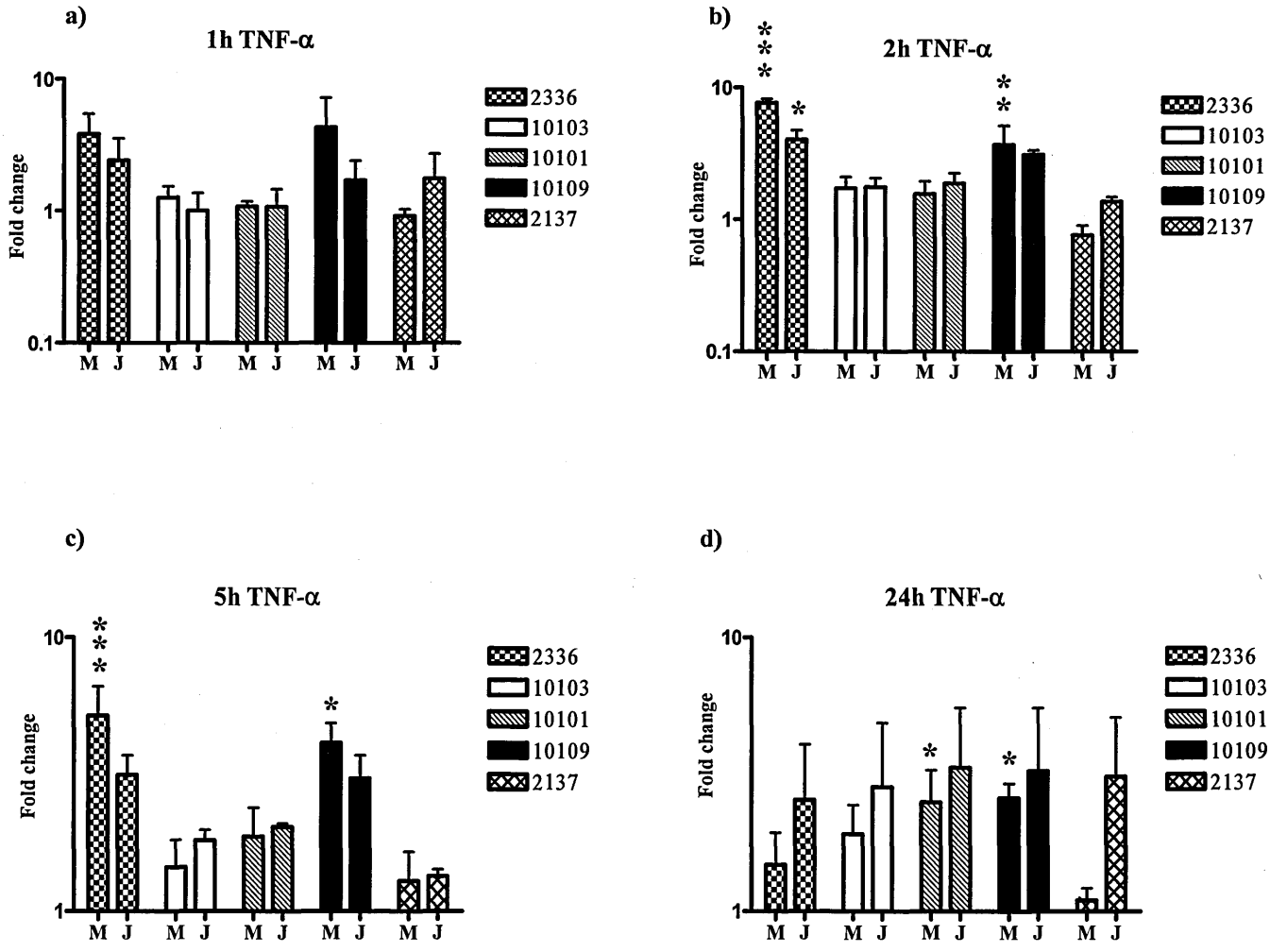

Figure 5.12. Changes in pro-inflammatory TNF-α cytokine mRNA expression. MH-S (M) and J774 (J) macrophages were stimulated with 75μg/ml CpG and analysed *via* RT-PCR. Graphs show changes in gene expression relative to unstimulated medium control wells after **(a)** 1 hour **(b)** 2 hours **(c)** 5 hours and **(d)** 24 hours CpG stimulation. Experiments performed in triplicate, values represent geometric mean of three separate experiments. Error bars ± SEM.

Significant differences between CpGs and cell-line specific non-CpG 2137 determined by three-way ANOVA with Bonferroni's post-tests and represented as:

** $p<0.05$, ** $p<0.01$, *** $p<0.001$.*

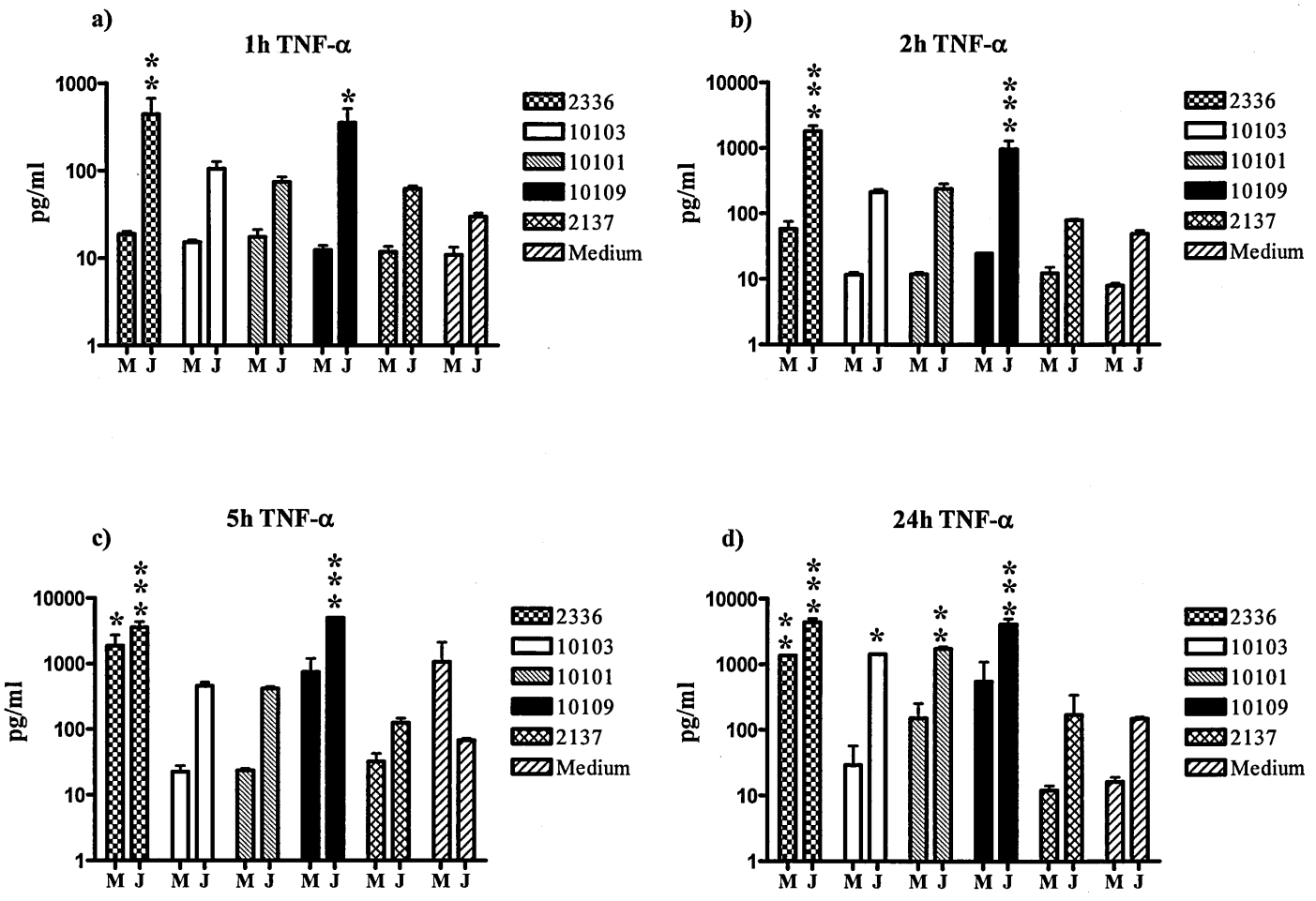

Figure 5.13. Changes in pro-inflammatory TNF-α protein release. MH-S (M) and J774 (J) macrophages were stimulated with 75μg/ml CpG and analysed *via* CBA. Graphs show levels of TNF-α (pg/ml) in supernatants of macrophage wells stimulated with CpGs 2336, 10103, 10101, 10109 and 2137 alongside unstimulated medium control wells after **(a)** 1 hour **(b)** 2 hours **(c)** 5 hours **(d)** 24 hours stimulation. Experiments performed in triplicate, values represent geometric mean of three separate experiments. Error bars ± SEM.

Significant differences between CpGs and cell-line specific non-CpG 2137 determined by three-way ANOVA with Bonferroni's post-tests and represented as:

** $p<0.05$, ** $p<0.01$, *** $p<0.001$;*

CpGs 2336 or 10109 stimulation resulted in significantly more TNF-α release than other CpGs ($p<0.001$) and this was true for both cell types.

5.3.5.3. IL-6

IL-6 mRNA expression in MH-S and J774 macrophages differed significantly following CpG-stimulation. Stimulation of J774 macrophages with CpG resulted in the up-regulation of significantly more IL-6 than that induced in MH-S macrophages ($p<0.001$) (Figure 5.14). Over the course of the experiment, the up-regulation of IL-6 was most significantly induced by CpG-A 2336 or CpG-sC 10109 ($p<0.001$) and peaked after 5 hours stimulation.

Protein levels of IL-6 are represented in Figure 5.15. Very little IL-6 was detectable within the first 2 hours of CpG stimulation (Figure 5.15 a-b). By 5 hours, release of IL-6 was most significant ($p<0.001$) in macrophages stimulated with CpG-A 2336 or CpG-sC 10109 (Figure 5.15c) and this was observed after 24 hours (Figure 5.15d). Analysis of IL-6 protein levels revealed that J774 cells secreted significantly more IL-6 than MH-S cells ($p<0.05$).

5.3.6. Replication of VACV in unstimulated MH-S and J774 macrophages

Previous experiments have shown that MH-S and J774 macrophages responded differently to CpG stimulation as measured by cytokine and NO production. To determine how CpG-treated macrophages responded to infection with VACV, it was first necessary to establish whether MH-S or J774 macrophages possessed an intrinsic ability to restrict VACV replication. An initial experiment was performed to assess the replication of VACV in unstimulated macrophages. Macrophages were incubated

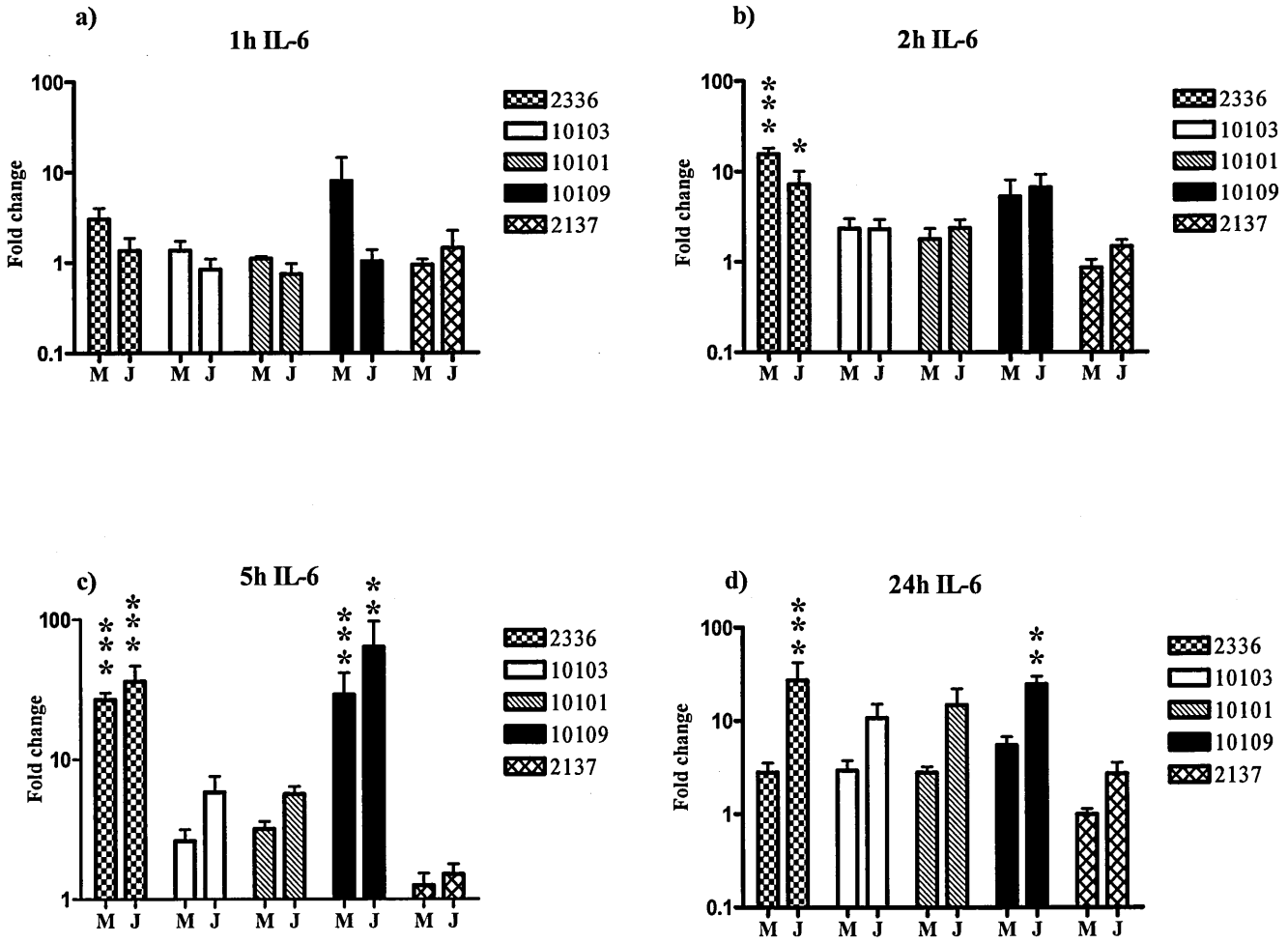

Figure 5.14. Changes in pro-inflammatory cytokine IL-6 mRNA expression. MH-S (M) and J774 (J) macrophages were stimulated with 75μg/ml CpG and analysed *via* RT-PCR. Graphs show changes in gene expression relative to unstimulated medium control wells after **(a)** 1 hour **(b)** 2 hours **(c)** 5 hours and **(d)** 24 hours CpG stimulation. Experiments performed in triplicate, values represent geometric mean of three separate experiments. Error bars ± SEM.

Significant differences between CpGs and cell-line specific non-CpG 2137 determined by two-way ANOVA with Bonferroni post-tests and represented as:

** $p<0.05$, ** $p<0.01$, *** $p<0.001$;*

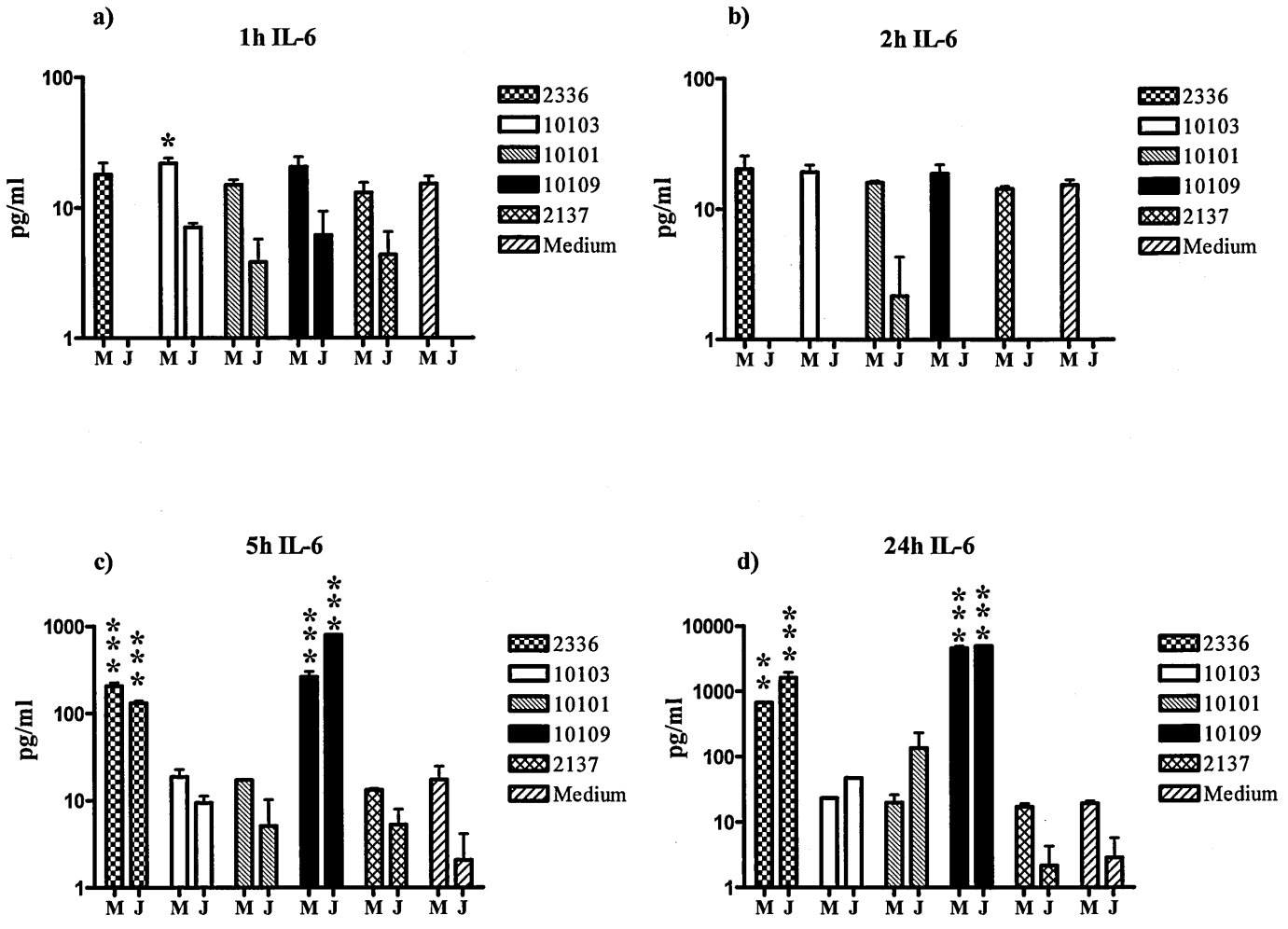

Figure 5.15. Changes in pro-inflammatory IL-6 protein release. MH-S (M) and J774 (J) macrophages were stimulated with 75μg/ml CpG and analysed *via* CBA. Graphs show levels of IL-6 (pg/ml) in supernatants of macrophage wells stimulated with CpGs 2336, 10103, 10101, 10109 and 2137 alongside unstimulated medium control wells after **(a)** 1 hour **(b)** 2 hours **(c)** 5 hours **(d)** 24 hours stimulation. Experiments performed in triplicate, values represent geometric mean of three separate experiments. Error bars ± SEM.

Significant differences between CpGs and cell-line specific non-CpG 2137 determined by two-way ANOVA with Bonferroni post-tests and represented as:

** $p<0.05$, ** $p<0.01$, *** $p<0.001$;*

overnight in 24-well plates at a concentration of 1 x 10^6 cells/ml and infected the following morning with 5 x 10^6 pfu VACV. Virus titres were then determined at time 1, 2, 5, 8, 12, 15, 18, 24 and 36 hours post infection as detailed in Section 2.2. VACV growth curves in each cell-line are represented in Figure 5.16 with each time-point representing the mean of three independent experiments. These studies found no significant difference in the ability of VACV to replicate in either macrophage cell-line over a 36 hour period (p=0.84) (Figure 5.16).

5.3.7. Replication of VACV in pre-stimulated MH-S and J774 macrophages

Replication of VACV in both MH-S and J774 macrophages was assessed following pre-stimulation of cells with a down-selected group of CpGs. As the most immunostimulatory CpG in our initial studies, CpG-sC 10109 was compared against CpG-B 10103, a similar CpG to CpG-B 7909 which conferred protection in the pre-exposure work *in vivo* (detailed in Chapter 3). Briefly, both MH-S and J774 macrophages were seeded at a concentration of 1x10^6 cells/ml onto 24-well plates and left to adhere overnight. The following morning, cells were stimulated in triplicate with 75 μg/ml of either CpG-sC 10109 or CpG-B 10103 for 24 hours prior to infection the following day with 5x10^6 pfu VACV. Viral titres were then calculated at 6, 12 and 24 hours and three independent experiments performed. Stimulation of cell-lines 24 hours prior to viral infection significantly effected the growth of VACV (Table 5.1). The extent of VACV inhibition was found to vary dramatically between cell-types and the class of CpG used to stimulate macrophages. Stimulation of MH-S macrophages with CpG-B 10103, and particularly CpG-sC 10109, resulted in significantly lower titres of VACV at both 12 and 24 hour time-points compared to unstimulated control samples (Figure 5.17a.). Here, stimulation with CpG-sC was

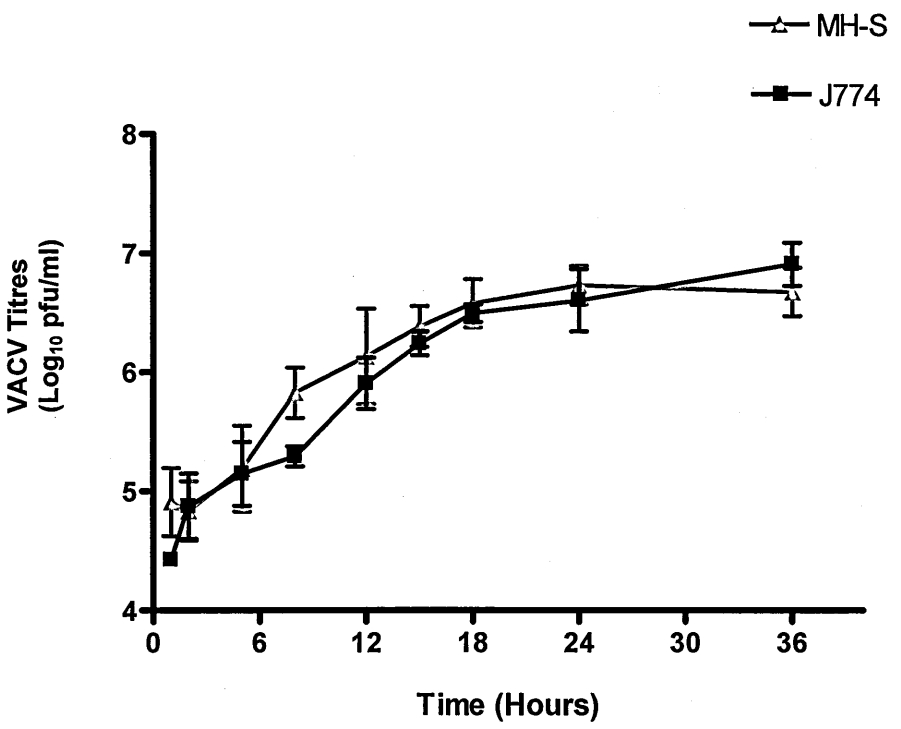

Figure 5.16. Growth of VACV in MH-S and J774 macrophage cell lines. Growth of VACV was determined at times 1, 2, 5, 8, 12, 15, 18, 24 and 36 hours. Data shown represents the geometric mean titre of three separate experiments. Error bars indicate ± SEM. No significant difference determined between cell-lines as determined by Two-way Anova with Bonferroni's post-tests.

Cell	Comparison	Time			
		1	6	12	24
MH-S	Medium:10103	-	-	*	***
MH-S	Medium:10109	-	-	***	***
MH-S	10103:10109	-	-	-	**
J774	Medium:10103	-	-	-	*
J774	Medium:10109	-	-	-	***
J774	10103:10109	-	-	-	-
MH-S and J774	Medium:Medium	-	-	-	-

Table 5.1. Both CpG-B 10103 and CpG-sC 10109 significantly restrict the growth of VACV in MH-S and J774 macrophages. Table indicates level of significance as determined by pair-matched two-way ANOVA of titres calculated from three separate experiments. Level of significance indicated by (-) n/s, (*) $p<0.05$, (**) $p<0.01$, (***) $p<0.001$.

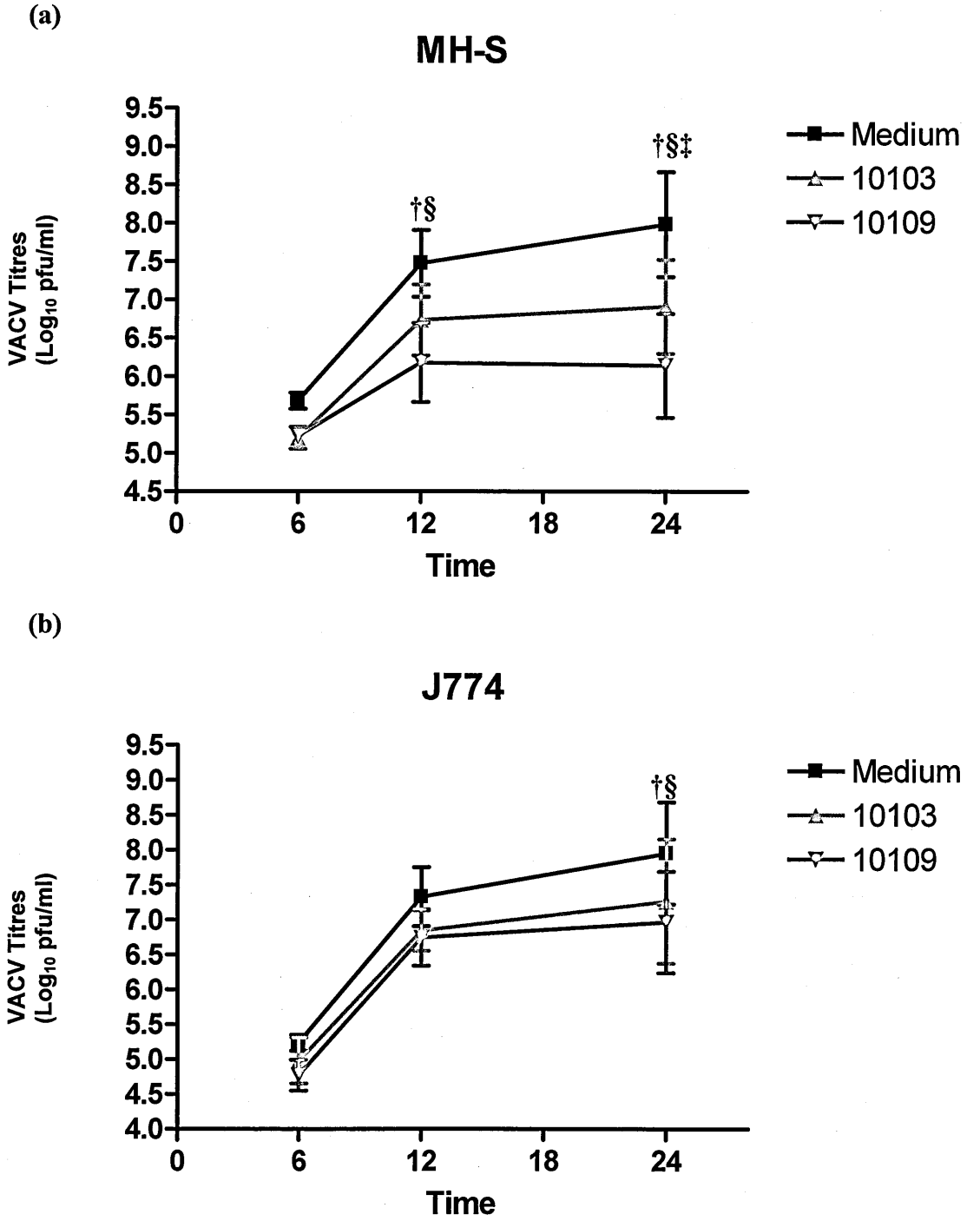

Figure 5.17. Growth of VACV in MH-S and J774 macrophage cell lines pre-stimulated with CpG. Growth of VACV was determined at time 6, 12 and 24 hours after pre-stimulation with 75μg/ml CpG-B 10103 and CpG-sC 10109 in **(a)** MH-S and **(b)** J774 macrophages. Data shown represents geometric mean of three separate experiments. Error bars indicate ± SEM. Significance determined by pair-matched two-way ANOVA of titres calculated from three separate experiments.

† 10103:Medium $p<0.05$; § 10109:Medium $p<0.05$; ‡ 10103:10109 $p<0.05$.

found to be significantly more effective at limiting the growth of VACV than CpG-B 10103 ($p<0.01$). Both CpG-B 10103 and CpG-sC 10109 were also able to reduce VACV viral titres significantly in J774 cells compared to medium controls although more modestly than in MH-S cells (and only at the 24 hour time-point) (Figure 5.17b). Interestingly, no significant differences were found between CpGs 10103 and 10109 in their ability to restrict the replication of VACV in J774 cells. Overall, these results indicated that at 24 hours post VACV-infection, viral titres were most significantly restricted in MH-S macrophages when stimulated with CpG-sC 10109. No significant differences were observed in VACV titres between stimulated and un-stimulated MH-S or J774 macrophages during the first six hours of infection (Table 5.1). This suggests the reduction in viral titres at 12 and 24 hours was unlikely to be a result of VACV failing to infect cells that had been pre-stimulated with CpG and was instead a result of CpG stimulation.

5.3.8. The effect of NO inhibition on VACV replication in MH-S and J774 macrophages

The initial investigation into differences between MH-S and J774 macrophages indicated the release of NO, following stimulation with CpG-sC 10109, was perhaps the most striking difference between the two cell-lines (Figure 5.8). As MH-S macrophages pre-stimulated with 10109 released significantly more NO than J774s, and 10109 pre-stimulated MH-S cells could restrict the growth of VACV, the effect of nitric oxide on VACV was investigated.

5.3.8.1. The inhibition of NO from MH-S macrophages

To assess whether the release of NO was responsible for limiting the growth of VACV in MH-S cells, it was first necessary to optimise the inhibition of NO synthesis in MH-S cells using the global nitric oxide synthetase inhibitor L-NMMA. Therefore, initial experiments were performed to determine the optimum time at which to introduce the inhibitor to MH-S cells, and the most effective dose to use. Figure 5.18 illustrates the inhibition of NO release from MH-S macrophages as determined by Griess reaction at 24 hours post-stimulation with CpG-sC 10109. Results show that the introduction of L-NMMA at the same time as CpG stimulation was most effective at inhibiting the synthesis of NO (Figure 5.18a). The optimum dose of L-NMMA was determined from three separate experiments introducing L-NMMA at the same time as CpG-sC 10109, and again measuring NO release at 24 hours (Figure 5.18b). From these experiments, an optimum concentration of 4000 μMol was determined.

5.3.8.2. Inhibition of NO does not alter the growth of VACV in CpG stimulated macrophages

The effect of NO inhibition prior to macrophage infection with VACV was investigated in MH-S cells. Macrophages were seeded onto 24-well plates at a concentration of $1x10^6$ cells/ml and left to adhere overnight. Cells were then stimulated in triplicate with 75 μg/ml CpG-sC 10109, or co-incubated with 75 μg/ml CpG-sC 10109 and 4000 μMol NMMA for 24 hours. These wells were run alongside macrophages that were incubated alone with 4000 μMol L-NMMA, or replenished with fresh medium. After 24 hours, an aliquot of medium was removed from each well for analysis of NO levels to confirm NO inhibition. All wells were then infected with $5x10^6$ pfu VACV and titres calculated at 1, 12 and 24 hours post-infection.

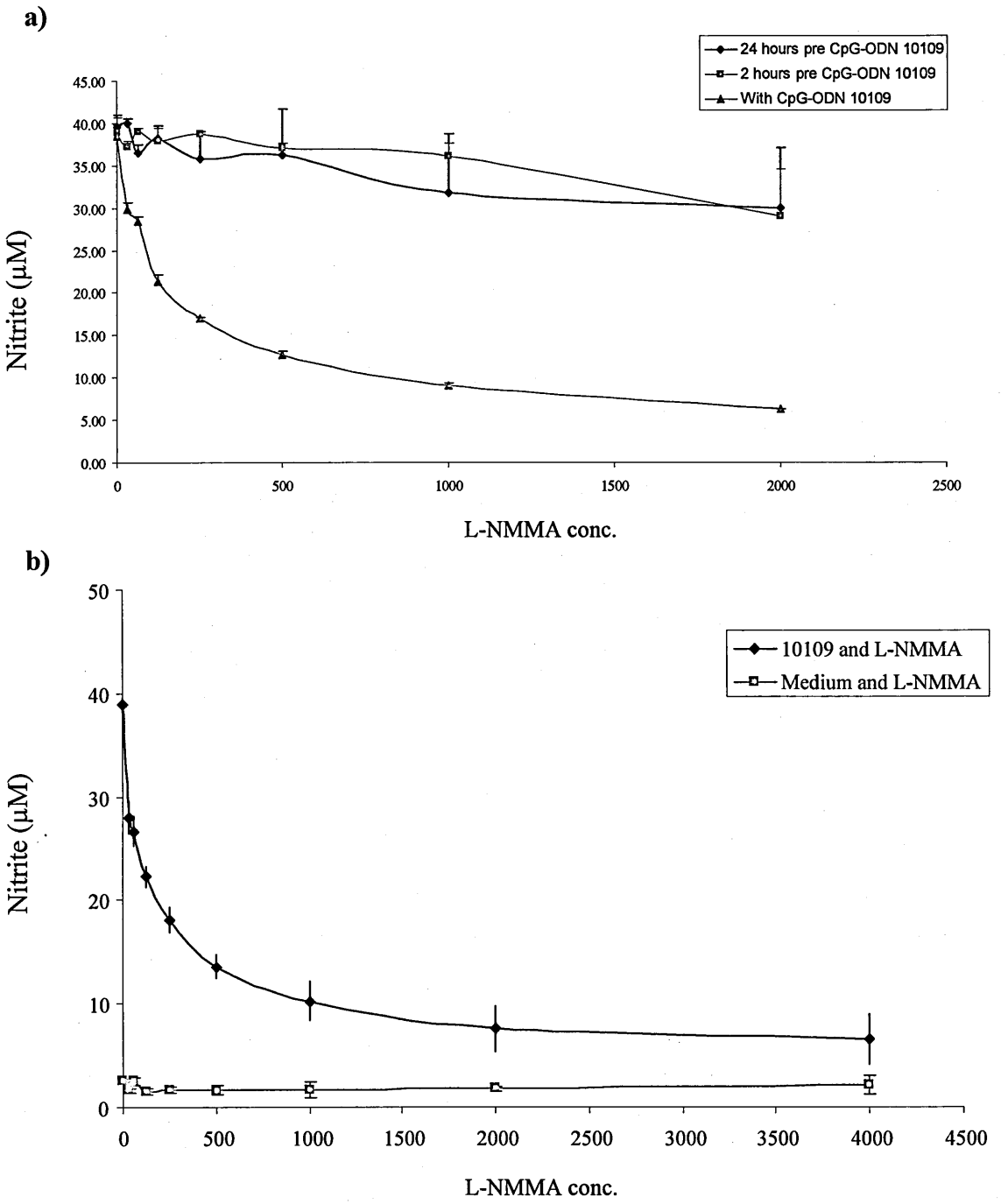

Figure 5.18. Effect of NO inhibitor L-NMMA on release of nitric oxide in MH-S macrophages following 24 hour stimulation with CpG-sC 10109. **(a)** 0-2000 µMol L-NMMA was added to wells in triplicate either 24 hours prior, 2 hours prior or concomitant to 75µg/ml CpG-sC 10109 stimulation. **(b)** Complete dose range of L-NMMA 0-4000 µMol. Cells were replenished with fresh medium or were stimulated with 75µg/ml CpG-sC 10109 for 24 hours. Graph representative of three independent experiments. Error bars represent ± 95% confidence limits.

VACV titres in macrophages supplemented with L-NMMA and CpG-sC 10109 did not differ significantly from macrophages given CpG alone ($p>0.05$) (Figure 5.19). Addition of CpG in both of these groups significantly reduced VACV titres compared to unstimulated control wells ($p<0.001$) suggesting that the restriction of VACV titres in CpG stimulated MH-S macrophages is not a result of NO production.

5.3.9. CpGs prevent apoptosis in both MH-S and J774 macrophage cells lines

NO has previously been shown to induce apoptosis in macrophages that have been stimulated with IFN-γ and LPS (Sarih *et al.*, 1993). Given the strength of the NO response generated in MH-S macrophages by CpG-sC 10109, an experiment was planned to investigate whether the reduction in VACV titres seen in MH-S macrophages was a result of CpG-induced apoptosis prior to viral infection due to a high concentration of CpG. Therefore, both MH-S and J774 macrophages were stimulated with either CpG-B 10103 or CpG-sC 10109 for 24 hours and analysed using Annexin-V as a marker of apoptosis *via* flow cytometry. Stimulation of both macrophage cell-lines with CpG significantly reduced the percentage of cells that were either in the end stages of apoptosis, undergoing necrosis or already dead, relative to unstimulated samples ($p<0.001$) (Figure 5.20). No significant difference between class of CpG or cell-line was found in the percentages of apoptotic macrophages after 24 hours of stimulation ($p>0.05$).

5.3.10. CpG-sC 10109 is protective against VACV

The identification of CpG-sC 10109 as a potent stimulator of macrophages led to the examination of its ability to protect in the pre-exposure model of VACV infection. Groups of mice ($n=6$) were pre-treated with 75 μg CpG-sC 10109 on day -7, -3, or -1

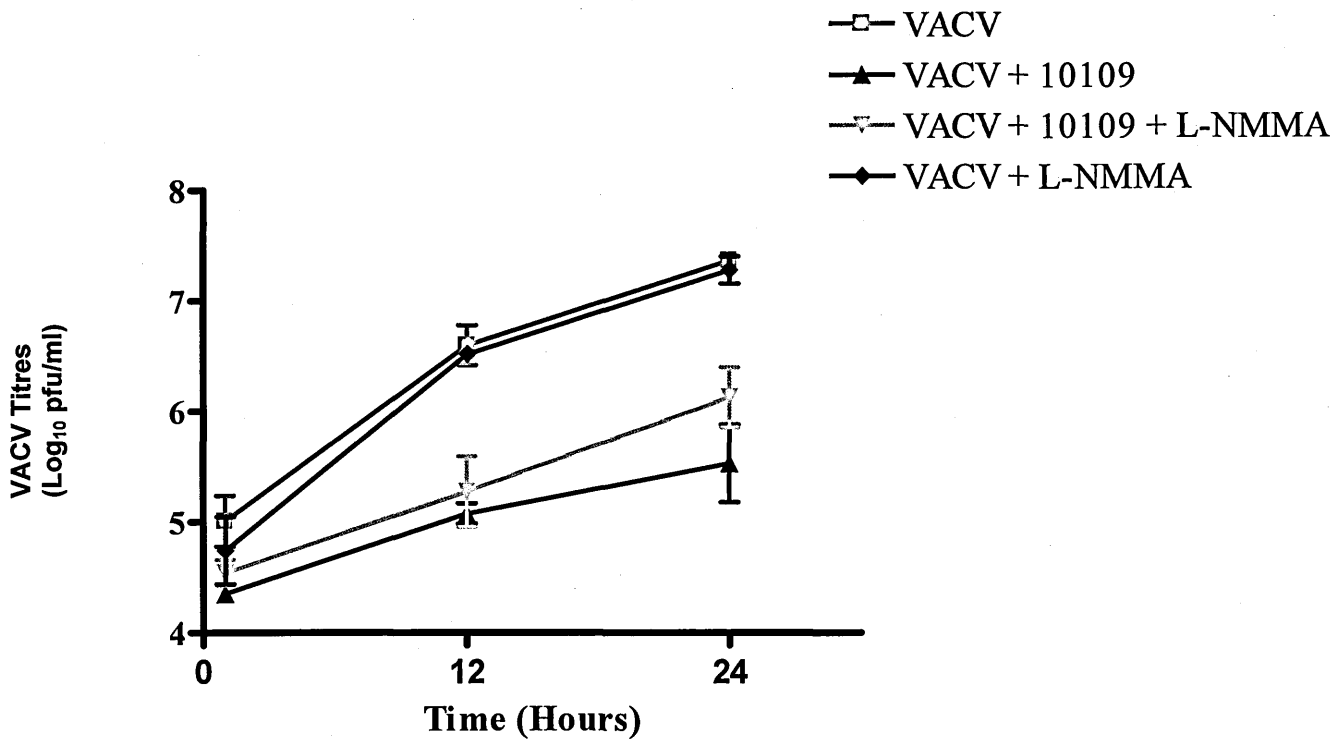

Figure 5.19. Effect of L-NMMA NO inhibition on growth of VACV in MH-S cells. Prior to infection with VACV, macrophages were incubated for 24 hours with RPMI medium (VACV), CpG-sC 10109 (VACV + 10109), CpG-sC 10109 and L-NMMA (VACV + 10109 + L-NMMA) or L-NMMA alone (VACV + L-NMMA). Growth of VACV was determined at time 1, 12 and 24 hours post-infection. Data shown represents geometric mean of three separate experiments. Error bars indicate ± SEM. Significance determined by pair-matched two-way ANOVA of titres calculated from three separate experiments.

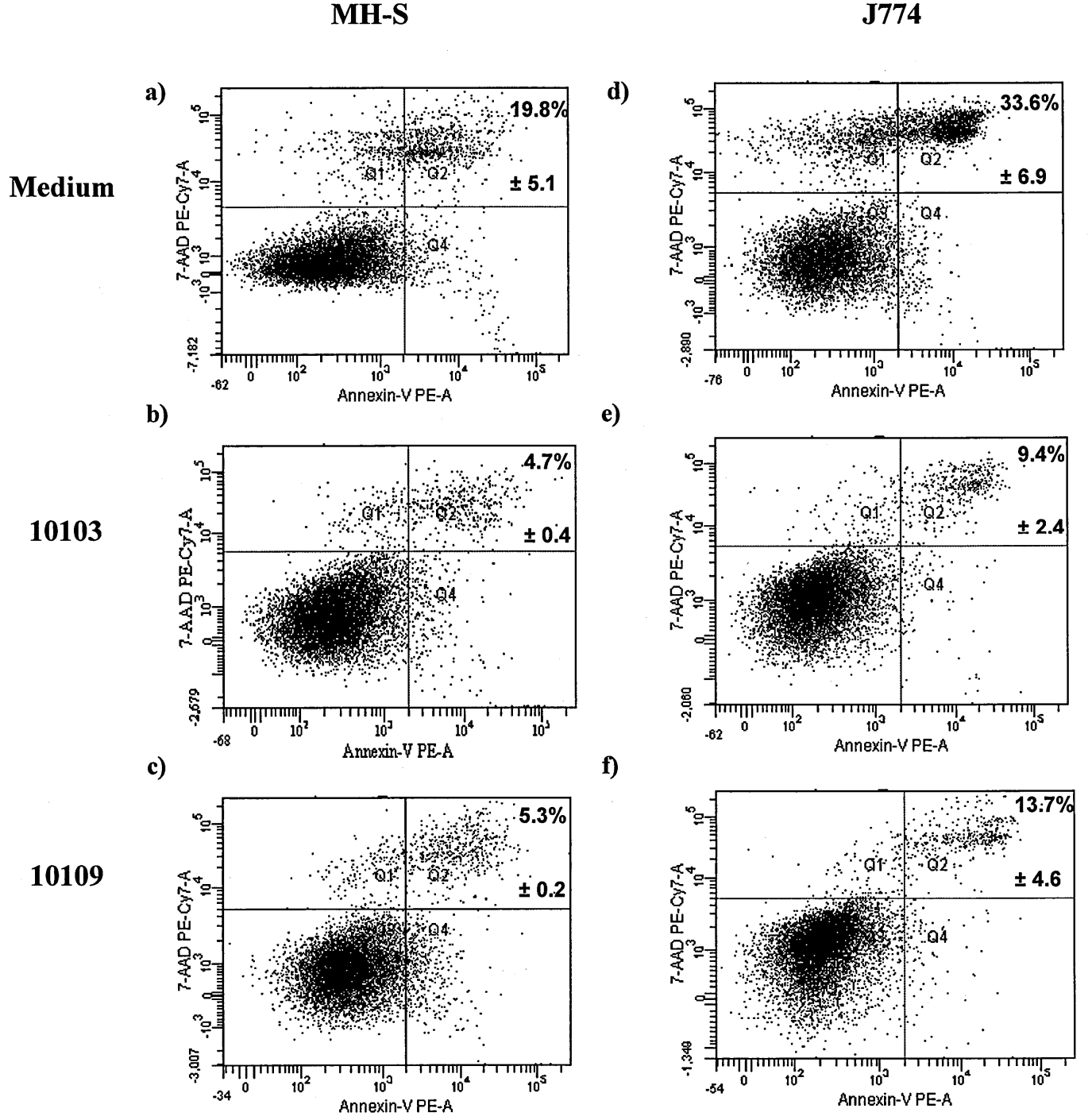

Figure 5.20. CpGs prevent apoptosis in both MH-S and J774 macrophages. Staining of Annexin-V, a Ca^{2+}-dependent phospholipid-binding protein, allows for identification of cells within a population that are actively undergoing apoptosis. MH-S macrophages were stained for Annexin-V and 7-AAD 24 hours after **(a)** fresh medium replacement **(b)** 75μg/ml CpG-B 10103 stimulation **(c)** 75μg/ml CpG-sC 10109 stimulation. Apoptosis in J774 macrophages was also examined 24 hours after **(d)** fresh medium replenishment **(e)** 75μg/ml CpG-B 10103 stimulation **(f)** 75μg/ml CpG-sC 10109 stimulation. Values in quadrants represent % of cells gated ± SEM. Figures representative of three separate experiments.

relative to intranasal infection with 10 MLD VACV. A separate group of mice were treated with CpG-sC 10109 and challenged with VACV concomitantly on day 0. Control groups included mice treated with CpG-B 7909 on day -3 and a group given PBS. Results represented in Figure 5.21 show that pre-treatment with CpG-sC 10109 provided complete protection when given 7 days prior to challenge and 80% protection when given on days -3 or -1. Treatment given on the day of challenge failed to confer any protection against virus infection. Mice given CpG-B 7909 on day -3 of infection as a positive control were fully protected.

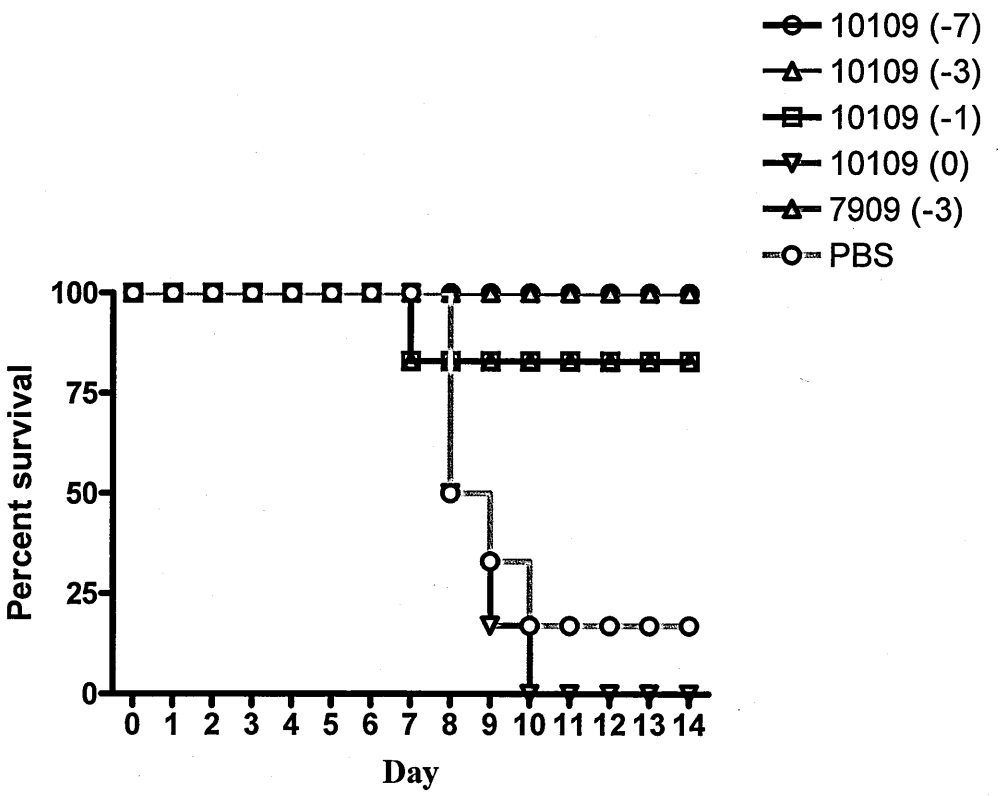

Figure 5.21. CpG-sC 10109 confers protection against VACV. Graph shows survival data of mice (n=6) treated intranasally with 75μg doses of CpG or PBS, prior to challenge on day 0 with 10 MLD VACV infection.

5.4. Discussion

A number of studies have suggested that the response of macrophages during infection depends significantly on the type of macrophage encountered by the invading organism (Gordon & Taylor, 2005; Laskin *et al.*, 2001; Dorger *et al.*, 2001). This makes the comparison of different macrophage responses important in understanding their likely contribution to the immune response. The development of *in vitro* macrophage cell-lines has enabled researchers to model the role of primary macrophages without the need for extensive animal use. Hence, the use of the MH-S macrophage cell-line has become a well-established tool for studying the alveolar macrophage (Mbawuike & Herscowitz, 1989; Sankaran & Herscowitz, 1995). Using this cell-line as a model for primary alveolar macrophages, the studies presented herein have highlighted a number of differences between MH-S macrophages and the non-alveolar macrophage cell-line J774 following stimulation with different classes of CpG. In addition, the investigation of CpGs that combine the characteristic features of individual classes has identified the newly designed semi-soft CpG 10109 as a potent stimulator of macrophages with antiviral properties.

Macrophages actively participate in the inflammatory response by releasing cytokines, chemokines and a range of other inflammatory mediators such as reactive oxygen and nitrogen species. Studies using alveolar macrophages (AMs) have shown them to be quiescent cells that are functionally regulated by alveolar epithelial cells through the expression of the TGF-β, activating integrin αvβ6 and the constitutive release of anti-inflammatory cytokines such as IL-10 (Fernandez *et al.*, 2004; Takabayshi *et al.*, 2006). Once activated, AMs play a fundamental role in regulating lung inflammation by being able to act as both initiator and suppressor of

inflammatory responses (Holt, 1986; Oshikawa & Sugiyama, 2003; Ogle *et al.*, 1994; Holt *et al.*, 1993; Strickland *et al.*, 1993). Whilst, many macrophage sub-types recognise and respond directly to CpG stimulation (Stacey *et al.*, 1996), the ability of alveolar macrophages to respond to CpGs has been a subject of some controversy. Several groups have documented the successful activation of primary alveolar macrophages using CpG alone or in combination with IFN-γ or LPS (Huang *et al.*, 2005; Fernandez *et al.*, 2004), whilst others have suggested TLR9 expression on alveolar macrophages may be impaired and incapable of responding fully to binding of CpG (Suzuki *et al.*, 2005).

The results within this chapter have shown that primary AMs from Balb/C mice express TLR9 and suggest that they can be induced to up-regulate synthesis of TNF-α following stimulation with CpGs. In addition, both alveolar and non-alveolar macrophage cell-lines were found to express TLR9 and could be induced to secrete NO and up-regulate expression of pro-inflammatory cytokines following CpG stimulation. The release of NO by macrophages is a key effector mechanism for the killing of pathogens. NO also serves a dual role in the regulation of macrophage apoptosis and cell death (Bosca *et al.*, 2005). Here, results suggest a marked difference in the ability of different classes of CpG to induce NO release from macrophage cell-lines. CpG-A 2336 and CpG-sC 10109 were found to induce potent NO responses from the MH-S macrophage cell-line compared to all other classes of CpG investigated. These two CpGs induced comparable amounts of NO over the three time-points investigated although the earlier kinetics of NO production was not investigated. Previously, Sester and colleagues found that phosphorothioate (PS) CpGs were more potent than their phosphodiester (PO) counterparts in the induction

of pro-inflammatory cytokines such as IL-12 from murine Raw 264.7 macrophages and IFN-primed bone marrow derived macrophages (Sester *et al.*, 2000). In these studies, ODNs with a pure PS-backbone (CpG-B, CpG-C), were less capable of activating macrophages than those with a mixed PS-PO backbone. The presence of a complete PS-backbone within a CpG increases nuclease resistance and enhances cellular binding and uptake (Zhao *et al.*, 1993; Stein *et al.*, 1988). Of the CpGs investigated here, it is worth noting that CpG-A 2336 and CpG-sC 10109 did not have a complete PS backbone, and yet treatment with these CpGs resulted in enhanced stimulation.

The frequency and spacing of CpG motifs within a CpG, as well as the regions peripheral to the CpG motifs, are factors that contribute to the stimulatory effects of individual ODNs. Mixed ODN backbones are predominantly built with a PO backbone and modified 5' and 3' PS ends which are typically palindromic or complemented with poly-G motifs (Krieg, 2002). The inclusion of these regions peripheral to the central CpG motif has been shown to facilitate interactions between homologous regions on adjacent ODNs, promoting duplex formation that contributes to IFN-α induction (Kerkmann *et al.*, 2005; Vollmer *et al.*, 2004). Collectively, these properties have also been shown to improve cellular uptake and may help explain the ability of CpGs 2236 and 10109 to activate macrophages so effectively. This finding is not unique to macrophages, as ODNs with a mixed PS-PO backbone have also been reported to be more stimulatory for NK cells than pure PS or PO-backbones (Boggs *et al.*, 1997). Previous studies have observed a non-specific stimulatory effect of oligonucleotide backbone chemistry on the activation of macrophages (Roberts *et al.*, 2005). The inclusion of a control non-CpG with a mixed PS-PO background in these

assays failed to induce NO from cells suggesting that enhanced NO production was unlikely to be a non-specific effect of a mixed PS-PO oligonucleotide backbone.

Interestingly, the extent of NO release was found to differ significantly between MH-S and J774 macrophages. Here, only CpG-sC 10109 was able to induce a mild NO response from the J774 macrophage cell-line. The reason for this difference in NO production between the two cell-lines is currently unclear. The release of NO from AMs has been well documented and has been shown to facilitate the down-regulation of immune responses *via* suppression of T-cell proliferation and pulmonary dendritic cell functions (Strickland *et al.*, 1993; Holt *et al.*, 1993). Furthermore, it has been shown to exert a very strong influence on its own and other cells' apoptotic pathways (Bingisser & Holt, 2001). The induction of apoptosis *via* NO is thought to involve the release of cytochrome *c* from the mitochondria and targeting of members of the BCL-2 family (Bosca *et al.*, 2005). However, studies have suggested that macrophages are more resistant to the anti-apoptotic effects of NO than other cell-types which may prolong their ability to phagocytose invading organisms or prolong their influence on the outcome of infection. As such, stronger NO responses by alveolar macrophages *in vivo* and MH-S cells *in vitro*, may be a strategy to preserve macrophage numbers and cellular integrity. Previous studies have also indicated that AM preservation may act to control inflammation by phagocytic clearance of other local apoptotic or necrotic cells such as neutrophils (Haslett, 1999; Knapp *et al.*, 2003). Here, stimulation of MH-S and J774 cells with CpG-sC 10109 and CpG-B 10103 prevented onset of apoptosis equally following 24 hours incubation despite differences in NO release. In contrast to previous studies, it was not possible to induce NO production from J774 cells using B or C-class CpGs (Ghosh *et al.*, 2001). This may be a result of the CpG

motifs in our study being optimally designed to stimulate human cells (GTCGTT), rather than those motifs used in other studies that are characteristically more stimulatory for mouse cells (GACGTT) (Hartmann & Krieg, 2000).

No CpG class investigated throughout these studies was capable of altering the expression of TLR9 more than 2-fold on macrophage cell-lines over a 24 hour period. This suggests the immunostimulatory properties of CpG-A 2336 and CpG-sC 10109 were not a result of TLR9 up-regulation or its cellular re-distribution. However, a limited examination of CpG-stimulated primary AMs suggested that CpG-sC 10109 could induce a 2-fold increase in expression. This finding was the result of a single experiment using a pool of four BAL samples and would be strengthened by obtaining similar results in repeat experiments.

CpGs 2336 and 10109 were also found to promote more vigorous IL-6 responses than other CpGs in macrophage cell-lines. Statistical analysis revealed MH-S macrophages were induced to express significantly lower amounts of IL-6 than that from J774 macrophages at both the level of mRNA transcript and quantity of translated protein. IL-6 is a potent inflammatory cytokine that has been suggested to regulate the transition from neutrophil to monocyte recruitment during the early stages of inflammation (Kaplanski *et al.,* 2003). Given the proposed anti-inflammatory nature of alveolar macrophages, the weaker induction of IL-6 in MH-S cells, an alveolar macrophage cell line, may be a result of these cells limiting the degree of inflammation they evoke. As such, the release of IL-6 from non-alveolar macrophages (modelled here by J774 cells) in response to CpG stimulation may model monocyte recruitment to the site of infection *in vivo* or promote a more potent pro-inflammatory

response. The MH-S cell-line secreted significantly less TNF-α protein than the J774 macrophage cell-line, despite having synthesised comparable levels of TNF-α mRNA. TNF-α is a pleiotropic pro-inflammatory cytokine with a variety of diverse immunological functions which can promote cellular proliferation and activation or contribute to the onset of septic shock if over-expressed (Rahman & McFadden, 2006). If also true in an *in vivo* setting, the muted release of TNF-α from alveolar macrophages could help prevent an undesirable or excessive inflammatory response in the lung.

Phagocytic cells of the immune system such as macrophages play a central role in the control of virus infection and the replication of VACV in a number of these cell-types has been investigated (Humlova *et al.*, 2002; Rivera *et al.*, 2007). Replication of VACV in both MH-S and J774 macrophages was comparable over the duration of repeated time-course experiments which indicated that these cells were equally permissive of VACV. Stimulation of both cell-lines with CpG was found to restrict viral titres over a 24 hour period, although this effect was far more pronounced in MH-S macrophages when stimulated with CpG-sC 10109. As both CpG-B 10103 and CpG-sC 10109 restricted apoptosis equally in both cell-lines, it is unlikely that the reduction of VACV titres in CpG-sC 10109 primed MH-S macrophages was due to enhanced macrophage apoptosis prior to VACV infection. As CpG-sC 10109 induced greater quantities of NO in MH-S and J774 cells, a role for NO in the inhibition of VACV replication was investigated using a global NO synthase inhibitor. Inclusion of the NO inhibitor failed to restore growth of VACV despite almost complete prevention of NO release. This suggested that CpG induced suppression of VACV replication was unrelated to NO production. Previous studies investigating the growth

of VACV in macrophages have shown that IFN-γ induced NO release from RAW 264.7 macrophages can limit VACV replication and that its inhibition can restore VACV growth (Harris *et al.*, 1995; Karupiah & Harris, 1995; Karupiah *et al.*, 1993). The difference in these findings may be a consequence of CpGs and IFN-γ activating different signaling pathways upon receptor binding or alternatively a difference in the ability of RAW 264.7 and MH-S macrophages to control VACV infection following stimulation. In these models, this is perhaps unlikely to involve enhanced phagocytosis of virus particles as no differences in VACV titres were found between cell-types in the early stages of infection. It is possible that the restriction of VACV replication following CpG stimulation could be a result of IFN-α production. IFN-α is a potent antiviral cytokine and its induction has been shown previously to restrict VACV replication in macrophage cell lines (Liu *et al.*, 2004). CpG-C ODNs are hybrids of CpG-A and CpG-B ODNs and are known to induce more potent IFN-α responses from pDCs than CpG-B (Jurk *et al.*, 2004). A similar ability to induce IFN-α from macrophages may explain the enhanced ability of CpG-sC 10109 to restrict VACV replication over CpG-B 10103. Recently, Rivera and colleagues have also reported that MH-S macrophages can limit the replication of VACV *in vitro*, as well as demonstrating an essential role for primary AMs *in vivo* (Rivera *et al.*, 2007).

Finally, the immunostimulatory properties of CpG-sC 10109 and its ability to restrict VACV replication in MH-S macrophages made it a candidate for testing in an *in vivo* model of VACV infection. Pre-treatment of Balb/C mice intranasally prior to an intranasal challenge with 10 MLD VACV was able to confer complete protection. Interestingly, protection with CpG-sC 10109 was optimal when given 7 days prior to challenge. This differs from the protection afforded by CpG-B 7909 which requires

administration three days prior to challenge for optimum efficacy (Rees *et al.*, 2005). These findings are not so surprising given the structural and immunomodulatory differences between the two classes of CpG. Here, significant differences between the two classes of CpG and their effects on macrophages have been presented. The effect of CpG-sC 10109 on cell-types other than macrophages has yet to be published by Coley Pharmaceuticals or any other group. However, it is conceivable that other significant differences exist between CpG-B and CpG-sC in the effects they exert on particular cell-types. Theoretically, the mixed oligonucleotide backbone of CpG-sC 10109 is likely to induce a much stronger IFN-α response from cells such as pDCs than CpG-B 7909 (Kerkmann *et al.*, 2005). In addition, CpG motifs present in CpG-sC 10109 that resemble those found in CpG-B ODNs, may stimulate B-cells to secrete pro-inflammatory cytokines and non-specific levels of IgM in a manner similar to CpG-B 7909 (Vollmer *et al.,* 2004). Collectively, these effects are likely to contribute to a different, yet equally effective immune response to VACV infection. Recently, the use of CpG-sC 10109 as an adjuvant in anthrax studies has been investigated and reported to significantly boost the immunogenicity of the BioThrax® vaccine (Gu *et al.*, 2007).

The results presented within this chapter suggest that primary alveolar macrophages do express TLR9 which makes them potential candidates for direct stimulation *in vivo*. The stimulation of an alveolar macrophage cell-line using CpGs results in the release of a variety of pro-inflammatory cytokines and chemokines as well as the secretion of NO and a reduction in macrophage apoptosis. In addition, pre-stimulation of MH-S macrophages *in vitro* with CpG establishes an antiviral state that restricts the replication of VACV independently of NO production over a 24 hour period. It is

possible that some or all of these *in vitro* observations may also occur *in vivo* and contribute to the development of the protective immune response against VACV infection observed during infection of mice.

Chapter 6: Summary Discussion

The threat of a new smallpox epidemic has dramatically increased efforts to identify new antiviral compounds against orthopoxviruses. Currently, the smallpox vaccine is cited by most countries as the post-exposure therapeutic of choice for use in the event of a smallpox epidemic. In this case, the vaccine would need to be administered within the first few days of infection to be effective. This may be problematic due to the incubation period of variola virus and delayed onset of characteristic symptoms (Stanford *et al.,* 2007). More importantly, this vaccine carries with it a small but significant risk of serious complications (Fulginiti *et al.*, 2003) which emphasises the need for new therapies. The restrictions placed upon research using variola virus, along with its exquisite host specificity, have led to the development of a variety of animal models to study smallpox pathogenesis and assess potential treatments. These have often used closely related viruses such as VACV in mouse models of infection, as has been used throughout this thesis.

The initiation of the inflammatory response requires recognition by host cells of a perceived threat from invading organisms. This recognition is often facilitated by PRRs of which the TLR-family are the best studied. Synthetic agonists have been developed that can initiate this inflammatory response and prove to be of huge therapeutic value (Krieg, 2006). One group of such synthetic TLR9 agonists, are CpG oligodeoxynucleotides which mimic immunostimulatory motifs present in prokaryotic DNA. A variety of classes of CpGs have been developed over recent years, each with unique characteristics and immunostimulatory properties (Vollmer *et al.,* 2004). This thesis has investigated the therapeutic efficacy of CpGs as both a pre- and post-

exposure antiviral against VACV. In doing so, insight has been provided into the type of immune response generated by VACV infection in naïve mice. In addition, the immunomodulatory effects of CpGs have been examined to understand how these responses may contribute to a protective response against VACV.

6.1. The immune response to VACV in naïve mice

This work has provided insight into the immune response of naïve mice following intranasal VACV challenge. Intranasal administration of VACV leads to an acute infection and a wide spread immune response in both the lungs and spleens of infected mice. Following infection, the cell numbers of various immune effector cells, including neutrophils, macrophages, DCs and B-cells, increase in the lung and become activated (Figure 6.1). During this time, the release of cytokines such as IFN-γ contribute to an antiviral immune response and chemokines like CCL2 recruit cells such as macrophages to the site of infection. The influx of immune effector cells into the lung attempts to control VACV replication and limit viral dissemination around the body. In the spleen, immune cells are alerted to the presence of infection, either through migration of cells from the infected lung or recognition of viral ligands from VACV itself. In response, pro-inflammatory cytokines such as TNF-α, IL-6 and type I and type II interferons are released, further amplifying the immune response (Figure 6.2). Throughout the remainder of infection, immune cells in the lungs and spleen continue to exhibit an activated phenotype and an adaptive response involving B and T-lymphocytes develops. Occasionally, this immune response enables mice to survive infection and recover from clinical signs of disease. Studies suggest that humoral and cell-mediated immunity are important at this stage to promote virus clearance (Reading & Smith, 2003b). In addition, the roles of complement and pox-virus

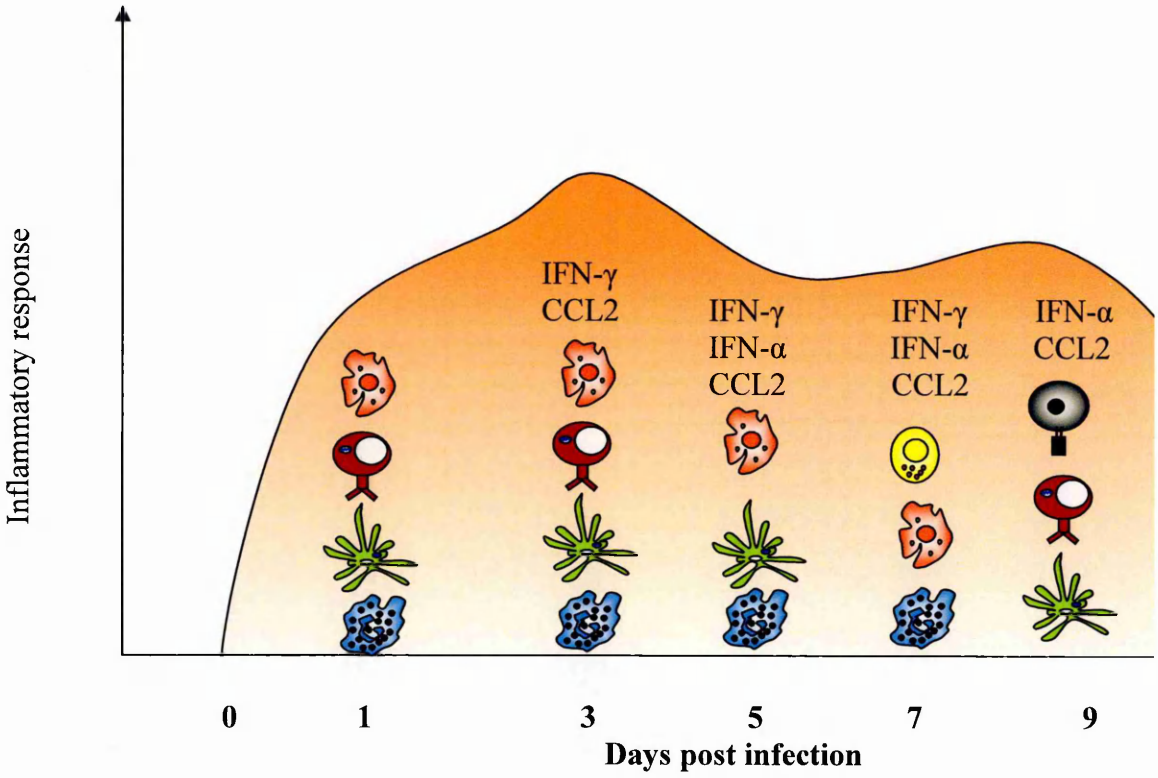

Figure 6.1. Increased inflammatory responses in the lungs of untreated VACV infected mice. Figure shows increased immune activity in the lungs of mice following intranasal infection with VACV.

Key:

Macrophage

Neutrophil

DC

NK cell

B-cell

T-cell

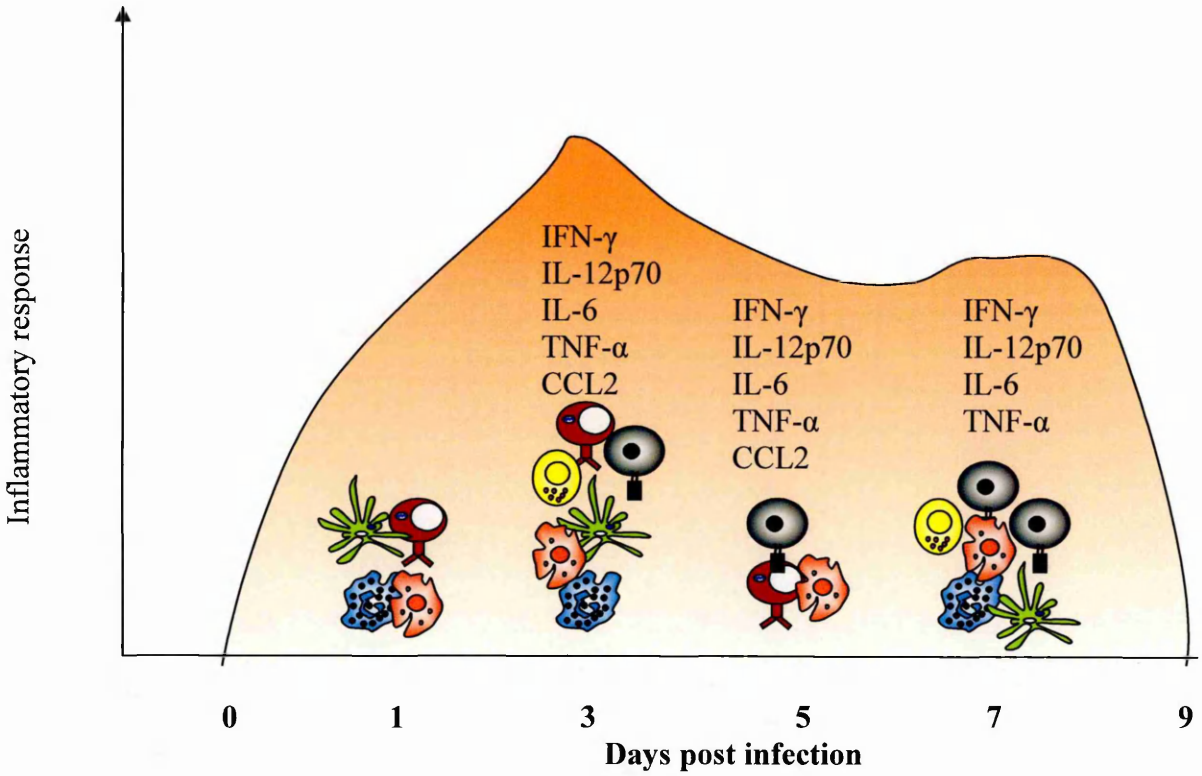

Figure 6.2. Increased inflammatory responses in the spleens of untreated VACV infected mice. Figure shows increased immune activity in the spleens of mice following intranasal infection with VACV.

Key:

Macrophage

Neutrophil

DC

NK cell

B-cell

T-cell

specific antibodies, although not examined in this work, are thought to play a major role in combating orthopoxvirus infection (Smith & Kotwal, 2002).

Data presented by Rees and colleagues suggests VACV rapidly establishes itself in the lungs of infected mice, reaching a peak on day +3 of infection (Rees *et al.,* 2005) (Figure 6.3b). At this stage, viral titres also peak in the spleen and significant levels of VACV can be isolated from the brain (Rees *et al.,* 2005) (Figure 6.4b and Figure 6.5). By day +5, viral titres begin to decrease in the lungs and spleen, although titres in the brain increase. By day +9 of infection, titres in the spleen are very low but high titres persist in both the lung and the brain. This titration data correlates with the immunological data obtained throughout this thesis. Increases in VACV titres during early infection results in a strong local inflammatory response in the lung. The arrival of VACV in the spleen also initiates a strong inflammatory response, characterised by very high levels of IFN-γ. As the inflammatory response amplifies in the lungs, viral titres stabilise, and begin to reduce steadily over the remainder of infection. This implies that the immune response in the lung is eventually able to control local VACV replication. In the spleen, viral titres begin to drop post-day +3 of infection when the inflammatory response is at its strongest. The clearance of VACV from the spleen may be due to the antiviral effects of IFN-γ and the involvement of B and T-lymphocytes as the adaptive immune response develops. Ultimately in this model, these responses fail to prevent lethality and mice succumb to infection. This may be a consequence of high viral titres in the brain. The role of the immune response in controlling VACV titres in the brain is unclear and may involve resident immune cells such as astrocytes and microglial cells.

6.2. The effect of CpG-B 7909 on the immune response to VACV

The intranasal administration of CpG-B 7909 has previously been shown to completely protect mice from a subsequent intranasal challenge with VACV (Rees *et al.,* 2005). Here, viral titres in the lungs of CpG-treated animals were found to be significantly lower than in mice that had not received any CpG treatment. This suggested that pre-treatment with CpG may result in a more effective inflammatory response capable of controlling virus infection. The work presented in Chapter 3 of this thesis provides an immunological assessment of the lungs and spleens of mice given CpG or PBS prior to VACV challenge. Stimulation with CpG-B 7909 resulted in the release of pro-inflammatory cytokines such as IFN-α, IFN-γ, TNF-α and IL-6 along with chemotactic messengers such as CCL2 as has been shown in a number of other studies (Schwartz *et al.*, 1997; Klinman *et al.*, 1996; Krieg, 2002; Deng *et al.*, 2004). In addition, effector cells such as macrophages, neutrophils, dendritic cells and NK cells were identified in high numbers in the lungs of CpG-treated mice. Consequently, at the time of VACV challenge (day 0), the lungs of CpG-treated mice had elevated numbers of activated immune effector cells and increased levels of powerful pro-inflammatory and antiviral cytokines (Figure 6.3a). In addition, the strength of immune response in the lungs of CpG-treated animals persisted over the first three days of infection compared to the more muted response observed in control animals. It is likely that the strength of this response restricted the growth and dissemination of VACV, as has been shown in other studies using CpGs as a prophylactic against viruses and bacteria (Ashkar *et al.,* 2003; Sajic *et al.,* 2003; Waag *et al.,* 2006; Wongratanacheewin *et al.,* 2004; Elkins *et al.,* 1999b). Figure 6.3b is recreated with kind permission from the authors of the Rees study (Rees *et al.,* 2005). Here, pre-treatment of mice with CpG-B 7909 resulted in significantly lower

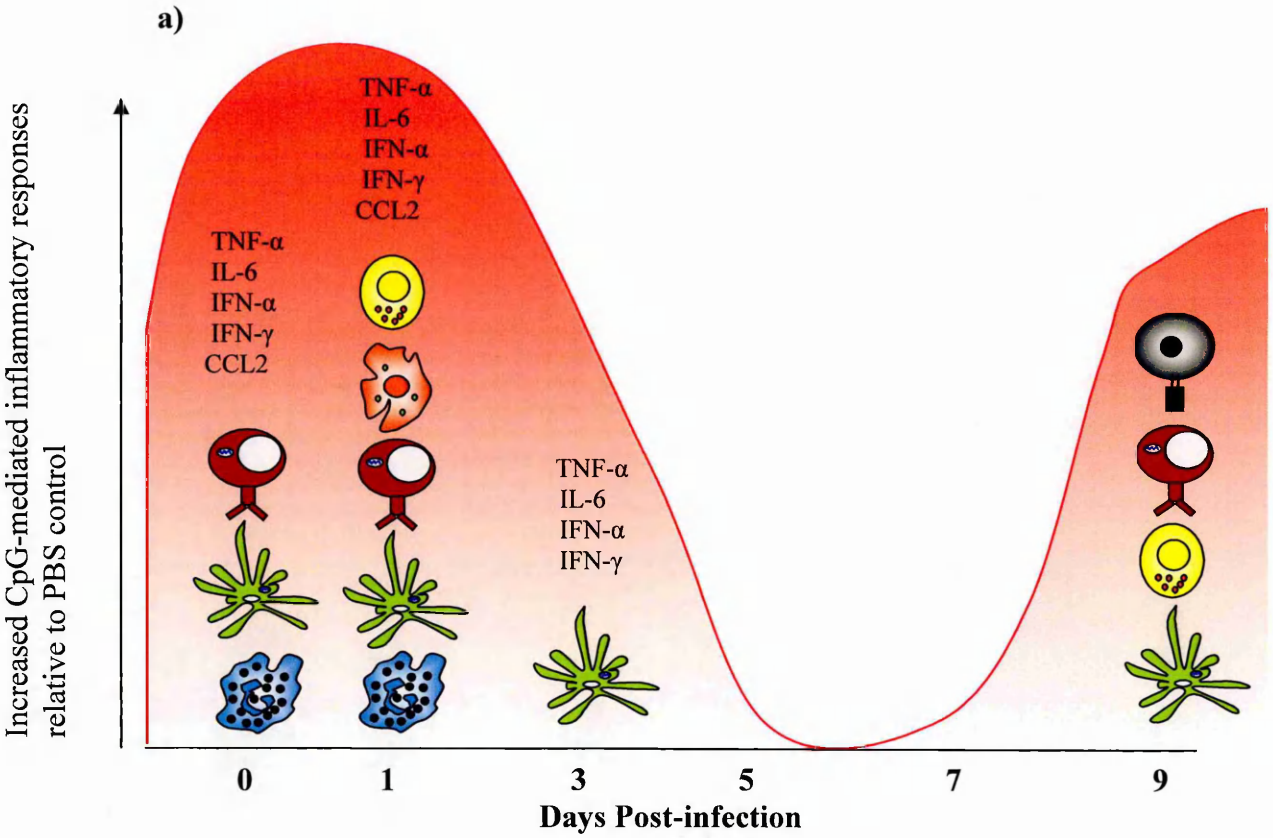

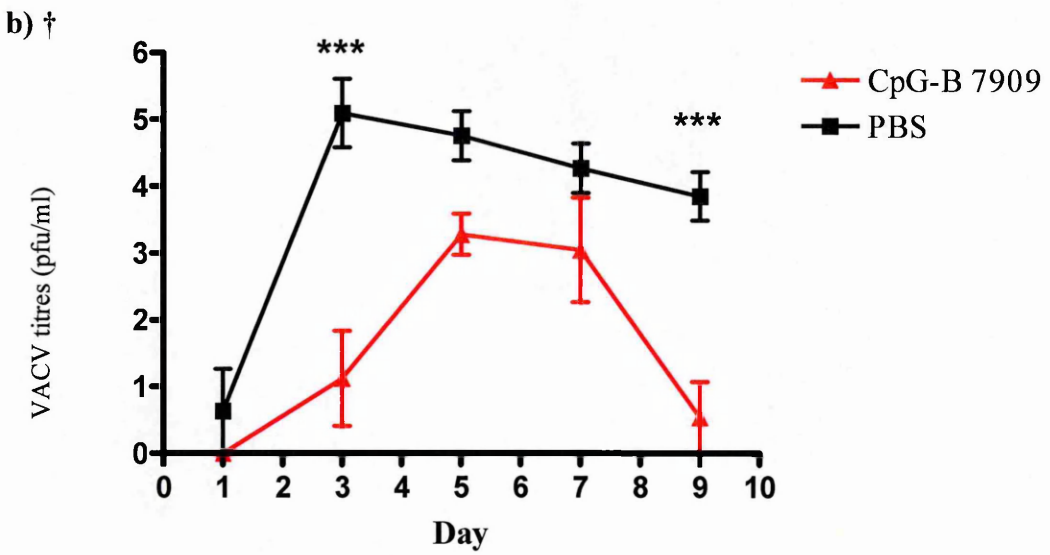

Figure 6.3. Immunological impact of CpG-B 7909 in the lung and effect on viral titres. **(a)** CpG-B 7909 delivery results in increased immune responses in the lung. **(b)** Prophylactic CpG-B 7909 delivery can significantly affect viral titres in the lung. Statistical significance determined by two-way ANOVA and Bonferroni's post-tests. Significance denoted by *** $p<0.001$. Error bars indicate ± SEM.

† *Reproduced with kind permission of authors (Rees et al., 2005.)*

titres of VACV in the lung on day +3 than those from control animals. This reduction in viral replication seems to be a direct result of a pre-formed and primed local inflammatory response at the site of infection. In this sense, the pre-positioning of effector cells in the lung prior to challenge provides the immune response with a critical "head-start" in the race between host response and pathogen. As a consequence, VACV titres in the lungs of CpG-treated mice do not reach as high a level as those in un-treated mice. In addition, whilst viral titres persist in untreated animals, they are almost cleared in CpG-treated mice. This clearance may be related to a second-wave of inflammation evident on day +9 of infection in CpG-treated mice (Figure 6.3a). Here, DCs, NK cells and B and T-lymphocytes may contribute significantly to this reduction in viral titres.

Few immunological differences were identified in the spleens of CpG-treated and un-treated groups at the time of VACV challenge. Prior to VACV challenge, small increases in neutrophil numbers, B-cell activation and IFN-γ were detected (Figure 6.4a). In the days following VACV infection, little additional immune activity beyond that caused by VACV infection was identified in the spleen. Interestingly, this correlates with splenic VACV titres obtained in the Rees study (Rees *et al.,* 2005) (Figure 6.4b). Here, viral titres reach a peak on day +3 of infection whereas titres in CpG-B 7909 treated animals are significantly lower. This is likely to be a direct consequence of the successful immune response launched in the lung, slowing the dissemination of VACV to distal sites like the spleen. This effect on viral dissemination may be the key factor to CpG-mediated protection. For instance, viral titres obtained from the brain in the Rees study show that CpG-treatment prevented VACV from reaching the brain in the majority of animals (Figure 6.5). In comparison,

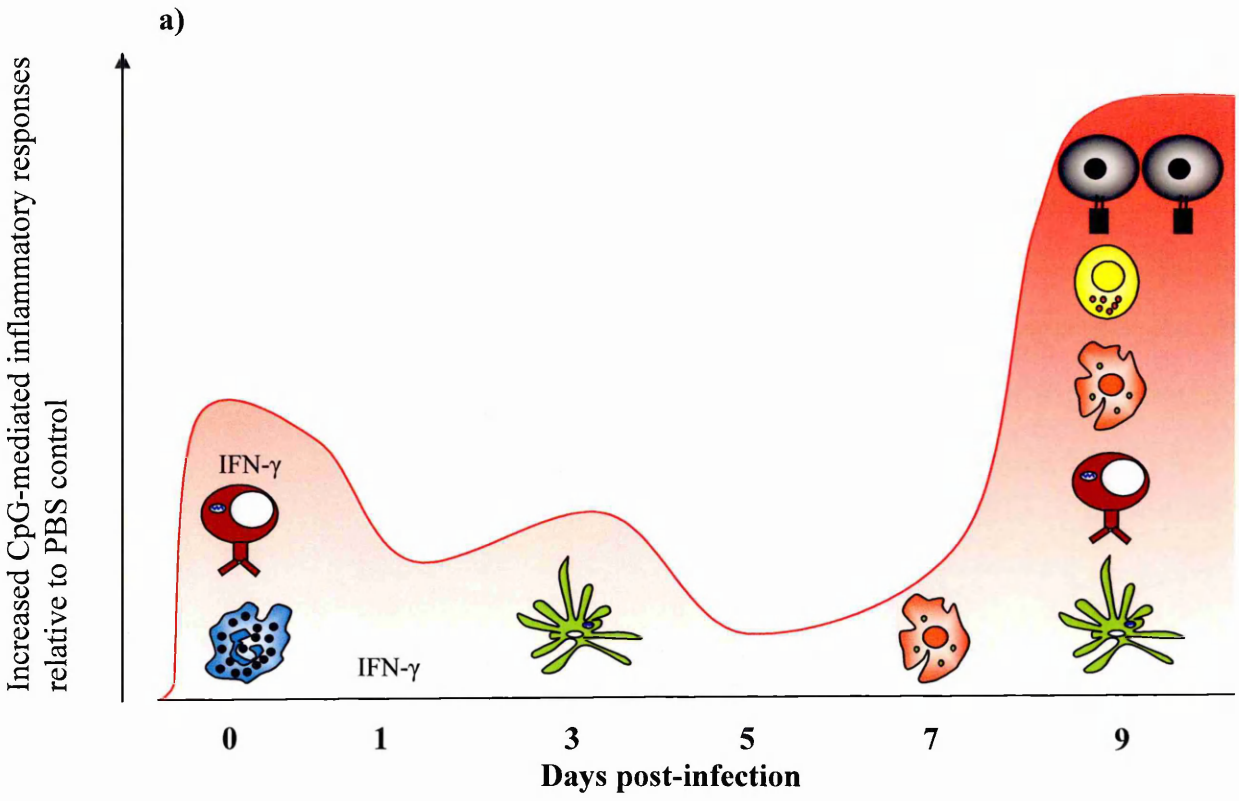

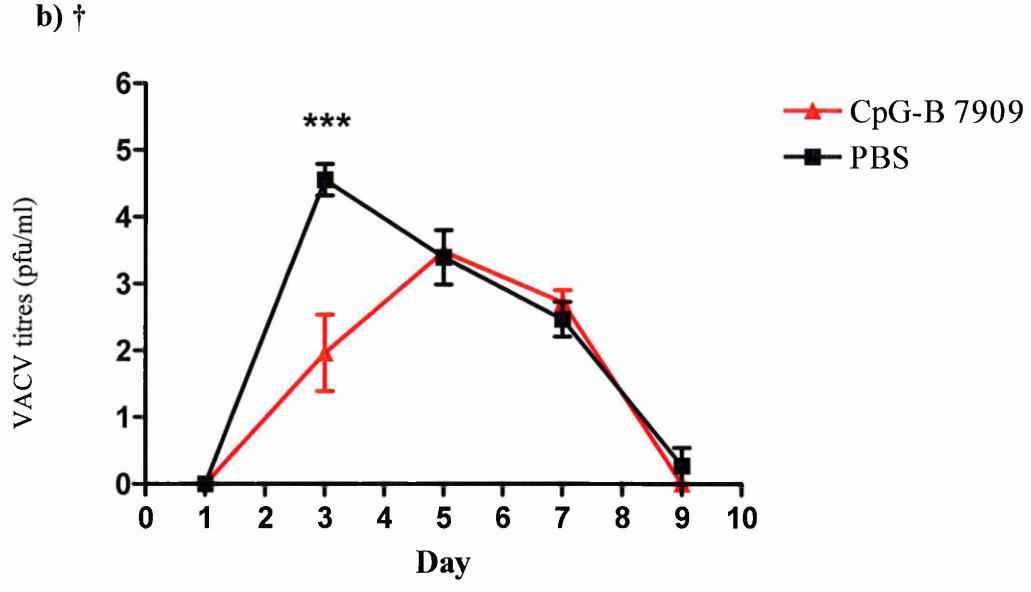

Figure 6.4. Immunological impact of CpG-B 7909 in the spleen and effect on viral titres. **(a)** CpG-B 7909 delivery results in increased immune responses in the spleen. **(b)** Prophylactic CpG-B 7909 delivery can significantly affect viral titres in the spleen. Statistical significance determined by two-way ANOVA and Bonferroni's post-tests. Significance denoted by *** $p<0.001$. Error bars indicate ± SEM.

† *Reproduced with kind permission of authors (Rees et al., 2005.)*

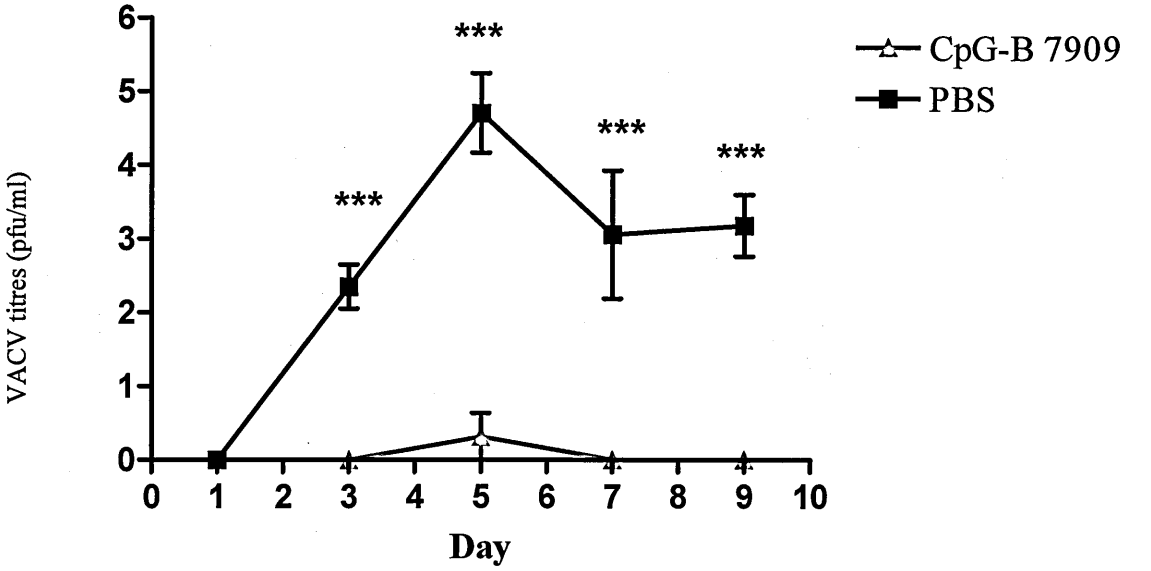

Figure 6.5. VACV titres in the brains of infected mice treated prophylactically with CpG-B 7909. Statistical significance determined by two-way ANOVA and Bonferroni's post-tests. Significance denoted by *** $p<0.001$. Error bars indicate ± SEM.

† *Reproduced with kind permission of authors (Rees et al., 2005.)*

high titres were determined in the brains of untreated mice and studies have suggested this contributes significantly to lethality (Hayasaka, Ennis & Terajima, 2007).

This data may suggest that the success of CpGs as a prophylactic relies on the generation of a powerful but local response at the site of pathogen challenge. This ensures the creation of a hostile environment for any invading pathogen. In support of this, other studies have lost the prophylactic effect of CpGs when delivered at sites distal from infection (Pedras-Vasconcelos *et al.*, 2006; Ashkar *et al.,* 2003; Sajic *et al.,* 2003). However, it is possible that the immune response to VACV in the spleen becomes important later in infection. This is suggested by the observation from day +7 of infection, the numbers of activated cell-types in CpG-treated animals, including macrophages, neutrophils, DCs, NK cells and $CD4^+$ and $CD8^+$ T-cells, become significantly higher than those from untreated groups (Figure 6.3a). It is at this time that clinical signs begin to alleviate in the animal model used throughout this study or, conversely, the time when control mice succumb to infection. Further studies using VACV could investigate the importance of local CpG delivery in a pre-exposure system and examine how the kinetics of the immune response alters if given by different routes.

How the protective immune response against VACV is launched by CpG-B 7909 in this pre-exposure system is unclear. CpG-B ODNs are predominantly thought to activate B-cells most potently (Krieg *et al.,* 1995). Here, B-cell stimulation could result in enhanced antigen presentation and antibody release as well as cytokine release such as IL-6 which in turn cascades the inflammatory signal throughout the lung. In this sense, it may well be that B-cells do facilitate the initiation of this

protective response. However, it is apparent from these studies using a B-cell KO mouse model that protection against VACV is still induced by pre-treatment with CpG-B 7909. This suggests that CpG-B 7909 can also stimulate other TLR9 expressing cell types in the lung and that this stimulation is sufficient to induce protection. Candidates for this direct stimulation include cells such as pDCs, myeloid DCs and alveolar macrophages. In addition it suggests that CpG-mediated protection does not rely upon the generation of VACV specific antibodies.

Studies that depleted neutrophils during the initial stages of infection did not affect the outcome of VACV infection. However, the role of neutrophils as a mediator of the protective response following CpG stimulation remains a question of interest. Although absent during the initial stages of infection, neutrophils may respond to CpG stimulation and recruit cells to the lung through release of chemotactic compounds like chemerin and cathepsin-G (Bennouna *et al.,* 2003; Chertov *et al.,* 1997; Wittamer *et al.,* 2005). In addition, neutrophils may prime other cells types through release of cytokines such as TNF-α and IFN-γ (Ethuin *et al.,* 2004) prior to VACV challenge and the importance of this is also a question that could be addressed in future work. In this present study, neutrophils were only depleted 24 hours prior to challenge. Repeated doses of neutralising antibody are usual in studies investigating the complete loss of neutrophils throughout infection. Thus, it would be interesting to examine whether the loss of neutrophils throughout the duration of the infection significantly affected the hosts ability to resolve VACV infection. The use of the RB6-85 monoclonal antibody remains the preferred method of depleting neutrophils by investigators despite the unavoidable loss of other Gr-1 expressing cell-types including $CD8^+$ T-cells and some monocytes. Studies have suggested that the extent

of this collateral depletion can be limited by altering the dose and timing of antibody treatment (Seilier *et al.*, 2003). Other studies have induced neutropenia using low doses of cyclophosphamide (Zuluaga *et al.*, 2006) or prevented neutrophil recruitment by blocking CXCR2 (Tsai *et al.*, 2000). Both of these approaches have problems though as cyclophosphomide also depletes monocytes and lymphocytes, and because neutrophils can also be recruited in response to stimuli not involving CXCR2.

6.3. Post-exposure treatment of VACV with CpG-B 7909

In a post-exposure model of VACV infection, CpG-B 7909 was found to be less protective against VACV than in the pre-exposure model. This drop in protection (100% to 60%), is consistent with a wide range of studies which have also seen protective levels fall if treatment with CpG is withheld (Wongratanacheewin *et al.*, 2004; Waag *et al.*, 2006; Deng *et al.*, 2004; Sajic *et al.*, 2003; Harandi, Eriksson, & Holmgren, 2003). In other studies, the host response failed to control the growth and replication of pathogens such as *Klebsiella* in the lung, *Burkholderia*, and HSV-2 in the genital mucosa. It may be that in this system, VACV rapidly reaches high titres in the lung and quickly disseminates to other sites of the body which future studies could confirm.

The post-exposure administration of CpG-B 7909 was still found to have a significant effect on the inflammatory response initiated by VACV. CpG-B 7909 delivery resulted in increased cellular recruitment and activation of macrophages, neutrophils and DCs in the lung (Figure 6.6a). In addition, NK cell activity on day +3 was increased and significant increases in cytokine and chemokine levels were also determined. Beyond this initial effect, no significant cellular differences between

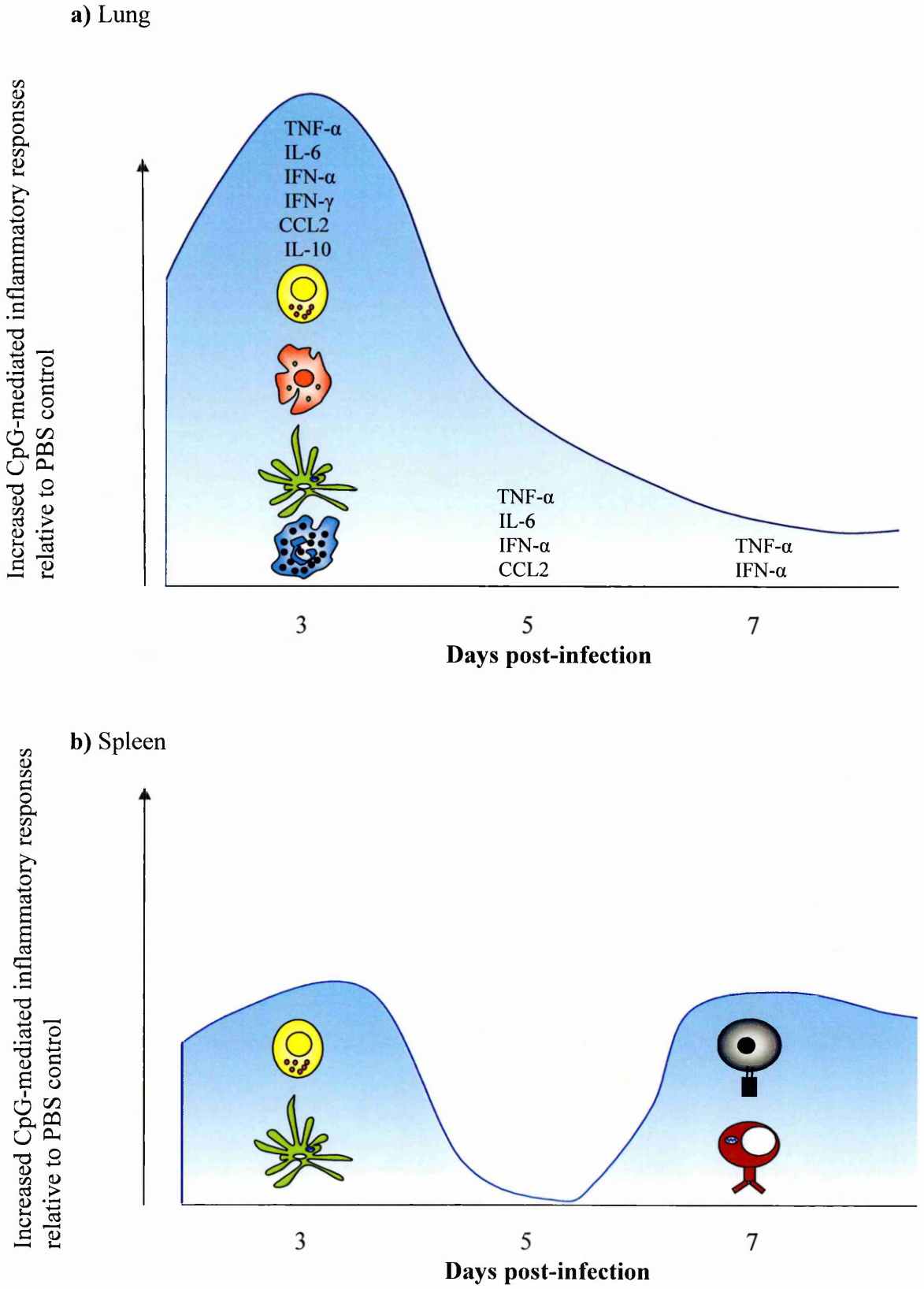

Figure 6.6. Increased inflammatory responses following administration of CpG-B 7909 post-infection with VACV. Figures show increased responses in **(a)** lungs and **(b)** spleens of mice over the course of infection with VACV.

CpG-treated and untreated mice were determined throughout the remainder of infection. In the spleen, it appears only NK cells and DC numbers were bolstered by CpG delivery (Figure 6.6b). Interestingly, B-cell and T-cell numbers on day +7 were significantly higher in CpG-treated mice which may suggest CpG-treatment contributed to the development of an adaptive response. Despite these effects, it appears that post-exposure delivery of CpG-B 7909 can not orchestrate an immune response that can undo the "damage" already caused by VACV infection. The absence of the pre-formed immune response, which protects in a pre-exposure model, enables VACV to replicate rapidly and establish systemic infection. Therefore, the delayed administration of CpG-B 7909 may provide a degree of "damage-limitation", sufficient to grant protection in some but not all of those infected. This is supported by the fact that as a post-exposure therapy, CpGs have only yielded success against slow growing organisms such as *M.tuberculosis*, *C.neoformans* and FLV (Juffermans *et al.,* 2002; Edwards *et al.,* 2005; Olbrich *et al.,* 2002). These results suggest that CpGs alone as a monotherapy may struggle to protect against pathogens such as VACV which replicates rapidly, or variola, which can also replicate to high titres quickly in key organs during infection.

Results reported here also support the requirement for local delivery of CpG to the site of infection as intraperitoneal, subcutaneous or intramuscular delivery of CpG failed to offer equivalent protection in a post-exposure model. In addition, the use of multiple doses of CpG was not found to be of therapeutic benefit. It is possible that other dosing regimens or a combination of optimised CpG doses may grant more success in this area. However, given the inflammatory nature of CpGs, it may be that multiple doses of CpG could enhance host tissue damage and accelerate time to death

due to an over-zealous immune response. CpG toxicity has been reported in the literature. Here, liver necrosis and lymphoid tissue disruption were reported following repeated CpG doses in a mouse model (Heikenwalder *et al.*, 2004). As such, investigations of this type need to proceed with caution. It is of note that toxicity studies of this type may not transition directly to humans given the more limited repertoire of human immune cells that express TLR9. Thus it is possible that these studies may over-estimate any negative effect of repeated CpG stimulation.

The role of VACV immunomodulatory proteins in infection was not investigated in these studies. However, this is an area of particular interest and one that may contribute significantly to the loss of protection in a post-exposure system. Poxviruses, such as VACV, possess a wealth of proteins that aim to disrupt many different arms of the host immune response (Haga & Bowie, 2005). Many of these proteins are synthesised early during infection and their release into the surrounding area prior to CpG delivery may allow the virus to obtain a vital foothold and subsequently hinder the effectiveness of the innate immune response. Many of these proteins have been shown to increase virulence in *in vivo* studies (Stack *et al.*, 2005; Reading & Smith, 2003) which makes their targeted disruption by siRNA or other technologies of potential therapeutic benefit. It would be interesting to see whether protection with CpG-B 7909 was boosted in systems where selected immunomodulatory proteins were disabled, possibly as part of a combination therapy approach. Maybe then, the inflammatory response induced by CpG-B 7909 may be stronger and more effective at combating VACV infection.

Collectively, these analyses find CpGs are more protective when given pre-exposure than when given after the event of VACV infection. This is likely to be a direct result of the initiation of a prominent local pro-inflammatory response pre-exposure, which primes the host immune system prior to infection. Of equal significance is the location of this response. Intranasal delivery of CpG ensures the effects of CpG are most strongly felt in the lung (Figure 6.7a). This ensures when VACV arrives in the lung, it is swiftly controlled and efficiently contained by the immune system. This ultimately enables the control of VACV infection and restriction of the lethal dissemination throughout the host. In addition, immune activity in the spleen is also boosted prior to VACV arrival (Figure 6.7b). In a post-exposure system, the addition of CpGs exacerbates an on-going pro-inflammatory response in both the lung and the spleen. This response seems sufficient to protect mice in some cases but insufficient in others. This suggests the necessary immune response initiated by CpG delivery is typically initiated too late. Consequently, the failure of CpGs to protect in this instance results from the inability of the host to control virus spread to multiple organs. These findings re-affirm the importance of local delivery of CpG to ensure activated cells are very much in the right place at the right time.

6.4. CpGs activate macrophages and restrict VACV titres *in vitro*

Studies using B-cell KO mice and neutrophil ablating antibodies (Section 3.3.7/8) suggested that neither B-cells nor neutrophils were crucial in conferring CpG mediated protection against VACV. This led to the investigation of other cell-types that may be important in mediating defence against VACV. Macrophages were identified in Chapter 3 as cells that were both highly activated and present in high numbers in the lungs of CpG-treated mice. The prevalence of alveolar macrophages in

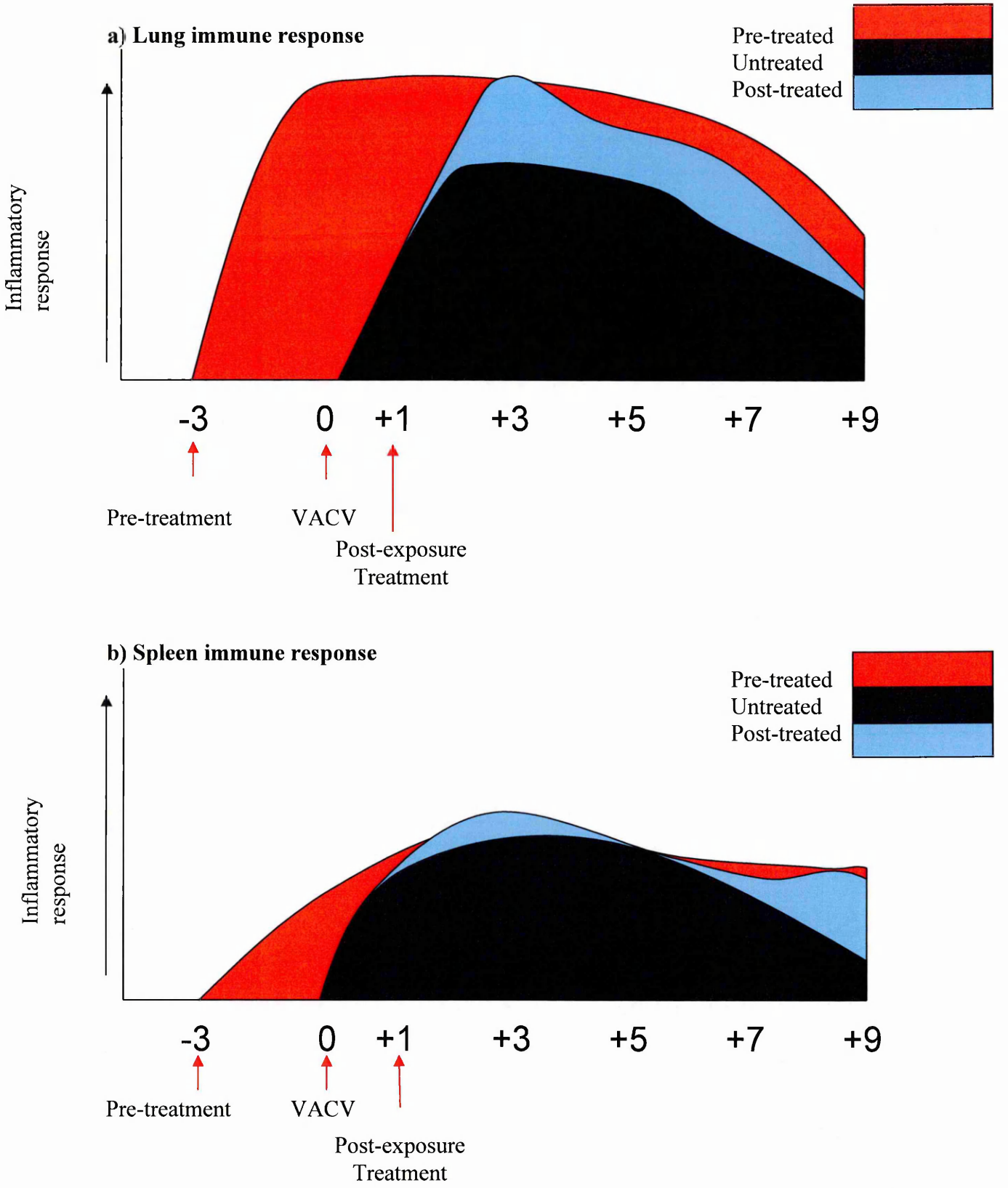

Figure 6.7. Timing of CpG delivery influences the immune response during VACV infection. Different Immune profiles are generated in the **(a)** lungs and **(b)** spleens of mice infected with VACV. Generation of a strong immune response prior to infection correlates with protection.

the lung and reports that they also express TLR9 (Huang *et al.,* 2005) made them a prime candidate cell-type to investigate. In addition, other studies have suggested that macrophages actively ingest and respond to CpG stimulation (Stacey *et al.*, 1996; Sester *et al.,* 2000; Roberts *et al.,* 2005). The expression of TLR9 on primary AMs was confirmed using RT-PCR and these studies suggested that CpG stimulation could enhance levels of TNF-α transcription in AMs. This observation makes them potential candidates for direct CpG stimulation *in vivo*. Reports that macrophages exhibit considerable heterogeneity (Gordon & Taylor, 2005) led to the investigation of CpG responses by AMs using an *in vitro* cell-line (MH-S) alongside a commonly studied non-alveolar macrophage cell-line (J774).

The degree of macrophage stimulation was found to vary dramatically according to the class of CpG used. In all studies, CpG-A 2336 and CpG-sC 10109 were identified as the most potent activators of macrophages. Here, stimulation with these CpGs typically induced significantly stronger NO, cytokine and chemokine responses than other CpGs. Interestingly, CpG-B 10103 (substituted for CpG-B 7909) was unable to stimulate strong pro-inflammatory cytokine and chemokine responses in either cell-line. However, stimulation of macrophages with CpG-B 10103 increased expression of the activation marker CD54 suggesting that incubation with CpG-B 10103 did activate both macrophage cell-lines. In addition, CpG-B 10103 significantly reduced levels of apoptosis in both MH-S and J774 macrophages further suggesting it can stimulate macrophages. Apoptosis is often a significant component of the host immune response and in an *in vivo* setting, prevention of apoptosis may prolong the ability of macrophages to secrete cytokines, phagocytose pathogens or necrotic neutrophils and present antigen to naïve T-cells (Haslett, 1999). The role of

macrophage apoptosis in an *in vivo* VACV infection has not been fully defined but it is known that VACV encodes a number of anti-apoptotic proteins such as v-GAAP, SPI-2, crmE (Dobbelstein & Shenk, 1996; Gubser *et al.,* 2007), which suggests cellular apoptosis may play a significant role in VACV infection. Therefore, determining whether apoptosis plays a significant role in CpG mediated protection and how VACV may modify this response would be a valid area to investigate.

The growth of VACV in MH-S and J774 macrophages did not identify any difference in the ability of VACV to replicate within either cell-line. However, pre-stimulation of macrophages with CpG-B 10103 or CpG-sC 10109 identified a significant difference in the ability of VACV to grow in pre-stimulated macrophages. Here, CpG-sC 10109 restricted growth of VACV significantly more than CpG-B 10103. The mechanism for this inhibition was found to be unrelated to NO release as has been suggested in other studies (Harris, Buller, & Karupiah, 1995; Karupiah & Harris, 1995; Karupiah *et al.,* 1993), as inhibition of NO did not significantly affect viral titres. Importantly, these studies suggest that pre-stimulation of macrophages with CpG-B can restrict growth of VACV. This may have important implications for the role of macrophages in understanding the mechanistic nature of CpG-B prophylaxis.

Investigation of the ability of CpG-sC 10109 to protect against VACV *in vivo* suggested that pre-treatment could provide full protection. Optimum protection was achieved when CpG-sC 10109 was administered 7 days before challenge, compared to three days before for CpG-B 7909. This result, along with the *in vitro* observations made, suggests that these two CpGs may confer protection against VACV *via* different means. If so, the role of the macrophage in this model would be worth

investigating. Studies using clodronate liposomes to deplete macrophages *in vivo* have suggested that macrophages may be crucial to resolving VACV infection (Karupiah *et al.,* 1996; Rivera *et al.,* 2007). If macrophages are key to providing defence against orthopoxvirus infection, it is possible that a more potent macrophage stimulator such as CpG-sC 10109 may be able to provide enhanced protection against VACV in a post-exposure model of infection.

Collectively, these studies also identified significant differences between MH-S and J774 macrophage responses to CpG stimulation. MH-S macrophages were found to transcribe less IL-6 than J774s and secrete significantly less TNF-α and IL-6 following CpG stimulation. These *in vitro* cytokine observations concur with the view that AMs are typically quiescent cells that limit inflammation in the lung environment (Takabayshi *et al.*, 2006; Holt, 1986; Holt *et al.*, 1993). It may be that this controlled release of pro-inflammatory cytokines by AMs contributes to a protective immune response against pathogens such as VACV. MH-S macrophages were found to secrete significantly more NO than their J774 counterparts when stimulated with CpG. NO is thought to play a dual role in inflammation, being toxic to invading pathogens but also being capable of suppressing T-cell and DC functions and promoting apoptosis (Strickland *et al.*, 1993; Holt *et al.,* 1993). In this sense, high NO release by MH-S macrophages may model an *in vivo* situation whereby AMs cause the destruction of invading pathogens whilst restricting overall levels of inflammation. This could help preserve lung integrity and homeostasis.

6.5. Concluding remarks

The investigation into CpGs as candidates to fill the current void in available antivirals against orthopoxvirus, has resulted in a number of key observations. CpG-B and CpG-sC classes of CpG are capable of protecting mice against a lethal dose of VACV if given at an optimum time prior to challenge. This protection is thought to be a direct result of the release of pro-inflammatory and antiviral cytokines that promote the recruitment of an array of host effector cells. This in turn prevents the invading virus from establishing itself and restricts its dissemination around the host. Key to this response may be macrophages and their ability to modulate the host response through release of pro-inflammatory cytokines and chemokines. In addition, activated macrophages infected with VACV may be able to restrict viral growth and limit virus dissemination. Despite the effectiveness of CpGs as a prophylactic, in reality, pre-empting orthopoxvirus infection is unlikely to ever prove a workable solution. Of greater interest is the ability of antivirals to protect after virus infection. In this case, therapy with CpG-B falls some way short of other antivirals such as ST-246, which are currently leading the way in research trials (Yang *et al.,* 2005a). Potentially, the key factor in CpGs failing to confer protection in a post-exposure setting is their inability to orchestrate an immune response rapidly enough to control VACV growth. Whether investigation of other CpG classes such as CpG-sC could improve in this area, is unclear. However, it is perhaps doubtful that any improvement will be improvement enough. Antiviral compounds such as ST-246 target the virus itself and prevent its maturation (Yang *et al.,* 2005b). This may slow the replication of virus sufficiently for the host immune system to mount an appropriate and protective response. In addition, these newly formulated drugs are highly effective in an orally available format which makes them extremely desirable. In contrast, the loss of

protection observed when CpGs are not delivered to the site of infection further detracts from their applicability.

Whilst the mono-therapeutic use of CpGs may not be the solution to viral infection, CpGs are proving valuable immunomodulatory agents in other medically important areas. Although recently withdrawn from non-small cell lung cancer trials (Schmidt, 2007), CpGs are proving effective against other types of malignancies (Murad *et al.*, 2007) and still have the potential to be invaluable as allergy treatments or as adjuvants to new vaccines (Krieg, 2006; Jurk & Vollmer, 2007). Furthermore, the use of CpGs in a combined antiviral approach is something that could prove to be of benefit. Combination approaches currently lead the way in the treatment of HIV and in other viral infections. It is feasible that where current antiviral compounds target the virus but are not fully effective, CpG therapy could help promote an immune response that resolves infection and generates adaptive immunity. Ultimately, understanding the differing kinetics of the immune response following CpG stimulation may allow for a more tailored approach to CpG mediated therapy in many areas.

Finally these studies have helped underpin our knowledge of the host response to VACV infection and response to CpG stimulation. Characterisation of the immune response during pathogen infection is paramount to understanding disease pathology and in determining correlates of protection in treatment studies. These studies have highlighted the importance of a rapid immune response to infection and revealed that the host response to VACV infection involves a diverse array of cell-types including macrophages, neutrophils, DCs and NK cells, in addition to B and T-lymphocytes. This response is likely to be orchestrated through the involvement of a wide variety of

pro-inflammatory cytokines and chemokines and release of NO. Understanding this response may enable a more tailored approach to immunomodulatory therapy and make the development of new and effective antiviral therapies a more likely prospect.

Chapter 7: References

Akira, S., Uematsu, S. & Takeuchi, O. (2006). Pathogen recognition and innate immunity. *Cell* **124**, 783-801.

Alcami, A. & Smith, G. L. (1992).A soluble receptor for interleukin-1β encoded by vaccinia virus: A novel mechanism of virus modulation of the host response to infection. *Cell* **71**, 153-167.

Alcami, A. & Smith, G. L. (1995). Vaccinia, cowpox, and camelpox viruses encode soluble gamma interferon receptors with novel broad species specificity. *J Virol* **69**, 4633-4639.

Alcami, A., Symons, J. A. & Smith, G. L. (2000). The vaccinia virus soluble alpha/beta interferon (IFN) receptor binds to the cell surface and protects cells from the antiviral effects of IFN. *J Virol* **74**, 11230-11239.

Aldern, K. A., Ciesla, S. L., Winegarden, K. L. & Hostetler, K. Y. (2003). Increased antiviral activity of 1-O-hexadecyloxypropyl-[2-(14)C]cidofovir in MRC-5 human lung fibroblasts is explained by unique cellular uptake and metabolism. *Mol Pharmacol* **63**, 678-681.

Alexopoulou, L., Holt, A. C., Medzhitov, R. & Flavell, R. A. (2001). Recognition of double-stranded RNA and activation of NF-κB by Toll-like receptor 3. *Nature* **413**, 732-738.

An, H., Xu, H., Yu, Y. & other authors (2002). Up-regulation of TLR9 gene expression by LPS in mouse macrophages *via* activation of NF-κB, ERK and p38 MAPK signal pathways. *Immunology Letters* **81**, 165-169.

Andrejeva, J., Childs, K. S., Young, D. F., Carlos, T. S., Stock, N., Goodbourn, S. & Randall, R. E. (2004). The V proteins of paramyxoviruses bind the IFN-inducible RNA helicase, mda-5, and inhibit its activation of the IFN-β promoter. *PNAS* **101**, 17264-17269.

Antoine, G., Scheiflinger, F., Dorner, F. & Falkner, F. G. (1998). The complete genomic sequence of the modified vaccinia Ankara strain: Comparison with Other Orthopoxviruses. *Virology* **244**, 365-396.

Armstrong, J. A., Metz, D. H. & Young, M. R. (1973). The mode of entry of vaccinia virus into L cells. *J Gen Virol* **21**, 533-537.

Arvanitakis, L., Geras-Raaka, E., Varma, A., Gershengorn, M. C. & Cesarman, E. (1997). Human herpesvirus KSHV encodes a constitutively active G-protein-coupled receptor linked to cell proliferation. *Nature* **385**, 347-350.

Ashkar, A. A., Bauer, S., Mitchell, W. J., Vieira, J. & Rosenthal, K. L. (2003). Local delivery of CpG oligodeoxynucleotides induces rapid changes in the genital mucosa and inhibits replication, but not entry, of herpes simplex virus type 2. *J Virol* **77**, 8948-8956.

Askew, D., Chu, R. S., Krieg, A. M. & Harding, C. V. (2000). CpG DNA induces maturation of dendritic cells with distinct effects on nascent and recycling MHC-II antigen-processing mechanisms. *J Immunol* **165**, 6889-6895.

Asselin-Paturel, C., Boonstra, A., Dalod, M. & other authors (2001). Mouse type I IFN-producing cells are immature APCs with plasmacytoid morphology. *Nat Immunol* **2**, 1144-1150.

Bablanian, R., Goswami, S. K., Esteban, M., Banerjee, A. K. & Merrick, W. C. (1991). Mechanism of selective translation of vaccinia virus mRNAs: differential role of poly(A) and initiation factors in the translation of viral and cellular mRNAs. *J Virol* **65**, 4449-4460.

Bailey, T. R., Rippin, S. R., Opsitnick, E. & other authors (2007).N-(3,3a,4,4a,5,5a,6,6a-Octahydro-1,3-dioxo-4,6- ethenocycloprop[f]isoindol-2-(1H)-yl)carboxamides: Identification of novel orthopoxvirus egress inhibitors. *J Med Chem* **50**, 1442-1444.

Ballas, Z. K., Rasmussen, W. L. & Krieg, A. M. (1996). Induction of NK activity in murine and human cells by CpG motifs in oligodeoxynucleotides and bacterial DNA. *J Immunol* **157**, 1840-1845.

Bao, M., Zhang, Y., Wan, M. & other authors (2006). Anti-SARS-CoV immunity induced by a novel CpG oligodeoxynucleotide. *Clin Immunol* **118**, 180-187.

Bartlett, N., Symons, J. A., Tscharke, D. C. & Smith, G. L. (2002). The vaccinia virus N1L protein is an intracellular homodimer that promotes virulence. *J Gen Virol* **83**, 1965-1976.

Bartlett, N. W., Buttigieg, K., Kotenko, S. V. & Smith, G. L. (2005). Murine interferon lambdas (type III interferons) exhibit potent antiviral activity *in vivo* in a poxvirus infection model. *J Gen Virol* **86**, 1589-1596.

Bauer, S., Kirschning, C. J., Hacker, H., Redecke, V., Hausmann, S., Akira, S., Wagner, H. & Lipford, G. B. (2001). Human TLR9 confers responsiveness to bacterial DNA *via* species-specific CpG motif recognition. *PNAS* **98**, 9237-9242.

Beloeil, L., Tomkowiak, M., Angelov, G., Walzer, T., Dubois, P. & Marvel, J. (2003).*In vivo* impact of CpG1826 oligodeoxynucleotide on CD8 T-Cell primary responses and survival. *J Immunol* **171**, 2995-3002.

Belyakov, I. M., Earl, P., Dzutsev, A. & other authors (2003). Shared modes of protection against poxvirus infection by attenuated and conventional smallpox vaccine viruses. *PNAS* **100**, 9458-9463.

Belyakov, I. M., Isakov, D., Zhu, Q., Dzutsev, A., Klinman, D. & Berzofsky, J. A. (2006). Enhancement of CD8+ T-cell immunity in the lung by CpG oligodeoxynucleotides increases protective efficacy of a modified vaccinia Ankara vaccine against lethal poxvirus infection even in a CD4-deficient host. *J Immunol* **177**, 6336-6343.

Benedict, C. A., Norris, P. S. & Ware, C. F. (2002). To kill or be killed: viral evasion of apoptosis. *Nat Immunol* **3**, 1013-1018.

Bennouna, S., Bliss, S. K., Curiel, T. J. & Denkers, E. Y. (2003). Cross-talk in the innate immune system: Neutrophils instruct recruitment and activation of dendritic cells during microbial infection. *J Immunol* **171**, 6052-6058.

Beutler, B. (2000). Tlr4: central component of the sole mammalian LPS sensor. *Curr Immunol* **12**, 20-26.

Bieback, K., Lien, E., Klagge, I. M. & other authors (2002). Hemagglutinin protein of wild-type measles virus activates Toll-like receptor 2 signaling. *J Virol* **76**, 8729-8736.

Bingisser, R. M. & Holt, P. G. (2001). Immunomodulating mechanisms in the lower respiratory tract: nitric oxide mediated interactions between alveolar macrophages, epithelial cells, and T-cells. *Swiss Med Wkly* **131**, 171-179.

Bird, A. P. (1987). CpG islands as gene markers in the vertebrate nucleus. *Trends in Genetics* **3**, 342-347.

Boggs, R. T., McGraw, K., Condon, T., Flournoy, S., Villiet, P., Bennett, C. F. & Monia, B. P. (1997). Characterization and modulation of immune stimulation by modified oligonucleotides. *Antisense Nucleic Acid Drug Dev* **7**, 461-471.

Bonfield, T. L., Konstan, M. W., Burfeind, P., Panuska, J. R., Hilliard, J. B. & Berger, M. (1995). Normal bronchial epithelial cells constitutively produce the anti-inflammatory cytokine interleukin-10, which is downregulated in cystic fibrosis. *Am J Respir Cell Mol Biol* **13**, 257-261.

Boom, R., Sol, C. J. A., Salimans, M. M. M., Jansen, C. L., Wertheim-Van Dillen, P. M. E. & Van Der Noordaa, J. (1990). Rapid and simple method for purification of nucleic acids. *J Clin Microbiol* **28**, 495-503.

Borchardt, R. T., Keller, B. T. & Patel-Thombre, U. (1984). Neplanocin A. A potent inhibitor of S-adenosylhomocysteine hydrolase and of vaccinia virus multiplication in mouse L929 cells. *J Biol Chem* **259**, 4353-4358.

Bosca, L., Zeini, M., Traves, P. G. & Hortelano, S. (2005). Nitric oxide and cell viability in inflammatory cells: a role for NO in macrophage function and fate. *Toxicology* **208**, 249-258.

Boulter, E. A. & Appleyard, G. (1973). Differences between extracellular and intracellular forms of poxvirus and their implications. *Prog Med Virol* **16**, 86-108.

Bowie, A., Kiss-Toth, E., Symons, J. A., Smith, G. L., Dower, S. K. & O'Neill, L. A. J. (2000).A46R and A52R from vaccinia virus are antagonists of host IL-1 and toll-like receptor signaling. *PNAS* **97**, 10162-10167.

Brannen, A. L. & Chandler, D. B. (1988). Alveolar macrophage subpopulations' responsiveness to chemotactic stimuli. *Am J Pathol* **132**, 161-166.

Brown, J. P., Twardzik, D. R., Marquardt, H. & Todaro, G. J. (1985). Vaccinia virus encodes a polypeptide homologous to epidermal growth factor and transforming growth factor. *Nature* **313**, 491-492.

Buller, R. M. & Palumbo, G. J. (1991). Poxvirus pathogenesis. *Microbiol Mol Biol Rev* **55**, 80-122.

Burns, J. M., Dairaghi, D. J., Deitz, M., Tsang, M. & Schall, T. J. (2002). Comprehensive mapping of poxvirus vCCI chemokine-binding protein. Expanded range of ligand interactions and unusual dissociation kinetics. *J Biol Chem* **277**, 2785-2789.

Byrd, C. M. & Hruby, D. (2005).A conditional-lethal vaccinia virus mutant demonstrates that the I7L gene product is required for virion morphopgenesis. *Virology Journal* **2**.

Byrd, C. M., Bolken, T. C., Mjalli, A. M. & other authors (2004). New class of orthopoxvirus antiviral drugs that block viral maturation. *J Virol* **78**, 12147-12156.

Cao, J. X., Gershon, P. D. & Black, D. N. (1995). Sequence analysis of HindIII Q2 fragment of capripoxvirus reveals a putative gene encoding a G-protein-coupled chemokine receptor homologue. *Virology* **209**, 207-212.

Cao, Z., Henzel, W. J. & Gao, X. (1996).IRAK: a kinase associated with the interleukin-1 receptor. *Science* **27**, 1128-1131.

Carter, G. C., Rodger, G., Murphy, B. J., Law, M., Krauss, O., Hollinshead, M. & Smith, G. L. (2003). Vaccinia virus cores are transported on microtubules. *J Gen Virol* **84**, 2443-2458.

Chang, H., Watson, J. C. & Jacobs, B. L. (1992). The E3L gene of vaccinia virus encodes an inhibitor of the interferon-induced, double-stranded RNA-dependent protein kinase. *PNAS* **89**, 4825-4829.

Chaudhri, G., Panchanathan, V., Bluethmann, H. & Karupiah, G. (2006). Obligatory requirement for antibody in recovery from a primary poxvirus infection. *J Virol* **80**, 6339-6344.

Chen, X., Schneller, S. W., Ikeda, S., Snoeck, R., ndrei, G., Balzarini, J. & e Clercq, E. (1993). Synthesis and antiviral activity of 5'-deoxypyrazofurin. *J Med Chem* **36**, 3727-3730.

Chertov, O., Ueda, H., Xu, L. L., Tani, K., Murphy, W. J., Wang, J. M., Howard, O. M. Z., Sayers, T. J. & Oppenheim, J. J. (1997). Identification of human neutrophil-derived cathepsin G and azurocidin/CAP37 as chemoattractants for mononuclear cells and neutrophils. *J Exp Med* **186**, 739-747.

Chomczynski, P. & Sacchi, N. (1987). Single-step method of RNA isolation by acid guanidinium thiocyanate-phenol-chloroform extraction. *Anal Biochem* **162**, 156-159.

Chu, R. S., Askew, D., Noss, E. H., Tobian, A., Krieg, A. M. & Harding, C. V. (1999). CpG oligodeoxynucleotides down-regulate macropahge class II MHC antigen processing. *J Immunol*, 1188-1194.

Chung, C. S., Hsiao, J. C., Chang, Y. S. & Chang, W. (1998).A27L Protein mediates vaccinia virus interaction with cell surface heparan sulfate. *J Virol* **72**, 1577-1585.

Ciesla, S. L., Trahan, J., Wan, W. B., Beadle, J. R., Aldern, K. A., Painter, G. R. & Hostetler, K. Y. (2003). Esterification of cidofovir with alkoxyalkanols increases oral bioavailability and diminishes drug accumulation in kidney. *Antiviral Res* **59**, 163-171.

Colamonici, O. R., Domanski, P., Sweitzer, S. M., Larner, A. & Buller, R. M. (1995). Vaccinia virus B18R gene encodes a type I interferon-binding protein that blocks interferon α/β transmembrane signaling. *J Biol Chem* **270**, 15974-15978.

Coley, W. B. (1893). The treatment of malignant tumors by repeated inoculations of erypsipelas: With a report of ten original cases. *Am J Med Sci*, 487.

Compton, T., Kurt-Jones, E. A., Boehme, K. W., Belko, J., Latz, E., Golenbock, D. T. & Finberg, R. W. (2003). Human cytomegalovirus activates inflammatory cytokine responses *via* CD14 and Toll-like receptor 2. *J Virol* **77**, 4588-4596.

Concha, N. O. & Abdel-Meguid, S. S. (2002). Controlling apoptosis by inhibition of caspases. *Curr Med Chem* **9**, 713-726.

Cooper, C. L., Davis, H. L., Morris, M. L. & other authors (2004). Safety and immunogenicity of CPG-B 7909 injection as an adjuvant to Fluarix influenza vaccine. *Vaccine* **22**, 3136-3143.

Crocker, P. L. (2005). Siglecs in innate immunity. *Curr Opin Pharmacol* **5**, 431-437.

Crowell, R. E., Heaphy, E., Valdez, Y. E., Mold, C. & Lehnert, B. E. (1992). Alveolar and interstitial macrophage populations in the murine lung. *Exp Lung Res* **18**, 435-446.

Cudmore, S., Cossart, P., Griffiths, G. & Way, M. (1995). Actin-based motility of vaccinia virus. *Nature* **378**, 636-638.

Cundy, K. C. (1999). Clinical pharmacokinetics of the antiviral nucleotide analogues cidofovir and adefovir. *Clin Pharmacokinet* **36**, 127-143.

Dajani, R., Zhang, Y., Taft, P. J., Travis, S. M., Olsen, A., Zabner, J., Welsh, M. J. & Engelhardt, J. F. (2005). Lysozyme secretion by submucosal glands protects the airway from bacterial infection. *Am J Respir Cell Mol Biol* **32**, 548-552.

Dales, S. (1990). Reciprocity in the interactions between the poxviruses and their host cells. *Ann Rev Micro* **44**, 173-192.

Datta, S. K., Redecke, V., Prillman, K. R. & other authors (2003).A subset of Toll-like recpetor ligands induces cross-presentation by bone marrow-derived dendritic cells. *J Immunol* **170**, 4102-4110.

Davies, M. V., Elroy-Stein, O., Jaqus, R., Moss, B. & Kaufman, R. J. (1992). The vaccinia virus K3L gene product potentiates translation by inhibiting double-stranded-RNA-activated protein kinase and phosphorylation of the alpha subunit of eukaryotic initiation factor 2. *J Virol* **66**, 1943-1950.

De Clercq, E. (1980). Antiviral and antitumor activities of 5-substituted 2'-deoxyuridines. *Methods Find Exp Clin Pharmacol* **2**, 253-267.

De Clercq, E. (2002). Cidofovir in the treatment of poxvirus infections. *Antiviral Res* **55**, 1-13.

De Clercq, E. (2007). Acyclic nucleoside phosphonates: Past, present and future: Bridging chemistry to HIV, HBV, HCV, HPV, adeno-, herpes-, and poxvirus infections: The phosphonate bridge. *Biochem Pharmacol* **73**, 911-922.

De Clercq, E., Bergstrom, D. E., Holy, A. & Montgomery, J. A. (1984). Broad-spectrum antiviral activity of adenosine analogues. *Antiviral Res* **4**, 119-133.

De Clercq, E. & Montgomery, J. A. (1983). Broad-spectrum antiviral activity of the carbocyclic analog of 3-deazaadenosine. *Antiviral Res* **3**, 17-24.

De Clercq, E., Murase, J. & Marquez, V. E. (1991). Broad-spectrum antiviral and cytocidal activity of cyclopentenylcytosine, a carbocyclic nucleoside targeted at CTP synthetase. *Biochem Pharmacol* **41**, 1821-1829.

Deane, D., McInnes, C. J., Percival, A. & other authors (2000). Orf virus encodes a novel secreted protein inhibitor of granulocyte-macrophage colony-stimulating factor and interleukin-2. *J Virol* **74**, 1313-1320.

Dehring, D. J. & Wismar, B. L. (1989). Intravascular macrophages in pulmonary capillaries of humans. *Am Rev Respir Dis* **139**, 1027-1029.

Demedts, I. K., Bracke, K. R., Maes, T., Joos, G. F. & Brusselle, G. G. (2006). Different roles for human lung dendritic cell subsets in pulmonary immune defense mechanisms. *Am J Respir Cell Mol Biol* **35**, 387-393.

Deng, J. C., Moore, T. A., Newstead, M. W., Zeng, X., Krieg, A. M. & Standiford, T. J. (2004). CpG oligodeoxynucleotides stimulate protective innate immunity against pulmonary Klebsiella infection. *J Immunol* **173**, 5148-5155.

Diebold, S. S., Kaisho, T., Hemmi, H., Akira, S. & Reis e Sousa, C. (2004). Innate antiviral responses by means of TLR7-medaited recognition of single-stranded RNA. *Science* **303**, 1531.

DiPerna, G., Stack, J., Bowie, A. G. & other authors (2004). Poxvirus protein N1L targets the I-κB kinase complex, inhibits signaling to NF-κB by the tumor necrosis factor superfamily of receptors, and inhibits NF-κB and IRF3 signaling by toll-like receptors. *J Biol Chem* **279**, 36570-36578.

Dobbelstein, M. & Shenk, T. (1996). Protection against apoptosis by the vaccinia virus SPI-2 (B13R) gene product. *J Virol* **70**, 6479-6485.

Dorger, M., Munzing, S., Allmeling, A. M., Messmer, K. & Krombach, F. (2001). Phenotypic and functional differences between rat alveolar, pleural, and peritoneal macrophages. *Exp Lung Res* **27**, 65-76.

Easton, A., Haque, A., Chu, K., Lukaszewski, R., Bancroft, G. J. (2007). A critical role for neutrophils in resistance to experimental infection with Burkholderia pseudomallei. *J.Infect Dis* **195**, 99-107.

Edwards, L., Williams, A. E., Krieg, A. M., Rae, A. J., Snelgrove, R. & Hussell, T. (2005). Stimulation *via* Toll-like receptor 9 reduces Cryptococcus neoformans-induced pulmonary inflammation in an IL-12-dependent manner. *Eur J Immunol* **35**, 273-281.

Elkins, K. L., Bosio, C. M. & Rhinehart-Jones, T. R. (1999a). Importance of B cells, but not specific antibodies, in primary and secondary protective immunity to the intracellular bacterium *Francisella tularensis* live vaccine strain. *Infect Immun* **67**, 6002-6007.

Elkins, K. L., Rhinehart-Jones, T. R., Stibitz, S., Conover, J. S. & Klinman, D. M. (1999b). Bacterial DNA containing CpG motifs stimulates lymphocyte-dependent protection of mice against lethal infection with intracellular bacteria. *J Immunol* **162**, 2291-2298.

Este, J. A. & Telenti, A. (2007).HIV entry inhibitors. *Lancet* **370**, 81-88.

Ethuin, F., Gerard, B., Benna, J. E., Boutten, A., Gougereot-Pocidalo, M. A., Jacob, L. & Chollet-Martin, S. (2004). Human neutrophils produce interferon gamma upon stimulation by interleukin-12. *Lab Invest* **84**, 1363-1371.

Fathi, M., Johansson, A., Lundborg, M., Orre, L., Skold, C. M. & Camner, P. (2001). Functional and morphological differences between human alveolar and interstitial macrophages. *Exp Mol Pathol* **70**, 77-82.

Fenner, F., Anderson, D. A., Arita, I., Jezek, Z. & Ladnyi, I. D. (1998). Smallpox and its eradication. *World Health Organisation, Geneva.*

Fernandez, S., Jose, P., Avdiushko, M. G., Kaplan, A. M. & Cohen, D. A. (2004). Inhibition of IL-10 receptor function in alveolar macrophages by toll-like receptor agonists. *J Immunol* **172**, 2613-2620.

Fokkens, W. J. & Scheeren, R. A. (2000). Upper airway defence mechanisms. *Paediatr Respir Rev* **1**, 336-341.

Freeman, S. & Gardiner, J. M. (1996). Acyclic nucleosides as antiviral compounds. *Mol Biotechnol* **5**, 125-137.

Fulginiti, V. A., Papier, A., Lane, J. M., Neff, J. M. & Henderson, D. A. (2003). Smallpox vaccination: a review, part II. Adverse events. *Clin Infect Dis* **37**, 251-271.

Gao, J., Diesl, V., Wittmann, T., Morrison, D. C., Ryan, J. L., Vogel, S. N. & Follettie, M. T. (2002). Regulation of gene expression in mouse macrophages stimulated with bacterial CpG-DNA and lipopolysaccharide. *J Leukoc Biol* **72**, 1234-1245.

Garcel, A., Crance, J. M., Drillien, R., Garin, D. & Favier, A. L. (2007). Genomic sequence of a clonal isolate of the vaccinia virus Lister strain employed for smallpox vaccination in France and its comparison to other orthopoxviruses. *J Gen Virol* **88**, 1906-1916.

Gardner, J. D., Tscharke, D. C., Reading, P. C. & Smith, G. L. (2001). Vaccinia virus semaphorin A39R is a 50-55 kDa secreted glycoprotein that affects the outcome of infection in a murine intradermal model. *J Gen Virol* **82**, 2083-2093.

Gedey, R., Jin, X. L., Hinthong, O. & Shisler, J. L. (2006). Poxviral regulation of the host NF-κB response: the vaccinia virus M2L protein inhibits induction of NF-κB activation *via* an ERK2 pathway in virus-infected human embryonic kidney cells. *J Virol* **80**, 8676-8685.

Geissmann, F., Jung, S. & Littman, D. R. (2003). Blood monocytes consist of two principal subsets with distinct migratory properties. *Immunity* **19**, 71-82.

Ghosh, D. K., Misukonis, M. A., Reich, C., Pisetsky, D. S. & Weinberg, J. B. (2001). Host response to infection: the role of CpG DNA in induction of cyclooxygenase 2 and nitric oxide synthase 2 in murine macrophages. *Infect Immun* **69**, 7703-7710.

Giamila, F. & Charles, A. D. (1999). Interleukin-18 and interleukin-1β: Two cytokine substrates for ICE (Caspase-1). *J Clin Immunol* **V19**, 1-11.

Goebel, S. J., Johnson, G. P., Perkus, M. E., Davis, S. W., Winslow, J. P. & Paoletti, E. (1990). The complete DNA sequence of vaccinia virus. *Virology* **179**, 247, 513-266, 563.

Gorden, K. K. B., Qiu, X., Battiste, J. J. L., Wightman, P. P. D., Vasilakos, J. P. & Alkan, S. S. (2006). Oligodeoxynucleotides differentially modulate activation of TLR7 and TLR8 by imidazoquinolines. *J Immunol* **177**, 8164-8170.

Gordon, S. & Taylor, P. R. (2005). Monocyte and macrophage heterogeneity. *Nat Rev Immunol* **5**, 953-964.

Graham, K. A., Lalani, A. S., Macen, J. L. & other authors (1997). The T1/35kDa family of poxvirus-secreted proteins bind chemokines and modulate leukocyte influx into virus-infected tissues. *Virology* **229**, 12-24.

Gramzinski, R. A., Doolan, D. L., Sedegah, M., Davis, H. L., Krieg, A. M. & Hoffman, S. L. (2001). Interleukin-12- and gamma interferon-dependent protection against malaria conferred by CpG oligodeoxynucleotide in mice. *Infect Immun* **69**, 1643-1649.

Greene, W. C. (2004). The brightening future of HIV therapeutics. *Nat Immunol* **5, 867 - 871**, 867-871.

Gu, M., Hine, P. M., James Jackson, W., Giri, L. & Nabors, G. S. (2007). Increased potency of BioThrax(R) anthrax vaccine with the addition of the C-class CpG oligonucleotide adjuvant CPG 10109. *Vaccine* **25**, 526-534.

Gubser, C., Bergamaschi, M., Hollinshead, M., Lu, X., van kuppeveld, F. J. & Smith, G. L. (2007).A new inhibitor of apoptosis from vaccinia virus and eukaryotes. *PLoS Pathog* **3**, e17.

Gursel, I., Gursel, M., Yamada, H., Ishii, K. J., Takeshita, F. & Klinman, D. M. (2003). Repetitive elements in mammalian telomeres suppress bacterial DNA-induced immune activation. *J Immunol* **171**, 1393-1400.

Hacker, H., Mischak, H., Miethke, T., Liptay, S., Schmid, R., Sparwasser, T., Heeg, K., Lipford, G. B. & Wagner, H. (1998). CpG-DNA-specific activation of antigen-presenting cells requires stress kinase activity and is preceded by non-specific endocytosis and endosomal maturation. *EMBO J* **17**, 6230-6240.

Hadziyannis, S. J., Tassopoulos, N. C., Heathcote, E. J. & other authors (2005). Long-term therapy with adefovir dipivoxil for HBeAg-negative chronic hepatitis B. *New Engl J Med* **352**, 2673-2681.

Haga, I. R. & Bowie, A. G. (2005). Evasion of innate immuntiy by vaccinia virus. *Parasitology* **130**, S11-S25.

Haller, O., Kochs, G. & Weber, F. (2006). The interferon response circuit: Induction and suppression by pathogenic viruses. *Virology* **344**, 119-130.

Halperin, S. A., Van Nest, G., Smith, B., Simin, A., Whiley, H. & Eiden, J. J. (2003).A phase I study of the safety and immunogenicity of recombinant hepatitis B surface antigen co-administered with animmunostimulatory phosphorothioate oligonucleotide adjuvant. *Vaccine* **21**, 2461-2467.

Harandi, A. M., Eriksson, K. & Holmgren, J. (2003).A protective role of locally administered immunostimulatory CpG oligodeoxynucleotide in a mouse model of genital herpes infection. *J Virol* **77**, 953-962.

Harris, N., Buller, R. M. & Karupiah, G. (1995). Gamma interferon-induced, nitric oxide-mediated inhibition of vaccinia virus replication. *J Virol* **69**, 910-915.

Harte, M. T., Haga, I. R., Maloney, G., Gray, P., Reading, P. C., Bartlett, N. W., Smith, G. L., Bowie, A. & O'Neill, L. A. J. (2003). The poxvirus protein A52R targets toll-like receptor signaling complexes to suppress host defense. *J Exp Med* **197**, 343-351.

Hartmann, G., Battiany, J., Poeck, H., Wagner, M., Kerkmann, M., Lubenow, W., Rothenfusser, S. & Endres, S. (2003). Rational design of new CpG oligonucleotides that combine B cell activation with high IFN-alpha induction in plasmacytoid dendritic cells. *Eur J Immunol* **33**, 1633-1641.

Hartmann, G. & Krieg, A. M. (2000). Mechanism and Function of a Newly Identified CpG DNA Motif in Human Primary B Cells. *J Immunol* **164**, 944-953.

Hasan, U., Chaffois, C., Gaillard, C., Saulnier, V., Merck, E., Tancredi, S., Guiet, C., Brière, J., Vlach, J & other authors. (2005). Human TLR10 is a functional receptor, expressed by B cells and plasmacytoid dendritic cells, which activates gene transcription through MyD88. *J Immunol* **174**, 2942-2950.

Haslett, C. (1999). Granulocyte apoptosis and its role in the resolution and control of lung inflammation. *Am J Respir Crit Care Med* **160**, 5S-11.

Hayasaka, D., Ennis, F.A. & Terajima, M. (2007). Pathogeneses of respiratory infections with virulent and attenuated vaccinia viruses. *Virol J* **4**, 22.

Hayashi, F., Means, T. K. & Luster, A. D. (2003). Toll-like receptors stimulate human neutrophil function. *Blood* **102**, 2660-2669.

Hayden, F. G., Osterhaus, A. D. M. E., Treanor, J. J. & other authors (1997). Efficacy and Safety of the neuraminidase inhibitor zanamivir in the treatment of influenza virus infections. *New Engl J Med* **337**, 874-880.

He, B., Qiao, X. & Cerutti, A. (2004). CpG DNA induces IgG class switch DNA recombination by activating human B Cells through an innate pathway that requires TLR9 and cooperates with IL-10. *J Immunol* **173**, 4479-4491.

He, H., Crippen, T. L., Farnell, M. B. & Kogut, M. H. (2003). Identification of CpG oligodeoxynucleotide motifs that stimulate nitric oxide and cytokine production in avian macrophage and peripheral blood mononuclear cells. *Dev Comp Immunol* **27**, 621-627.

Heikenwalder, M., Polymenidou, M., Junt, T., Sigurdson, C., Wagner, H., Akira, S., Zinkernagel, R. & Aguzzi, A. (2004). Lymphoid follicle destruction and immunosuppression after repeated CpG oligodeoxynucleotide administration. *Nat Med* **10**, 187-192.

Heil, F., Hemmi, H., Hochrein, H., Ampenberger, F., Kirschning, C. J., Akira, S., Lipford, G. B., Wagner, H. & Bauer, S. (2004). Species-specific recognition of single-stranded RNA *via* toll-like recetor 7 and 8. *Science* **303**, 1526-1529.

Hemmi, H., Takeuchi, O., Kawai, T. & other authors (2000). A Toll-like receptor recognizes bacterial DNA. *Nature* **408**, 740-745.

Holt, P. G. (1986). Down-regulation of immune responses in the lower respiratory tract: the role of alveolar macrophages. *Clin Exp Immunol* **63**, 261-270.

Holt, P. G., Oliver, J., Bilyk, N., McMenamin, C., McMenamin, P. G., Kraal, G. & Thepen, T. (1993). Downregulation of the antigen presenting cell function(s) of pulmonary dendritic cells *in vivo* by resident alveolar macrophages. *J Exp Med* **177**, 397-407.

Honda, K. & Taniguchi, T. (2006).IRFs: master regulators of signaling by Toll-like receptors and cytosolic pattern-recognition receptors. *Nat Rev Immunol* **6**, 644-658.

Hornung, V., Ellegast, J., Kim, S. & other authors (2006).5'-Triphosphate RNA is the ligand for RIG-I. *Science* **314**, 994-997.

Hornung, V., Rothenfusser, S., Britsch, S., Krug, A., Jahrsdorfer, B., Giese, T., Endres, S. & Hartmann, G. (2002). Quantitative expression of toll-like receptor 1-10 mRNA in cellular subsets of human peripheral blood mononuclear cells and sensitivity to CpG oligodeoxynucleotides. *J Immunol* **168**, 4531-4537.

Hsiao, J. C., Chung, C. S. & Chang, W. (1999). Vaccinia virus envelope D8L protein binds to cell surface chondroitin sulfate and mediates the adsorption of intracellular mature virions to cells. *J Virol* **73**, 8750-8761.

Huang, H., Jiang, J. X., Zhu, P. F., Wang, Z. G., Zhang, D. J. & Yang, C. (2005). The synergistic effects of lipopolysaccharide, bacterial lipoprotein and bacterial DNA on mouse alveolar macrophage activation. *Zhonghua Yi Xue Za Zhi* **85**, 1468-1472.

Humlova, Z., Vokurka, M., Esteban, M. & Melkova, Z. (2002). Vaccinia virus induces apoptosis of infected macrophages. *J Gen Virol* **83**, 2821-2832.

Hutchens, M., Luker, K. E., Sottile, P., Sonstein, J., Lukacs, N. W., Nunez, G., Curtis, J. L. & Luker, G. D. (2008).TLR3 increases dieases morbidity and mortality from vaccinia infection. *J Immunol* **180**, 483-491.

Husain, M. & Moss, B. (2003). Intracellular trafficking of a palmitoylated membrane-associated protein component of enveloped vaccinia virus. *J Virol* **77**, 9008-9019.

Ichihashi, Y. A. S. U. (1996). Extracellular enveloped vaccinia virus escapes neutralization. *Virology* **217**, 478-485.

Ichihashi, Y., Matsumoto, S. & Dales, S. (1971). Biogenesis of poxviruses: Role of A-type inclusions and host cell membranes in virus dissemination. *Virology* **46**, 507-532.

Imlach, W., McCaughan, C. A., Mercer, A. A., Haig, D. & Fleming, S. B. (2002). Orf virus-encoded interleukin-10 stimulates the proliferation of murine mast cells and inhibits cytokine synthesis in murine peritoneal macrophages. *J Gen Virol* **83**, 1049-1058.

Isaacs, S. N., Kotwal, G. J. & Moss, B. (1992). Vaccinia virus complement-control protein prevents antibody-dependent complement-enhanced neutralization of infectivity and contributes to virulence. *PNAS* **89**, 628-632

Ishii, K. K., Coban, C., Kato, H., Takahashi, K., Torii, Y., Takeshita, F., Ludwig, H., Sutter, G., Suzuki, K & other authors. (2006). A Toll-like receptor-independent antiviral response induced by double-stranded B-form DNA. *Nat Immunol* **7**, 40-48.

Iwasaki, A. & Medzhitov, R. (2004). Toll-like receptor control of the adaptive immune responses. *Nat Immunol* **5**, 987-995.

Jain, V. V., Kitagaki, K., Businga, T., Hussain, I., George, C., O'shaughnessy, P. & Kline, J. N. (2002). CpG-oligodeoxynucleotides inhibit airway remodeling in a murine model of chronic asthma. *J Allergy Clin Immunol* **110**, 867-872.

Jegerlehner, A., Maurer, P., Bessa, J., Hinton, H. J., Kopf, M. & Bachmann, M. F. (2007).TLR9 signaling in B Cells determines class switch recombination to IgG2a. *J Immunol* **178**, 2415-2420.

Juffermans, N. P., Leemans, J. C., Florquin, S., Verbon, A., Kolk, A. H., Speelman, P., van Deventer, S. J. H. & van der Poll, T. (2002). CpG oligodeoxynucleotides enhance host defense during murine tuberculosis. *Infect Immun* **70**, 147-152.

Jung, J., Yi, A. K., Zhang, X., Choe, J., Li, L. & Choi, Y. S. (2002). Distinct response of human B Cell subpopulations in recognition of an innate immune signal, CpG DNA. *J Immunol* **169**, 2368-2373.

Jurk, M., Schulte, B., Kritzler, A., Noll, B., Uhlmann, E., Wader, T., Schetter, C., Krieg, A. M. & Vollmer, J. (2004).C-Class CpG ODN: sequence requirements and characterization of immunostimulatory activities on mRNA level. *Immunobiol* **209**, 141-154.

Jurk, M. & Vollmer, J. (2007). Therapeutic applications of synthetic CpG oligodeoxynucleotides as TLR9 agonists for immune modulation. *BioDrugs* **21**, 387-401.

Kaplanski, G., Marin, V., Montero-Julian, F., Mantovani, A. & Farnarier, C. (2003).IL-6: a regulator of the transition from neutrophil to monocyte recruitment during inflammation. *Trends Immunol* **24**, 25-29.

Karlin, S., Doerfler, W. & Cardon, L. R. (1994). Why is CpG suppressed in the genomes of virtually all small eukaryotic viruses but not in those of large eukaryotic viruses? *J Virol* **68**, 2889-2897.

Karupiah, G., Buller, R. M., Van Rooijen, N., Duarte, C. J. & Chen, J. (1996). Different roles for CD4+ and CD8+ T lymphocytes and macrophage subsets in the control of a generalized virus infection. *J Virol* **70**, 8301-8309.

Karupiah, G. & Harris, N. (1995). Inhibition of viral replication by nitric oxide and its reversal by ferrous sulfate and tricarboxylic acid cycle metabolites. *J Exp Med* **181**, 2171-2179.

Karupiah, G., Xie, Q. W., Buller, R. M., Nathan, C., Duarte, C. & MacMicking, J. D. (1993). Inhibition of viral replication by interferon-gamma-induced nitric oxide synthase. *Science* **261**, 1445-1448.

Kato, H., Takeuchi, O., Sato, S., Yoneyama, M., Yamamoto, M., Matsui, K., Uematsu, S., Jung, A., Kawai, T & other authors. (2006). Differential roles of MDA5 and RIG-I helicases in the recognition of RNA viruses. *Nature* **441**, 101-105.

Katze, M. G., He, Y. & Gale, M. (2002). Viruses and interferon: A fight for supremacy. *Nat Rev Immunol* **2**, 675-687.

Kawai, T. & Akira, S. (2007).TLR signaling. *Sem Immunol* **19**, 24-32.

Kawai, T., Sato, S., Ishii, K. J. & other authors (2004). Interferon-α induction through Toll-like receptors involves a direct interaction of IRF7 with MyD88 and TRAF6. *Nat Immunol* **5**, 1061-1068.

Keith, K. A., Wan, W. B., Ciesla, S. L., Beadle, J. R., Hostetler, K. Y. & Kern, E. R. (2004). Inhibitory activity of alkoxyalkyl and alkyl esters of cidofovir and cyclic cidofovir against orthopoxvirus replication *in vitro*. *Antimicrob Agents Chemother 2004* **48**, 1869-1871.

Kerkmann, M., Costa, L. T., Richter, C. & other authors (2005). Spontaneous formation of nucleic acid-based nanoparticles is responsible for high interferon-α induction by CpG-A in plasmacytoid dendritic cells. *J Biol Chem* **280**, 8086-8093.

Kern, E. R., Hartline, C., Harden, E., Keith, K., Rodriguez, N., Beadle, J. R. & Hostetler, K. Y. (2002). Enhanced inhibition of orthopoxvirus replication *in vitro* by alkoxyalkyl esters of cidofovir and cyclic cidofovir. *Antimicrob Agents Chemother* **46**, 991-995.

Kettle, S., Blake, N. W., Law, K. M. & Smith, G. L. (1995). Vaccinia virus serpins B13R (SPI-2) and B22R (SPI-1) encode Mr 38.5 and 40K, intracellular polypeptides that do not affect virus virulence in a murine intranasal model. *Virology* **206**, 136-147.

Kibler, K. V., Shors, T., Perkins, K. B., Zeman, C. C., Banaszak, M. P., Biesterfeldt, J., Langland, J. O. & Jacobs, B. L. (1997). Double-stranded RNA is a trigger for apoptosis in vaccinia virus- infected cells. *The Journal of Virology* **71**, 1992-2003.

Kilby, J. M., Hopkins, S., Venetta, T. M. & other authors (1998). Potent suppression of HIV-1 replication in humans by T-20, a peptide inhibitor of gp41-mediated virus entry. *Nat Med* **4**, 1302-1307.

Kitagaki, K., Jain, V. V., Businga, T., Hussain, I. & Kline, J. N. (2002). Immunomodulatory effects of CpG oligodeoxynucleotides on established th2 responses. *Clin Diagn Lab Immunol* **9**, 1260-1269.

Klesney-Tait, J., Turnbull, I. R. & Colonna, M. (2006). The TREM receptor family and signal integration. *Nat Immunol* **7**, 1268-1273.

Kline, J. N., Waldschmidt, T. J., Businga, T. R., Lemish, J. E., Weinstock, J. V., Thorne, P. S. & Krieg, A. M. (1998). Cutting Edge: Modulation of airway inflammation by CpG oligodeoxynucleotides in a murine model of asthma. *J Immunol* **160**, 2555-2559.

Klinman, D. M. (2006). CpG oligonucleotides accelerate and boost the immune response elicited by AVA, the licensed anthrax vaccine. *Expert Rev Vaccines* **5**, 365-369.

Klinman, D. M., Conover, J. & Coban, C. (1999). Repeated administration of synthetic oligodeoxynucleotides expressing CpG motifs provides long-term protection against bacterial infection. *Infect Immun* **67**, 5658-5663.

Klinman, D. M., Gursel, I., Klaschik, S., Dong, L., Currie, D. & Shirota, H. (2005). Therapeutic potential of oligonucleotides expressing immunosuppressive TTAGGG motifs. In *Therapeutic oligonucleotides: Transcriptional and translation strategies for silencing gene expression, Annals of the New York academy of sciences* 87-95.

Klinman, D. M., Yi, A. K., Beaucage, S. L., Conover, J. & Krieg, A. M. (1996). CpG motifs present in bacterial DNA rapidly induce lymphocytes to secrete interleukin 6,interleukin 12,and interferon gamma. *PNAS* **93**, 2879-2883.

Knapp, S., Leemans, J. C., Florquin, S., Branger, J., Maris, N. A., Pater, J., van Rooijen, N. & van der Poll, T. (2003). Alveolar macrophages have a protective antiinflammatory role during murine pneumococcal pneumonia. *Am J Respir Crit Care Med* **167**, 171-179.

Kobzik, L., Godleski, J. J., Barry, B. E. & Brain, J. D. (1988). Isolation and antigenic identification of hamster lung interstitial macrophages. *Am Rev Respir Dis* **138**, 908-914.

Kopf, M., Baumann, H., Freer, G., Freudenberg, M., Lamers, M., Kishimoto, T., Zinkernagel, R., Bluethmann, H. & Kohler, G. (1994). Impaired immune and acute-phase responses in interleukin-6-deficient mice. *Nature* **368**, 339-342.

Kotenko, S. V., Gallagher, G., Baurin, V. V. & other authors (2003).IFN-λs mediate antiviral protection through a distinct class II cytokine receptor complex. *Nat Immunol* **4**, 69-77.

Kotwal, G. J., Isaacs, S. N., McKenzie, R., Frank, M. M. & Moss, B. (1990). Inhibition of the complement cascade by the major secretory protein of vaccinia virus. *Science* **250**, 827-830.

Kotwal, G. J. & Moss, B. (1988). Vaccinia virus encodes a secretory polypeptide structurally related to complement control proteins. *Nature* **335**, 176-178.

Krieg, A. M. (2002). CpG motifs in bacterial DNA and their immune effects. *Annu Rev Immunol* **20**, 709-760.

Krieg, A. M. (2006). Therapeutic potential of Toll-like receptor 9 activation. *Nat Rev Drug Discovery* **5**, 471-484.

Krieg, A. M. (2007). Development of TLR9 agonists for cancer therapy. *J Clin Invest* **117**, 1184-1194.

Krieg, A. M., Matson, S. & Fisher, E. (1996). Oligodeoxynucleotide modifications determine the magnitude of B cell stimulation by CpG motifs. *Antisense Nucleic Acid Drug Dev* **6**, 133-139.

Krieg, A. M., Wu, T., Weeratna, R., Efler, S. M., Love-Homan, L., Yang, L., Yi, A. K., Short, D. & Davis, H. L. (1998). Sequence motifs in adenoviral DNA block immune activation by stimulatory CpG motifs. *PNAS* **95**, 12631-12636.

Krieg, A. M., Yi, A. K., Matson, S., Waldschmidt, T. J., Bishop, G. A., Teasdale, R., Koretzky, G. A. & Klinman, D. M. (1995). CpG motifs in bacterial DNA trigger direct B-cell activation. *Nature* **374**, 546-549.

Krug, A., Luker, G. D., Barchet, W., Lieb, D. A., Akira, S. & Colonna, M. (2004). Herpers simplex virus type-1 activates murine natural interferon-producing cells through Toll-like receptor 9. *Blood* **103**, 1433-1437.

Krug, A., Rothenfusser, S., Hornung, V., Jahrsdorfer, B., Blackwell, S., Ballas, Z. K., Endres, S., Krieg, A. M. & Hartmann, G. (2001). Identification of CpG oligonucleotide sequences with high induction of IFN-alpha/beta in plasmacytoid dendritic cells. *Eur J Immunol* **31**, 2154-2163.

Kruzel, M. L., Bacsi, A., Choudhury, B., Sur, S. & Boldogh, I. (2006). Lactoferrin decreases pollen antigen-induced allergic airway inflammation in a murine model of asthma. *Immunology* **119**, 159-166.

Kumagai, Y., Takeuchi, O. & Akira, S. (2008).TLR9 as a key receptor for the recognition of DNA. *Adv Drug Deliv Rev*, In press.

Kumagai, Y., Takeuchi, O., Kato, H., Kumar, H., Matsui, K., Morii, E., Aosaza, K., Kawai, T. & Akira, S. (2007). Alveolar macrophages are the primary interferon-alpha producer in pulmonary infection with RNA viruses. *Immunity* **27**, 240-252.

Kuramoto, E., Yano, O., Kimura, Y., Baba, M., Makino, T., Yamamoto, S., Yamamoto, T., Kataoka, T. & Tokunaga, T. (1992). Oligonucleotide sequences required for natural killer cell activation. *Jpn J Cancer Res* **83**, 1128-1131.

Kurt-Jones, E. A., Popova, L., Kwinn, L. & other authors (2000). Pattern recognition receptors TLR4 and CD14 mediate response to respiratory syncytial virus. *Nat Immunol* **1**, 398-401.

Lalani, A. S., Graham, K., Mossman, K., Rajarathnam, K., Clark-Lewis, I., Kelvin, D. & McFadden, G. (1997). The purified myxoma virus gamma interferon receptor homolog M-T7 interacts with the heparin-binding domains of chemokines. *J Virol* **71**, 4356-4363.

Lalezari, J. P. (1997). Cidofovir: a new therapy for cytomegalovirus retinitis. *J Acquir Immune Defic Syndr Hum Retrovirol* **14**, S22-S26.

Lane, J. M., Ruben, F., Neff, J. M. & Millar, J. D. (1970). Complications of smallpox vaccination, 1968: results of ten statewide surveys. *J Infect Dis* **122**, 303-309.

Langland, J. O., Kash, J. C., Carter, V., Thomas, M. J., Katze, M. G. & Jacobs, B. L. (2006). Suppression of proinflammatory signal transduction and gene expression by the dual nucleic acid binding domains of the vaccinia virus E3L proteins. *J Virol* **80**, 10083-10095.

Laskin, D. L., Weinberger, B. & Laskin, J. D. (2001). Functional heterogeneity in liver and lung macrophages. *J Leukoc Biol* **70**, 163-170.

Latz, E., Schoenemeyer, A., Visintin, A. & other authors (2004).TLR9 signals after translocating from the ER to CpG DNA in the lysosome. *Nat Immunol* **5**, 190-198.

Latz, E., Verma, A., Visintin, A. & other authors (2007). Ligand-induced conformational changes allosterically activate Toll-like receptor 9. *Nat Immunol* **8**, 772-779.

Lauw, F. N., Pajkrt, D., Hack, C. E., Kurimoto, M., van Deventer, S. J. H. & van der Poll, T. (2000). Proinflammatory effects of IL-10 during human endotoxemia. *J Immunol* **165**, 2783-2789.

Lehmann, C., Sprenger, H., Nain, M., Bacher, M. & Gemsa, D. (1996). Infection of macrophages by influenza A virus:characteristics of tumour necrosis factor-alpha (TNF-a) gene expression. *Res Virol* **147**, 123-130.

Lehrer, R. I. (2004). Primate defensins. *Nat Rev Microbiol* **2**, 727-738.

Lemaitre, B., Nicolas, E., Michaut, L., Reichhart, J. M. & Hoffmann, J. A. (1996). The dorsoventral regulatory gene cassette spatzle/Toll/cactus controls the potent antifungal response in drosophila adults. *Cell* **86**, 973-983.

Levy, H. B. & Lvovsky, E. (1978). Topical treatment of vaccinia virus infection with an interferon inducer in rabbits. *J Infect Dis* **137**, 78-81.

Ley, K., Laudanna, C., Cybulsky, M. I., Nourshargh, S. (2007). Getting to the site of inflammation: the leukocyte adhesion cascade updated. *Nat Rev Imm* **7**, 678-689.

Li, N., Fan, X. G., Chen, Z. H., Zhu, C., Liu, H. B. & Huang, Y. (2006). Inhibition of the hepatitis B virus replication *in vitro* by an oligodeoxynucleotide containing cytidine-guanosine motifs. *Immunol Lett* **102**, 60-66.

Li, Q. & Verma, I. M. (2002).NF-κB regulation in the immune system. *Nat Rev Immunol* **2**, 725-734.

Lidbury, B. A., Ramshaw, I. A. & Sambhi, S. K. (1995). The role for host-immune factors in the *in vivo* antiviral effects of tumour necrosis factor. *Cytokine* **7**, 157-164.

Lin, C. L., Chung, C. S., Heine, H. G. & Chang, W. (2000). Vaccinia virus envelope H3L protein binds to cell surface heparan sulfate and is important for intracellular mature virion morphogenesis and virus infection *in vitro* and *in vivo*. *J Virol* **74**, 3353-3365.

Lin, L., Gerth, A. J. & Peng, S. L. (2004). CpG DNA redirects class-switching towards "Th-1-like" Ig isotype production *via* TLR9 and MyD88. *European J Immunol* **34**, 1483-1487.

Link, B. K., Ballas, Z. K., Weisdorf, D., Wooldridge, J. E., Bossler, A. D., Shannon, M., Rasmussen, W. L., Krieg, A. M. & Weiner, G. J. (2006). Oligodeoxynucleotide CpG-B 7909 delivered as intravenous infusion demonstrates immunologic modulation in patients with previously treated non-Hodgkin lymphoma. *J Immunother* **29**, 558-568.

Liu, G., Zhai, Q., Schaffner, D., Popova, T., Hayford, A., Bailey, C. & Alibek, K. (2004). Bacillus alcalophilus peptidoglycan induces IFN-alpha-mediated inhibition of vaccinia virus replication. *FEMS Immunol Med Microbiol* **42**, 197-204.

Livak, K. J. & Schmittgen, T. D. (2001). Analysis of relative gene expression data using real-time quantitative PCR and the 2-[Delta][Delta]CT Method. *Methods* **25**, 402-408.

Locker, J. K., Kuehn, A., Schleich, S., Rutter, G., Hohenberg, H., Wepf, R. & Griffiths, G. (2000). Entry of the two infectious forms of vaccinia virus at the plasma membane is signaling-dependent for the IMV but not the EEV. *Mol Biol Cell* **11**, 2497-2511.

Loparev, V. N., Parsons, J. M., Knight, J. C., Panus, J. F., Ray, C. A., Buller, R. M., Pickup, D. J. & Esposito, J. J. (1998).A third distinct tumor necrosis factor receptor of orthopoxviruses. *PNAS* **95**, 3786-3791.

Lucas, S., Schroder, M., Bowie, A. G. & Smith, G. L. (2007). Vaccinia virus protein K7 is an immunomodulator that inhibits multiple inflammatory signaling pathways. *SGM conference* **March 2007.**

Lund, J., Sato, A., Akira, S., Medzhitov, R. & Iwasaki, A. (2003). Toll-like recpetor 9-meidated recognition of Herpes simplex virus-2 by plasmacytoid dendritic cells. *J Exp Med* **198**, 513-520.

Macen, J. L., Garner, R. S., Musy, P. Y., Brooks, M. A., Turner, P. C., Moyer, R. W., McFadden, G. & Bleackley, R. C. (1996). Differential inhibition of the Fas- and granule-mediated cytolysis pathways by the orthopoxvirus cytokine response modifier A/SPI-2 and SPI-1 protein. *PNAS* **93**, 9108-9113.

Magee, W. C., Hostetler, K. Y. & Evans, D. H. (2005). Mechanism of inhibition of vaccinia virus DNA polymerase by cidofovir diphosphate. *Antimicrob Agents Chemother* **49**, 3153-3162.

Malmgaard, L., Melchjorsen, J., Bowie, A. G., Mogensen, S. C. & Paludan, S. R. (2004). Viral activation of macrophages through TLR-dependent and independent pathways. *J Immunol* **173**, 6890-6898.

Mariathasan, S. & Monack, D. M. (2007). Inflammasome adaptors and sensors: intracellular regulators of infection and inflammation. *Nat Rev Immunol* **7**, 31-40.

Marko, M., Chipperfield, R. & Birnboim, H. C. (1982).A procedure for the large-scale isolation of highly purified plasmid DNA using alkaline extraction and binding to glass powder. *Anal Biochem* **121**, 382-387.

Marshall, J. D., Fearon, K., Abbate, C., Submaranian, S., Yee, P., Gregorio, J., Coffman, R. L. & Van Nest, G. (2003). Identification of a novel CpG DNA class and motif that optimally stimulate B cell and plasmacytoid dendritic cell functions. *J Leukoc Biol* **73**, 781-792.

Marshall, J. D., Heeke, D. S., Abbate, C., Yee, P. & Van Nest, G. (2006). Induction of interferon-gamma from natural killer cells by immunostimulatory CpG DNA is mediated through plasmacytoid-dendritic-cell-produced interferon-alpha and tumour necrosis factor-alpha. *Immunology* **117**, 38-46.

Martin, T. R. & Frevert, C. W. (2005). Innate immunity in the lungs. *PATS* **2**, 403-411.

Martinon, F., Burns, K. & Tschopp, J. (2002). The inflammasome: A molecular platform triggering activation of inflammatory caspases and processing of proIL-β. *Molecular Cell* **10**, 417-426.

Massung, R. F., Jayarama, V. & Moyer, R. W. (1993).DNA sequence analysis of conserved and unique regions of swinepox virus: Identification of genetic elements supporting phenotypic observations including a novel G protein-coupled receptor homologue. *Virology* **197**, 511-528.

Matsuzaki, J., Tsuji, T., Chamoto, K., Takeshima, T., Sendo, F. & Nishimura, T. (2003). Successful elimination of memory-type CD8+ T cell subsets by the administration of anti-Gr-1 monoclonal antibody *in vivo*. *Cell Immunol* **224**, 98-105.

Maxeiner, J. H., Karwot, R., Hausding, M., Sauer, K. A., Scholtes, P. & Finotto, S. (2007).A method to enable the investigation of murine bronchial immune cells, their cytokines and mediators. *Nat Protoc* **2**, 105-112.

Mbawuike, I. N. & Herscowitz, H. B. (1989).MH-S, a murine alveolar macrophage cell line: morphological, cytochemical, and functional characteristics. *J Leukoc Biol* **46**, 119-127.

McHutchison, J. G., Bacon, B. R., Gordon, S. C. & other authors (2006). Early clinical results with CPG 10101, a new investigational antiviral TRL9 agonist being developed for treatment of subjects chronically infected with hepatitis C virus. *J Clin Virol* **36**, S31.

McIntosh, A.A. & Smith, G.L. (1996). Vaccinia virus glycoprotein A34R is required for infectivity of extracellular enveloped virus. *J Virol* **70**, 272-281.

Meadows, K. P., Tyring, S. K., Pavia, A. T. & Rallis, T. M. (1997). Resolution of recalcitrant molluscum contagiosum virus lesions in human immunodeficiency virus-infected patients treated with cidofovir. *Arch Dermatol* **133**, 987-990.

Medzhitov, R. & Janeway, J. (1997). Innate immunity: The virtues of a nonclonal system of recognition. *Cell* **91**, 295-298.

Medzhitov, R., Preston-Hurlburt, P. & Janeway, C. A., Jr. (1997).A human homologue of the Drosophila Toll protein signals activation of adaptive immunity. *Nature* **388**, 394-397.

Messina, J. P., Gilkeson, G. S. & Pisetsky, D. S. (1991). Stimulation of *in vitro* murine lymphocyte proliferation by bacterial DNA. *J Immunol* **147**, 1759-1764.

Messina, J. P., Gilkeson, G. S. & Pisetsky, D. S. (1993). The influence of DNA structure on the *in vitro* stimulation of murine lymphocytes by natural and synthetic polynucleotide antigens. *Cell Immunol* **147**, 148-157.

Meylan, E., Tschopp, J. & Karin, M. (2006). Intracellular pattern recognition receptors in the host response. *Nature* **442**, 39-44.

Milligan, G. N. (1999). Neutrophils aid in protection of the vaginal mucosae of immune mice against challenge with herpes simplex virus type 2. *J Virol* **73**, 6380-6386.

Morales-Montor, J. (2005). The role of the pleiotropic cytokine interleukin-6 (IL-6) during disease. *Mod Asp Immunobiol* **16**, 21-25.

Moss, B. (2006). Poxvirus entry and membrane fusion. *Virology* **344**, 48-54.

Mossman, K., Upton, C. & McFadden, G. (1995). The Myxoma virus-soluble Interferon-γ receptor homolog, M-T7, inhibits interferon-γ in a species-specific manner. *J Biol Chem* **270**, 3031-3038.

Muller, U., Steinhoff, U., Reis, L. F., Hemmi, S., Pavlovic, J., Zinkernagel, R. M. & Aguet, M. (1994). Functional role of type I and type II interferons in antiviral defense. *Science* **264**, 1918-1921.

Murad, Y. M., Clay, T. M., Lyerly, H. K. & Morse, M. A. (2007).CPG-7909 (PF-3512676, ProMune): toll-like receptor-9 agonist in cancer therapy. *Expert Opin Biol Ther* 7, 1257-1266.

Nakashima, H., Matsui, T., Harada, S., Kobayahsi, N., Matsuda, A., Ueda, T. & Yamamoto, N. (1986). Inhibition of replication and cytopathic effect of human T cell lymphotropic virus type III/lymphadenopathy-associated virus by 3'-azido-3'-deoxythymidine *in vitro*. *Antimicrob Agents Chemother* **30**, 933-937.

Nathan, C. (2006). Neutrophils and immunity: challenges and opportunities. *Nat Rev Immunol* **6**, 173-182.

Neujahr, D. C., Reich, C. F. & Pisetsky, D. S. (1999). Immunostimulatory properties of genomic DNA from different bacterial species. *Immunobiology* **200**, 106-119.

Neyrolles, O., Gicquel, B. & Quintana-Murci, L. (2006). Towards a crucial role for DC-SIGN in tuberculosis and beyond. *Trends Microbiol* **14**, 383-387.

Nicholson, K. G., Aoki, F. Y., Osterhaus, A. D. M. E., Trottier, S., Carewicz, O., Mercier, C. H., Rode, A., Kinnersley, N. & Ward, P. (2000). Efficacy and safety of oseltamivir in treatment of acute influenza: a randomised controlled trial. *Lancet* **355**, 1845-1850.

Ogle, C. K., Wu, J. Z., Mao, X., Szczur, K., Alexander, J. W. & Ogle, J. D. (1994). Heterogeneity of Kupffer cells and splenic, alveolar, and peritoneal macrophages for the production of TNF, IL-1, and IL-6. *Inflammation* **18**, 511-523.

Okabe, Y., Kawane, K., Akira, S., Taniguchi, T. & Nagata, S. (2005). Toll-like receptor-independent gene induction program activated by mammalian DNA escaped from apoptotic DNA degradation. *J Exp Med* **202**, 1333-1339.

Olbrich, A. R. M., Schimmer, S., Heeg, K., Schepers, K., Schumacher, T. N. M. & Dittmer, U. (2002). Effective postexposure treatment of Retrovirus-induced disease with immunostimulatory DNA containing CpG motifs. *J Virol* **76**, 11397-11404.

O'Neill, L. A. J. & Bowie, A. G. (2007). The family of five: TIR-domain-containing adaptors in Toll-like receptor signalling. *Nat Rev Immunol* 7, 353-364.

Oshikawa, K. & Sugiyama, Y. (2003). Gene expression of Toll-like receptors and associated molecules induced by inflammatory stimuli in the primary alveolar macrophage. *Biochem Biophys Res Commun* **305**, 649-655.

Parr, M. B. & Parr, E. L. (2000). Immunity to vaginal herpes simplex virus-2 infection in B-cell knockout mice. *Immunology* **101**, 126-131.

Parrino, J., McCurdy, L. H., Larkin, B. D. & other authors. (2007). Safety, immunogenicity and efficacy of modified Vaccinia Ankara (MVA) against Dryvax challenge in vaccinia-naïve and vaccinia-immune individuals. *Vaccine* **25**, 1513-1525.

Patick, A. K. & Potts, K. E. (1998). Protease inhibitors as antiviral agents. *Clin Microbiol Rev* **11**, 614-627.

Pedras-Vasconcelos, J. A., Goucher, D., Puig, M., Tonelli, L. H., Wang, V., Ito, S. & Verthelyi, D. (2006). CpG oligodeoxynucleotides protect newborn mice from a lethal challenge with the neurotropic Tacaribe arenavirus. *J Immunol* **176**, 4940-4949.

Penfold, M. E. T., Dairaghi, D. J., Duke, G. M., Saederup, N., Mocarski, E. S., Kemble, G. W. & Schall, T. J. (1999). Cytomegalovirus encodes a potent alpha chemokine. *PNAS* **96**, 9839-9844.

Pestka, S. (1986). Interferon standards and general abbreviations. *Methods Enzymol* **119**, 14-23.

Pilette, C., Ouadrhiri, Y., Godding, V., Vaerman, J. P. & Sibille, Y. (2001). Lung mucosal immunity: immunoglobulin-A revisited. *Eur Respir J* **18**, 571-588.

Platanias, L. C. (2005). Mechanisms of type-I- and type-II-interferon-mediated signaling. *Nat Rev Immunol* **5**, 375-386.

Platz, J., Beisswenger, C., Dalpke, A., Koczulla, R., Pinkenburg, O., Vogelmeier, C. & Bals, R. (2004). Microbial DNA induces a host defense reaction of human respiratory epithelial cells. *J Immunol* **173**, 1219-1223.

Pulford, D., Gates, A. J., Bridge, S. H., Robinson, J. H. & Ulaeto, D. O. (2004). Differential efficacy of vaccinia virus envelope proteins administered by DNA immunisation in protection of Balb/C mice from a lethal poxvirus challenge. *Vaccine* **22**, 3358-3566.

Quenelle, D. C., Collins, D. J., Wan, W. B., Beadle, J. R., Hostetler, K. Y. & Kern, E. R. (2004). Oral Treatment of cowpox and vaccinia virus infections in mice with ether lipid esters of cidofovir. *Antimicrob Agents Chemother* **48**, 404-412.

Racila, D. M. & Kline, J. N. (2005). Perspectives in asthma: Molecular use of microbial products in asthma prevention and treatment. *J Allergy Clin Immunol* **116**, 1202-1205.

Rahman, M. M. & McFadden, G. (2006). Modulation of tumor necrosis factor by microbial pathogens. *PLoS Pathog* **2**, e4.

Rankin, R., Pontarollo, R., Ioannou, X., Krieg, A. M., Hecker, R., Babiuk, LA. & van Drunen Littel-van den Hurk, S. (2001). CpG motif identification for veterinary and laboratory species demonstrates that sequence recognition is highly conserved. *Antisense Nucleic Acid Drug Dev* **11**, 333-340.

Rassa, J. C., Meyers, J. L., Zhang, Y., Kudaravalli, R. & Ross, S. R. (2002). Murine retroviruses activate B-cells *via* interaction with toll-like receptor 4. *PNAS* **99**, 2281-2286.

Razin, A. & Friedman, J. (1981).DNA methylation and its possible biological roles. *Prog Nucleic Acid Res Mol Biol* **25**, 33-52.

Reading, P. C. & Smith, G. L. (2003a). Vaccinia Virus interleukin-18-binding protein promotes virulence by reducing gamma interferon production and natural killer and T-cell activity. *J Virol* **77**, 9960-9968.

Reading, P. C. & Smith, G. L. (2003b). A kinetic analysis of immune mediators in the lungs of mice infected with Vaccinia virus and comparison of intradermal infection. *J Gen Virol* **84,** 1973-1983.

Reading, P. C., Khanna, A. & Smith, G. L. (2002). Vaccinia virus CrmE encodes a soluble and cell surface tumor necrosis factor receptor that contributes to virus virulence. *Virology* **292**, 285-298.

Reed, L. J. & Muench, H. (1938).A simple method of estimating fifty percent endpoints. *Am J Hyg* **27**, 493-497.

Rees, D. G. C., Gates, A. J., Green, M., Eastaugh, L., Lukaszewski, R. A., Griffin, K. F., Krieg, A. M. & Titball, R. W. (2005). CpG-DNA protects against a lethal orthopoxvirus infection in a murine model. *Antiviral Res* **65**, 87-95.

Reeves, P. M., Bommarius, B., Lebeis, S. & other authors (2005). Disabling poxvirus pathogenesis by inhibition of Abl-family tyrosine kinases. *Nat Med* **11**, 731-739.

Rivera, R., Hutchens, M., Luker, K. E., Sonstein, J., Curtis, J. L. & Luker, G. D. (2007). Murine alveolar macrophages limit replication of vaccinia virus. *Virology* **363**, 48-58.

Robbins, B. L., Srinivas, R. V., Kim, C., Bischofberger, N. & Fridland, A. (1998). Anti-Human immunodeficiency virus activity and cellular metabolism of a potential prodrug of the acyclic nucleoside phosphonate 9-R-(2-phosphonomethoxypropyl)adenine(PMPA), Bis(isopropyloxymethylcarbonyl) PMPA. *Antimicrob Agents Chemother* **42**, 612-617.

Roberts, T. L., Dunn, J. A., Terry, T. D., Jennings, M. P., Hume, D. A., Sweet, M. J. & Stacey, K. J. (2005). Differences in macrophage activation by bacterial DNA and CpG-containing oligonucleotides. *J Immunol* **175**, 3569-3576.

Robins, R. K., Revankar, G. R., McKernan, P. A., Murray, B. K., Kirsi, J. J. & North, J. A. (1985). The importance of IMP dehydrogenase inhibition in the broad spectrum antiviral activity of ribavirin and selenazofurin. *Adv Enzyme Regul* **24**, 29-43.

Robinson, M. J., Sancho, D., Slack, E. C., LeibundGut-Landmann, S. & Reis e Sousa, C. (2006). Myeloid C-type lectins in innate immunity. *Nat Immunol* **7**, 1258-1265.

Rosales, R., Sutter, G. & Moss, B. (1994).A cellular factor is required for transcription of vaccinia viral intermediate-stage genes. *PNAS* **91**, 3794-3798.

Rotem, Z., Cox, R. A. & Isaas, A. (1963). Inhibition of virus multiplication by foreign nucleic acid. *Nature* **197**, 564-566.

Rudd, B. D., Schaller, M. A., Smit, J. J., Kunkel, S. L., Neupane, R., Kelley, L., Berlin, A. A. & Lukacs, N. W. (2007). MyD88-mediated instructive signals in dendritic cells regulate pulmonary immune responses during respiratory virus infection. *JImmunol* **178**, 5820-5827.

Sahu, A., Isaacs, S. N., Soulika, A. M. & Lambris, J. D. (1998). Interaction of vaccinia virus complement control protein with human complement proteins: Factor I-mediated degradation of C3b to iC3b1 inactivates the alternative complement pathway. *J Immunol* **160**, 5596-5604.

Sajic, D., Ashkar, A. A., Patrick, A. J., McCluskie, M. J., Davis, H. L., Levine, K. L., Holl, R. & Rosenthal, K. L. (2003). Parameters of CpG oligodeoxynucleotide-induced protection against intravaginal HSV-2 challenge. *J Med Virol* **71**, 561-568.

Sakala, I. G., Chaudhri, G., Buller, R. M., Nuara, A. A., Bai, H., Chen, N. & Karupiah, G. (2007). Poxvirus-encoded gamma interferon binding protein dampens the host immune response to infection. *J Virol* **81**, 3346-3353.

Sanderson, C. M., Hollinshead, M. & Smith, G. L. (2000). The vaccinia virus A27L protein is needed for the microtubule-dependent transport of intracellular mature virus particles. *J Gen Virol* **81**, 47-58.

Sandron, D., Reynolds, H. Y., Venet, A., Laval, A. M., Israel-Biet, D. & Chretien, J. (1986). Human alveolar macrophage subpopulations isolated on discontinuous albumin gradients: functional data in normals and sarcoid patients. *Eur J Respir Dis* **69**, 226-234.

Sankaran, K. & Herscowitz, H. B. (1995). Phenotypic and functional heterogeneity of the murine alveolar macrophage-derived cell line MH-S. *J Leukoc Biol* **57**, 562-588.

Saraiva, M. & Alcami, A. (2001). CrmE, a novel soluble tumour necrosis factor receptor encoded by poxviruses. *J Virol* **75**, 226-233.

Sarih, M., Souvannavong, V. & Adam, A. (1993). Nitric oxide synthase induces macrophage death by apoptosis. *Biochem Biophys Res Commun* **191**, 503-508.

Sato, S., Sanjo, H., Takeda, K., Ninomiya-Tsuji, J., Yamamoto, M., Kawai, T., Matsumoto, K., Takeuchi, O. & Akira, S. (2005). Essential function for the kinase TAK1 in innate and adaptive immune responses. *Nat Immunol* **6**, 1087-1095.

Saunders, L. R. & Barber, G. N. (2003). The dsRNA binding protein family: critical roles, diverse cellular functions. *FASEB J* **17**, 961-983.

Schmelz, M., Sodeik, B., Ericsson, M., Wolffe, E., Shida, H., Hiller, G. & Griffiths, G. (1994). Assembly of vaccinia virus: the second wrapping cisterna is derived from the trans Golgi network. *J Virol* **68**, 130-147.

Schmidt, C. (2007). Clinical setbacks for toll-like receptor 9 agonists in cancer. *Nat Biotech* **25**, 825-826.

Schnare, M., Holt, A. C., Takeda, K., Akira, S. & Medzhitov, R. (2000). Recognition of CpG DNA is mediated by signaling pathways dependent on the adaptor protein MyD88. *Curr Biol* **10**, 1139-1142.

Schreiber, M., Rajarathnam, K. & McFadden, G. (1996). Myxoma virus T2 protein, a tumor necrosis factor (TNF) receptor homolog, is secreted as a monomer and dimer that each bind rabbit TNFalpha , but the dimer is a more potent TNF inhibitor. *J Biol Chem* **271**, 13333-13341.

Schroder, M. & Bowie, A. G. (2005).TLR3 in antiviral immunity: key player or bystander ? *Trends Immunol* **26**, 462-468.

Schwartz, D. A., Quinn, T. J., Thorne, P. S., Sayeed, S., Yi, A. K. & Krieg, A. M. (1997). CpG motifs in bacterial DNA cause inflammation in the lower respiratory tract. *J Clin Invest* **100**, 68-73.

Seilier, P., Aichele, P., Bandermann, S. & other authors (2003). Early granuloma formation after aerosol *Mycobacterium tuberculosis* infection is regulated by neutrophils *via* CXCR3-signaling chemokines. *Eur J Immunol* **33**, 2676-2686.

Senkevich, T. G., Ward, B. M. & Moss, B. (2004). Vaccinia virus entry into cells is dependent on a virion surface protein encoded by the A28L gene. *J Virol* **78**, 2357-2366.

Sester, D. P., Brion, K., Trieu, A., Goodridge, H. S., Roberts, T. L., Dunn, J., Hume, D. A., Stacey, K. J. & Sweet, M. J. (2006). CpG DNA activates survival in murine macrophages through TLR9 and the phosphatidylinositol 3-kinase-Akt pathway. *J Immunol* **177**, 4473-4480.

Sester, D. P., Naik, S., Beasley, S. J., Hume, D. A. & Stacey, K. J. (2000). Phosphorothioate backbone modification modulates macrophage activation by CpG DNA. *J Immunol* **165**, 4165-4173.

Shirota, H., Gursel, M. & Klinman, D. M. (2004). Suppressive oligodeoxynucleotides inhibit Th-1 differentiation by blocking IFN-γ and IL-12-mediated signaling. *J Immunol* **173**, 5002-5007.

Shisler, J. L. & Jin, X. L. (2004). The vaccinia virus K1L gene product inhibits host NF-κB activation by preventing IκBα degradation. *J Virol* **78**, 3553-3560.

Sibille, Y. & Reynolds, H. Y. (1990). Macrophages and polymorphonuclear neutrophils in lung defense and injury. *Am Rev Respir Dis* **141**, 471-501.

Sidwell, R. W., Allen, L. B., Khare, G. P., Huffman, J. H., Witkowski, J. T., Simon, L. N. & Robins, R. K. (1973). Effect of 1-beta-D-ribofuranosyl1-1,2,4-triazole-3-carboxamide (virazole, ICN 1229) on herpes and vaccinia keratitis and encephalitis in laboratory animals. *Antimicrob Agents Chemother* **3**, 242-246.

Sivori, S., Carlomagno, S., Moretta, L. & Moretta, A. (2006). Comparison of different CpG oligodeoxynucleotide classes for their capability to stimulate human NK cells. *Eur J Immunol* **36**, 961-967.

Smee, D. F., Bailey, K. W. & Sidwell, R. W. (2001a). Treatment of lethal vaccinia virus respiratory infections in mice with cidofovir. *Antivir Chem Chemother* **12**, 71-76.

Smee, D. F., Huffman, J. H., Morrison, A. C., Barnard, D. L. & Sidwell, R. W. (2001b). Cyclopentane neuraminidase inhibitors with potent *in vitro* anti-influenza virus activities. *Antimicrob Agents Chemother* **45**, 743-748.

Smith, S.A. & Kotwal, G.J. (2002). Immune response to poxvirus infection in various animals. *Crit Rev Microbiol* **28**, 149-185.

Smith, V. P., Bryant, N. A. & Alcami, A. (2000). Ectromelia, vaccinia and cowpox viruses encode secreted interleukin-18-binding proteins. *J Gen Virol* **81**, 1223-1230.

Sparwasser, T., Vabulas, R. M., Villmow, B., Lipford, G. B. & Wagner, H. (2000). Bacterial CpG-DNA activates dendritic cells *in vivo*: T helper cell-independent cytotoxic T-cell responses to soluble proteins. *Eur J Immunol* **30**, 3591-3597.

Speiser, D. E., Lienard, D., Rufer, N., Rubio-Godoy, V., Rimoldi, D., Lejeune, F., Krieg, A. M., Cerottini, J. C. & Romero, P. (2005). Rapid and strong human CD8(+) T cell responses to vaccination with peptide, IFA, and CpG oligodeoxynucleotide 7909. *J Clin Invest* **115**, 739-746.

Spriggs, M. K. (1999). Shared resources between the neural and immune systems: semaphorins join the ranks. *Curr Opin Immunol* **11**, 387-391.

Stacey, K. J., Sweet, M. J. & Hume, D. A. (1996). Macrophages ingest and are activated by bacterial DNA. *J Immunol* **157**, 2116-2122.

Stacey, K. J., Young, G. R., Clark, F., Sester, D. P., Roberts, T. L., Naik, S., Sweet, M. J. & Hume, D. A. (2003). The molecular basis for the lack of immunostimulatory activity of vertebrate DNA. *J Immunol* **170**, 3614-3620.

Stack, J., Haga, I. R., Schroder, M., Bartlett, N. W., Maloney, G., Reading, P. C., Fitzgerald, K. A., Smith, G. L. & Bowie, A. G. (2005). Vaccinia virus protein A46R targets multiple Toll-like-interleukin-1 receptor adaptors and contributes to virulence. *J Exp Med* **201**, 1007-1018.

Stanford, M. M., McFadden, G., Karupiah, G. & Chaudhri, G. (2007). Immunopathogenesis of poxvirus infections: forecasting the impending storm. *Immunol Cell Biol* **85**, 93-102.

Stein, C. A., Subasinghe, C., Shinozuka, K. & Cohen, J. S. (1988). Physicochemical properties of phosphorothioate oligodeoxynucleotides. *Nucleic Acids Res* **16**, 3209-3221.

Stokes, G. V. (1976). High-voltage electron microscope study of the release of vaccinia virus from whole cells. *J Virol* **18**, 636-643.

Strickland, D. H., Thepen, T., Kees, U. R., Kraal, G. & Holt, P. G. (1993). Regulation of T-cell function in lung tissue by pulmonary alveolar macrophages. *Immunology* **80**, 266-272.

Sun, S., Beard, C., Jaenisch, R., Jones, P. & Sprent, J. (1997). Mitogenicity of DNA from different organisms for murine B cells. *J Immunol* **159**, 3119-3125.

Sun, S., Cai, Z., Langlade-Demoyen, P., Kosaka, H., Brunmark, A., Jackson, M. R., Peterson, P. A. & Sprent, J. (1996). Dual function of Drosophila cells as APCs for naive CD8+ T cells: Implications for tumor immunotherapy. *Immunity* **4**, 555-564.

Suvas, S., Singh, V., Sahdev, S., Vohra, H. & Agrewala, J. N. (2002). Distinct role of CD80 and CD86 in the regulation of the activation of B cell and B cell lymphoma. *J Biol Chem* **277**, 7766-7775.

Suzuki, K., Suda, T., Naito, T., Ide, K., Chida, K. & Nakamura, H. (2005). Impaired Toll-like receptor 9 expression in alveolar macrophages with no sensitivity to CpG DNA. *Am J Respir Crit Care Med* **171**, 707-713.

Tabeta, K., Georgel, P., Janssen, E. & other authors (2004). Toll-like receptors 9 and 3 as essential components of innate immune defense against mouse cytomegalovirus infection. *PNAS* **101**, 3516-3521.

Takabayshi, K., Corr, M., Hayashi, T., Redecke, V., Beck, L., Guiney, D., Sheppard, D. & Raz, E. (2006). Induction of a homeostatic circuit in lung tissue by microbial compounds. *Immunity* **24**, 475-487.

Takaoka, A., Wang, Z., Choi, M. & other authors (2007).DAI (DLM-1/ZBP-1) is a cytosolic DNA sensor and an activator of innate immune response. *Nature* **448**, 501-505.

Takaoka, A., Yanai, H., Kondo, S. & other authors (2005). Integral role of IRF-5 in the gene induction programme activated by Toll-like receptors. *Nature* **434**, 243-249.

Takaoka, A. & Yanai, H. (2006). Interferon signaling network in innate defence. *Cell Microbiol* **8**, 907-922.

Takeshita, S., Takeshita, F., Haddad, D. E., Ishii, K. J. & Klinman, D. M. (2000). CpG oligodeoxynucleotides induce murine macrophages to up-regulate chemokine mRNA expression. *Cell Immunol* **206**, 101-106.

Tokunaga, T., Yamamoto, H., Shimada, S. & other authors (1984). Antitumor activity of deoxyribonucleic acid fraction from *Mycobacterium bovis* BCG. I. Isolation, physicochemical characterization, and antitumor activity. *J Natl Cancer Inst* **72**, 955-962.

Tomioka, H., Shimizu, T., Maw, W. W. & Ogasawara, K. (2000). Roles of tumour necrosis factor-alpha (TNF-alpha), transforming growth factor-beta (TGF-beta), and IL-10 in the modulation of intercellular adhesion molecule-1 (ICAM-1) expression by macrophages during mycobacterial infection. *Clin Exp Immunol* **122**, 335-342.

Tomura, M., Zhou, X. Y., Maruo, S. & other authors (1998).A critical role for IL-18 in the proliferation and activation of NK1.1+CD3- cells. *J Immunol* **160**, 4738-4746.

Tooze, J., Hollinshead, M., Reis, B., Radsak, K. & Kern, H. (1993). Progeny vaccinia and human cytomegalovirus particles utilize early endosomal cisternae for their envelopes. *Eur J Cell Biol* **60**, 163-178.

Tsai, W. C., Strieter, R. M., Mehrad, B., Newstead, M. W., Zeng, X. & Standiford, T. J. (2000).CXC chemokine receptor CXCR2 is essential for protective innate host response in murine *Pseudomonas aeruginosa* pneumonia. *Infect Immun* **68**, 4289-4296.

Tscharke, D. C., Reading, P. C. & Smith, G. L. (2002). Dermal infection with vaccinia virus reveals roles for virus proteins not seen using other inoculation routes. *J Gen Virol* **83**, 1977-1986.

Tumpey, T. M., Chen, S. H., Oakes, J. E. & Lausch, R. N. (1996). Neutrophil-mediated suppression of virus replication after herpes simplex virus type 1 infection of the murine cornea. *J Virol* **70**, 898-904.

Tzahar, E., Moyer, J. D., Waterman, H. & other authors (1998). Pathogenic poxviruses reveal viral strategies to exploit the ErbB signaling network. *EMBO J* **17**, 5948-5963.

Upton, C., Slack, S., Hunter, A. L., Ehlers, A. & Roper, R. L. (2003). Poxvirus orthologous clusters: toward defining the minimum essential poxvirus genome. *J Virol* **77**, 7590-7600.

Utaisincharoen, P., Anuntagool, N., Chaisuriya, P., Pichyangkul, S. & Sirisinha, S. (2002). CpG ODN activates NO and iNOS production in mouse macrophage cell line (RAW 264.7). *Clin Exp Immunol* **128**, 467-473.

Utaisincharoen, P., Kespichayawattana, W., Anuntagool, N., Chaisuriya, P., Pichyangkul, S., Krieg, A. M. & S, Sirisinha. (2003). CpG ODN enhances uptake of bacteria by mouse macrophages. *Clin Exp Immunol* **132**, 70-75.

Vabulas, R. M., Pircher, H., Lipford, G. B., Hacker, H. & Wagner, H. (2000). CpG-DNA activates *in vivo* T cell epitope presenting dendritic cells to trigger protective antiviral cytotoxic T cell responses. *J Immunol* **164**, 2372-2378.

van Eijl, H., Hollinshead, M., Rodger, G., Zhang, W. H. & Smith, G. L. (2002). The vaccinia virus F12L protein is associated with intracellular enveloped virus particles and is required for their egress to the cell surface. *J Gen Virol* **83**, 195-207.

van Reeth, K. & Adair, B. (1997). Macrophages and respiratory viruses. *Path Biol* **45**, 183-192.

Vanderplasschen, A., Hollinshead, M. & Smith, G. L. (1998). Intracellular and extracellular vaccinia virions enter cells by different mechanisms. *J Gen Virol* **79**, 877-887.

Verthelyi, D., Ishii, K. J., Gursel, M., Takeshita, F. & Klinman, D. M. (2001). Human peripheral blood cells differentially recognize and respond to two distinct CpG motifs. *J Immunol* **166**, 2372-2377.

Vollmer, J., Weeratna, R., Payette, P. & other authors (2004). Characterization of three CpG oligodeoxynucleotide classes with distinct immunostimulatory activities. *Eur J Immunol* **34**, 251-262.

von Itzstein, M., Wu, W. Y., Kok, G. B. & other authors (1993). Rational design of potent sialidase-based inhibitors of influenza virus replication. *Nature* **363**, 418-423.

Waag, D. M., McCluskie, M. J., Zhang, N. & Krieg, A. M. (2006).A CpG oligonucleotide can protect mice from a low aerosol challenge dose of *Burkholderia mallei*. *Infect Immun* **74**, 1944-1948.

Waibler, Z., Anzaghe, M., Ludwig, H., Akira, S., Weiss, S., Sutter. & Kalinke., U. (2007). Modified Vaccinia virus Ankara induces toll-like receptor-independent type I interferon responses. *J Virol* **81**, 12102-12110

Walzer, T., Galibert, L. & De Smedt, T. (2005). Poxvirus semaphorin A39R inhibits phagocytosis by dendritic cells and neutrophils. *Eur J Immunol* **35**, 391-398.

Weighardt, H., Feterowski, C., Veit, M., Rump, M., Wagner, H. & Holzmann, B. (2000). Increased resistance against acute polymicrobial sepsis in mice challenged with immunostimulatory CpG oligodeoxynucleotides is related to an enhanced innate effector cell response. *J Immunol* **165**, 4537-4543.

Wesche, H., Henzel, W. J., Shillinglaw, W., Li, S. & Cao, Z. (1997). MyD88: An adapter that recruits IRAK to the IL-1 receptor complex. *Immunity* **7**, 837-847.

West, B. C., Eschete, M. L., Cox, M. E. & King, J. W. (1987). Neutrophil uptake of vaccinia virus *in vitro*. *J Infect Dis* **156**, 597-606.

Wharton, M., Strikas, R. A., Harpaz, R. & other authors (2003). Recommendations for using smallpox vaccine in a pre-event vaccination program. Supplemental recommendations of the Advisory Committee on Immunization Practices (ACIP) and the Healthcare Infection Control Practices Advisory Committee (HICPAC). *MMWR Recomm Rep* **52**, 1-16.

Wietek, C., Miggin, S. M., Jefferies, C. A. & O'Neill, L. A. J. (2003). Interferon regulatory factor-3-mediated activation of the interferon-sensitive response element by Toll-like receptor (TLR) 4 but not TLR3 requires the p65 subunit of NF-κB. *J Biol Chem* **278**, 50923-50931.

Wise, L. M., Veikkola, T., Mercer, A. A. & other authors (1999). Vascular endothelial growth factor (VEGF)-like protein from orf virus NZ2 binds to VEGFR2 and neuropilin-1. *PNAS* **96**, 3071-3076.

Wittamer, V., Bondue, B., Guillabert, A., Vassart, G., Parmentier, M. & Communi, D. (2005). Neutrophil-mediated maturation of chemerin: A link between innate and adaptive immunity. *J Immunol* **175**, 487-493.

Wongratanacheewin, S., Kespichayawattana, W., Intachote, P., Pichyangkul, S., Sermswan, R. W., Krieg, A. M. & Sirisinha, S. (2004). Immunostimulatory CpG oligodeoxynucleotide confers protection in a murine model of infection with *Burkholderia pseudomallei*. *Infect Immun* **72**, 4494-4502.

Woodworth, B. A., Neal, J. G., Newton, D., Joseph, K., Kaplan, A. P., Baatz, J. E. & Schlosser, R. J. (2007). Surfactant protein A and D in human sinus mucosa: a preliminary report. *ORL J Otorhinolaryngol Relat Spec* **69**, 57-60.

Xu, R., Johnson, A. J., Liggitt, D. & Bevan, M. J. (2004). Cellular and humoral immunity against Vaccinia Virus infection of mice. *J Immunol* **172**, 6265-6271.

Yamamoto, S., Yamamoto, T., Kataoka, T., Kuramoto, E., Yano, O. & Tokunaga, T. (1992a). Unique palindromic sequences in synthetic oligonucleotides are required to induce IFN and augment IFN-mediated natural killer activity. *J Immunol* **148**, 4072-4076.

Yamamoto, S., Yamamoto, T., Shimada, S., Kuramoto, E., Yano, O., Kataoka, T. & Tokunaga, T. (1992b).DNA from bacteria, but not from vertebrates, induces interferons, activates natural killer cells and inhibits tumor growth. *Microbiol Immunol* **36**, 983-997.

Yang, G., Pevear, D. C., Davies, M. H. & other authors (2005a). An orally bioavailable antipoxvirus compound (ST-246) inhibits extracellular virus formation and protects mice from lethal orthopoxvirus challenge. *J Virol* **79**, 13139-13149.

Yang, H., Kim, S. K., Kim, M., Reche, P. A., Morehead, T. J., Damon, I. K., Welsh, R. M. & Reinherz, E. L. (2005b). Antiviral chemotherapy facilitates control of poxvirus infections through inhibition of cellular signal transduction. *J Clin Invest* **115**, 379-387.

Yi, A. K., Chace, J. H., Cowdery, J. S. & Krieg, A. M. (1996a).IFN-gamma promotes IL-6 and IgM secretion in response to CpG motifs in bacterial DNA and oligodeoxynucleotides. *J Immunol* **156**, 558-564.

Yi, A. K., Klinman, D. M., Martin, T. L., Matson, S. & Krieg, A. M. (1996b). Rapid immune activation by CpG motifs in bacterial DNA. Systemic induction of IL-6 transcription through an antioxidant-sensitive pathway. *J Immunol* **157**, 5394-5402.

Yoneyama, M., Kikuchi, M., Natsukawa, T., Shinobu, N., Imaizumi, T., Miyagishi, M., Taira, K., Akira, S. & Fujita, T. (2004). The RNA helicase RIG-I has an essential function in double-stranded RNA-induced innate antiviral responses. *Nat Immunol* **5**, 730-737.

Zhang, D., Zhang, G., Hayden, M. S., Greenblatt, M. B., Bussey, C., Flavell, R. A., Ghosh, S. (2004). A Toll-like receptor that prevents infection by uropathogenic bacteria. *Science* **303**, 1522-1526.

Zhao, Q., Matson, S., Herrera, C. J., Fisher, E., Yu, H. & Krieg, A. M. (1993). Comparison of cellular binding and uptake of antisense phosphodiester, phosphorothioate, and mixed phosphorothioate and methylphosphonate oligonucleotides. *Antisense Res Dev* **3**, 53-66.

Zhou, Q., Snipas, S., Orth, K., Muzio, M., Dixit, V. M. & Salvesen, G. S. (1997). Target protease specificity of the viral serpin CrmA. Analysis of five caspases. *J Biol Chem* **272**, 7797-7800.

Zhu, J., Martinez, J., Huang, X. & Yang, Y. (2007). Innate immunity against vaccinia virus is mediated by TLR2 and requires TLR-independent production of IFN-beta. *Blood* **109**, 619-625.

Zimmermann, K. C., Bonzon, C. & Green, D. R. (2001). The machinery of programmed cell death. *Pharmacol Ther* **92**, 57-70.

Zimmermann, S., Hausmann, S., Lipford, G. B., Wagner, H. & Heeg, K. (1998a). Prevention of lethal murine toxoplasmosis by CpG oligonucleotides in susceptible mice. *10Th International Congress on Immunology, Vols 1 and 2*, 1407-1410.

Zimmermann, S., Egeter, O., Hausmann, S., Lipford, G. B., Rocken, M., Wagner, H. & Heeg, K. (1998b). Cutting edge: CpG oligodeoxynucleotides trigger protective and curative Th-1 responses in lethal murine leishmaniasis. *J Immunol* **160**, 3627-3630.

Zsengeller, Z., Otake, K., Hossain, S. A., Berclaz, P. Y. & Trapnell, B. C. (2000). Internalization of adenovirus by alveolar macrophages initiates early proinflammatory signaling during acute respiratory tract infection. *J Virol* **74**, 9655-9667.

Zuluaga, A., Salazar, B., Rodriguez, C., Zapata, A., Agudelo, M. & Vesga, O. (2006). Neutropenia induced in outbred mice by a simplified low-dose cyclophosphamide regimen: characterization and applicability to diverse experimental models of infectious diseases. *BMC Infectious Diseases* **6**, 55.